Stellingen/Propositions

Fungal Fermentation : technological aspects

Y.Q.Cui

1. Harder roeren leidt niet tot sterkere pellets (*zie Hoofdstuk 5*).
   Stirring harder does not lead to the formation of stronger pellets (*see Chapter 5*).

2. De dichtheid van pellets is evenredig met de concentratie van het limiterende substraat (*zie Hoofdstuk 5*).
   Pellet density is proportional to the concentration of the limiting substrate (*see Chapter 5*).

3. Viskeuze systemen zijn het minst inhomogeen op "pilot plant" schaal (*zie Hoofdstuk 9*).
   Viscous systems are most homogeneous on the pilot plant scale (*see Chapter 9*).

4. De mogelijkheid van schimmels om te veranderen zorgt er voor dat hun overlevingskansen op aarde groot zijn.
   The ability of fungi to change gives them a competitive advantage on our planet.

5. Een grondige beschrijving van schimmelfermentaties is een onmogelijke opgave.
   A rigorous description of fungal fermentation is impossible.

6. Een benadering van een precieze beschrijving van een natuurlijk verschijnsel is nuttiger dan de exacte.
   An approximate description of a natural phenomenon is more useful than an exact one.

7. Het gemiddelde kennisniveau van wiskunde op universiteiten neemt af met het toenemende gebruik van computers en rekenprogrammatuur.
   The average level of understanding of mathematics in Universities decreases with the use of computers and calculation software.

8. Computers genereren geen extra vrije tijd.
   Computers do not generate more leisure time.

9. Het nastreven van een hogere productiviteit in de levensmiddelenindustrie verlaagt de smaak van de voedingsmiddelen.
   The pursuit of higher efficiency in food production diminishes the taste of the foodstuffs.

10. De grootste fout in het leven is het voornemen geen fouten te maken
    The biggest mistake in life is the intention to make no mistakes.

11. De mening van de meerderheid is niet persé de juiste.
    The opinion of a majority is not necessarily the right one.
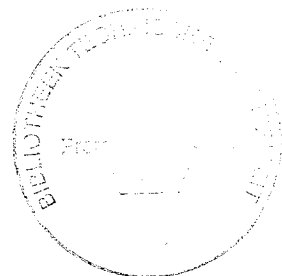
Fungal Fermentation

technological aspects

Yi Qing Cui

Fungal Fermentation

technological aspects

Thesis / Proefschrift

ter verkrijging van de graad van doctor
aan de Technische Universiteit Delft
op gezag van de Rector Magnificus Prof. dr.ir J. Blaauwendraad,
in het openbaar te verdedigen ten overstaan van een commissie,
door het College van Dekanen aangewezen,
op dinsdag 9 december 1997 te 16.00 uur
door

Yi Qing CUI

Master of Science in Chemical Engineering, Technical Institute of Dalian, China

Geboren te Shenyang, China

Dit proefschrift is goedgekeurd door de promotor:
Prof. ir. K.Ch.A.M. Luyben

Samenstelling promotiecommissie:

Rector Magnificus, voorzitter
Prof. ir. K.Ch.A.M. Luyben (promotor)   Technische Universiteit Delft
Prof. dr. C.A.M.J.J. v.d. Hondel   RU-Leiden, Fac Wisk./TNO-voeding
Prof. Dr.Ing. R. King   Technische Universität Berlin
Prof. dr.ir. J.J. Heijnen   Technische Universiteit Delft
Prof. A.W. Nienow. F.Eng.   U-Birmingham, Engeland
Dr.ir. J.P. van Dijken   Technische Universiteit Delft
Dr.ir. M.L.F. Guiseppin   Unilever Research, Vlaardingen

Dr. ir. R.G.J.M. van der Lans heeft als begeleider in belangrijke mate aan het totstandkomen van het proefschrift bijgedragen

CONTENTS

CHAPTER 1

Introduction

Y.Q.Cui

Background

Filamentous fungi are eukaryotic organisms and represent a physiologically divers group of microorganisms. Their capacity to change and adapt makes them a strong competitor on our planet. They can be found in a wide range of habitats: in fresh water and the sea, in soil, litter, decaying remains of plants and animals, in dung, in living plants, animals and often in exposed foodstuffs. The traditional utilization of filamentous fungi by humans is especially on and with foods. For example, certain filamentous fungi have been used to improve the flavour of cheese, while some fungi are used in Asian cultures to produce foods such as soy sauce and fermented bean curd. Mushrooms similarly have a long history of being used as food.

The rapid expansion of industrial applications of filamentous fungi started this century. One of the most economically important uses of fungi is the industrial production of biochemicals such as organic acids (e.g. citric, fumaric, lactic, itaconic and gluconic acids). Now the annual world production of citric acid is more than 200 000 tonnes (Wainwright,1992) which are mainly produced using *Aspergillus niger or Aspergillus wentti* as the producer organism (Schrickx, 1994).

Penicillin, a fungal product from pharmaceutical industry, is considered to have revolutionised medicine. The use of filamentous fungi for the commercial production of enzymes was amplified by the introduction of enzyme-containing washing powders. The enzyme production trend over the past 30 years shows that the new products are almost invariably derived from bacteria and fungi. There are several reasons for this phenomenon: (1) microorganisms grow rapidly and are ideal for intensive cultivation; (2) medium constituents are cheap and generally comprise agricultural products available in bulk and (3) the choice of producer organisms is wide and they mostly can be improved by genetic modification (Priest, 1984). The largest emerging application of biotechnology is in the production of pharmaceutical products, and particularly biopharmaceutical therapeutic protein (Slater, 1993). The high levels of secretion of native proteins by filamentous fungi makes these organisms excellent potential hosts for the production of homologous and heterologous proteins (Korman et al, 1990; Saunders et al., 1989 and Van den Hondel et al., 1992, Gouka, 1996).

Exciting developments are also made in the use of fungi for agricultural and environmental reasons. In agricultural biotechnology, attempts are being made to use fungi as biological control agents to reduce the damage caused by populations of insects, weeds and plant-pathogenic micro-organisms (Wainwright, 1992). The use of fungi in environmental biotechnology presently focusses on the treatment of hazardous wastes such as cyanide (Wainwright 1992), on the remediation of soil polluted by pesticides and other chemical

compounds (Wainwright 1992), and on the removal of pollutants, such as styrene (Cox, 1994), from air.

Fungal fermentation

Industrial filamentous fungal fermentations are usually carried out in submerged cultures in stirred bioreactors. The stirred tank reactor consists of a cylindrical vessel, mechanical stirrers, baffles and mostly a sparger as well. The vessels vary in volume as well as geometry. In general, the height over diameter ratio (aspect ratio) of an industrial fermenter is larger than unity and the fermenter is equipped with multiple stirrers. The most often used and studied stirrer is the Rushton turbine with six blades. Baffles are used to prevent rotation of the contents as a whole and the formation of a vortex. The sparger, mounted usually below the bottom impeller, is used to supply gas (air, gas mixture or oxygen) into the fermenter.

For operation of a stirred bioreactor, the controlled parameters are stirrer speed and gas flow rate. The mechanical energy input by the rotating stirrers is used to disperse the gas and create an overall convection flow and turbulence in the bioreactor. The dispersion of gas is needed to achieve mass transfer between the gas and the liquid phase. Overall convection flow and turbulence are required for a good homogenization (both macromixing and micromixing) and mass and heat transfer.

To run a submerged fungal fermentation, one usually starts with making an inoculum which could be a spore suspension, a preculture from shaking flasks or a preculture in stirred vessels through one or several steps. After the obtained inoculum is inoculated into a chosen fermenter filled with culture medium, fermentation begins. The fermentation will be tuned to produce the desired products. The design and operation of the bioreactor for a given process has to be done such that the costs of the pertinent products with a desired quality are minimized within the biological and technological constrains. The growth-form of filamentous fungi in submerged culture can be long, thin, branched threads of mycelia, or compact mycelial pellets. Often both forms are present. A schematic drawing of the two kinds of morphology is given in Fig.1.
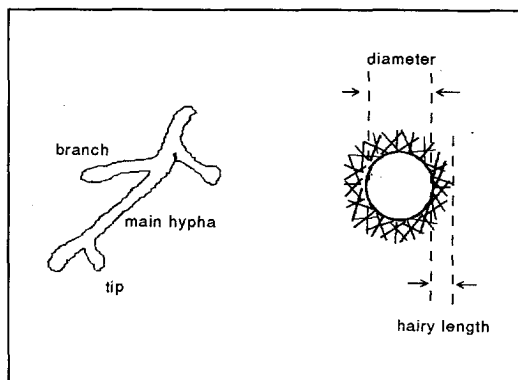

Figure 1. A schematic drawing of fungal morphology

Mycelial hyphae have a length in the order of 50-500 μm and a diameter of 2-10 μm. The pellets have a diameter in the order of 500-5000 μm. The filamentous growth-form at a high concentration of biomass (10-50 kg/m^3 of dry mass) gives a high viscous culture fluid and consequently a low gas -liquid (G-L) oxygen transfer rate and a poor mixing efficiency. The growth in pellet form does improve the gas-liquid oxygen transfer and mixing efficiency in comparison with the filamentous form but the pellets may be subject to internal oxygen limitation. The growth of a pellet only occurs in its peripheral zone, while the hyphae in the centre may be lysed. Attempts to describe the factors that influence growth in pellet or filamentous form led to contradictory reports (Schrickx J., 1994). The complex morphology makes fungi rather difficult to handle and introduces various kinds of problems for their industrial application. Fungal growth, morphology, mass and heat transfer, mixing, broth rheology and product formation and secretion interact with each other in a complex way and are very sensitive for scale-up/down, operation conditions, procedures, and bioreactor geometry. Fig.2 presents the relevant mechanisms and their interaction in the fungal fermentation process.
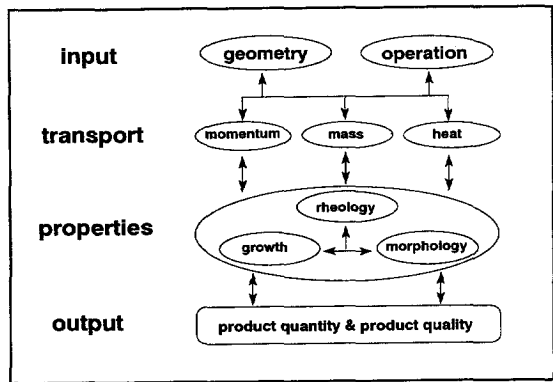

Figure 2. Schematic description of a fungal fermentation

An engineer working on the production with fungal fermentation, often faces the task to scale up a fermentation with a newly developed strain, to improve a existing process, or to even construct a new plant and optimize the fungal fermentation. However, in general there is a lack of knowledge on how fungi respond physiologically and morphologically to a change in the environment in a bioreactor, how to design and operate an industrial bioreactor and how this bioreactor will perform with a given fungal fermentation broth. Besides that, there are several industrial constraints for scale-up: to maintain the product quality, to meet the market demands quickly, to obtain a proper return on invested capital and revenue costs and to minimize the impact on the environment. Profitability projections are as a rule based on results obtained from the process in lab and pilot scale. Any changes in efficiency or quality caused by the increase in scale will influence the profit and may even jeopardize the project. It is therefore of great importance for the industrial application of new biotechnological developments that the bioreactor performance for the production at full scale can be predicted accurately. However, due to the complexity of fungal fermentations, the predictability in its performances is very limited today. For example, the optimization of the more than 50 year

old and well known industrial penicillin production still relies on a combination of empiricism and tradition rather than on a thorough understanding (Nielsen, 1994).

Aim, scope and outline of the thesis

A joint research programme on fungal fermentation, involving Unilever Research Vlaardingen, Hannover University and Delft University of Technology, was set up. *Aspergillus awamori* (CBS 115.52) was chosen as a model fungal microorganism. The fermentations were performed in both synthetic medium and complex medium. Stirred bioreactors equipped with Rushton turbines were used to achieve mixing, gas dispersion, mass and heat transfer and to provide the desired physical and chemical environment for cell growth. In this progamme Hannover focused on physiological aspects while the technological aspects was studied in Delft. The research described in this thesis mainly focuses on these technological aspects of a fungal fermentation.

The aim of this thesis is to reduce the uncertainty in the scale-up of a given fungal fermentation process and to facilitate process optimization. This aim is approached by three aspects of research: to study the hydrodynamics of a stirred bioreactor; to generate information on morphology and growth of fungi at various conditions; and to model fungal fermentation and map relevant mechanisms.

Hydrodynamics in the bioreactor
In Chapter 2 a compartment model is developed to predict the mixing behaviour of a multi-impeller stirred bioreactor. Pulse response curves were measured in a production scale bioreactor at different operation conditions and different geometries.

In Chapter 3 the local power uptake of Rushton turbines in a multi-impeller reactor is discussed. A large amount of data were gathered from the literature. The power uptake of both bottom impeller and middle and top impellers are correlated with operation conditions and tank geometries.

Generating information on morphology and growth at various conditions
In Chapter 4 morphological parameters, such as pellet size, pellet density and hairy length of pellets, obtained from fermentations that were run parallel at different agitation intensities are presented.

Chapter 5 is focussed on the effects of dissolved oxygen tension and mechanical forces on fungal morphology. Parallel fermentations at different dissolved oxygen tensions but at the same agitation intensities were perfomed. Combining the data of these parallel fermentations

with the previous ones results in a picture on how dissolved oxygen tension and mechanical forces affect morphology.

In Chapter 6 the results from fermentations performed at various conditions, are reported. Specific growth rate, maintenance coefficient, and autolysis constant were determined and the time profile of fermentations and morphology are presented. The effect of scale on morphology was looked at.

Aspergillus awamori was also cultivated in a complex medium (wheat bran) at different conditions (Chapter 7) . Growth kinetics and the influence of complex medium and inoculation on morphology were investigated.

Modelling growth and morphology and mapping the relevant mechanisms
In Chapter 8 a model is developed for a suspension growth of filamentous mycelia and pellets. Gas-liquid mass transfer, shave-off of hairs from pellets, reseed of the growth of filamentous mycelia and internal mass transfer limitation are taken into account.

In Chapter 9 the relevant mechanisms for a fungal fermentation are mapped. The important subprocesses discussed are mixing, oxygen transfer and consumption, and the behaviour of fungal particles in turbulent flow in bioreactors.

References

Cox, H.H.J., 1994, "Styrene removal from waste gas by the fungus *Exophiala jeanselmei* in a biofilter", the Ph.D thesis of Rijksuniversiteit Groningen.

Gouka, R.J., 1996, Analysis of heterologous protein production by the filamentous fungus *Aspergillus awamori*, Ph.D thesis of Universiteit Utrecht, the Netherlands..

Korman, D.R., Bayliss, F.T., Barnett, C.C., Carmona, C.L., Kodama, K.H., Royer, T.J., Thompson, S.A., Ward, M., Wilson, L.J., Berka,R.M., 1990, "Cloning, characterization, and expression of two α-amylase genes from *Aspergillus niger var. awamori*", *Curr. Genet*, **17**, 203-212

Nielsen,J., 1994, "Physiological Aspects of Penicillium chrysogenum", Proceedings of European conference on Modelling of filamentous fungi, 15-16 September 1994, Otočec, Slovenia, 15-18

Priest, F.G., 1984,: Aspects of Microbiology 9: Extracellular enzymes. Wokingham UK: van Nostrand Reinhold (UK)

Saunders, G., Picknett, T.M., Tuite, M.F. and Ward, M. 1989, "Heterologous gene expression in filamentous fungi", *Tr. Biotechnol.* **7**, 283-287

Schrickx,J., 1994, "Physiology of growth and product formation in wild-type and a glucoamylase overproducing transformant of *Aspergillus niger*", *Ph.D Thesis Vrije Universiteit te Amsterdam*

Slater,N.K.H., 1993, "Scale-up problems", Proceedings of Bioreactor performance, 15-17 March, 1993 Helsingør, Denmark, pp:15-21

Van den Hondel, C.A.M.J.J., Punt, P.J. and van Gorcom, R.F.M., 1992, "Production of extracellular proteins by the filamentous fungus *Aspergillus*", *Antonie van Leeuwenhoek*, **61**, 153-160

Wainwright,M 1992, An introduction to fungal biotechnology, John Wiley & Sons, New York

CHAPTER 2

Compartment Mixing Model For Stirred Reactors with Multiple Impellers

Y.Q.Cui, R.G.J.M. van der Lans, H.J.Noorman and K.Ch.A.M.Luyben

Abstract

Mixing determines the micro-environment for most (bio)chemical conversions. Estimation of mixing behaviour is therefore of major importance for the design and study of stirred reactors. To predict the mixing behaviour of stirred (bio)reactors with multiple impellers, commonly used in industry, a multi-compartment mixing model was developed. Experimental data on mixing behaviour were obtained with a fluorescent tracer pulse response technique. Various pulse-response curves have been measured in a large scale bioreactor (30 m³) with different geometries. Working volume, number of impellers, clearance between impellers and operating conditions were changed. Comparison between the simulated data and the experimental data shows that the developed model predicts the measured pulse-response curves rather well. The model parameters are obtained from available knowledge on hydrodynamics instead of fitting experimental data. This will increase the applicability of the model.

Keywords: compartment model; mixing; stirred vessel; multiple impellers

INTRODUCTION

Determination and quantification of mixing behaviour

Pulse response techniques are often used to determine the mixing behaviour of stirred reactors. Usually, the pulse (tracer or heat) is injected at a chosen location (surface, stirrer region or other place) in the stirred reactor by means of a special device. Then a sensor, mounted at the same or a different location, measures the local signal. The mixing process can be characterized by a characteristic time or mixing time. This is the time span needed to reach a certain degree of homogeneity in a given vessel after a disturbance. Because the physical meaning of this parameter is clear, and its quantification and comparison are relatively straightforward, the concept of mixing time is quite common in the literature. However, large deviations in obtained values may occur due to different injection and detection positions in different situations. Besides that, the characteristic time for mixing only represents the time span to reach the given homogeneity at the detected point. It provides no information on how the local environment actually reaches this homogeneity. It therefore does not contain any information on phenomena such as overshoot and oscillations.

Mixing Times

Despite its intrinsic limitation, mixing time is still the most commonly used parameter to quantify the mixing behaviour of a particular system. In the literature, correlations can be found for various systems.

Single-phase / single-impeller systems
Many attempts[1, 2, 3] have been made to correlate mixing times in unaerated stirred vessels to the impeller speed and the geometry of vessels and stirrers. For a low viscous medium, the mixing time in stirred vessels with standard geometry or not too far away from that, can be predicted based on the information in the literature. Equation (1) is an example[2] of the correlations.

$$Nt_{95\%} = \frac{3}{N_P^{1/3}} \left(\frac{T}{D} \right)^3 \qquad Re > 10000 \qquad (1)$$

$t_{95\%}$ is the time span to reach a 95% homogeneity.

Two-phase / single-impeller systems
Two-phase systems are especially of interest for fermentation, where aeration is commonly used. How does an air flow influence the mixing behaviour in a given situation? This type

of information is rather scarce [2]. When a gas flow is introduced into a stirred vessel, the flow becomes very complex. Increasing the air flow rate will finally lead to flooding. A flow map[4] can be used to predict the operation regime of aerated stirred vessels. Several regimes are distinguished such as: '3-3' structure of the cavity formed behind impeller blades, complete gas recirculation, flooding, and so on. Although aeration reduces the pumping capacity of impellers, it also induces an extra axial flow and may change the flow pattern. By comparing the experimental data from Einsele et al.[5] and others, van 't Riet[2] concluded that aeration will lead to approximately a doubling of the mixing time compared to unaerated conditions at the same stirrer speed. However, Pedersen et al.[6] stated that the mixing time under aerated conditions decreases. Groen et al.[7] demonstrated that the influence of aeration depends on the prevailing flow regime at the given aeration rate. An aeration at the same stirrer speed reduces the mechanical power input of an impeller, but adds the pneumatic power input into the system. So far it is still very difficult to quantify the influence of the gas flow on the mixing behaviour for a given system. The mixing time for unaerated conditions can only be used as a first approximation.

Single-phase / multi-impeller systems
Industrial fermenters are often equipped with multiple impellers. The introduction of multiple radial pumping impellers into the system creates a segregation of circulation flows between the impellers. The circulation flows also interact with each other. These interactions will not only influence the power consumption for each impeller but may also change the flow pattern. Three flow patterns (parallel flow, merging flow and diverging flow) have been found[8] by changing stirrer speed and the distance between impellers. It is recommend that an impeller spacing of 2 to 3 times the impeller diameter should be used to maximize the power consumption and therefore the potential for gas-liquid mass transfer[9]. Generally speaking, the mixing behaviour of a multi-impeller system will be quite different from that of single-impeller systems even under unaerated conditions. Unfortunately, the published correlations about mixing in stirred vessels are mainly based on single impeller tanks with limited geometries in aqueous systems. Recently, a formula was published[7] for the mixing time, $t_{95\%}$, as a function of the geometry of a tank, the size of the Rushton impellers, the number of impellers and the operating conditions [equation (2)]. For turbulent conditions, this equation was tested for stirred vessels at a scale of 0.025 m^3 up to 150 m^3.

$$\frac{t_m \varepsilon^{1/3}}{T^{2/3}} = C \left(\frac{D_h}{T} \right)^{-4/3} \left(\frac{L_s}{H} \right)^2 \left(\frac{H}{T} \right)^2 \tag{2}$$

Where $C=0.11$ for 95% homogeneity mixing time, top injection and bottom detection in water, and $L_s = H + N_i T$, T is the diameter of the tank, D_h the height of the stirrer blade, ε the power input per mass, and N_i the number of impellers. The relation predicts that mixing

gets worse fast with an increase in the number of impellers, assuming H/T to be proportional to the number of impellers.

Large scale bioreactors often differ from laboratory scale vessels with respect to the number of impellers, ratio of height to diameter, distance between stirrers, type of impeller, hydrostatic effects, and the rheology of the broth. Therefore, the extrapolation of many literature data to a given large scale bioreactor is unreliable. This makes further study of mixing behaviour in large bioreactors necessary.

Multi-phase / multi-impeller systems
Little is known about mixing behaviour in large scale bioreactors with multiple impellers under aerated conditions. To our knowledge, there are no correlations for such systems available in the literature. But most industrial fermentations are carried out in such systems. Perhaps, the unaerated data can be used as a reference. Before a conclusion can be reached, intensive research is needed.

Model approaches

A continuously changing environment may influence the (bio)conversion[3, 10, 11] . The local conditions encountered by organisms flowing through the nonhomogeneous turbulent and bubbly flow field, need to be studied. This can be done experimentally or by means of simulation. Two common simulation approaches are computational fluid dynamics (CFD) and the compartment model. Both can be extended relatively easily using a kinetic model. This makes the local quantification of biological and chemical processes possible.

Computational Fluid Dynamics (CFD)

To reach some theoretical understanding of turbulent mixing, particularly its local effects, detailed knowledge of flow and characteristics of turbulence within the stirred vessel is first required. In the literature, several articles on the simulations of single phase flow patterns in relatively simple systems can be found[12, 13, 14, 15]. Experimental data are always needed either for providing boundary conditions or due to uncertainties in the simulation[16]. The experimental support can be obtained by measuring the velocity at different locations by means of photographic techniques, hot-wire, hot-film, laser-doppler anemometry or others. Then a comparison of the simulated data with measured data is possible.

It is known that multi-impeller systems are difficult to simulate because of the interaction between the impellers. Nevertheless, some CFD results of multi-impeller systems have been

reported[17, 18, 19]. For industrial scale stirred bioreactors, the verification of the simulation is often difficult. Sometimes it is impossible to accomplish and sometimes the installation of an appropriate sensor in such a system is too costly. This inhibits the application of CFD for large scale stirred vessels. Multi-phase and multi-impeller systems are important subjects in the CFD research area. CFD is very promising but in our opinion there is still a long way to go before CFD can be used as a practical tool to predict the flow in large scale fermenters with industrial media.

Compartment models

During the last few decades several compartment models for stirred tanks have been developed[20, 21, 22, 23, 24]. The simplest model[24] has only two compartments for a single impeller system. The most complex one[22] contains a huge number of compartments for a single impeller system. In the literature[21], a compartment model is presented for a multi-impeller system. Figure 1 gives a schematic representation of the configuration around one impeller in this model[21]. The model contains four adjustable (fitting) parameters:
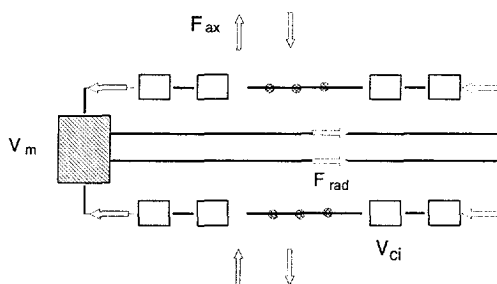

Figure 1. Configuration of compartments around one impeller[15].

1. the ratio of the ideally mixed volume (stirrer region) to the total liquid volume (V_m/V_{tot}),
2. the radial circulation time ($t_{c,RAD} = V_{tot}/(nF_{rad})$) (for n stirrers),
3. the axial circulation time ($t_{c,AX} = V_{tot}/F_{ax}$),
4. the number of ideally mixed tanks (N) in the cascade representing the circulation flow within a stirrer compartment.

Based on the Monte-Carlo optimization method, these parameters have been estimated by fitting pulse-response curves measured in a 2.5 m³ bioreactor. The model described the experimental data relatively well. However, four parameters are needed in this model, which are variable (changing with used operating conditions and geometry) and cannot be predicted beforehand.

Although several compartment models are available in the literature, up to now there is no model which is based on extensive and exact measurements applied in industrial scale bioreactors and which can **predict** the mixing behaviour in bioreactors with different

geometries. The structure and the parameters of the model should be based, as far as possible, on available knowledge of the hydrodynamics, such as flow patterns, circulation velocity, and turbulent mixing. Such a mechanistic background will enlarge the chance of proper prediction outside the range of experimental verification.

Present work

A multi-compartment model for single-phase stirred bioreactors with multiple radial pumping impellers has been developed. Its structure is based on the dominating radial parallel flow pattern (see Figure 4) for the liquid which is often reported in literature. A relation for the axial exchange flow rate between the vicinal compartments is derived. The model parameters come from hydrodynamics in stirred vessels. These values are based on the reported data. This will increase the applicability of the model. To study the mixing behaviour of a multi-impeller stirred vessel, various pulse-response curves were measured in such a system. The model was then used to simulate these curves. The comparison of the predicted and measured data will be presented.

EXPERIMENTAL

A cylindrical tank (2.07 m diameter and 6.55 m in height) with four vertical baffles has been used (Figure 2). It is originally mounted with four disk turbines with six flat blades ($T/D=3$). By changing the level of the liquid and changing the clearance between the impellers, several different geometries could be investigated using the same tank. Table I gives an overview of the different geometries used in the experiments. The first and second column in table II give the configuration and the corresponding experimental conditions.

Tap water was used as the medium. The pulse-response technique with fluorescent tracers[7] was adopted to determine the mixing behaviour. During a measurement, the tank is kept dark. Fluorescent tracer was introduced at the top. Optical detectors were located at the outflows of both bottom and middle impellers (see Fig. 2). The detectors
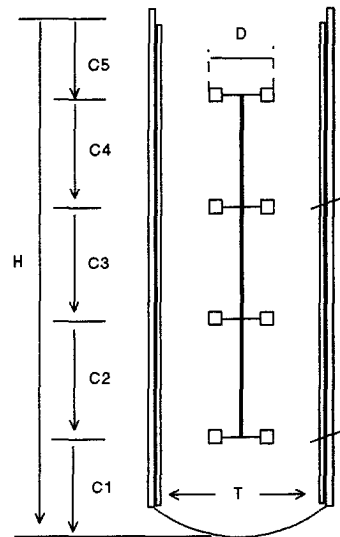

Figure 2. Configuration of the used fermenter.

Table I. Geometry of the used configurations. $T=2.07m$; $D=0.7m$; $D_h=0.14m$; $D_L=0.175m$.

Geometry	A#	B#	C#	D#	E#	F#
V (m³)	22.0	15.8	10.8	5.4	10.8	22.0
Ni (-)	4	3	2	1	1	2
H (m)	6.55	4.63	3.18	1.73	3.18	6.55
C_1 (m)	1.0	1.0	1.0	1.0	1.0	1.0
C_2 (m)	1.45	1.45	1.45	--	--	2.9
C_3 (m)	1.45	1.45	--	--	--	2.9
C_4 (m)	1.45	--	--	--	--	--
B (m)	0.167	0.167	0.167	0.167	0.167	0.167

B: width of baffle, Ni: number of impellers

Table II. Analysis of Simulation of Pulse-response data

Geometry	N (min⁻¹)	Probe	Sample size	Mean Residual²	S_e^2	F	Bias	F'
A#	133	B	100	0.002551	0.002022	1.2829	-0.04545	0.261622
A#	115	B	98	0.003772	0.003459	0.12221	-0.01624	0.090489
A#	95	B	112	0.003412	0.002579	0.81324	-0.03841	0.3265
A#	70	B	125	0.00274	0.002407	0.1469	-0.00195	0.1383
B#	115	B	82	0.002591	0.001392	1.06998	-0.01702	0.8614
C#	115	B	55	0.011804	0.007898	0.56401	0.0234	0.4946
D#	115	B	45	0.10417	0.005709	79.414	0.1023	17.246
E#	115	B	55	0.02505	0.003078	11.06	0.1097	7.1384
F#	115	B	85	0.003025	0.00204	0.7257	-0.02203	0.4828
F#	95	B	96	0.004144	0.003946	0.05086	0.00168	0.0502
A#	115	Mid	59	0.007349	0.002773	8.6535	0.04937	1.6503

B: bottom; S_e^2 : mean square of pure error; F ratio$=MS_L/S_e^2$ (MS_L:Lack of fit); F' ratio $= MS_L'$ $/S_e^2$ (MS_L': Lack of fit taking Bias into account); Bias: mean residual.

consist of two optical fibre cables. One of them is used to send an excitation light beam with a certain wavelength into the front of the detector. The other will guide the light emitted by the tracer to an photomultiplier. The intensity of the signal from the photomultiplier is proportional to the local tracer concentration under the conditions used (the concentration of the tracer < 2 g m⁻³). Since this is an optical system, it responds very quickly. This makes it suitable for measuring a pulse-response curve.

For such a large scale experiment, the amount of water to be used and coloured has to be taken into account. Besides that, the time needed to fill a 30 m³ tank with water should be

considered as well. Therefore in our experiments, the amount of tracer for each injection is minimized in order to carry out as many measurements as possible in each tank of water. In consequence, the measured pulse-reponse signals contain a certain amount of noise. By varing the amount of tracer for each injection, the level of this noise is controlled to be less than 15% of the magnitude of the measured signals.

QUANTIFICATION OF SIMULATION QUALITY

Figure 3 visualizes a comparison between the experimental data and the corresponding simulation. Although such a visual comparison gives a good impression of whether or not the model matches the measured data, an objective quantification of such a comparison is preferred. But how can we quantify this comparison?

In classical regression analysis, F is a statistical parameter often used to check whether or not a fitted regression is good. It can be expressed[25] by equation (3).

$$F = \frac{MS_L}{S_e^{\,2}} \tag{3}$$

Where MS_L is the mean square due to lack of fit, and S_e^2 the mean square due to pure error. In Figure 3, individual lack of fit and pure error are schematically illustrated.

In general, the residual between the regression model and the actual data can be seen to consist of two parts: the pure error in the actual data and the lack of fit from the model.

$$Y_j - \hat{Y}_j = (Y_j - E_j) - (\hat{Y}_j - E_j) \tag{4}$$

Here Y_j is the observation, E_j the mathematical expectation, and $\hat{Y}_j$ the prediction. For regression, the square of both sides and summation over all data will give the following expression:

$$\sum (Y_j - \hat{Y}_j)^2 = \sum (Y_j - E_j)^2 - \sum (\hat{Y}_j - E_j)^2 \tag{5}$$

The cross product vanishes in the summation. The left side of equation (5) is the residual sum of squares; the first term on the right side is the pure error sum of squares. The remainder is called lack of fit sum of squares. If two of these three terms are known, then F can be determined. Since the compartment model is different from a regression model, a modification is needed to use the above method for checking whether or not the model predicts well.
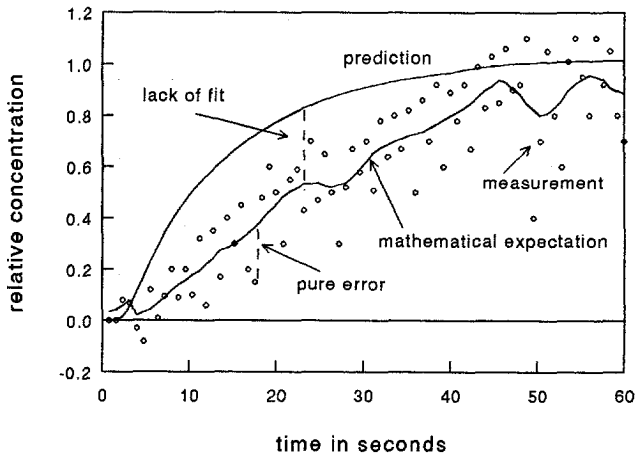
Figure 3. General comparison of experimental data and corresponding simulation.

From response curves, the residual sum of squares (the left-hand term in equation (5)) can easily be obtained. The other terms are unknown. However, the pure error sum of squares can be estimated by using the actual data from the pseudo steady state, assuming the pure error to be distributed equally over the whole curve. It should be noted that the averaged bias between model prediction and experimental data is not likely to be zero. The influence of this bias on F can be partly removed by subtracting the bias from each residual. In addition, the sensitive part of the response curve is located before the moment when homogeneity has been reached. Therefore, the calculation of F will be based on the data from 0 to 99% homogeneity.

MODEL

Flow pattern

The structure of a desired physical model should depend on the flow pattern that the model is to describe. The flow pattern is normally a function of geometry. For a stirred vessel with a single disk turbine, Figure 4a gives the general flow pattern. However the situation becomes more complicated when multiple impellers are introduced into the system. Different flow patterns may occur depending on the geometry and operating conditions. Especially, the clearance between the impellers has a strong influence. In the literature only a few publications could be found on this subject.
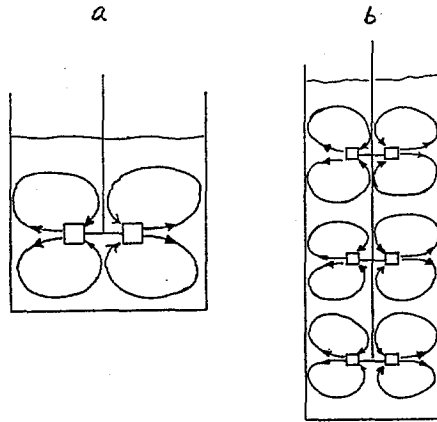
Figure 4. (a) Flow pattern in a single-phase and single-impeller system. (b) Flow pattern in a singlephase and multi-impeller system.

When the impeller spacing is greater than 1.5 times the impeller diameter, the two independent flow patterns are generated by two impellers[26]. It is stated that for unaerated as well as aerated conditions, an impeller spacing of two to three times the impeller diameter will maximize the total power draw and the potential for oxygen transfer[9]. In a study on the effect of impeller spacing on the flow patterns and mixing times in a stirred vessel[8], three different flow patterns, parallel flow, merging flow, and diverging flow, were observed for different spacings. The flows from two impellers were nearly horizontal and parallel (parallel flow) when the spacing between the two impellers was roughly larger than 1.2 times the impeller diameter.

The impeller spacing in fermenters is usually larger than 1.2-1.5 times the impeller diameter and therefore a parallel flow pattern can be expected. Figure 4b presents this common flow pattern. In this example one can distinguish three 'stages', one around each impeller.

Physical structure of the model

The impeller spacing of the studied vessel is larger than twice the impeller diameter. This means that the parallel flow pattern is dominant which is also the case in the industrial vessels with multiple Rushton impellers. Based on this parallel flow pattern, a compartment model was developed. The schematic structure for the *i-th* impeller of this model is depicted in Figure 5.
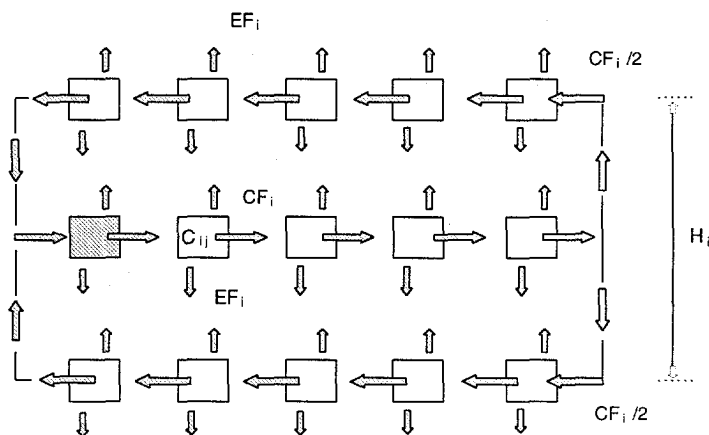
Figure 5. Schematic structure of compartments around the i-th impeller.

The volumes of all compartments are taken as equal. One compartment is located in the impeller region. Two circulation loops, upper and bottom, are formed per impeller, which corresponds to the flow pattern in Figure 4a. The circulation loops are modelled as ideal mixed tanks-in-series with axial exchange. In Figure 5, CF_i is the circulation flow rate, EF the axial exchange flow rate between the stream layers, C_{ij} the concentration of tracer, i the stage-number or impeller number (the upward and downward loop together form one stage for each impeller), j the number of compartments per stage, H_i the axial distance between impellers. The exchange flow rate, EF, occurs both within the stage and between the stages. It is logical that axial mass exchange will occur as long as the flow layers contact each other. However, in the literature[21, 27, 28], the axial exchange within a stage is often neglected or described by radial mixing. Actually, EF cannot be equivalently described by means of radial back mixing or by changing the number of tanks in series.

Based on mass balances, the governing equations can now be derived. Numerical calculation of the system with any number of impellers can be done by means of a simulation program such as **Psi-C** (**Psi** was originally developed at the TU Delft and is now sold by BOZA, Nuenen, the Netherlands).

Determination of parameters

For unaerated conditions, the model contains three parameters, the circulation flow rate (CF), the exchange flow rate (EF), and the number of compartments (N).

Circulation flow

From a theoretical point of view, the circulation flow should be calculated by integrating the radial-velocity profile and multiplying this with the corresponding area. Lacking any experimental data, it can be determined from the discharge flow rate. Equation (6) presents a correlation[29] for calculating the impeller discharge flow rate under ungassed conditions:

$$Q_p = K_p N D^3 \qquad K_p = 0.75 \pm 0.15 \qquad (6)$$

Equation 7 is given to estimate K_p by taking into account the effect of impeller geometry[30]:

$$K_p = 6.2 \left(\frac{D_h}{D}\right) \left(\frac{D}{T}\right)^{0.3} \qquad (7)$$

The circulation flow rate (*CF*) is usually considered to be twice the impeller pumping capacity at the front of the impeller[2, 20]. In this model, *CF* is considered constant in the radial direction as a simplification although part of the circulation stream follows a short path in the whole loop. Therefore, the averaged circulation flow rate in the whole path should be used. Here, the averaged *CF* is assumed to be 80% of that given by doubling equation (6). That means that *CF* can be calculated from equation (8) and K_c ($K_c = 0.8 \times 2 \times K_p$) is 1.2 for the standard geometry.

$$CF = K_c N D^3 \qquad (8)$$

Exchange Flow

The exchange flow rate (*EF*) describes the intensity of exchange flow between vicinal compartments in the axial direction. The flow in a stirred vessel is commonly considered to be isotropic turbulent. For isotropic turbulent flow, the root mean square fluctuation velocity (*rms*) of energy-containing eddies can be calculated[31] by equation (9).

$$\tilde{u}' = (\epsilon l_e)^{1/3} \qquad (9)$$

Where ϵ is the specific power dissipation, l_e the length of energy-containing eddies and $l_e \approx 0.08D$, and $\tilde{u}'$ the root mean square fluctuation velocity (*rms*). ϵ is defined as equation (10).

$$\epsilon = \frac{\rho N_p N^3 D^5}{\pi \left(\frac{T}{2}\right)^2 H_i \rho} \qquad (10)$$

N_p: power number (5-6), *N*: stirrer speed, *D*: diameter of impeller, *T*: diameter of tank, H_i: individual height of working volume for each impeller.

Since we assume the flow to be isotropic turbulent, then

$$\tilde{u}_z^{\,\prime} \sim \tilde{u}^{\,\prime} \qquad (11)$$

Here, $\tilde{u}_z^{\,\prime}$ is the root mean square fluctuation velocity (*rms*) in axial direction. The combination of equation (9) with equation (10) and equation (11) gives equation (12). $K_z^{\prime}$ is a constant.

$$\tilde{u}_z^{\,\prime} = \frac{K_z^{\prime} N_p^{\,1/3} N D^2}{(T^2 H_i)^{1/3}} \qquad (12)$$

EF should be proportional to the axial turbulent velocity $(\tilde{u}_z^{\,\prime})$ and the contact area between the concerned streams. This means, with $K_z = \pi K_z^{\prime} N_p^{1/3}/4$

$$EF = \tilde{u}_z^{\,\prime} \pi \left(\frac{T}{2}\right)^2 = K_z N D^3 \left[\left(\frac{T}{D}\right)^{4/3} \left(\frac{H_i}{D}\right)^{-1/3}\right] \qquad (13)$$

or

$$EF = K_E N D^3 \qquad (14)$$

K_E is a fraction coefficient of the flow in axial direction induced by an impeller and it is a function of geometry, power number, and K_z. From equation (13), we see that *EF* is proportional to the pumping capacity and the dimensionless geometry factor of a stirred tank. Increasing the height of the working medium per impeller will reduce the *EF* because of a lower *rms*. On the other hand, a larger diameter of the tank will raise *EF* since the exchange area becomes larger.

Some measurements of the axial exchange flow rate have been reported in the literature[20,32,33]. By means of magnetic particles used as flow-follower, the exchange flow frequency between two stages was determined[32]. From the experimental results, it was concluded that the ratio of exchange flow rate to circulation flow rate is independent of the power consumption. The exchange flow rate was found to be a function of pumping capacity[20]. This is in agreement with equation (13). Based on the results[20, 32], K_E in equation (14) equals 0.59 for the ungassed case. If we assume that this fraction coefficient is correct, K_z in equation (13) will be 0.1747. EF_i in Figure 5 is $EF/5$.

PARAMETER SENSITIVITY ANALYSIS

Number of compartments per impeller stage

In general, the number of compartments is a function of backmixing. For the circulation flow

to be close to plug flow, a large number of compartments should be used. However, the effect of the number of the compartments is reduced due to the existence of exchange flow. In the above calculations, 15 compartments for each impeller stage were chosen. Here, the effect of this number on the simulation will be discussed.
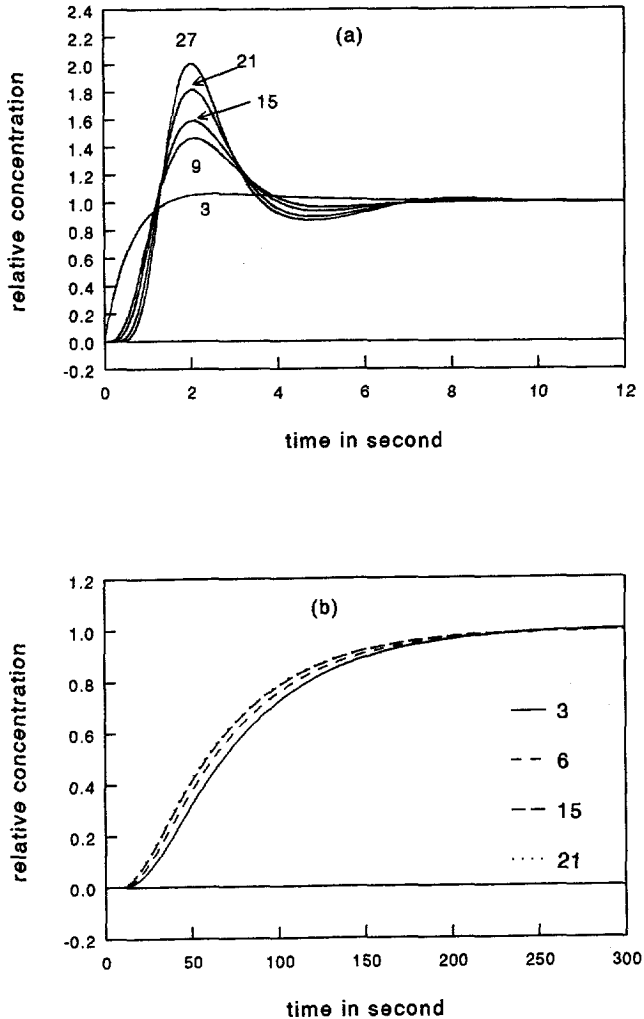

Figure 6. (a) Simulated pulse response curves of the model with different number of compartments in a single-impeller system. (b) Simulated pulse response curves with different number of compartments in a 4-impeller system.

Figure 6a and 6b show the results from the simulations using different numbers of compartments. From the figures it is clear that:

(1) For one impeller systems, the overshoot of the pulse-response curve becomes less with a decreasing number of compartments.

(2) For multi-impeller systems, a decreasing number of compartments gives a slightly slower response curve.

This tendency is easy to understand because more compartments mean less backmixing. However, the magnitude of this difference is less than expected. This can be explained as follows: For multi-impeller systems with the given circulation flow rate, the response-curves are mainly dominated by the axial exchange flow rate. Multiple stages will work as a filter, so that the effect of the number of compartments per stage becomes less visible. This does not mean that only three compartments should be used. One of the possible applications of the compartment model is to simulate the variations of process variables in different parts of the bioreactor. Radial distribution of mechanical stress, oxygen concentration, and other nutrients are often expected. This can become a serious problem in production scale fermenters with a high viscous broth or with non-Newtonian media. Therefore, the model to be developed should contain at least six compartments (see Figure 5). In addition, the response curve of one-impeller systems often shows an overshoot which cannot be simulated by three compartments. Roughly, the number of compartments should be 9 or more to simulate the distribution in radial directions. The proper number of compartments depends on the distribution of the concerned variables.

Exchange flow

The exchange flow rate is a very important parameter for a system with multiple impellers because it describes the extent of segregation between stages. In this work, it is calculated from equation (13). The coefficient in equation (13) is based on literature data[20, 28]. Information on the effect of this parameter will be helpful for understanding its use. Figure 7a presents the calculated response curves using different coefficients for the exchange flow.

From the figure, it is clear that K_z is a very sensitive parameter in the model. When K_z is increased, the response becomes faster which means less segregation. Otherwise, the response will be slower and in the extreme case of $K_z = 0$, the mixing time becomes infinite.

MODEL CALCULATION

The numerical calculation of the developed compartment model has been implemented in Psi-C. In the simulation, 15 compartments are used for each impeller stage of standard geometry

and K_z, the coefficient of exchange flow rate in equation (13), is taken to be 0.1747, based on the reported data[20, 28]. The circulation flow is then calculated using equation (8).
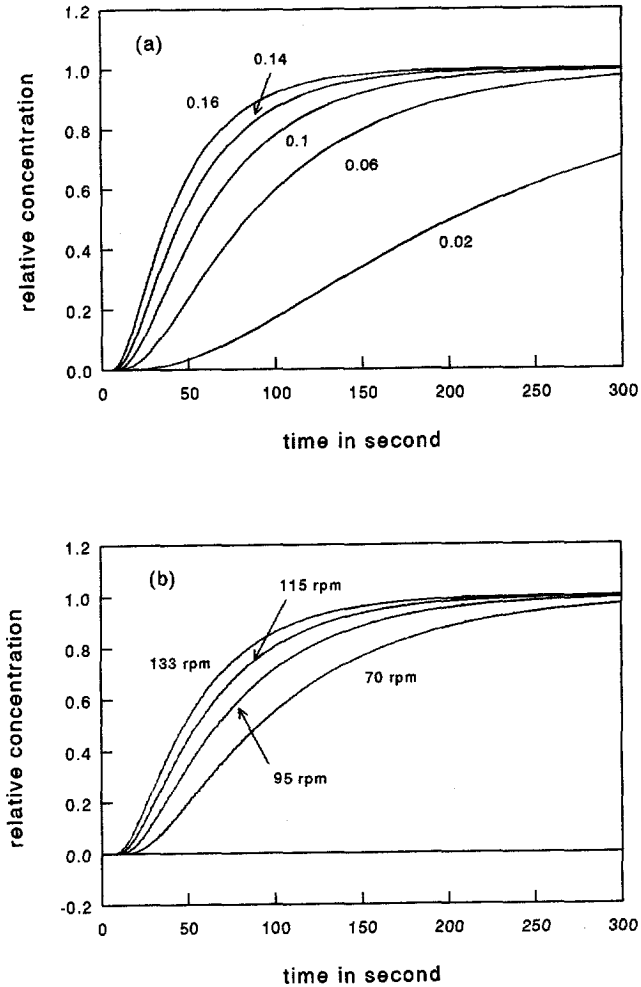

Figure 7. (a) Simulated pulse response curves with different coefficients of the exchange flow (K_z) in a 4-impeller system. (b) Predicted relative concentration of tracer at bottom with different stirrer speeds. The operating conditions: N = 70-115 rpm; V = 22.4 m^3; 4-stirrers.

Effect of stirrer speed

By changing the rotation speed, which is an input parameter in the model, the pulse-response curves at different stirrer speeds can be obtained. Figure 7b presents the calculated change of tracer concentration with time for four different stirrer speeds. From Fig.7b we see thatthe pulse response and mixing become quicker with increasing stirrer speed.

Effect of the number of impellers

Based on the parallel flow pattern in stirred vessels with multiple impellers, the number of impellers should have an obvious influence on the overall mixing behaviour of the system. It is very important to know quantitatively the influence of the number of impellers on the mixing behaviour of the stirred reactor. This can easily be obtained from the model. Figure 8 shows the pulse-response curves in reactors which have 1, 2, 3 and 4 impellers, respectively. It is clear that according to the model calculations, the mixing in a multi-impeller system is much worse than that in a single-impeller one.
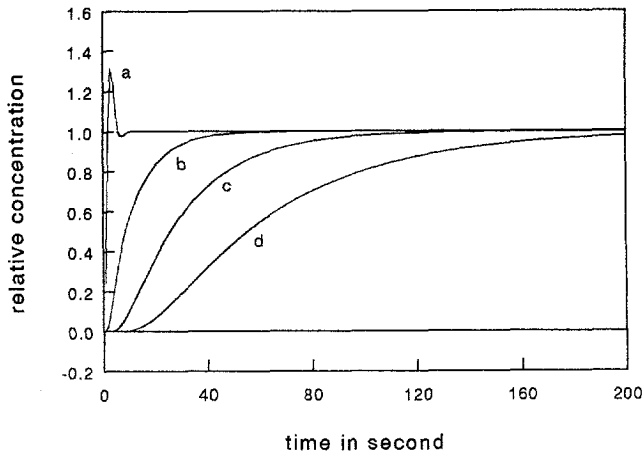
Figure 8. Predicted relative concentration of tracer at bottom. The number of used impellers is varied. The working volume per impeller is constant. Operating conditions: N = 115 rpm; Curve a: 1 stirrer and 5.4 m³; b: 2 stirrers and 10.8 m³; c: 3 stirrers and 15.8 m³; d: 4 stirrers and 22.4 m³.

Effect of clearance between impellers

It is logical that the mixing behaviour of a bioreactor will change when the specific power input is reduced. This can be done in two ways. One way is to reduce the stirrer speed. This has been demonstrated above. Another way is by increasing the distance between the

impellers. Some extreme cases have been calculated by doubling the working volume per impeller. Figure 9a gives the simulated pulse response curves for two such systems. From this graph, one can see that the doubled clearance improves the mixing.
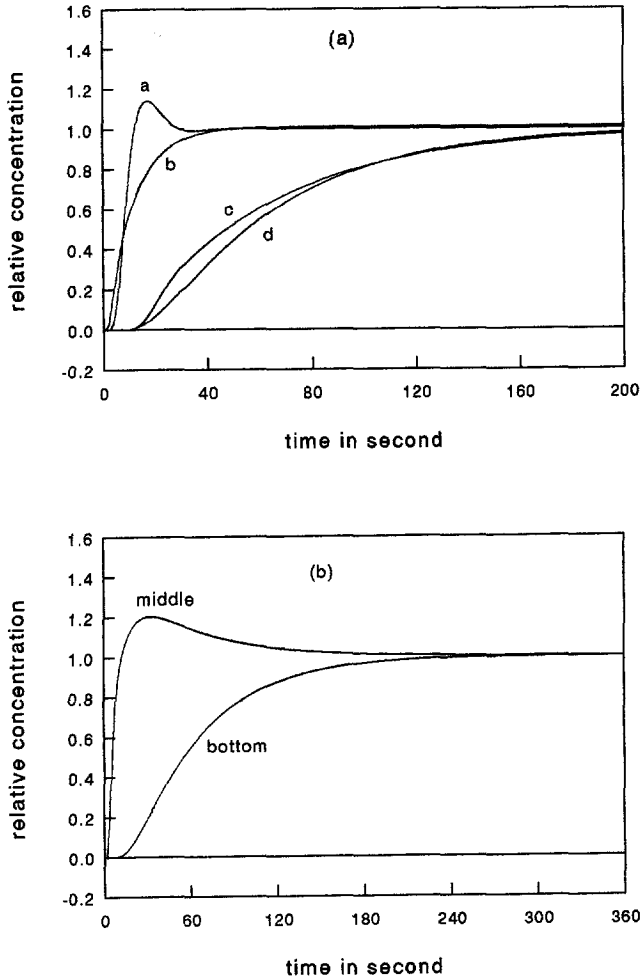
Figure 9. (a) Predicted relative concentration of tracer at bottom. Curve a is for 10.8 m³ of working volume and one stirrer, b for 10.8 m³ of working volume and two stirrers, c for 22.4 m³ of working volume and two stirrers, d for 22.4 m³ of working volume and four stirrers. The operating conditions: N = 115 rpm. (b) Predicted relative concentration of tracer at bottom and middle. The operating conditions: N = 115 rpm; V = 22.4 m³; 4 stirrers.

Effect of location of detection

The model can also be used to simulate the response of the tracer concentration at different location. The simulated pulse-response curves for the middle and the bottom of the reactor are depicted in Figure 9b.

COMPARISON OF MODEL CALCULATIONS AND EXPERIMENTAL RESULTS

Pulse-response curves have been measured in a stirred vessel with several different geometries and under different operating conditions. Corresponding dimensions and operating conditions are given in Table I and II, respectively. To check whether the model matches the experimental results and to study the mixing behaviour of multi-impeller reactors, these measured data will be compared with calculated curves.

Figure 10. Predicted and measured relative concentration of tracer at bottom. The operating conditions: N = 70 and 115 rpm; V = 22.4 m^3, 4 stirrers.

Figure 10 compares pulse response curves in a 22 m^3 fermenter with four impellers at 115 rpm and 70 rpm . The F value (see equation (3)), which is a statistical parameter that gives an indication of how much the measured and calculated curves match, is given in Table II for all comparisons. The smaller the F value, the better the curves match. From Figure 10, it can be seen that the calculated curves are very close to the experimental data. In the measured pulse-response curves, the lag time is about 20 second for the stirrer speed of 70 rpm and

about 15 second for 115 rpm. The curves calculated by the model give almost the same lag time as the measured one, respectively. Besides that, Figure 10 and Table II show that the model is able to predict the pulse-response curves of a multi-impeller stirred tanks with different stirrer speeds.

The effect of the number of impellers on the mixing behaviour of stirred vessels has also been studied experimentally. The number was varied by filling the vessel to different levels. The experimental and calculated pulse-response curves for one and two-impeller systems are shown in Figure 11. The pulse-response curve of one-impeller system had an overshoot. The overshoot predicted by the model started at almost the same time as the measured one. But its magnitude is lower than that of the measured one. This can actually be improved by increasing the number of the used compartments as has been discussed before (see Figure 6a). But more compartments mean longer calculation time. From Figure 11 and Table II, it can be seen that although the visual comparison for the one-impeller tank looks reasonable, it corresponds with the highest F-value in the table. This gives a feeling for the F-value and in general we can say that the calculations match the measured data well. Both model and measurement indicate that the overall mixing behaviour gets worse by increasing the number of impellers.
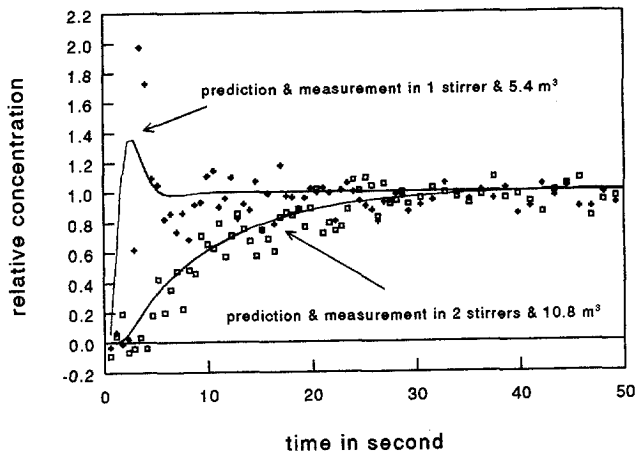
Figure 11. Predicted and measured relative concentration of tracer at bottom. The operating conditions: N = 115 rpm; 5.4 m^3 and 1 stirrer or 10.8 m^3 and 2 stirrers.
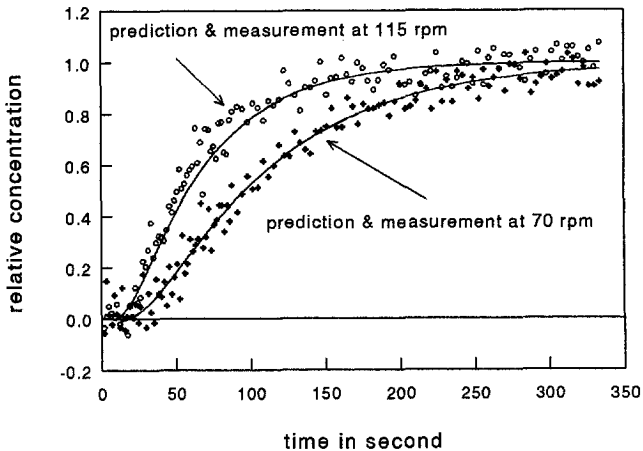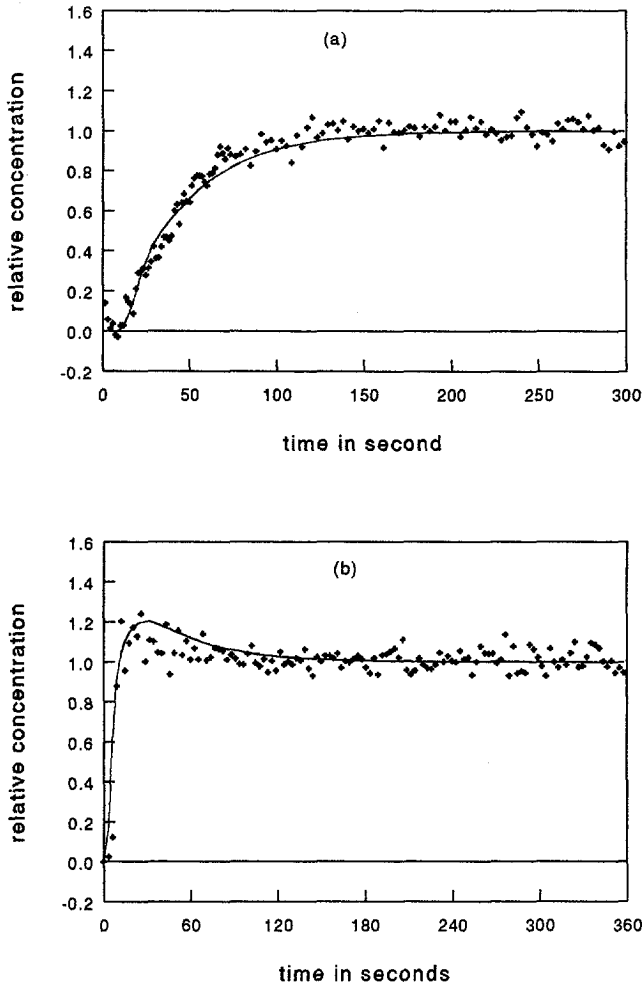
Figure 12. (a) Predicted and measured relative concentration of tracer at bottom. The operating conditions: N = 115 rpm; V = 22.4 m³, 2 stirrers. (b) Predicted and measured relative concentration of tracer at bottom. The operating conditions: N = 115 rpm; V = 22.4 m³, 4 stirrers.

According to the model calculations, a doubled clearance between the impellers improve the overall mixing behaviour. The relevant experiments have been performed by removing every second impeller. The data obtained in this way and the curve predicted by the model are given in Figure 12a. The predictions are quite close to the actual pulse-response data. If we compare Figure 12a with Figure 10 and Figure 9a, we will find that the doubled clearance

indeed improves the overall mixing behaviour of the stirred vessel. This means that extra impellers in industrial reactors do not improve the mixing, but mainly contribute to the mass transfer between the phases.

After relocating the optical detector halfway up the reactor height, another pulse-response curve was measured. Because this detection point is much closer to the injection position than the detection point at the bottom, the pulse-response curve is expected to be different. This can be simulated by monitoring the pulse response in the corresponding compartment in the multi-compartment model. The experimental data and their prediction are given in Fig.12b. The comparison shows that the simulation describes the measured pulse-response curve well.

Comparison of mixing time

The mixing time can be obtained by processing the measured pulse-response data. Based on the common shape of these curves, equation (15) is chosen to fit the experimental data.

$$C(t) = \alpha_1 (1 + \alpha_2 \exp (\alpha_3 t) \cos (\alpha_4 t + \alpha_5)) \tag{15}$$

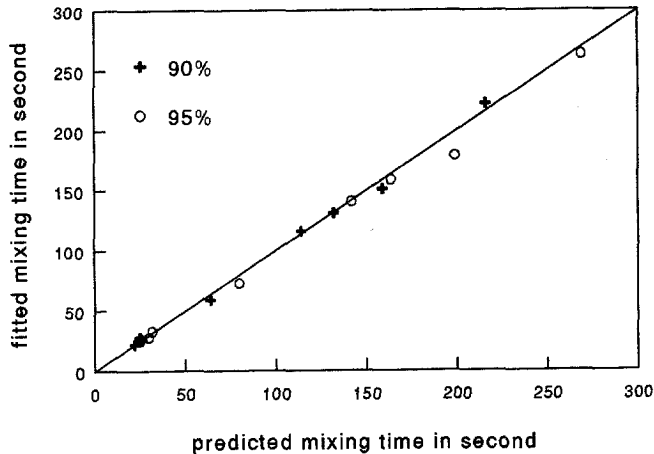Where α_k are the parameters which can be estimated using a fitting program.

Figure 13. Predicted and fitted mixing times by using 90% and 95% homogeneity as criteria. The operating conditions: N = 70-133 rpm; V = 5.4-22.4 m³, 1-4 stirrers.

The mixing times obtained from the fitted curves are compared with those coming from the model in a parity plot, given in Figure 13. It is clear that the simulation results are close to those obtained from fitting the experimental data. Based on these mixing times, $Nt_{95\%}$ has been calculated. For the same geometry, $Nt_{95\%}$ is constant for both predictions and measurements. But it varies with the change of the geometry.

CONCLUSIONS

For single phase flow, the mixing behaviour of several geometries of a large scale bioreactor is successfully predicted by the developed multi-compartment model. This holds for the pulse-response curves determined under very diverse situations, such as different number of impellers, working volume, detection positions, stirrer speeds, and clearance between the impellers. This certifies the good performance of the model. It is important to stress that no fitted parameters were used in these predictions. The application of this model is considered very promising. Further work is intended to quantify the aeration effect on the mixing behaviour in a large reactor with different number of impellers.

List of symbols

B:	width of baffle	m
C:	coefficient of equation 2	-
C_i:	distance between impellers	m
C_{ij}:	concentration of tracer	ppm
CF:	circulation flow rate	$m^3\ s^{-1}$
D:	diameter of impeller	m
D_h:	height of impeller blade	m
D_L:	length of impeller blade	m
E_j:	mathematical expectation at compartment j	-
EF:	exchange flow rate	$m^3\ s^{-1}$
F:	statistical parameter	-
H:	height of working medium in tank	m
H_i:	height of working medium for each individual impeller	m
K_c:	coefficient of circulation flow capacity	-
K_E:	ratio of exchange flow to circulation flow	-
K_Z:	coefficient of exchange flow capacity	-

K_P: coefficient of pumping capacity   -

l_e: eddy length of energy-containing eddies   m

MS_L: mean square due to lack of fit   -

N: rotation speed of impeller s^{-1}

N_p: power number   -

N_s: number of impellers   -

P: power input per volume   W m^{-3}

Q_P: pumping capacity of impeller   m^3 s^{-1}

Re: Reynolds number ($Re = uD\rho/\mu$)   -

S_e^2: mean square due to pure error   -

t: time   s

T: tank diameter   m

t_m: mixing time   s

V: working volume of tank   m^3

Y: axial distance between impeller and compartment   m

Y_j: sample observation   -

$\hat{Y}_j$: prediction.   -

α: parameter of fitting function   -

μ: viscosity   Pa.s

ρ: fluid density   kg m^{-3}

ϵ: specific energy dissipation   W kg^{-1}

Subscripts

i: number of stage   -

j: number of compartment   -

k: number of parameter in fitting function   -

REFERENCES

1. Brennan, D.J., Lehrer, I.H., 1976. Impeller mixing in vessels: experimental studies on the influence of some parameters and the formulation of a general mixing time equation, Trans. Inst. Chem. Engrs. **54**:139-152;

2. Van 't Riet, K., and Tramper, J. 1991. Basic Bioreactor Design, Marcel Dekker, New York, p. 190.

3. Sweere, A.P.J., Luyben,K.Ch.A.M., Kossen, N.W.F., 1987. Regime analysis and scale-down: tools to investigate the performance of bioreactors, Enzyme.Micro Technol., **9**:386-

397

4. Warmoeskerken, M., 1986. Gas-liquid dispersing characteristics of turbine agitators, Ph.D. thesis, Technical University of Delft, the Netherlands.

5. Einsele, A. and Finn, R.K., 1980. Influence of gas flow rates and gas hold up on blending efficiency in stirred tanks, Ind. Eng. Chem. Proc. Des. Dev., **19**:600-603

6. Pedersen, A.G., Nielsen, J., Villadsen, J., 1994. Characterization of bioreactors using isotope tracer techniques, Proc. 6th European Congress on Biotechnology, Elsevier Science B.V., p. 931-934.

7. Groen, D.J., 1994. Macromixing in Bioreactors, Ph.D. thesis, Technical University of Delft, the Netherlands.

8. Mahmoudi, S.M., Yianneskis, M., 1991. The variation of flow pattern and mixing time with impeller spacing in stirred vessels with two Rushton impellers, Proc. of 7th Europ.Conf. On Mixing, Brugge, Belgium 18-20th Sept., p. 17-24

9. Hudcova, V., Machon, V., Nienow, A.W., 1989. Gas-liquid dispersion with dual Rushton turbine impellers, Biotechnol. Bioeng., **34**:617-628.

10. Griot, M., Saner, U., Heinzle, E., Dunn, I.J., Bourne,J.R., 1988. Experiments with an oxygen-sensitive culture for fermenter scale-up, Proc. 2th International Conference on Bioreactor Fluid Dynamics, Cambridge, England: 21-23th Sept., p. 17-35

11. Oosterhuis, N.M.G., 1984. Scale-up of bioreactor: a scale-down approach, Ph.D. thesis, Technical University of Delft, the Netherlands.

12. Bakker, A., 1992. Hydrodynamics of stirred gas-liquid dispersions, Ph.D. thesis, Technical University of Delft, the Netherlands.

13. Hjertager, B.H., Morud, K, 1993. Computational fluid dynamics simulation of bioreactors, Proc. of Bioreactor performance, 15-17th March, Helsingør, Denmark, p.47-61.

14. Kresta, S.M., Wood, P.E., 1991. Prediction of the three-dimensional turbulent flow in stirred tanks, AIChE Journal, **37**:448-460.

15. Ranade, V.V., Joshi, J.B., 1990. Flow generated by a disc turbine: part 2 Mathematical

modelling and comparison with experimental data, Trans IChemE, **68**:34-50.

16. Lou, J.Y., Gosman, A.D., Issa, R.I., Middleton, J.C., Fitzgerald, M.K., 1993. Full flow field computation of mixing in baffled stirred vessels, Trans IChemE, **71**:342-344.

17. Noorman, J.H., 1993. CFD modelling and verification of flow and conversion in a 1m³ bioreactor, Proc. of 3th International Conference on Bioreactor & Bioprocess Fluid Dynamics, Cambridge, UK, on 14-16th Sept.

18. Smith, T.J., Rielly, C.D., 1988. Predictions of the flow in fermenters and the implication for scale-up, Proc. of 2th international Conference on Bioreactor Fluid Dynamics, Cambridge,England, 21-23th Sept., p. 431-441

19. Trägårdh, Ch., 1993. Scale-up using integrated models, Proc. of Bioreactor Performance, 15-17th March, Helsingør, Denmark. p. 221-231,

20. Alves, S.S., Jorge, M.T. Vasconcelos, 1993. Mixing and oxygen transfer in aerated tanks agitated by multiple impellers, Proc. of Bioreactor and Bioprocess Fluid Dynamics, Cambridge, UK, on 14-16th Sept., p:3-14.

21. Mayr, B., Horvat, P., Nagy, E., Moser, A., 1993. Mixing-models applied to industrial batch bioreactors, Bioprocess Engineering, **9**:1-12;

22. Mann, R., Mavros, P., 1982. Analysis of unsteady tracer dispersion and mixing in a stirred vessel using interconnected net works of ideal flow zones, 4th European Conference on mixing, 27-29th April, BHRA Fluid Engineering, Cranfield, England, B3: 35-47.

23. Reuss, M., Jenne, M., 1993. Compartment models, Conference on Bioreactor performance, Helsingør, Denmark, 15-17th March, p. 63-75.

24. Sinclair, C.G., Brown,D.E., 1970. Effect of incomplete mixing on the analysis of the static behaviour of continuous cultures, Biotech. Bioeng., **12**:1001-1017.

25. Draper, N.R., Smith, H., 1981. Applied Regression Analysis, Jonn Wiley & Sons, New York.

26. Mishra, R.V., Joshi, J.B., 1994. Flow generated by a disc turbine, Part IV:multiple impellers, Trans IChemE, **72**:657-668.

27. Nagy, E., Mayr, B., Moser, A., 1994. Bioprocess scale-up using a structured mixing model., Computers Chem. Engng., Suppl., **18**:663-667

28. Singh, V., Fuche, R., Constantinides, A., 1987. A new method for fermentation scale-up incorporating both mixing and mass transfer effects, Biotechnology Processes on Scale-up and Mixing, Edited by Chester S. Ho and J. Oldshue, p. 200-214.

29. Revill, B.K., 1982. Pumping capacity of disc turbine agitators-a literature review, 4th European Conference on Mixing, BHRA, Fluid Engineering, 24 April, B1, 11-24

30. Bowen, R.L., Tensco, J., 1986. Unraveling the mysteries of shear-sensitive mixing systems, Chemical Engineering, **9**:56-63.

31. Davies, J.T., 1972. Turbulence Phenomena. p. 62-68, Academic Press, New York, London.

32. Mukataka Sukekuni, Kataoka Hiroshi, and Takahashi Joji, 1981. Circulation time and degree of fluid exchange between upper and lower circulation regions in a stirred vessel with a dual impeller, J.Ferment. Technol., **59**:303-307.

33. Nienow, A.W., Kuboi, R., 1984, A technique for studying intervortex mixing rates in a dual impeller agitated vessel in high viscosity fluids, IChemE Symposium series, **89**:97-106

CHAPTER 3

Local Power Uptake in Gas-Liquid Systems with Single and Multiple Rushton Turbines

Y.Q.Cui, R.G.J.M. van der Lans and K.Ch.A.M.Luyben

Abstract

Prediction of the power uptake of impellers is crucial for a successful scale-up, operation, and design of stirred tank reactors (STR). However, for gas-liquid systems equipped with multiple impellers, commonly used in industry, information on the local power uptake is scarce in literature. For single-impeller stirred vessels, inconsistency between the experimental data on power uptake under gassed conditions and available relations in literature is often reported. In this paper empirical correlations on the local gassed power uptake of impellers are derived both for single-impeller and multi-impeller systems, based on a large body of experimental data from literature. Under gassed conditions the bottom impeller of a multiple impeller configuration or a single impeller draws relatively less power than an impeller in the middle or at the top. The power uptake by impellers in a gassed STR shows two regimes. It is found that middle and top impellers reach their second regime at a much higher gas flow rate than single or bottom impellers under the same conditions.

Keywords: Impeller power uptake, Rushton turbine, Aerated stirred vessel, Multiple impellers, Local power uptake, Impeller hydrodynamics.

INTRODUCTION

Homogenization, dispersion, interphase mass and heat transfer rates, and hydrodynamic stress in mechanically agitated gas-liquid reactors are controlled by power dissipation and gas flow. Accurate estimations of the power input and control of the hydrodynamic regime of an impeller are important factors in the scale-up, operation, and design of such reactors.

The power uptake of an impeller in an ungassed stirred tank reactor (STR) with a Newtonian liquid can be predicted fairly well from the power number. Since the transfer of power from the impeller to the fluid is influenced very much by aeration, the power uptake for the gassed situation is lower than that for the ungassed situation. This reduction in power uptake is due to the formation of cavities behind the blades of a Rushton turbine impeller. Much research has been done on measuring this reduction in various systems under different operating conditions, searching for a relation between the reduction and some physical parameters. Fluid hydrodynamics of two-phase flow in a STR is a relevant subject. Papers in which the above subjects are treated include the articles from Hughmark (1980), Midoux and Charpentier (1984), Michel and Miller (1962), Nagata (1975), Nienow et al. (1977, 1988), Van't Riet and Tramper (1991), Rushton et al. (1950), Smith et al. (1977 and 1993), Warmoeskerken (1986) and Warmoeskerken and Smith (1988).

In literature, the correlations from Michel and Miller (1962) and Hughmark (1980) are often used or referred to for the estimation of the gassed power reduction. In the review paper of Midoux and Charpentier (1984), the correlation from Michel and Miller (1962) is recommended for estimating the gassed power uptake by impellers. Similar correlations have been presented by Loiseau et al. (1977), Pharamond et al. (1975) and Masami et al. (1991). Van 't Riet and Tramper (1991) stated that the correlation from Michel and Miller was not proper since not all the variables were varied enough. The correlation of Michel and Miller is considered to be applicable in a limited range (Nagata 1975).

Hughmark (1980) presented Eq.1 which was based on 391 data points for a turbine stirrer including those of Michel and Miller (1962).

$$\frac{P_g}{P_u} = 0.1 \left(\frac{Q_g}{NV}\right)^{-0.25} \left(\frac{N^2 D^4}{g D_i V^{2/3}}\right)^{-0.2} \tag{1}$$

The average absolute deviation between calculated and experimental values was 0.117. Although such a deviation is rather high, this correlation is considered to be quite good (Hughmark 1980, Van 't Riet and Tramper 1991) since accurate power uptake measurements are rather difficult to perform (Nienow et al. 1977). However, Koloini et al. (1989) reported that Hughmark's correlation predicted systematically higher values for the power uptake compared to their experimental data (T=0.33 m, D=0.1 m, H=0.33 m, C=0.11 m). Warmoeskerken (1986) has compared his data with the correlations from both Michel and Miller and Hughmark. Under his experimental conditions, both relations overestimated the

reduction of the gassed power demand.

Research reported on gassed power uptake in multi-impeller reactors is scarce although such reactors are most commonly used in industry. The correlation obtained from a single impeller system is often applied for multi-impeller systems. For multi-impeller systems, very little experimental data on the power uptake by individual impellers have been published. We only found data from Warmoeskerken and Smith (1988), Nienow et al. (1988) and Hudcova et al. (1989). The data used by the latter two are based on the same measurements. Fig. 1 present the experimental data of bottom, top and middle impellers from Warmoeskerken and Smith (1988). Their results clearly show that the reduction in power uptake by the bottom impeller is much more significant than that of the other impellers. This is commonly explained by the fact that most of the gas from the sparger will go through the bottom impeller, but only part of this gas passes through the other impellers. Up to now, no correlation for the gassed power uptake by the individual impellers in such multi-impeller systems can be found in literature according to our knowledge.
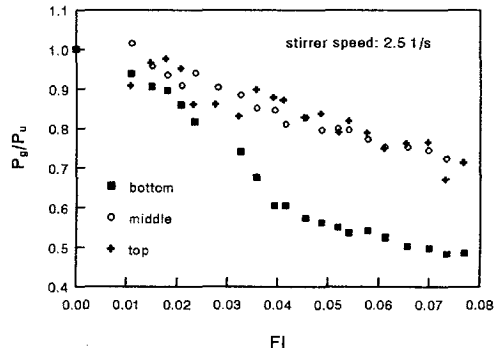

Figure 1. Power uptake by top, middle and bottom impellers in the gassed STR from Warmoeskerken and Smith (1988). [T=0.625m, D=0.256m, H=2.2m, 3 impellers]

DATA ANALYSIS ON POWER REQUIREMENT

A considerable body of data on gassed power uptake especially on single-impeller systems can be found in literature. Most of these data are plotted as a function of dimensionless numbers or groups of variables. Due to this, the extraction of the original data from literature is sometimes difficult. We have extracted 739 data points from literature by scanning and ungraphing. Table 1 gives the sources, the corresponding operating conditions, and geometries of the stirred vessels. Based on those data, an analysis of impeller power uptake was performed. For simplification, the gas volume flow rate is often based on a standard condition of 1 bar and 25 °C in literature. However, the interaction between gas flow and impeller blade should be related with the actual gas volume flow rate. For the data collected in the present study, the local condition is rather close to the standard condition. Therefore, no correction has been taken into account. The power uptake of an impeller in a gassed STR is a function of the physical properties of the working medium as well. Since all the data were determined in water, the effect of the physical properties of the working medium on the reduction of power uptake will not be studied here.

Table 1. The sources, geometry, and operating conditions of the scanned literature data.

source	T (m)	D (m)	H (m)	T/D (-)	Number of Impellers.	N s^{-1}
Bruijn et al. (1974)	0.23*	0.076	0.23	3	1	10
Nagata (1975)	0.585	0.293	0.585	2	1	2.2
Nienow et al. (1977)	0.29	0.143	0.29	2	1	2.3-5.4
Nienow et al. (1977)	0.91	0.303	0.91	3	1	1.7-5
Smith et al. (1977)	1.83	0.915	1.83	2	1	0.917-1.5
Warmoeskerken (1986)	0.44	0.176	0.44	2.5	1	2-8
Warmoeskerken (1986)	1.2	0.48	1.2	2.5	1	1.5-3.5
Warmoeskerken and Smith (1988)	0.64	0.256	2.2	2.5	3	2.5-5
Hudcova et al. (1989)	0.56	0.19	1.12	3	2	2.5-3.25

* Equivalent diameter for the baffled square vessel

Single impeller or bottom impeller

In stirred vessels, the spargers are normally installed below the bottom impeller or the single impeller. Except for the difference in local static pressure, the interaction of gas flow with a rotating single impeller above a sparger should be very similar to that with a bottom impeller of a multiple impeller configuration at different scales. Therefore, the single impeller and bottom impeller are discussed together. For single impellers and bottom impellers, 526 experimental points have been scanned from literature in total. Fig. 2 shows the plots of P_g/P_u against flow number (*Fl*) from Warmoeskerken (1986). These data are measured in a single-impeller vessel with a diameter of 1.2 m. From these curves, we may conclude that the gassed power reductions can vary considerably at the same flow number, which means that the flow number alone is not sufficient to describe the value of P_g/P_u .

The expressions from Hughmark (1980) and Michel and Miller (1962) have a common drawback, being that P_g/P_u does not equal 1 for the ungassed condition. In this study, we have chosen $1-P_g/P_u$ as a function of the gas volume flow rate, the stirrer speed, the diameter of impeller and the diameter of stirred tank. Multiple regression of $1-P_g/P_u$ with the variables Q_g , N, D and T leads to a conclusion that the data can be related as

$$1 - \frac{P_g}{P_u} = f(\frac{Q_g N^{0.25}}{D^2})\tag{2}$$

Based on this correlation, the data in Fig. 2 are replotted in Fig. 3. All data come into one line in Fig. 3. This means that $Q_g N^{0.25} D^{-2}$ correlates these experimental data better than *Fl* does. Eq. 2 does not contain the diameter of the reactor (*T*). The question is whether *T* influences the gassed power uptake of impellers. The correlated data were obtained not only at different scales (diameter:0.23-1.83 m) and under various operating conditions (N:0.9-10 1/s, *Fl*:0-0.23) but also at different *T/D* ratios (3-2) which is in the range commonly used in

practice. No obvious influence has been found. The conclusion is that T/D has no or a very weak effect on P_g/P_u. So it can be neglected from an engineering point of view.
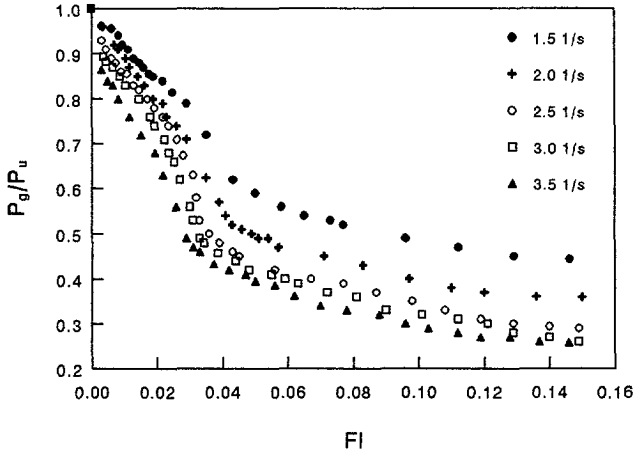

Figure 2. Power uptake by a single impeller in a gassed STR from Warmoeskerken (1986) [T=1.2 m, D=0.48 m, H=T]
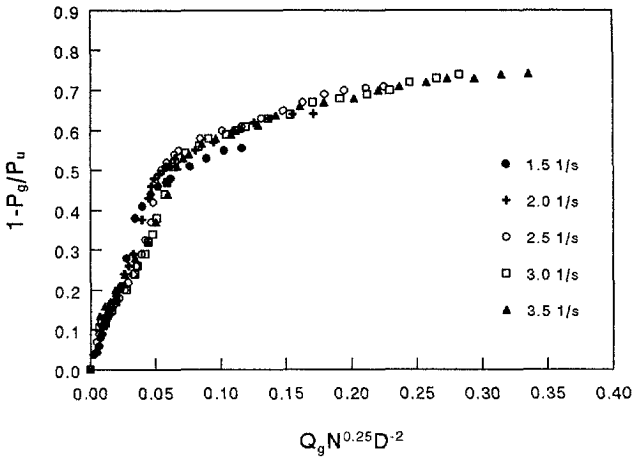

Figure 3. Reduction of power uptake by single impeller in a gassed STR from Warmoeskerken (1986) [T=1.2 m, D=0.48 m, H=D]

Fig. 4 plots the data of $1-P_g/P_u$ from Bruijn et al. (1974), Hudcova et al. (1989), Nagata (1975), Nienow (1977), Smith et al. (1977), Warmoeskerken (1986), Warmoeskerken and Smith (1988) against $Q_g N^{0.25} D^{-2}$. Table 1 gives the used experimental conditions at which these data were measured. Although the geometry of the vessels ($T=0.238$-1.83 m; $D/T=1/3$-$1/2$), stirrer speeds ($N=0.9$-10 s^{-1}), and flow number ($Fl=0$-0.26) change considerably, we see that
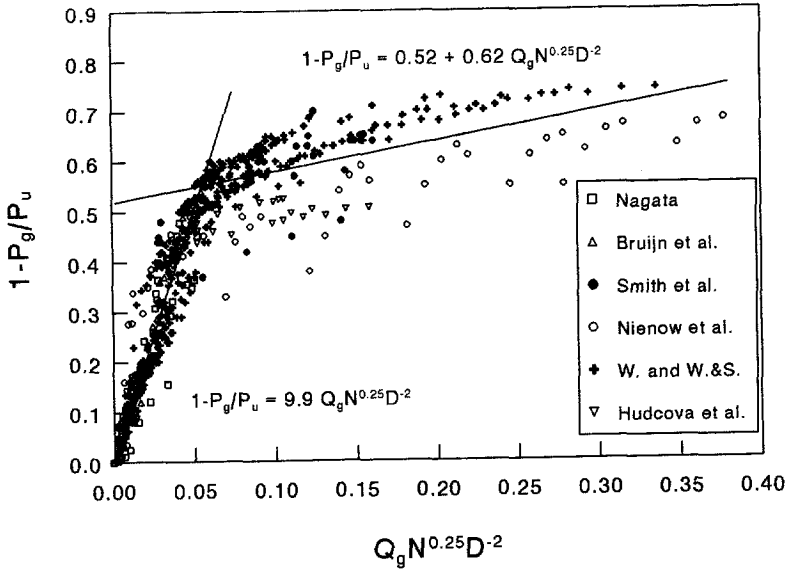

Figure 4. Comparison of Egs. 3 and 4 with the reduction of power uptake of all single and bottom impellers in the gassed STR.

all the data fall approximately into one line in Fig. 4. Therefore it can be concluded that Eq. 2 is indeed a good basic correlation for both single impellers and bottom impellers. The comparison between the data for bottom and single impellers demonstrates that the bottom impeller behaves similar to the single impeller.

From the shape of the cloud of data in Fig.4, one can notice that the data can roughly be divided into two parts. When $Q_g N^{0.25} D^{-2}$ is lower than about 0.055, $1-P_g/P_u$ is approximately a linear function of $Q_g N^{0.25} D^{-2}$ with a steep slope (about 9.9). For $Q_g N^{0.25} D^{-2}$ above 0.055, it can be approximated by a linear function of $Q_g N^{0.25} D^{-2}$ with a much smaller slope (about 0.62). The transection between the two parts occurs at $Q_g N^{0.25} D^{-2} = 0.055$ and $P_g/P_u \approx 0.5$. Assuming that the two parts correspond with two regimes, we call this intersection as a regime transition. For simplicity, the data clouds are now separated and correlated in two

$$\frac{Q_g N^{0.25}}{D^2} \leq 0.055 : \qquad 1 - \frac{P_g}{P_u} = 9.9 \left(\frac{Q_g N^{0.25}}{D^2}\right) \qquad (3)$$

$$\frac{Q_g N^{0.25}}{D^2} > 0.055 : \qquad 1 - \frac{P_g}{P_u} = 0.52 + 0.62 \left(\frac{Q_g N^{0.25}}{D^2}\right) \qquad (4)$$

parts. The obtained correlations are given in Eqs. 3 and 4. For these two correlations, 526 experimental points are used and the relative errors are below 6% for both. Eqs. 3 and 4 are plotted in Fig. 4. The comparison of the actual data with the prediction shows that Eqs .3 and 4 give a rather good estimation for the gassed power uptake although these data were determined under very diverse conditions.

Top impeller and middle impeller

For multi-impeller systems, the individual power uptake by the different impellers can be determined by installing more than one torque meter on the shaft. Results obtained with this approach have been published in literature (see table 1). From Fig. 1, we know that the top and middle impellers behave differently from the bottom impeller. Fig. 5, 7 and 8 presents the gassed power uptake data of the top and middle impellers from Hudcova et al. (1989) and Warmoeskerken and Smith (1988). If one calculates the value of $1 - P_g/P_u$ with Eqs. 3 and 4 and compares with experimental data in Fig. 5, 7 and 8, it will be seen that the reduction of
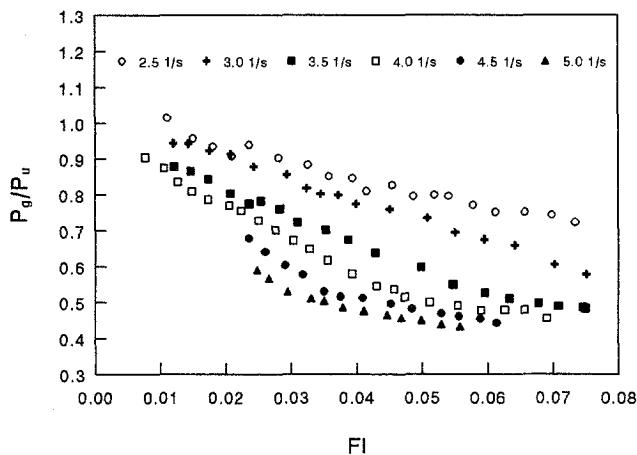

Figure 5. Power uptake by a middle impeller in the gassed STR from Warmoeskerken and Smith (1988) [T=0.625 m, D=0.256 m, H=2.2m, 3 impellers]

power uptake at the bottom impellers is much higher than those at the middle or top impellers under the same operating conditions. This phenomenon was also shown in Fig. 1. Therefore, we may assume that the size of the cavity behind the bottom impeller is larger than that behind the other impellers. It indicates that the way in which the aeration influences the power uptake of the impellers (top, middle and bottom) differs and thus the correlations are supposed also to be different. Based on the distribution of the gas phase, it can be imagined that the reduction in power uptake of the bottom impeller is more directly influenced by air flow and that of the other impellers more by the local gas hold up. P_g/P_u can again be expressed as the function of operating conditions and the geometry of the reactor.
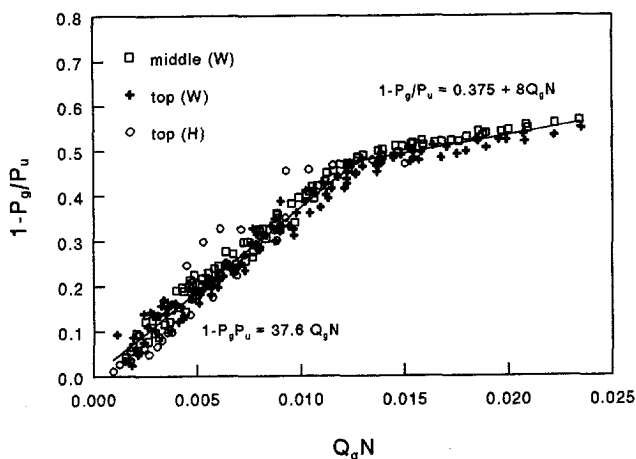
Figure 6. $1-P_g/P_u$ of top and middle impellers as a function of Q_gN from Hudcova et al. (1989) and Warmoeskerken and Smith (1988). See Table.1 for the geometries

Following the same approach that has been used for single and bottom impellers, the multiple regression of $1-P_g/P_u$ against Q_g and N was tried. For both the top and the middle impellers from the work of Warmoeskerken and Smith (1988), $1-P_g/P_u$ was found to be a function of Q_gN.

The question arises why the top impeller behaves the same as the middle one in this respect. If one considers the local conditions of two-phase flow in a STR, one could imagine that except for the difference in static pressures, the interactions between aeration and impeller blade are similar. For the available data, the difference between the static pressures at middle

and top is about 0.064 bar. Comparing such a difference with the operating pressure (1 bar), this can be neglected under the given conditions. In Fig. 6, $1-P_g/P_u$ of top and middle impellers are plotted against $Q_g N$. It is clear that the relative power uptake by the two impellers is identical. Therefore, the top and middle impellers can be treated together.

Fig. 6 shows that the relation of $1-P_g/P_u$ with $Q_g N$ can again be approximated by two linear relations. At the intersection point between the two parts, the value of P_g/P_u is about 0.5 which is almost the same as that for bottom and single impellers. The first part has a steep slope (about 37.6) and the second a small slope (about 8). The regression of $1-P_g/P_u$ for the top and middle impellers against $Q_g N$ gives the intercept and slope of the correlations for the available data ($D=0.256$ m and $T=0.625$ m). Eqs. 5 and 6 show the obtained correlations.

$$Q_g N \leq 0.013 : \qquad 1-\frac{P_g}{P_u}=K_1\,Q_g N \qquad\qquad (5)$$

$$Q_g N > 0.013 : \qquad 1-\frac{P_g}{P_u}=K_2+K_3\,Q_g N \qquad\qquad (6)$$

Where K_1, K_2, and K_3 depend on the geometry of the stirred vessel and equal respectively 37.6, 0.375 and 8 in the case ($D=0.256$ m and $T=0.64$ m). In total, about 213 experimental
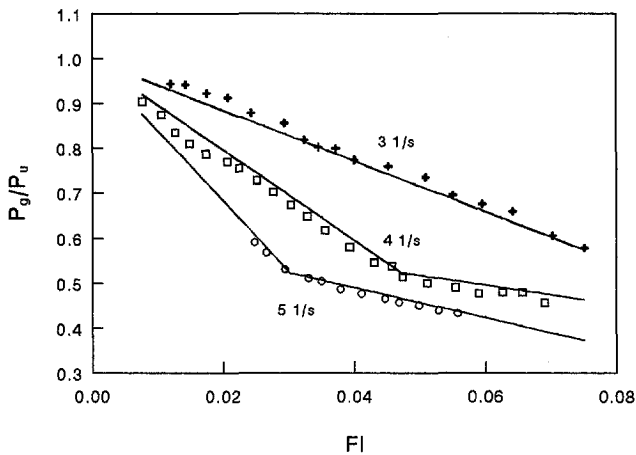

Figure 7. Comparison of Eq.5 and 6 with actual power uptake by middle impeller from Warmoeskerken and Smith (1988) [T=0.625 m, D=0.256 m, H=2.2 m, 3 impellers]

data points have been used. The relative errors are 2.3% for Eq. 5 and 1.4% for Eq. 6. The values according to Eqs. 5 and 6 are given in Fig. 6, 7 and 8 as well. The comparison of the actual data with the curves calculated by using Eqs. 5 and 6 can be seen in Fig. 6, 7 and 8. Clearly, Eqs. 5 and 6 predict the experimental data rather well.
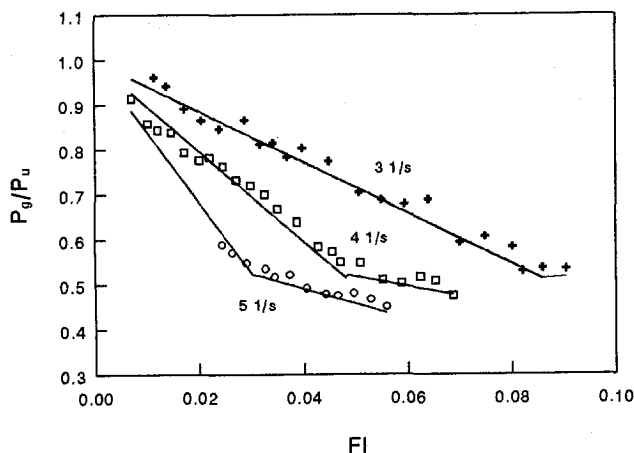

Figure 8. Comparison of Eqs.5 and 6 with actual power uptake by a top impeller from Warmoeskerken and Smith (1988) [T=0.625 m, D=0.256 m, H=2.2 m, 3 impellers]

Eqs. 5 and 6 do not contain geometry parameters. This is because they have been obtained from the data measured in one stirred vessel ($T=0.64$ m, $D=0.256$ m, $H=2.2$ m) only. Extra data from reactors with different geometries are needed for a complete correlation. Unfortunately such data are extremely scarce. One other data set found in literature is from Hudcova et al. (1989) (see Fig. 6). However they claimed that the flooding of both bottom impeller and top impeller occurred at the same time and that the top impeller started flooding even at $P_g/P_u =0.9$-0.85. Based on the common knowledge, the top impeller should be far away from flooding when P_g/P_u ranges from 0.9 to 0.85. Since it is agreed that flooding is related to a certain size or structure of the cavities formed behind impeller blades, such cavities will reduce severely the gassed power consumption drawn by impellers. This means that the accuracy of their measurement may be not very good. Therefore, no attempt has been made to correlate the geometry into Eqs. 5 and 6 using these data. In spite of this, Fig. 6 still gives some idea on how Eqs. 5 and 6 match with these data.

In order to build up the relation between the geometry parameter and the gassed power uptake of the top and middle impeller, measurements of local power uptake under gassed conditions

in multi-impeller systems with a different size of that of Warmoeskerken and Smith (1988) are needed.

Fig. 4 and Fig. 8 show that the transition for the gassed power uptake by impellers always occurs at $P_g/P_u \approx 0.5$, which is independent of the location of the impeller. For the bottom and single impellers the transition can be predicted by $Q_g N^{0.25} D^{-2}$ (see Eqs. 3 and 4) and for the top and middle impellers $Q_g N$ (see Eqs. 5 and 6) should be used. The knowledge of the hydrodynamic characteristics in a gassed STR may be essential for a good quantitative understanding of this transition. In literature, several two-phase flow regimes and various structures of cavities formed behind impeller blades have been reported (Nienow et al., 1977 and Warmoeskerken and Smith, 1988). The comparison of the transition with these reported characteristics in a gassed STR is the subject of a forthcoming publication.

CONCLUSION

The correlations of the local gassed power uptake by impellers have been derived for single and multi-impeller stirred vessels. The bottom impeller shows the same behaviour as a single impeller. Eqs. 3 and 4 describe rather good P_g/P_u of both impellers as a function of operating conditions and impeller geometry. At $Q_g N^{0.25} D^{-2} = 0.055$, a transition occurs from Eq. 3 to Eq. 4.

With respect to the interaction between impeller and gas flow, top and middle impellers behave almost identical to each other. But they are much different from the single and bottom impellers. A relation of $1 - P_g/P_u$ with operating conditions (Q_g and N) has been established. Depending on the value of $Q_g N$ (< 0.013 or > 0.013), Eq. 5 or Eq. 6 should be used for the prediction of the reduction of the power uptake by the top or middle impellers. The geometry effect needs further investigation. Top and middle impellers reach their second regime at a much higher gas flow rate than a single or bottom impeller under the same condition. With respect to the gassd power uptake, the transition between the two regimes occurs at $P_g/P_u \approx 0.5$ and this is independent of the location of the impeller.

Nomenclature

D	:	diameter of impeller	m
D_i	:	impeller blade width	m
C	:	clearance	m
Fl	:	Flow number of an impeller (Q_g/ND^3)	-
Fr	:	impeller Froude number (N^2D/g)	-
g	:	acceleration of gravity	m s^{-2}
H	:	height of reactor	m
N	:	impeller speed	s^{-1}
K_i	:	coefficient in Eq.6 and 7	-

P_g	:	impeller power uptake under gassed condition	W
P_u	:	impeller power uptake under ungassed condition	W
Q_g	:	real local gas volume flow rate	$m^3 \, s^{-1}$
Re	:	Reynolds number $(\rho D^2 N/\mu)$	-
T	:	diameter of stirred vessel	m
V	:	working volume	m^3

Literature

Bruin, W., van't Riet, K. and Smith, J.M., 1974, "Power consumption with aerated Rushton turbines", *Trans. Inst. Chem. Engrs.*, **52**, 88.

Hudcova, V., Machton, V and Nienow, A.W., 1989, "Gas-liquid dispersion with dual Rushton turbine impellers", *Biotechno. Bioeng.*, **34**, 617-628.

Hughmark, A.Gordon, 1980, "Power requirements and interfacial area in gas-liquid turbine agitated systems", *Ind. Eng. Chem. Process Des. Dev.*, **19**, 641-646.

Kipke Klaus, 1978, "Gas Dispersion in non-newtonian liquids", *Proc. Int. Symp. on Mixing*, C5. Mons, Belgium, 21-24 Feb.

Koloini, T., Plazl, I. and Zumer, M., 1989, "Power consumption, gas hold-up and interfacial area in aerated non-Newtonian suspensions in stirred tanks of square cross-section", *Chem. Eng. Res. Des,* **67**, 526-536.

Loiseau, B., Midoux, N. and Charpentier, J.C., 1978, "Some hydrodynamics and power input data in mechanical power requirements of gas-liquid contactors", *A.I.Ch.E. Journal*, **23**, 931.

Michel, B.J. and Miller, S.A., 1962, "Power requirements of gas-liquid agitated systems", *A.I.Ch.E. Journal*, **8**, 262-266.

Midoux, N. and Charpentier, J.C., 1984, "Mechanically agitated gas-liquid reactors. Part 1. Hydrodynamics", *International Chemical Engineering*, **24**, 249-287.

Masami Yasukawa, Masayuki Onodera, Kazuaki Yamagiwa, and Akira Ohkawa, 1991, "Gas holdup, power consumption, and oxygen absorption coefficient in a stirred-tank fermentation under foam control", *Biotechnol. Bioeng.*, **38**, 629-636.

Nagata, S., 1975, "Mixing principle and applications", Kodansha LTD, A Halsted press,

Tokyo.

Nienow, A.W., Liu, H., Wang, H. , Allsford, K.V., Cronin, D., and Hudcova, V., 1988, "The use of large ring spargers to improve the performance of fermenters agitated by single and multiple standard rushton turbines", 2th Int. Conf. on Bioreactor fluid dynamics, Ed. King R. held at Cambridge, England:21-23. September.

Nienow, A.W., Wisdom, D.J. and Middleton, J.C., 1977, "The effect of scale and geometry on flooding, recirculation, and power in gassed stirred vessels", F1. Second European Conf. on Mixing, F6. Cambridge, England, 30th March-1st April.

Pharamond, J.C., Roustan, M. and Roques, H., 1975, Determination de la puissance concommee dans une cuve aeree et agitee, *Chem. Eng. Sci.,* **30**, 907-912.

Ranade, V.R. and Ulbrecht, J., 1977, "Gas Dispersion in agitated viscous inelastic and viscoelastic liquids", Second European Conf. on Mixing, F6. Cambridge, England, 30th March-1st April.

Rushton, J.H., Costich, E.W. and Everett, H.J., 1950, "Power characteristics of mixing impellers", *Chem. Engg. Progr.,* **46**, 395.

Smith, J.M., Van't Riet, K. and Middleton, J.C., 1977, "Scale-up of agitated gas-liquid reactors for mass transfer", F4. Second European Conf. on Mixing, F6. Cambridge, England, 30th March-1st April.

Van't Riet, K. and Tramper,J., 1991, "Basic Bioreactor Design", Marcel Dekker,Inc. New York.

Warmoeskerken, M.M.C.G., 1986, "Gas-Liquid Dispersing characteristics of turbine agitators", Ph.D thesis at TU Delft.

Warmoeskerken, M.M.C.G. and Smith, M.J. 1988, "Impeller loading in multi turbine vessels" 2th Int. Conf. on Bioreactor fluid dynamics, Ed. King R. held at Cambridge, England, 21-23 September.

CHAPTER 4

Effect of Agitation Intensities on Fungal Morphology of Submerged Fermentation

Y.Q.Cui, R.G.J.M. van der Lans and K.Ch.A.M.Luyben

Abstract: Both parallel fermentations with *Aspergillus awamori* (CBS 115.52) and a literature study on several fungi have been carried out to determine a relation between fungal morphology and agitation intensity. The studied parameters include hyphal length, pellet size, surface structure or so-called hairy length of pellets and dry mass per wet pellet volume at different specific energy dissipation rates. The literature data from different strains, different fermenters, and different cultivation conditions can be summarized to say that the main mean hyphal length is proportional to the specific energy dissipation rate according to a power function with an exponent of -0.25 ± 0.08. Fermentations with identical inocula showed that pellet size was also a function of the specific energy dissipation rate and proportional to the specific energy dissipation rate to an exponent of -0.16 ± 0.03. Based on the experimental observations, we propose the following mechanism of pellet damage during submerged cultivation in stirred fermenters. Interaction between mechanical forces and pellets results in the hyphal chip-off from the pellet outer zone instead of the breakup of pellets. By this mechanism, the extension of the hyphae or hair from pellets is restricted so that the size of pellets is related to the specific energy dissipation rate. Hyphae chipped off from pellets contribute free filamentous mycelia and reseed their growth. So the fraction of filamentous mycelial mass in the total biomass is related to the specific energy dissipation rate as well. To describe the surface morphology of pellets, the hyphal length in the outer zone of pellets or the so-called hairy length was measured in this study. A theoretical relation of the hairy length with the specific energy dissipation rate was derived. This relation matched the measured data well. It was found that the porosity of pellets showed an inverse relationship with the specific energy dissipation rate and that the dry biomass per wet pellet volume increased with the specific energy dissipation rates. This means that the tensile strength of pellets increased with the increase of specific energy dissipation rate. The assumption of a constant tensile strength, which is often used in literature, is then not valid for the derivation of the relation between pellet size and specific energy dissipation rate. The fraction of free filamentous mycelia in the total biomass appeared to be a function of the specific energy dissipation in stirred bioreactors.

Keywords: fungal morphology, pellets, hypha, hair of pellets, agitation intensity.

INTRODUCTION

GENERAL ASPECTS

In order to perform a given bioconversion in a fermenter, mass and heat transfer, gas dispersion, and a certain homogenization are required. These are normally achieved by agitation with an impeller. In case of fungal fermentation, agitation not only fulfills the above functions, but as a side effect it may also influence the morphology of fungi. The morphology has an strong influence on the physical properties of a fungal cultivation broth which causes numerous problems in industrial fermenters with respect to gas dispersion, mass and heat transfer, and homogenization (Metz,1976; Braun and Vecht-Lifshitz, 1991). Fungal morphology is often considered as one of the key parameters in industrial production. For productions of fungal metabolic products, the desired morphology varies from one product to another (Braun and Vecht-Lifshitz, 1991). Therefore, it is important to study the influence of agitation on the morphology of fungi.

In case of submerged fermentation, two extreme types of morphology, pellets and free filaments, are generally known. Both of them are used in industrial fungal fermentations (Metz and Kossen, 1977). A culture of filamentous mycelia may be completely free of pellets whereas a culture containing pellets always contains some filamentous mycelia(Nielsen and Carlsen, 1996). The mechanical forces in a fermenter can have a profound effect on the morphology. Terms often used for describing the morphology of filamentous

Figure 1. Schematic drawing of pellets and hyphea.

mycelia are (Metz et al., 1981): main hyphal length, total hyphal length, number of tips per hyphae, diameter of the hyphae, etc. For pellet morphology, the reported quantitative parameter is the size of the pellets. Hyphae in the outer zone of pellets resemble hairs. A schematic drawing of pellets and hyphae is given in Fig.1. In this study, the hyphae in the outer zone of the pellets are called the hair of the pellets. A characteristic parameter is then the "hairy length" as defined in Fig.1.

In a typical mechanically stirred vessel filled with water, the Kolmogoroff scale of turbulence or the size of the smallest eddies is in the range 10-50 μm which corresponds to a maximum specific energy dissipation rate of 100 W/kg to 0.1 W/kg . The size of pellets is in the range 500-5000 μm and the main mean hyphal length of the free filamentous mycelia 100-400 μm.

The hairy length in this study falls in the range 100-300 μm. In general, three damaging mechanisms may exist, i.e. the interaction between particles and eddies, the impact between particles and impellers or baffles, and the collision between particles and particles. In literature, study and discussion on damaging mechanisms in stirred vessels have been reported for fungal particles (pellet and free filamentous hypha) and cells on microcarriers. Since the density and size of microcarriers are close to fungal pellets, the damaging mechanism for cells on microcarriers in stirred vessels is considered to be relevant.

Several studies (Ayazi Shamlou et al., 1994; Metz, 1976; Van Suijdam and Metz, 1981) suggest that the most plausible mechanisms of particle disruption are those based on the interaction between particle and eddies. For a microcarrier cell culture [loading: 2.0-10 g/L (approximately 2-10 % v/v), ρ_p: 1040 kg/m^3, d_p: 180 μm], it was concluded that the collision between particles and particles is a predominant mechanism of cell damage (Cherry and Papoutsakis, 1988). However, a theoretical calculation of the intensity of the microcarrier collisions in turbulent flows led to the conclusion that the collision between microcarriers and microcarriers cannot cause considerable cell damage in bioreactors (Beverloo and Tramper, 1994). In case of another microcarrier cell culture [loading: 1.5-30 g/L (approximately 1.5-23% v/v), ρ_p:1030 kg/m^3, d_p: 168 μm], it was reported (Croughan et al., 1988) that the collision between microcarriers and microcarriers was not the predominant mechanism for cell damage under a mild agitation, but that collisions and the interaction between microcarriers and eddies could contribute to the cell damage under strong agitation.

No experimental data have been found on the impact between impellers and microcarriers, filamentous pellets, or hyphae. Some data on the impact between impeller and glass beads (ρ_p:2400 kg/m^3, d_p: 1.38 mm) have been reported (Takahashi et al., 1993). The number of impacts between impeller and glass beads per time is roughly proportional to ϵ^4 (ϵ is the specific energy dissipation rate). This differs from the results found in the literature (Ayazi Shamlou et al., 1994; Beverloo and Tramper, 1994; Metz, 1976; Van Suijdam and Metz, 1981). The difference is likely due to the different particle densities used in different studies. Particles with a density close to water will follow the stream line of the liquid flow (Caulet et al., 1996), which diminishes the collisions of the particles with the particles or impellers. The wet densities of fungal pellets and hyphae are close to that of water. For fungal fermentation systems, the prevailing mechanism of damage to pellets and hyphae is considered to be the interaction of pellets or hyphae with eddies.

Most of the theoretical models described in the literature are based on the assumption that the turbulent flow is isotropic in a given stirred vessel. Actually, the turbulent flow in a stirred vessel is not fully isotropic. However, although the large eddies produced by a mechanical impeller are not isotropic, the small eddies may be considered to be isotropic (Davies, 1972). In the case of a very small object (such as pellets and hyphae) and a fully turbulence in a

relative large vessel, it is a reasonable assumption that turbulence of the relevant scale in the region nearby the impellers is isotropic. This region is commonly considered as the part of a bioreactor in which the damage to microorganisms occurs. So the assumption of isotropic turbulence is acceptable for the derivation of theoretical models to estimate the size of pellets and the main mean hyphal length, one of the most important parameters (Metz et al., 1981) for the morphology of filamentous mycelia.

The size of pellets and the main mean hyphal length are often considered to be proportional to ϵ^α. The reported values (Ayazi Shamlou et al., 1994; Bhavaraju and Blanch, 1976; Metz, 1976; Van Suijdam and Metz, 1981) for the exponent α differ. Due to the intrinsic complexity in biosystems and the limited accuracy in the quantification of fungal morphology, it is very difficult to judge from available data whether this relationship holds. In spite of this uncertainty, this correlation does make the comparison of both different experimental data and different models easier. The theoretical analysis of the interaction between particles and eddies and the derived models support this type of relationship (Ayazi Shamlou et al., 1994; Bhavaraju and Blanch, 1976; Metz, 1976; Van Suijdam and Metz, 1981). In this study, the general power function of Eq. 1 will be used for processing both our data and data from literature.

$$Y = \alpha_1 \epsilon^\alpha \qquad\qquad (1)$$

Where Y is a dependent variable such as the pellet size, the main mean hyphal length, the hairy length and so on, α_1 the coefficient, ϵ the specific energy dissipation rate and α the exponent of ϵ. The coefficient α_1 is the value for the fungal morphology at a specific energy dissipation rate of 1 W/kg. It is expected to be influenced by the tensile strength of hyphae (differs from strain to strain and depends on the age of cultivation), the mode of experiments, the geometry of the used stirred vessel, and the subjective factor in morphological measurements by each individual researcher. The tensile strength is the maximum force per cross area exerted before a hypha or pellet breaks. However the exponent α is less affected by these factors and gives the information on how severely the morphology is affected by the specific energy dissipation rate. In order to make it easy to compare the data and correlations from different systems, we will focus on the exponent of α only.

FREE FILAMENTOUS MYCELIA
Data on main mean hyphal length (L_e) at different specific energy dissipation rates (ϵ) have been collected from literature. Regression of these data versus specific energy dissipation rate is carried out in those cases in which the regression has not or not correctly been done. In Table I, a summary is given, together with correlations from the literature.

Table I. Regression of literature data on hyphal length and the published models (correlations: $L_e \propto \epsilon^{\alpha}$).

Strain	Exponents of ϵ in correlations	L_e μm	ϵ W/kg	Model	Sources	Remark
Pen.chrysogenum	-0.33	80-275	0.56-20.9[a]		Dion et al. (1954)	BC
A.niger	-0.33	130-370	0.56-18 [a]		Dion and Kaushal (1959)	BC
A.fumigatus	-0.31	156-400	0.56-18 [a]		Dion and Kaushal (1959)	BC
A.glaucus	-0.20	160-315	0.56-18 [a]		Dion and Kaushal (1959)	BC
Paecilomyces varioti	-0.25	160-305	0.56-18 [a]		Dion and Kaushal (1959)	BC
Pen.chrysogenum	-0.17	133-313	0.12-15.1	$L_e \propto C_1\mu^{0.5} \epsilon^{-5/12} + C_2 \epsilon^{-1/4}$	Metz (1976)	CC
Pen.chrysogenum	-0.17	110-429	0.24-48.4	$L_e \propto C_1\mu^{0.5} \epsilon^{-5/12} + C_2 \epsilon^{-1/4}$	Metz (1976)	BC
Pen.chrysogenum	-0.20[b]	58-105[b]	1.7-33	$L_e \propto \epsilon^{-4/7}$	Ayazi Shamlou et al. (1994)	BC

L_e is main hyphal length, ϵ the specific energy dissipation rate, μ the specific growth rate.
BC stands for batch culture and CC for continuous culture.
[a]Energy dissipation rate is calculated from the correlation for Rushton turbine since the so-called disk-turbine propeller in these two papers turned out to be a disk turbine.
[b]Regression of a part of their data which are accessible for readers

Dion et al. (1954) and Dion and Kaushal (1959) ran batch cultures with several strains to study the agitation effect on filamentous mycelia morphology. They called the impeller used in their fermenters "disk propeller" and referred to a publication of Chain et al. (1954). Indeed, the impellers cited in this publication were called "propeller"as well. However, the mechanical drawing of this so-called propeller (Chain et al., 1954) showed the impeller to be a disk turbine with eight blades. Therefore we recalculated energy dissipation rates in their systems at different stirrer speeds accordingly. The mean main hyphal length for five different strains against specific energy dissipation rate is plotted in Figure 2. The exponent of ϵ found by correlation varies from -0.20 to -0.33 for the different species (Table I).
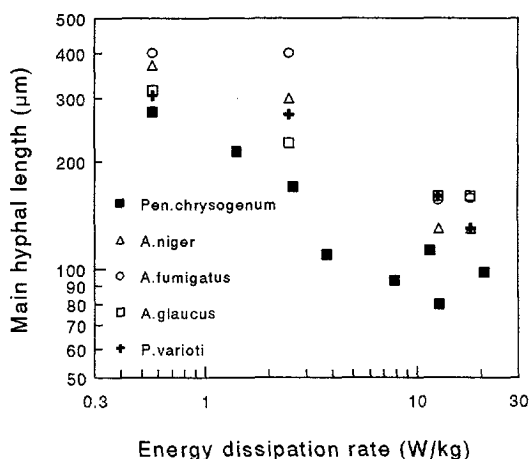
Figure 2. Mean main hyphal length of free filamentous mycelia of several strains at different specific energy dissipation rates [Dion et al. (1954); Dion and Kaushal (1959)]

Metz (1976) measured the hyphal length of filamentous mycelia of *P. chrysogenum* in both continuous and batch cultures. The experimental data are given in Fig. 3. The regression of his data in both systems gave exponent values of -0.17. This exponent is somewhat lower than that of Dion et al. (1954) and Dion and Kaushal (1959). Aware of the difference

between the growing and non-growing systems, Metz derived the following model to estimate the hyphal length:

$$L_e = C_1 \mu^{1/2} \epsilon^{-5/12} + C_2 \epsilon^{-1/4} \qquad (2)$$

Where C_1 and C_2 are constants which are only a function of the geometry of the bioreactors and μ is the specific growth rate. Metz's model is not very successful to describe his data. However, if the term containing the specific growth rate is ignored, the relation shows a reasonable agreement with the average results of Dion et al.(1954) and Dion and Kaushal (1959), and himself.

Ayazi Shamlou et al.(1994) presented a model in which the hyphal length is proportional to $\epsilon^{-4/7}$ (fermentations with *P. chrysogenum* as a model strain). From a regression of the accessible part of their data at pseudo steady state, we found an exponent of -0.2 (see Table I). This exponent is rather close to the one found by Metz (1976). Figure 3 shows that the values of Ayazi Shamlou et al. (1994) are lower than those of Metz (1976). The model from Ayazi Shamlou et al. (1994) is not successful in predicting the hyphal length at different specific energy dissipation rates.
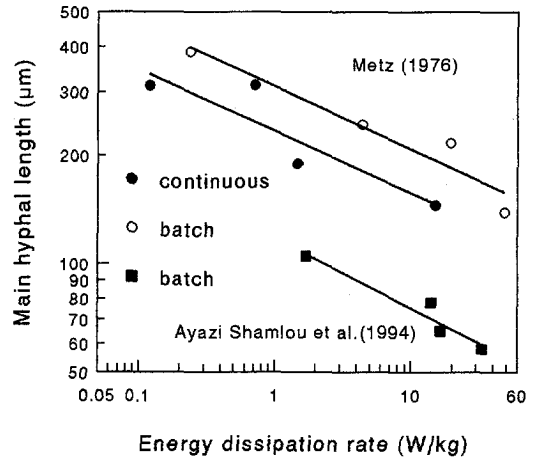
Figure 3. Mean main hyphal length of free filamentous mycelia of P. chrysogenum at different specific energy dissipation rates: (●) Metz (1976), (○) Metz (1976), (■) Ayazi Shamlou et al. (1994).

Summarizing the above-mentioned literature data (Ayazi Shamlou et al., 1994; Dion et al., 1954; Dion and Kaushal, 1959; Metz, 1976) on hyphal length at different energy dissipation rates results in an exponent between 0.17 and 0.33 or, if the exponent is averaged,

$$L_e \propto \epsilon^{-(0.25 \pm 0.08)} \qquad (3)$$

The Kolmogoroff eddy or the smallest scale of turbulence is a function of the specific energy dissipation rate ϵ and the kinematic viscosity of the fluid ν. The size of the smallest eddy can be described (Davies, 1972) as $\nu^{3/4} \epsilon^{-1/4}$. The size of particles in a turbulent flow is often

correlated to the size of eddies in the flow (Ayazi Shamlou et al., 1994; Metz, 1976; Van Suijdam and Metz, 1981). If one assumes that the hyphal length is proportional to the size of the Kolmogoroff eddies, a constant dimensionless number of $L_e \, v^{3/4} \epsilon^{-1/4}$ or a relationship of $L_e \propto v^{3/4} \epsilon^{-1/4}$ will be obtained. This is in accordance with Eq.3. It suggests that the size of the smallest eddy determines the hyphal length in a submerged fungal fermentation.

PELLETS

For pellets, it is known that agitation can influence the size of pellets and the structure of the pellet's surface (smooth or fluffy). During fermentations, autolysis of the cells at the pellet centre can occur (Clark, 1962). Quantitative studies on the effect of agitation on pellets found in literature focus only on the size of pellets. The reported quantitative effect of agitation intensity on pellet size is summarized in Table II.

Table II. Regression of data on pellet diameter and the models (correlations: $d_p \propto \epsilon^{\alpha}$).

Strain	Exponent of ϵ in correlations	d_p mm	ϵ W/kg	Model	Sources	Remark
Lentinus edodes	-0.13	2.2-4.3	0.0043-0.88		Taguchi et al. (1968)	dispersion
Pen.chrysogenum	-0.36	0.47-1.98	0.11-9.06	$d_p \propto \epsilon^{-0.4}$	Van Suijdam and Metz (1981)	fermentation and dispersion
				$d_p \propto \epsilon^{-0.4}$	Bhavaraju and Blanch (1976)	model and no experiment
A.awamori	-0.19	1.21-2.28	0.19-5.7	$d_p \propto \epsilon^{-0.16}$	present study	fermentation at 24 h
A.awamori	-0.15	1.42-2.39	0.19-5.7	$d_p \propto \epsilon^{-0.16}$	present study	fermentation at 41 h

d_p is the pellet diameter and ϵ the specific energy dissipation rate.

Taguchi et al. (1968) measured the diameter of pellets at different stirrer speeds by using *Lentinus edodes* in cold mold. In their experiments, fungal cultivation was carried out in shake flasks or fermenters and cultivated pellets (diameters 3.3-4.3 mm) were transferred into a stirred vessel filled with water and equipped with a Rushton turbine. The size of the pellets was measured at successive times under non-growing conditions. Such an experiment will be called a dispersion experiment in this study. The final pellet diameters are plotted as a function of specific energy dissipation in Figure 4. Regression of the data gives the relationship:

$$d_p = 2.18 \epsilon^{-0.133} \qquad (4)$$

Van Suijdam and Metz (1981) studied pellet size in both fermentations and dispersion experiments with *P. chrysogenum*. The actual data are presented in Figure 4 as well. Their experimental correlation for pellet size with specific energy dissipation rate is

$$d_p = 1.02 \epsilon^{-0.36} \qquad (5)$$

The exponent differs considerably from the one in Eq.4. In these two studies, both strains used (*Lentinus edodes* and *P. chrysogenum*) and experimental modes (dispersion and fermentation) are different. Since stronger agitation will result in a higher dissolved oxygen tension and more branching of hyphae, the pellets formed may be denser and stronger. So for a growing system or fermentation, the pellets subjected to a stronger agitation can be expected to have a higher tensile strength. Therefore, it is not justified to put both data from dispersion experiments (non-growing system) and those from fermentations (growing system) together for a

Figure 4. Size of fungal pellets as a function of specific energy dissipation rate in submerged fermentations: (●) P. chrysogenum from Van Suijdam and Metz (1981), (○) P. chrysogenum from Van Suijdam and Metz (1981), (■) Lentinus edodes from Taguchi et al. (1968).

regression. The data measured by Taguchi et al.(1968) in dispersion experiments cannot be compared with those from the growing systems, and should not be considered relevant for fermentation processes. The effect of agitation on pellet morphology should be studied in growing systems i.e. fermentation processes.
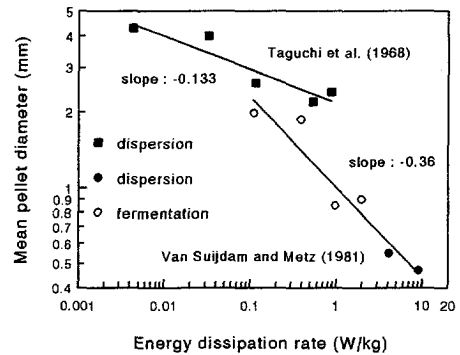
In spite of the inherent complexity, some models have been reported in the literature. Based on different derivations, Bhavaraju and Blanch (1976) and Van Suijdam and Metz (1981) present the same final form of the relation for the prediction of pellet size as a function of specific energy dissipation rate.

$$d_p \propto \epsilon^{-2/5} \tag{6}$$

This relation fits reasonable well with the experimental results of Van Suijdam and Metz (1981). However, the data of Van Suijdam and Metz (1981) are from both fermentations and dispersion experiments. Further, it is questionable to assume a constant tensile strength for the pellets cultivated at different conditions, as was used for the derivation of the model of Van Suijdam and Metz.

Eq. 6 is derived in analogy with the relation of drop size in stirred tanks. The model used to predict the liquid drop size in stirred tanks are (Kawase and Moo-Yang, 1990; Tsouris and Tavlarides, 1994):

$$D_d \propto \frac{\sigma^{3/5}}{\rho^{3/5} \, \epsilon^{2/5}} \qquad (7)$$

Where D_d is the diameter of a drop, σ the surface tension, ϵ the specific energy dissipation rate and ρ the density of the fluid. The size of liquid drops in stirred vessels is mainly determined by agitation intensity, surface tension, density of the liquid and the rheology of the medium. The surface tension is a constant for a given system. If one assumes that the tensile strength of pellets is constant and can be compared with the surface tension of drops in a liquid, the relations for both pellets and drops will be similar. However, the tensile strength of pellets is not necessarily constant and it may well be influenced by the agitation intensity. Therefore the relations for pellets and drops are expected to be different.

The extension of the hyphal tip is the way in which fungi grow (Nielsen and Krabben, 1995; Trinci, 1970). The hyphal length of free mycelia is sensitive to the intensity of agitation. The hairs on the pellets are probably comparable to the tips of hyphae and the hairy length of pellets will depend on agitation conditions. Therefore, attention should be paid to the quantification of the hairy length of fungal pellets. Until now, little has been known about the effect of operating conditions on the internal structure of fungal pellets. In this work, the biomass per wet volume of pellets and the porosity of pellets are measured as well. The studied parameters include hyphal length of free mycelia, pellet size, hairy length of pellets, and biomass per wet volume pellets at different specific energy dissipation rates.

The size, morphology and physiological state of inocula strongly influences the development of fungal morphology in fermentations (Metz and Kossen, 1977; Tucker and Thomas, 1992; Vecht-Lifshitz et al., 1990). In order to study the effect of other factors on morphology, the difference in morphology due to inoculation should be minimized. This can be achieved by inoculating with the same number of spores, the same amount of preculture with the same morphology into the same sterilized medium. Due to the difficulty in obtaining exactly the same spore viability, the same morphology of preculture, and the same sterilized medium in different successive batch fermentations, parallel fermentations were chosen in the present study.

Materials and Methods

Aspergillus awamori (CBS 115.52) was used as a model strain in all experiments. Cultures were maintained and spores produced on standard potato dextrose agar. The fermentations were carried out in 3 L fermentors. Figure 5 shows the geometry of the used fermentors. Sucrose was used as carbon source. The composition of the media used, is given in Table.III.

A seed culture was used for the inoculation of fermentation. The medium composition of the seed culture was the same as that of the fermentation medium. The shaking flask of 2 L was filled with 500 mL of the medium. The flask with medium was first sterilized and then 10 mL of a spore suspension with a concentration of 1.2×10^7 spores per mL was added. The flask was rotated in a rotary shaker at 200 rpm for 24 h. The temperature was kept at 25 °C. The obtained preculture was used for the inoculation of seven fermentors.
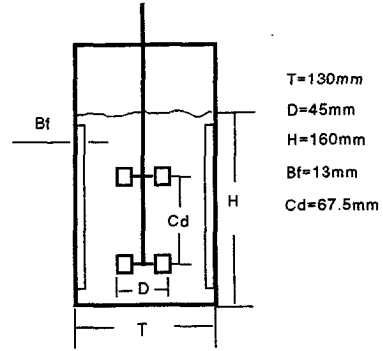

T=130mm
D=45mm
H=160mm
Bf=13mm
Cd=67.5mm

Figure 5. The geometry of the used fermentors.

The initial fungal morphology in preculture was controlled as so called small pellets. Compared with pellets from fermentors, these small pellets had a relative loose core. But the structure of hyphae in the centre was much denser than in the outer zone. Therefore, we still called these initial spherical colonies "pellets".

In a vessel 14 L of medium was prepared. Its composition is given in Table III. This medium was divided over the seven fermenters with the same geometry to be operated with different stirring rates. After sterilization in one batch, the fermenters were inoculated with 60 mL of the obtained preculture. The temperature set point was 25 °C. The pH was maintained at 4.5, using ammonia and phosphate.

Table IV. Composition of fermentation medium.

Ingredient	concentration	
Sucrose	10	g/L
NH_4Cl	9	g/L
KH_2PO_4	1.5	g/L
$NaNO_3$	1.0	g/L
$MgSO_4.7H_2O$	1.0	g/L
$CaCl.2H_2O$	0.3	g/L
Yeast Extract	1.0	g/L

Antifoam was added if needed. Table IV defines the stirrer speed, the specific energy dissipation rate, and the concentration of spores. The specific energy dissipation rate in the used gassed multi-impeller system was calculated according to an approach from literature (Cui et al., 1996). Samples were taken from the fermentors during the fermentation. In this way the influence of the specific energy dissipation rate on fungal morphology could be studied with *parallel* fermentations starting from the *same* inoculum.

Quantification of the morphology of pellets was achieved by means of Image Analysis which has been used often to quantify fungal morphology (Cox and Thomas, 1992; Reichl et al., 1992; Vecht-Lifshitz and Ison, 1992). Before the image analysis, each sample of fermentation broth was processed as followed: 30 mL of the sample was poured gently into a partly submerged 0.425 mm sieve and 1000 mL demineralized water was added slowly to wash the sample and remove the free mycelia. In order to check whether this washing procedure affected the pellet
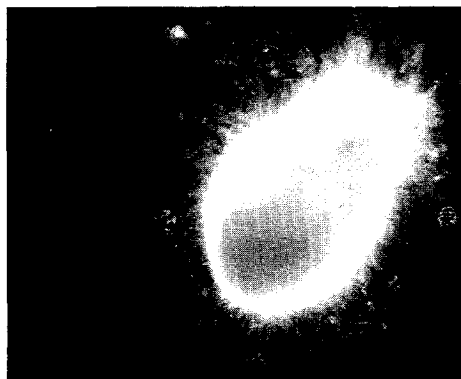

Figure 6. Pellet image. The size is about 1.5 mm

morphology, the results of several sample of a test fermentation broth before and after washing were compared using image analysis and microscopic visual observation. No difference was found. For the determination of the morphology of each sample, 150 objects were analyzed at least. The image analyzer system consisted of microscope, videocamera, monitor, computer (AST Premium II 486/33), and software (CUE-2 Galai Productions). For the pellet image analysis, magnification of 25-50 times was used. In order to characterize pellet surface morphology, pellets were described to have a hairy part and a core part. The hairy part was defined as the outer filamentous zone and the core part as the compact part (see Figs. 1, 6). Figure 6 is an image of a pellet under 50 fold magnification. The image of the hairy part has a clear different grey level compared to the compact core part. This difference in grey level was used for distinguishing the hairy part from the core part. The projection areas of both core part and hairy part were measured by means of Image analysis. Based on the measured areas of the core part and the hairy part, the equivalent radius of the core and the total equivalent radius of both hairy and core parts were calculated. The hairy length was obtained by subtracting the radius of the core from the total radius.

In order to know whether and how the internal structure of pellets changed with the surrounding environment, the dry mass per wet pellet volume was measured at different cultivation conditions. The procedures were: (1) the sample was washed with demineralized water, (2) a certain number of pellets (300) was counted and one half of them was dried in an oven (75°C for 24 h), and (3) the other half was analysed for their wet core volume by means of the Image Analyzer. The hairy volume of pellets was ignored for the measurement of biomass per wet pellet volume because the pellet hairy mass was negligible compared to the pellet core mass. From these data, the dry mass per wet pellet volume was calculated.

The fraction of free filamentous mycelia or pellets in the total biomass was determined in terms of dry biomass. The separation of the filamentous mycelia from the pellets was achieved by means of a sieve with pore size of 0.425 mm. So that the free filamentous mycelia could go through the sieve easier, the separation was carried out in water. The separated mycelia and pellets were dried in an oven (75°C for 24 h) to determine their dry mass.

Results and Discussion

The fermenters were inoculated with a pellet suspension cultivated in shaking flasks in which pellets (diameter about 1mm) were dominant and had a very fluffy outer part and a loose core. In the growth phase, the size of the pellets increased and filamentous mycelia appeared. The size of the pellets and the relative amount of filamentous mycelia varied with fermentation time and intensity of agitation. Before substrate was depleted, few broken pellets were observed in the studied range of power input (ϵ: 0.19 - 5.7 W/kg). In a later phase of the fermentation (depletion of substrate), broken pellets were very noticeable.
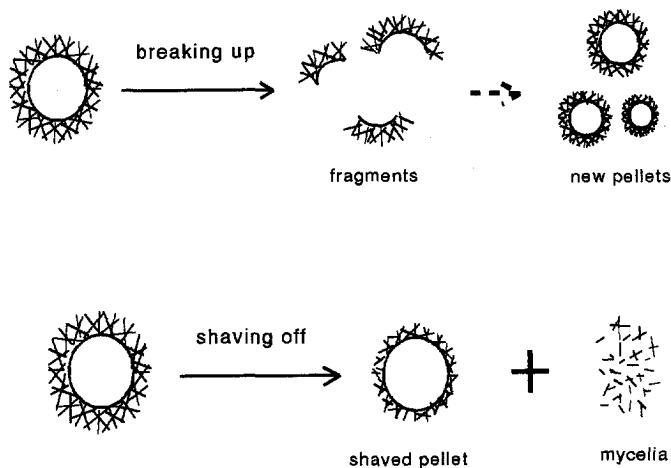

Figure 7. Schematic description of pellet damage mechanisms in stirred bioreactor.

Based on these observations, a shaving mechanism for the effects of agitation on the morphology of pellets is proposed and depicted in Figure 7. The hairs or outer zone of pellets are chipped off by mechanical forces induced by turbulent flow. The severity of this cutting

is a function of the hyphal strength and the magnitude of the mechanical forces. The chipped hyphae form filamentous mycelia and reseed the filamentous mycelial growth or the formation of new pellets. Such a shaving of hyphae from the pellets constricts the increase of the pellet size.

In the literature (Bhavaraju and Blanch, 1976; Lejeune, 1996; Van Suijdam and Metz, 1981; Metz and Kosen, 1977), it has been reported that pellets are damaged through breakage (see Fig.7). Both breakage and surface erosion were proposed to cause pellet damage (Taguchi et al., 1968; Edelstein, 1983). Surface erosion has not been described clearly as a pellet damage mechanism. A very recent paper (Lejeune, 1996) states that the mechanical damage of pellets is due to the breakup mechanism and that if erosion (fragmentation) is used, it should be considered as a synonym of breakage. To simulate the pellet size distribution produced in a shaking flask, Edelstein (1983) assumed that large pellets broke up and the fragments of the pellets were used to reseed other classes of pellets. Metz and Kossen (1977) states that "the pellet size decreases with increasing agitation intensity. However, literature data are not suitable to draw conclusions about the mechanism that is determining the process. This is caused by the fact that in most literature no distinction is made between size limitation by shearing forces and by nutrients in the growth medium". The models published for a relationship between the size of pellets and the specific energy dissipation rate are commonly based on a concept of an equilibrium pellet diameter. The pellets with a larger diameter than that will break up due to turbulent forces or pressures under a given condition (Bhavaraju and Blanch, 1976; Van Suijdam and Metz, 1981; Edelstein, 1983).

Because not many broken pellets have been found in our fermentations, the tensile strength of the pellets must have been higher than the break-up force faced by the pellets. The mechanism of pellet breakage did not govern the present pellet morphology. Since the breakup of hyphae or hairs of the pellets is expected to be easier than the breakup of pellets, it is proposed that in our case, pellets were mainly damaged by chipping hyphae off from their outer zone when oxygen and substrate were sufficiently available. Therefore, the shaving mechanism depicted in Figure 7 is proposed to govern fungal morphology in stirred vessels under the studied conditions.

The measured pellet size distributions of three samples taken at 24 h after inoculation are depicted in Figure 8. The figure shows that these distributions are similar and not very different from the normal distribution, but that the distributions shift from right to left with increase of the mean specific energy dissipation rate. From the distributions of each sample, the arithmetic mean pellet diameter is calculated and used to characterize and compare the pellet sizes at different conditions (Metz, 1976).

Figure 9 shows the mean diameter of pellets at different times as a function of the mean

specific energy dissipation rate in a logarithmic plot. The experimental points at the different specific energy dissipation rates come from independent fermentations performed in parallel. The size of the pellets increased rapidly from 0 h to 14 h. The higher the specific energy dissipation rate was, the less the size of the pellets increased. From 14 h to 24 h, only the size of pellets cultivated in low agitation shows an obvious increase and the rest seems to be more or less stable. In a period of 24-41 h, not much change in size can be found. If the size of pellets at 24-41 h is considered to have reached equilibrium, a linear regression of the two sets of data shows $d_p \propto \epsilon^{-0.19}$ at 24 h and $d_p \propto \epsilon^{-0.15}$ at 41 h (see Fig. 9 and Table II), respectively. The values of these exponents are different from -0.36 as reported by Van Suijdam and Metz (1981) but close to -0.133 as found in the regression of the data of Taguchi et al. (1968). However, the data of Taguchi et al. (1968) obtained from dispersion experiments are not relevant for the fermentation system in the present study. In previous

Figure 8. Distribution of pellet diameters at different energy dissipation rates at 24 h after inoculation

Figure 9. Size of pellets as a function of specific energy dissipation rate in submerged fermentations of A.awamori at different times. The open markers were measured in a duplicated fermentation.

experiments, it has been found that the size and morphology of inocula have a profound effect on the morphological development. To overcome this problem, our fermentations were run simultaneously, and seven fermentors were inoculated with the same amount of preculture from the same batch. Therefore, the measured data are expected to be correct.

In this study, the hairy length of pellets is used as a morphology parameter at different agitation intensities. The measured distributions of pellet hairy length of three samples at 24 h after inoculation are depicted in Figure 10. These distributions are not very different from a normal distribution and shift from right to left with the increase of mean specific energy
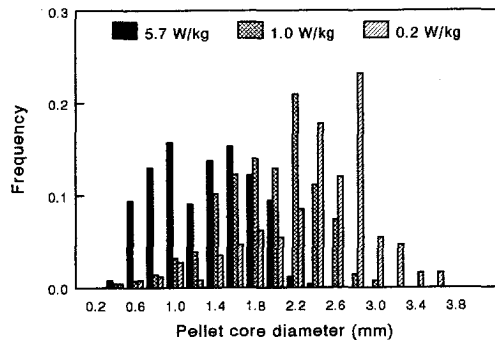
dissipation rate. The plot of the arithmetic mean data calculated for different mean specific

energy dissipation rates and at different fermentation times is given in Figure 11. It shows that the hairy length decreased within 14-24 h dramatically and that the change of this length was much less in the period of 24-41 h. If we assume that the hairy length reached its equilibrium after 24 h, a linear regression of the equilibrium hairy length with specific energy dissipation rate results in the correlation $L_h \propto \epsilon^{-0.25}$ at 24 h and at 41 h.

Figure 10. Distribution of pellet hairy lengths at different energy dissipation rates at 24 h after inoculation

In general, the cell wall is the only important structural element in hyphae. Whether a hair in the outer zone of a pellet will be chipped off by an interaction with eddies depends on the amount of energy contained in these eddies and the maximum energy which can be stored in a hair without breakup. This maximum energy in a hypha has almost nothing to do with the core of the pellets and is a function of the mechanical properties and the geometries of cell walls. If we assume that the hyphae will be elongated in the interaction with eddies and the elongation follows Hooke's law, then we arrive at:

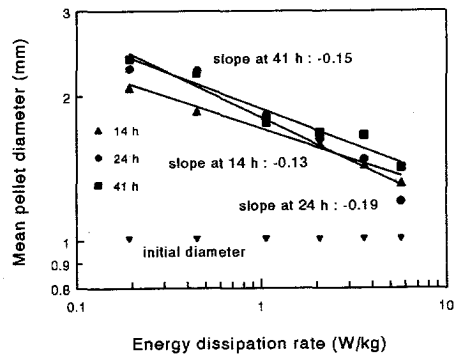**Figure 11.** Hairy length of pellets as a function of specific energy dissipation rate in submerged fermentations of A.awamori at different times. The open markers were measured in a duplicated fermentation.

$$F = \frac{L_h' - L_h}{L_h} \frac{\pi}{4} (d_h^2 - (d_h - 2Z_h)^2) H_C \approx \frac{L_h' - L_h}{L_h} \pi d_h Z_h H_C \qquad (8)$$

where F is the mechanical force from the interaction between hyphae and eddies, L_h' the length of the hypha after elongation, L_h the hyphal length without elongation, d_h the diameter of the hypha, Z_h the thickness of the hyphal cell wall and H_C Hooke's constant. d_h is much
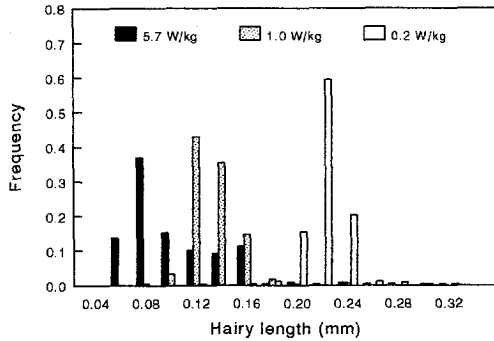
larger than Z_h. The energy stored in a hypha can be described by

$$E_h = \int_{L_h}^{L_h'} F \, d(L_h') = \frac{1}{2} \pi H_C Z_h d_h \frac{(L_h' - L_h)^2}{L_h}$$ (9)

E_h is the mechanical energy stored in a hyphal cell wall at an elongation from L_h to L_h'. The maximum mechanical energy stored in the hyphal cell wall (at breakup) will be:

$$E_{hb} = \frac{1}{2} \pi H_C Z_h d_h \frac{(L_{hb} - L_h)^2}{L_h}$$ (10)

L_{hb} is the hyphal length at breakup. Assuming that the mechanical properties of cell walls in hyphae are independent of hyphal length, the maximum magnitude of an hyphal elongation, $L_{hb} - L_h$, is proportional to the hyphal length, L_h. Therefore, the maximum energy stored in a hypha is:

$$E_{hb} \propto H_C Z_h d_h L_h$$ (11)

The kinetic energy contained in an eddy is a function of the specific energy dissipation rate and the eddy size or wavenumber. For isotropic turbulence one can write (Davies, 1972):

$$u_k^2 \propto \epsilon^{2/3} k^{-2/3}$$ (12)

where u_k is the root mean square of the velocity of the eddy with wavenumber k. The wavenumber of an eddy, k, is the reciprocal of its size (d_e). The kinetic energy contained in an eddy (size is d_e) with wavenumber k can be described as:

$$E_t(d_e) = \frac{1}{2} \rho \frac{\pi}{6} d_e^3 u_k^2$$ (13)

where E_t (d_e) is the kinetic energy in an eddy with a size of d_e and ρ the density of the fluid. A combination of Eq.12 and Eq. 13 gives:

$$E_t(d_e) \propto \rho \epsilon^{2/3} d_e^{11/3}$$ (14)

When a pellet is in a turbulent flow field in a stirred vessel, it will interact with eddies of different sizes. Assuming that the hairy breakup is mainly due to the interaction between hair and the eddies with a size equal to or smaller than the hairy length, then a critical Weber

(We) number may be defined as:

$$We = \frac{\rho\, \epsilon^{2/3} L_h^{11/3}}{H_C Z_h L_h d_h}$$ (15)

This leads to the following relationship:

$$L_h \propto \rho^{-3/8} Z_h^{3/8} d_h^{3/8} \epsilon^{-1/4}$$ (16)

The density of the fermentation medium varied from 1020 kg/m³ to 1050 kg/m³ and can be considered constant. If we assume that the diameter of the hyphae and the thickness of the hyphal cell walls in the outer zone of pellets was also constant, then $L_h \propto \epsilon^{-1/4}$. This dependence agrees well with the experimental data as shown in Figure 11.

Dry biomass per wet pellet volume gives an indication how dense the hyphae are constructed in pellets. This internal structure may be influenced by agitation intensity. To get this kind of information, the dry mass per wet pellet volume was determined for the fermentations run at different stirrer speeds. Figure 12 shows the measured data versus the mean specific energy dissipation rate. The dry biomass per wet pellet volume varies from 14 kg/m³ to 57 kg/m³ under the conditions studied (ϵ : 0.19 - 5.7 W/kg). The magnitude of this variation is rather large, which means that the rheology of the fungal broth can vary considerably for the pellet suspensions with the same amount of biomass since the rheology is a function of the volume fraction of particles. By increasing the dry biomass per wet pellet volume, the biomass per bioreactor volume can be increased without increasing broth viscosity. Of course, a highly packed pellet will enhance the limitation of internal oxygen transfer. The dry mass per wet pellet volume rises with the increase of the energy dissipation rate. Linear regression of the data in Figure 12 gives:
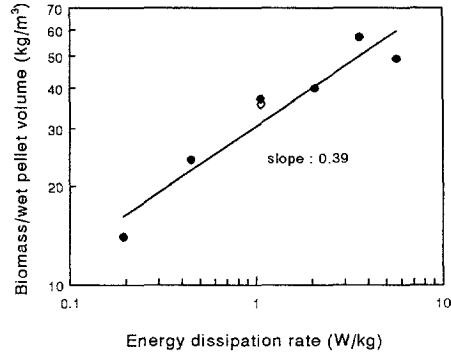

Figure 12. Biomass per-wet-pellet volume as a function of specific energy dissipation rate in submerged fermentations of A.awamori at different times. The open markers were measured in a duplicated fermentation.

$$\rho_{wp} = 31.2\, \epsilon^{0.39}$$ (17)

where ρ_{wp} is dry mass per wet pellet volume.

Eq.17 says that the biomass per wet pellet volume increases with the specific energy dissipation rate. It is expected that a denser packed pellet has a higher tensile strength. Hence, pellet strength will increase with an increase of the specific energy dissipation rate in fermentations. In the derivation of the model of Van Suijdam and Metz (1981), it has been assumed that the tensile strength of pellets is constant. Here, we see that this assumption is not valid. If the tensile strength of pellets is assumed to be proportional to ρ_{wp}, this will give:

$$T_{pb} \propto \epsilon^{0.39} \tag{18}$$

where T_{pb} is the tensile strength of pellets (N.m^{-2}).

If we apply this relation to derive the model of Van Suijdam and Metz (1981) or if we substitute the tensile strength of pellets for the surface tension term in Eq. 7 for the liquid drop size in stirred vessels, we get the following relationship:

$$d_p \propto \epsilon^{-0.16} \tag{19}$$

The exponent (-0.16) is rather close to the values from the regression of the measured pellet size versus specific energy dissipation rate (see Fig. 9 and Table II). The model of Van Suijdam and Metz (1981) is based on the mechanism that pellets will be broken if they are larger than a certain eddy size under a given specific energy dissipation rate. Since Eq.19 is modified from the model of Van Suijdam and Metz (1981) or Eq.7 for liquid drop sizes, it is based on the breakup mechanism as well. However, our experimental observations show that the size of pellets is mainly controlled by the "chip-off" of hair from the outer zone of the pellets instead of breakage. Therefore, we do not conclude that Eq.19 is correct although it matches our observations well.

From the data of the dry mass per wet pellet volume, we can estimate the porosity of the pellet. Assuming that the wet hyphae have a density of 1100 kg/m^3 and contain 80% of water (kg/kg), then the average porosity in pellets can be calculated from the data in Figure 12. The results of such a calculation show that the most dense pellet and the most loose pellet represented in Figure 12 have a porosity of 75% and 93%, respectively. From this we see that the pellets had a loose internal structure and most of the space in each pellet was occupied by liquid and not by hyphae. Regression of the data gives:

$$\epsilon_W = 0.84 \epsilon^{-0.064} \tag{20}$$

where ϵ_w is the porosity in pellets or the relative free water volume in pellets. The porosity decreases with the increase in specific energy dissipation rate.

Figure 13 shows the fraction of free filamentous mycelia in the total biomass as a function of specific energy dissipation rate at 14 h, 24 h and 41 h. The initial morphology was small uniform pellets with a diameter of about 1 mm coming from the preculture. The amount of free filamentous mycelia can be neglected. Figure 13 shows that the fraction of free filamentous mycelia increases from 0 h to 24 h. This can be the result of the "chipping-off" of hyphae from pellets and the growth of free filamentous mycelia without internal oxygen limitation. The fraction of free filamentous mycelia at 24 h and 41 h first decreases and then rises with the

Figure 13. Fraction of free filamentous mycelia in submerged fermentations of A.awamori as a function of specific energy dissipation rate. The open markers were measured in a duplicated fermentation.

specific energy dissipation rate. It has been reported in the literature (Metz and Kossen 1977; Vecht-Lifshitz et al., 1990) that a higher specific energy dissipation rate and a lower dissolved oxygen tension favor the growth of free filamentous mycelia over that of pellets. However, the dissolved oxygen tension is a function of the specific energy dissipation rate and fungal growth rate per bioreactor volume under the studied conditions. The lowest specific energy dissipation rate corresponds to the lowest dissolved oxygen tension. The counteraction of the mechanical forces and the dissolved oxygen tension on fungal growth could explain the minimum value in Figure 13. The samples taken at 14 h do not show such a minimum fraction. These samples are influenced strongly by the morphology in the preculture, which consists of uniform small pellets, and the energy dissipation rate has less effect on the dissolved oxygen tension at the beginning of the fermentations (0-14 h) because the biomass concentration is relatively low at 0-14 h.

The measured fraction of the free filamentous mycelia did not increase between 24 h and 41 h, in contrast to the period between 0 and 24 h. This may have been caused by wall growth and biomass adhesion on the wall. The 3 L fermenters used have a relative large surface area. Spraying the broth suspension on the wall of the fermenters by the rotating top impeller became more severe at a lower medium level which was caused by sampling. Wall growth
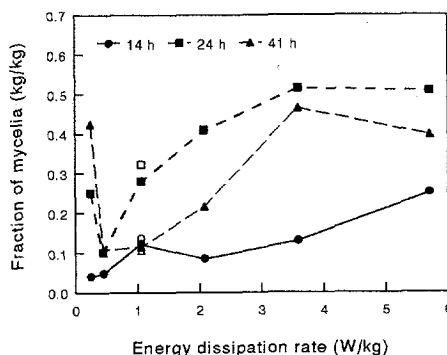
and spraying increased with time. The free filamentous mycelia seemed to attach and grow on the wall more easily than pellets. If so, the fraction of the free filamentous mycelia was underestimated since only the fraction in the bulk was measured.

If one compares Figures 9, 11, 12 and 13, the following picture emerges: higher energy dissipation rates resulted in more chipped hyphae from the pellets and a higher dissolved oxygen tension. More chipping of hyphae led to a smaller size of pellets with shorter hairs and the formation of more new centres for the growth of free filamentous mycelia, which gave a higher fraction of the mycelia. The denser and smaller pellets were formed under a higher specific energy dissipation rate. Such a picture confirms with the proposed shaving mechanism for the damage of pellets in a submerged fermentation (Fig. 7). The chipping of hyphae from pellets is the dominant mechanism for pellet damage which influences the fraction of free filamentous mycelia, the size of the pellets, the hairy length, and perhaps, the internal structure of the pellets as well.

Table IV shows that the parallel fermentations were carried out using the same aeration rate, preculture, and medium but with different stirrer speeds. The difference in stirrer speed influenced both the dissolved oxygen tension and the intensity of interaction between mechanical forces and fungal cells. Based on the present data, it is difficult to distinguish between those two. To study the direct interaction between mechanical forces and fungal cells, the dissolved oxygen tension in different fermenters should be kept the same. This is the subject of further research.

CONCLUSIONS

Effects of agitation intensities on fungal morphology were studied in both *parallel* fermentations with *Aspergillus awamori* and in a literature research on several fungi. The use of parallel fermentations improved the reliability of the obtained results. In the literature, pellet breakup is often assumed to be of great importance in the damage of pellets in fungal fermentations. However, our experimental observations showed that the damage of pellets was mainly due to "shaving of hair" from the pellet surface by mechanical forces. The consequence of this shaving is that the "hair" is chipped off from the pellets. The increase in size due to growth will be restricted. In this way, the size of pellets is related to the specific energy dissipation rate. The breakup of pellets seems to be of minor importance. The main mean hyphal length is influenced very much by the specific energy dissipation rate in a stirred fermenter. Literature data from different fermenters, different strains and different researchers can be correlated using a power function for the specific energy dissipation rate (ϵ). The obtained exponent seems to be independent of the strains used.

The pellet size is related to the specific energy dissipation rate in stirred vessels. The data

from this study could be correlated by $d_p \propto \epsilon^{-0.16}$ which is different from the relation reported in the literature (Bhavaraju and Blanch, 1976; Van Suijdam and Metz, 1981). Data from dispersion experiments (non-growing conditions) are not relevant for fermentation systems. The biomass per wet pellet volume increased with an increase of specific energy dissipation rate in the parallel fermentations. Therefore, the internal structure of the pellets was a function of specific energy dissipation rate as well. The average porosity in the pellets increased with a decrease of the specific energy dissipation rate. The biomass per wet pellet volume and the tensile strength of the pellets changed with fermentation conditions. The assumption of a constant strength is not valid. The fraction of free filamentous mycelia in the total biomass is a function of the specific energy dissipation rate.

Nomenclature

A_{hb}	: surface area of hypha at breakup	m^2
B_f	: width of baffles	m
C_d	: distance between two impellers	m
C_1	: coefficient in Eq.2	-
C_2	: coefficient in Eq.2	-
D	: diameter of impellers	m
d_e	: size of eddies	m
d_p	: diameter of pellets	m
d_h	: diameter of hypha	m
E_h	: mechanical energy stored in hypha	J
E_{hb}	: critical surface energy stored in hypha at breakup	J
E_t	: kinetic energy in an eddy	J
H	: level of liquid in stirred bioreactor	m
H_C	: Hooke's constant	$N\ m^{-2}$
k	: wavenumber	m^{-1}
L_e	: hyphal length	m
L_h	: hairy length of pellets	m
L_{hb}	: hairy length of pellets at breakup	m
Re	: Reynold number	-
T	: diameter of the stirred vessel	m
T_{pb}	: tensile strength of pellets	$N\ m^{-2}$
u'_k	: root mean square of fluctuation velocity	$m\ s^{-1}$
We	: Weber number	-
Y	: parameter of fungal morphology	-
Z_h	: thickness of hyphal cell wall in outer zone of pellets	m

Greek letters

α	: exponent in a power function	-
α_1	: coefficient in a power function	-
ρ	: density of fluid	kg m^{-3}
ρ_p	: density of particles (such as carriers and glass balls)	kg m^{-3}
ρ_{wp}	: dry biomass per wet pellet volume	kg m^{-3}
ν	: kinematic viscosity of fluid	m^2 s^{-1}
ϵ	: specific energy dissipation rate	W kg^{-1}
ϵ_w	: porosity in pellets	%
μ	: specific growth rate	s^{-1}

References

Ayazi Shamlou, P., Makagiansar, H.Y., Lilly, M. D., and Thomas, C.R., 1994, Turbulent breakage of filamentous microorganisms in submerged culture in mechanically stirred bioreactors, *Chem. Eng. Sci.,* **49**, 2621-2631.

Bhavaraju, S.M., and Blanch, H.W., 1976, A model for pellet breakup in fungal fermentations, *J. Ferment. Technol.,* **54**, 466-468.

Beverloo, W.A. and Tramper, J., 1994, Intensity of microcarrier collisions in turbulent flow, *Bioproc. Eng.,* **11**, 177-184.

Braun, S., Vecht-Lifshitz, S.E., 1991, Mycelia morphology and metabolite production, *Trends in Biotechnology,* **9**, 63-68.

Caulet, P.J.C., Van der Lans, R.G.J.M., Luyben, K.Ch.A.M., 1996, Hydrodynamical interactions between particles and liquid flows in biochemical applications, *Chem. Eng. J.,* **62**, 193-206.

Chain, E.B., Paladino, S., Ugolini, F., Callow, D.S., van der Sluis, J., 1954, A laboratory fermenter for vortex and sparger aeration, *Istituto Superiore di Sanita (Eng.ED)* , **17**, 59-85.

Cherry, R.S., Papoutsakis, E.T., 1988,Physical mechanisms of cell damage in microcarrier cell culture bioreactors, *Biotechnol. Bioeng.,* **32**, 1001-1014.

Clark, D.S., 1962, Submerged citric acid fermentation of ferrocyanide-treated beet molasses: Morphology of pellets of Aspergillus niger, *Can. J. Microbio.,* **8**, 133-136.

Cox, P.W., Thomas, C.R., 1992, Classification and measurement of fungal pellets by

automated image analysis, *Biotechnol. Bioeng.,* **39**, 945-952.

Croughan, M.S., Hamel, J-F.P., Wang, D.I.C., 1988, Effect of microcarrier concentration in animal cell culture, *Biotechnol. Bioeng.,* **32**, 975-982.

Cui, Y.Q., Van der Lans, R.G.J.M., Luyben, K.Ch.A.M., 1996, Local power uptake in Gas-Liquid systems with single and multiple Rushton turbines, 14 international symposium on chemical reaction engineering, *Chem. Eng. Sci.,* **51**, 2631-2636.

Davies, J.T., 1972, Turbulence Phenomena,p. 54. Academic Press, New York.

Dion, W.M., Calrilli, A., Sermonti, G., Chain, E.B., 1954, The effect of mechanical agitation on the morphology of penicillium chrysogenum thom in stirred fermenters, *Istituto Superiore di Sanita (Eng.ED)* , **17** 187-205.

Dion, W.M., Kaushal, R., 1959, The effect of mechanical agitation on the morphology of some common fungi grown in submerged culture, *Selected Scientific papers from Istituto Superiore di Sanita (Eng.ED)* , **2** 357-369.

Edelstein, L., 1983, A model for pellet size distributions in submerged mycelial cultures, *J. theor. Biol.,* **105**, 427-452.

Lejeune, R., 1996, From spores to pellets: modelling the growth and morphology of filamentous fungi, *Ph.D thesis, Vrije Universiteit Brussel.*

Kawase, Y., Moo-Yang, M., 1990, Mathematical models for design of bioreactors: Application of Kolmogoroff's theory of isotropic turbulence, *Chem. Eng. J.,* **43**, B19-B41.

Metz, B., 1976, From pulp to pellet, *Ph.D* thesis, Delft University of Technology.

Metz, B., De Bruijn, E.W., Van Suijdam, J.C., 1981, Method for quantitative representation of the morphology of molds, *Biotechnol. Bioeng.,* **23** 149-162.

Metz, B., Kossen, N.W.F., 1977, The growth of molds in the form of pellets-Literature Review, *Biotechnol. Bioeng.,* **19**, 781-799.

Nielsen, J., Carlsen, M., 1996, Fungal pellets, *in*: Immobilished living cell systems : modeling and experimental methods. (Willaert R.G., Baron G.V. and De Backer L. Eds. John Wiley & Sons Ltd).

Nielsen, J., Krabben, P., 1995, Hyphal growth and fragmentation of *Penicillium chrysogenum* in submerged cultures, *Biotechnol. Bioeng.*, **46**, 488-598.

Reichl, U., King, R., Gilles, E.D., 1992, Characterization of pellet morphology during submerged growth of *Streptomyces tendae* by image analysis, *Biotechnol. Bioeng.*, **39**, 164-170.

Van Suijdam, J.C., Metz, B., 1981, Fungal pellet breakup as a function of shear in a fermenter, *J. Ferment. Technol.*, **59**, 329-333.

Trinci, A.P.J., 1970, Kinetics of the growth of mycelial pellets of *Aspergillus nidulans*, *Archiv fur Mikrobiologie*, **73**, 353-367.

Taguchi, H., Yoshida, T., Tomita, Y., Teramoto, S., 1968, The effects of agitation on disruption of the mycelial pellets in stirred fermenters, *J. Ferment. Technol.*, **46**, 814-822.

Takahashi, K., Nakano, Y., Yokota, T., Nomura, T., 1993, Effect of scale on particle-impeller impact in an agitated vessel equipped with a Rushton turbine, *J. Chem. Eng. Japan*, **26**, 100-103.

Tsouris, C., Tavlarides, L.L., 1994, Breakage and coalescence models for drops in turbulent dispersions, *AIChE Journal*, **40**, 395-406.

Tucker, K., Thomas, C.R., 1992, Mycelial morphology: the effect of spore inoculum level, *Biotechnology Letters*, **14**, 1071-1074.

Vecht-Lifshitz, S.E., Magdassi, S., Braun, S., 1990, Pellet formation and cellular aggregation in *Streptomyces tendae*, *Biotechnol. Bioeng.*, **35**, 890-896.

Vecht-Lifshitz, S.E., Ison, P. A., 1992, Biotechnological applications of image analysis: present and future prospects, *J. Biotechnol.*, **23**, 1-18.

CHAPTER 5

Effects of Dissolved Oxygen Tension and Mechanical Forces on Fungal Morphology in Submerged Fermentation

Y.Q.Cui, R.G.J.M. van der Lans, K.Ch.A.M. Luyben

Abstract

The effect of the dissolved oxygen tension and mechanical forces on fungal morphology were both studied in the submerged fermentation of *Aspergillus awamori*. Pellet size, the hairy length of pellets and the free filamentous mycelial fraction in the total biomass were found to be a function of the mechanical force intensity and to be independent of the dissolved oxygen tension provided that the dissolved oxygen tension was neither too low(5%) or too high (330%). When the dissolved oxygen concentration was close to the saturation concentration corresponding to pure oxygen gas, *A. awamori* formed denser pellets and the free filamentous mycelial fraction was almost zero for a power input about 1 W/kg. In case of a very low dissolved oxygen tension, the pellets were rather week and fluffy so that they showed a very different appearance.

The amount of biomass per pellet surface area appeared to be affected only by the dissolved oxygen tension and was proportional to the average dissolved oxygen tension to the power of 0.33. From this it was concluded that molecular diffusion was the dominant mechanism for oxygen transfer in the pellets and that convection and turbulent flow in pellets were negligible in submerged fermentations. The biomass per wet pellet volume increased with the dissolved oxygen tension and decreased with the size of pellets. This means that the smaller pellets formed under a higher dissolved oxygen tension had a higher intrinsic strength. Correspondingly, the porosity of pellets was a function of the dissolved oxygen tension and the size of pellets. Within the studied range, the void fraction in the pellets was high and always much more than 50%.

INTRODUCTION

GENERAL ASPECTS
Fungal fermentation is widely recognized as a complex process with numerous problems. One of the reasons for this is the diverse fungal morphologies. In submerged fermentations, fungal morphology is usually classified into two extremes: individual filamentous mycelia and spherical dense colonies called pellets. Free filamentous mycelia leads to a highly viscous and pseudoplastic fermentation broth that reduces the gas-liquid (G-L) mass transfer and the homogeneity in fermenters. On the other hand pellets probably have internal mass transfer limitation. Hydrodynamic conditions in a bioreactor, dissolved oxygen tension, fungal morphology and growth, broth rheology, and the formation and secretion of products interact with each other. To understand and control this complex process, a detailed study of the mechanisms behind this interaction is necessary.

As a result of the low solubility and the limited volume mass transfer in bioreactors, oxygen is often one of the limiting components for fermentations. At 25°C its concentration in water saturated with air of 1 bar is only 8.4 g/m^3. The G-L mass transfer capacity in a fermenter is determined by the power input of impellers, the rheology of the broth and the gas flow rate. For a specific energy dissipation rate of 0.5-10 W/kg and a medium with a viscosity of 1-1000 mPa.s, k_La, the G-L mass transfer coefficient per volume, varies from 0.001 to 0.1 s^{-1}. Due to the high viscous fungal broth, k_La in a fungal fermentation is much lower than that in the fermentations with single cell microorganisms. Moreover, oxygen depletion in pellets even occurs at a high bulk dissolved oxygen tension. Therefore, the oxygen limitation in a fungal fermentation is more profound than in a single cell microorganism fermentation. In a fungal fermentation, the agitation by the impellers not only results in the dispersion of gas, mixing, and mass and heat transfer but also strongly affects fungal morphology. The dissolved oxygen tension and stirrer speed, to which mechanical forces are related, are important parameters for performing a desired fungal fermentation with a given strain and medium.

Oxygen tension effect on fungal fermentation
Reports in the literature have stated that the dissolved oxygen tension affects productivity, cell autolysis, the rigidness of the cell wall, and so on in fungal fermentations. Some of the observations contradict each other. Zetelaki and Vas (1968) bubbled air and oxygen through a culture of *Aspergillus niger* for the production of glucose oxidase. The oxygenated culture produced twice as much glucose oxidase as the aerated one. Sakurai and Imai (1992) found that the specific citric acid production rate increased with the dissolved oxygen tension in a rotating disk contactor using *A. niger*. Giuseppin (1984) showed that lipase production of *Rhizopus delemar* decreased when the dissolved oxygen tension was lower than about 18%

of air saturation. Wecker and Onken (1991) stated that in the cultivation of *Aureobasidium pullulans*, the yield of pullulan at 50% dissolved oxygen tension of air saturation was higher than that at 100% dissolved oxygen tension.

Clark (1962) found that the oxygen pressure in the fermentation of *A. niger* had a marked effect on the density of peripheral growth and on the rate and extent of cell autolysis. A higher oxygen pressure (1.7 atm) reduced the extent of cell autolysis in the pellets. However, with an oxygen pressure of 0.2 atm, the pellets were larger, possessed a uniform growth density throughout, and did not autolyse. With respect to the cell autolysis, Zetelaki and Vas (1968) reported that the cell autolysis in an oxygenated culture started earlier and was quicker than in an aerated one.

The most widely observed growth kinetics of pellets is the cube-root law (Carlsen et al., 1996; Emerson,1950; Marshall and Alexander, 1960; Trinci, 1970). The cube-root law is in accordance with the diffusion limitation of a substrate in the outer shell of a pellet. The profile of the dissolved oxygen tension measured within a pellet indicated that only a part of pellet was penetrated by dissolved oxygen (Schügerl et al., 1983; Wittler et al., 1986). The specific respiration rate of a pellet decreased with an increase in pellet size (Kobayashi et al., 1973). Limitation of oxygen within the pellets is expected if pellets are larger than a certain critical size. The critical size can be calculated by (Tramper and Van't Riet, 1991)

$$d_{crit} = \sqrt{\frac{24\,C_{O_2}D_{eff}}{R_{O_2}}} \qquad (1)$$

where d_{crit} is the critical diamter at which the internal oxygen limitation starts, C_{O2} is the dissolved oxygen tension in the bulk, D_{eff} is the effective diffusion coefficient of oxygen in the pellet, and R_{O2} is the oxygen consumption rate per pellet volume. D_{eff} is equal to the product of the molecular diffusion coefficient and the pellet porosity. R_{O2}, is equal to the product of the specific oxygen consumption rate and the density of pellets.

Critical pellet diameter is about 370 μm with a pellet porosity of 0.8 (Cui et al., 1997), a bulk dissolved oxygen concentration of 8.4 g/m^3, the specific oxygen consumption rate of 0.2 kg/kg h and the density of pellet of 50 kg/m^3. Pellets are larger than that in most cases. This means that the growth of pellets is controlled by oxygen limitation.

Summarizing, it is clear that the oxygen limitation controls the growth of pellets and that the dissolved oxygen tension does affect the fungal fermentation with respect to productivity and cell autolysis. However, the literature is not clear whether the observed results at different

dissolved oxygen tensions is caused by the change of the fungal physiology, the change of the fungal morphology, or the change of the oxygen transfer rate.

Oxygen tension effect on morphology

The effect of dissolved oxygen tension on fungal morphology has been observed but inconsistent results have been reported. Van Suijdam and Metz (1981a) reported that the morphology of free filamentous mycelia of *Penicillium. chrysogenum* hardly changed with the variation of the dissolved oxygen tension from 7.5 to 188% of air saturation. Dion et al. (1954) used oxygen gas instead of air to pass through the culture fluid of *P. chrysogenum*. A marked difference in the appearance of the mycelium was found in comparison to the normal conditions when air was used. The hyphae became thickened, more branched, and shorter. Zetelaki and Vas (1968) stated that the cell walls of *A. niger* were less rigid and less resistant to mechanical agitation in oxygenated cultures. Zetelaki and Vas (1968) found that the viscosity of the oxygenated culture of *A. niger* was half of that of the aerated culture. This implies that the oxygen tension influences morphology in a fungal culture. Some qualitative effects of oxygen tension on fungal morphology were reported in the literature, but due to the contradictions no clear picture emerges. A quantitative study is lacking.

Effect of mechanical forces on fungal cells

The isolated effects of mechanical forces on the fungal morphology in a submerged fermentation have seldom been studied. The most relevant type of work is the study on the effect of the agitation intensity on fungal morphology. The common approach is to run a fermentation at different agitation intensities and to observe the change in the fungal morphology. For free filamentous mycelia, the studied quantitative parameters include the main mean hyphal length, the number of branches, the total hyphal length, and the length per branch. The mean main hyphal length was found to decrease with an increasing energy dissipation rate (Aziya Smoulou et al., 1994; Doin et al, 1954; Metz, 1976). Correlations between hyphal length and energy dissipation rate were reported by Metz (1976) and Cui et al. (1997). For pellet morphology, Van Suijdam and Metz (1981b) and Cui et al. (1997) quantified the influence of the energy dissipation rate on pellet size. The former reported that the pellet size was proportional to the energy dissipation rate with an exponent of -0.4. The latter found from parallel fermentations an exponent of -0.16 instead of -0.4. In their article, the quantitative effects of the specific energy dissipation rate on the fungal pellet morphology were studied as well such as the hairy length of pellets, the biomass per wet pellet volume, the porosity of the pellets, and the fraction of free filamentous mycelia in the total biomass. However, increasing the agitation intensity also changed the dissolved oxygen tension. Whether the difference in morphology was due to the mechanical forces or the dissolved oxygen tension was not very clear. In this article, the new correlations will be presented and the mechanisms of the mechanical force effect on fungal morphology will be discussed.

Previous results

In our previous parallel fermentations (Cui et al., 1997), the fermentations were run at different agitation intensities but at the same gas flow rate. It was found that the pellet size, the hairy length, the pellet density, the pellet porosity, and the free filamentous mycelial fraction in the total biomass varied with the specific energy dissipation rate. The increase of the specific energy dissipation rate, however, enhances both the mechanical forces on the cells and the G-L mass transfer. The dissolved oxygen tension was registered during these batch parallel fermentations. Figure 1 shows the average dissolved oxygen tension that are averaged in a relevant period. This period is defined from the fermentation start time to the time at which the sample is taken. The average dissolved oxygen tension increased with the specific energy dissipation rate. To study the mechanisms of how mechanical forces and dissolved oxygen tension affect fungal morphology, it is necessary to distinguish the effect of the dissolved oxygen tension and the effect of the mechanical forces.

If the yield of biomass on oxygen is assumed to be constant for pellet growth, the biomass per pellet surface area will be the product of the accumulative mass of oxygen transferred per pellet surface area and the biomass yield on oxygen. The accumulative amount of oxygen transferred through the pellet surface is a function of the driving force for oxygen transfer in the pellets. The driving force is related to the bulk dissolved oxygen tension. Therefore, the biomass per pellet surface area can be expected to be related to the dissolved oxygen tension as well.

Figure 1. Averaged dissolved oxygen tension observed in the previous parallel batch fermentations run at different specific energy dissipation rate and in the present ones. The open marker is from a duplicate fermentation

If so, it will be a useful parameter for distinguishing between the effect of mechanical force and the effect of dissolved oxygen tension on fungal morphology. Thus our previous data (Cui et al., 1997) were processed. The biomass per wet pellet surface area was calculated from the total biomass and total pellet core surface area of 150 pellets. The obtained data are depicted in Figures 2 and 3. Figure 2 shows that the biomass per pellet surface area increased with the specific energy dissipation rate, and Figure 3 shows that the biomass per pellet
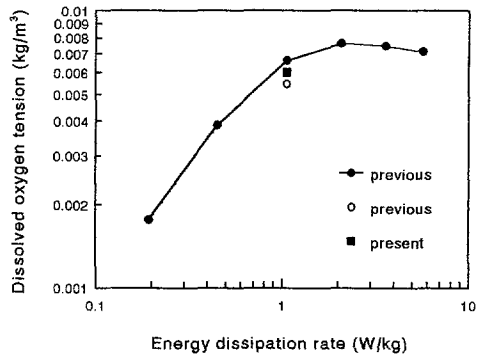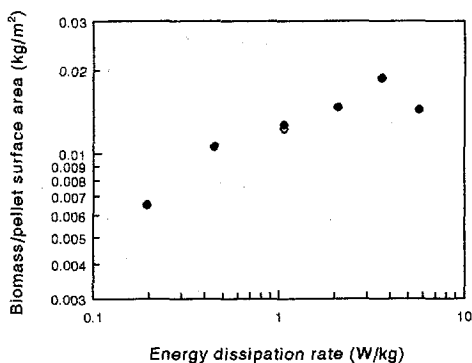
Figure 2. Biomass per pellet surface area observed in the parallel batch fermentation run at different specifc energy dissipation rates from our previous work. The open marker is for a duplicate fermentation.
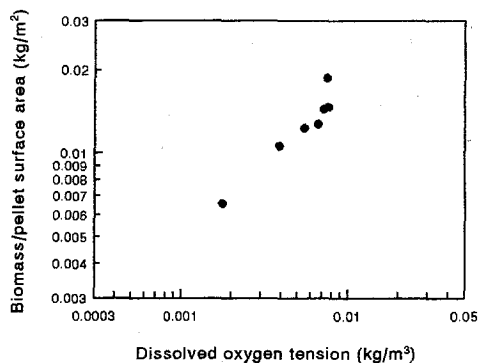
Figure 3. Biomass per pellet surface area versus the averaged dissolved oxygen tension observed in our previous parallel batch fermentations run at different specific energy dissipation rate.

surface area increased with the dissolved oxygen tension in the bulk. However, it is not clear whether the biomass per pellet surface area is actually influenced by the mechanical forces or by the dissolved oxygen tension.

To study the effects of the dissolved oxygen tension and the mechanical forces independently in the present work, a new set of batch parallel fermentations were performed at the same specific energy dissipation rates but with different dissolved oxygen tensions. This was achieved by varying the oxygen concentration in the inlet gas. The studied morphological parameters were the pellet size, the hairy length of the pellets, the biomass per pellet surface area, the biomass per wet pellet volume, the pellet porosity, and the fraction of free filamentous mycelia in the total biomass. To avoid frequent citation, the terms of our previous data, our previous study, or our previous parallel fermentation will be used to refer to the work from Cui et al. (1997). The combination of the new parallel fermentations and the previous parallel fermentations leads to a clear picture on how the dissolved oxygen tension effects the fungal morphology and on what the effects of mechanical forces are on the fungal morphology.

MATERIALS AND METHODS

A. awamori (CBS 115.52) was used as a model strain in all experiments. Cultures were maintained and spores produced on potato dextrose agar. The fermentations were carried out in 3 L fermenters. The geometry of the used fermenters is given in Figure 4 which is the

same as those used in our previous study. Sucrose was used as the carbon source. The composition of the used media is given in Table I. A preculture was used for the inoculation of fermentation. The preparation of the preculture was the same as our previous study. The fungal morphology in the preculture was controlled to be small pellets. Compared with the pellets from a fermenter, these small pellets had a relative loose core. But the structure of the hyphae in the centre was much denser than in the outer zone. Therefore, we still called these initial spherical colonies pellets.

Table I. Composition of the fermentation medium.

Ingredient	concentration	
Sucrose	10	g/L
NH_4Cl	9.0	g/L
KH_2PO_4	1.5	g/L
$NaNO_3$	1.0	g/L
$MgSO_4.7HO_2$	1.0	g/L
$CaCl_2.2HO_2$	0.3	g/L
Yeast Extract	1.0	g/L

T=130mm
D=45mm
H=160mm
Bf=13mm
Cd=67.5mm
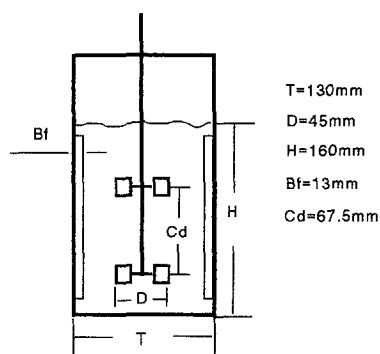
Figure 4. Geometry of the fermenters used.

After sterilization of the seven fermenters filled with the same medium (see Table I) from one batch, the fermenters were inoculated with 50 mL of the obtained preculture (parallel). The temperature set point was 25 ^{0}C. The pH was maintained at 4.5 using ammonia and phosphate. Antifoam was added if needed. Table II gives the operation conditions. The specific energy dissipation rate and the concentration of spores in each fermentation were kept constant. The different oxygen concentrations in the inlet gas were realized by mixing air with pure oxygen or with nitrogen gas. But the dissolved oxygen tensions were not controlled as constant values due to the lack of the control system of the dissolved oxygen tensions in the seven fermenters. Samples were taken from the fermenters during the fermentation. The dissolved oxygen tension in each fermenter was registered as a function of fermentation time. The average dissolved oxygen tension was calculated for a given sample from the fermentation start time to the time when the sample was taken.

Table II. Operating conditions for the fermentations. The aeration rate is the same for all fermentations and about 5×10^{-6} m³/s. The size of fermenters is 3 liter (see Fig.4 for the geometry).

Fermenter	Stirrer speed	Energy dissipation	Oxygen in inlet gas	number of spores	remark
	rpm	W/kg	%	1/m³	
F1	600	1.07	4	6.3×10^9	same preculture
F2	600	1.07	10	6.3×10^9	same preculture
F3	600	1.07	10	6.3×10^9	same preculture
F4	600	1.07	20	6.3×10^9	same preculture
F5	600	1.07	40	6.3×10^9	same preculture
F6	600	1.07	60	6.3×10^9	same preculture
F7	600	1.07	80	6.3×10^9	same preculture

The quantification of pellet morphology was achieved by means of image analysis, which has often been used to quantify the fungal morphology (Cox and Thomas, 1992; Reichl et al., 1992; Vecht-Lifshitz and Ison, 1992). The methods used for the morphology quantification and processing of samples were the same as the previous ones (Cui et al., 1997). To characterize pellet surface morphology, a compact core part and a hairy part defined as the outer filamentous zone were distinguished
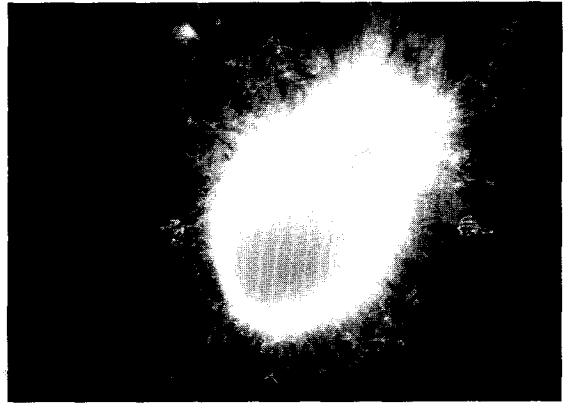
Figure 5. Pellet image. The pellet size is about 1 .5 mm.

(see Fig.5). A line is drawn in Figure 5 to illustrate how the core part and the hairy part are defined. For fluffy pellets this interface is less clear, which may influence the accuracy of the quantification of the hairy length. The image of the hairy part had a different grey level compared to the compact core part (see Figure 5). This difference in grey level was used for distinguishing the hairy part from the core part. Based on the measured areas of the core part and the hairy part, the diameter of the core and the thickness of the hairy layer (the hairy length) were calculated. Figure 6 showed the mean pellet core diameter and the mean hairy length that were measured by two researchers in a test fermentation. We see that the pellet size measurement was rather accurate and reproducible. The measurements of hairy length by one researcher had a good reproducibility and were very comparable with respect to time

development. But the measurements from the different researchers deviated about 20% from each other. This deviation was probably due to the difference in defining the interface between hairy part and core part (see Fig.5) by the different researches.
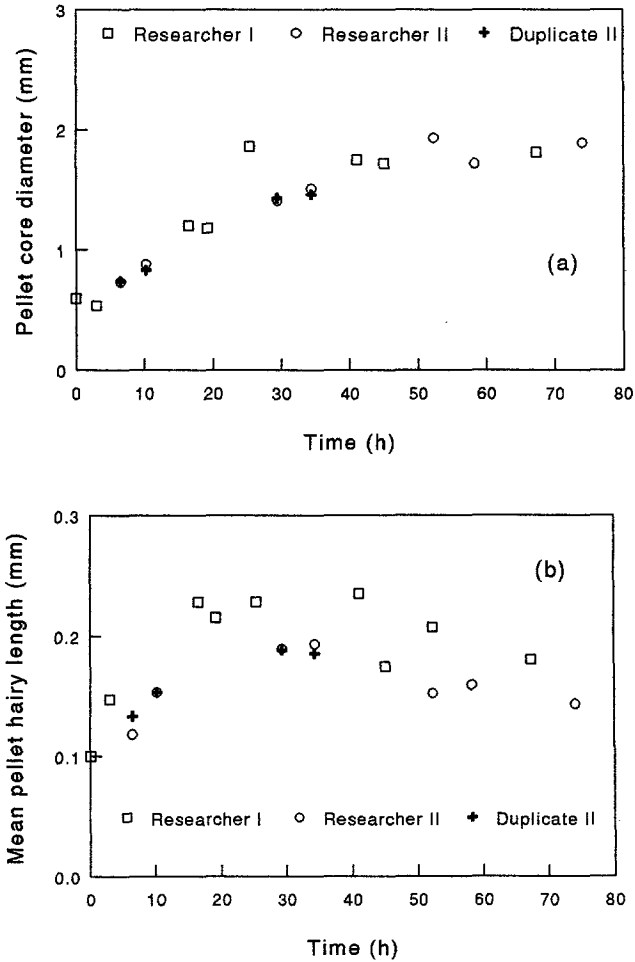
Figure 6. Pellet morphology measured by different researchers during a test fermentation. Cross marker is from a duplicate measurement by reasearcher II. **a**: pellet sizes; **b**: hairy length of pellets.

In order to know whether and how the internal structure of the pellets changes with the surrounding environment, the dry mass per wet pellet volume was measured at different dissolved oxygen tensions. The procedure was as follows. First the sample was washed with demineralized water. Then a certain number of pellets (600) was counted and half of them

were dried in an oven (75°C and 24 h) and weighed. The other half was analysed for their wet core surface area by means of the image analyzer. From these two results, the dry mass per wet pellet surface area was calculated. By using the wet biomass density of 1100 kg/m³ and knowing the size of pellets, the porosity and the density of the pellets were calculated.

The fraction of free filamentous mycelia or pellets in the total biomass was determined in terms of the dry biomass fraction. The separation of the filamentous mycelia from the pellets was achieved by means of a sieve with pore size of 0.425 mm. In order to let the free filamentous mycelia go though the sieve easier, the separation was carried out in water. The separated mycelia and pellets were dried in an oven (75°C and 24 h), then their dry mass was measured.

RRSULTS AND DISCUSSION

The pellet sizes were measured in the parallel fermentations performed at different dissolved oxygen tensions (0.1-30 g/m³) and a constant energy dissipation rate (1.0 W/kg). The distributions of pellet core diameters of three samples are depicted in Figure 7. The arithmetic mean approach was used for the calculation of the mean pellet size from the measured distributions as in our previous study. The average dissolved oxygen tension was calculated from the dissolved oxygen tension registered during the fermentations. Figure 8a shows the

Figure 7. Distributions of pellet diameters at different oxygen fractions (parameters with markers) in inlet gas at 38 h fermentation.

observed pellet size as a function of the oxygen fraction in the inlet gas. The energy dissipation rate in these gassed multi-impeller systems was calculated according to the literature (Cui et al., 1996). With a constant energy dissipation rate, the oxygen fraction in inlet gas hardly affected pellet size, although the oxygen fraction varied from 0.04 to 0.8. For a filamentous bacteria Vecht-Lifshitz et al. (1989) found that oxygen limitation reduced pellet size. Figure 8b shows the pellet size versus specific energy dissipation rate from our previous work in which the specific energy dissipation rate varied from 0.2 to 5.7 W/kg. Pellet size decreased with the specific energy dissipation rate and was correlated with

$$d_p \propto \epsilon^{-0.16} \qquad\qquad (2)$$

Figure 8. Diameter of pellets from the parallel batch fermentations. **a**: run at different oxygen fractions in inlet gas but at the same specific energy dissipation rate (see table II); **b**: run at different specific energy dissipation rates from our previous parallel batch fermentations.

Combining the results depicted in Figure 8a and 8b leads to the conclusion that the pellet size is determined by mechanical forces and is independent of the dissolved oxygen tension. It must be noted that the data obtained in this study and those from the previous study with the same conditions (1.0 W/kg, oxygen fraction of about 0.2 in inlet gas) do not result in exactly the same pellet size (1.8 vs 2.0 mm after 40 h) although the differences are relatively small. This may be due to the different inoculations in the different parallel experiments.

The physical picture behind the correlation [Eq.(2)] is clearer than in our previous study. Mechanical forces, related to the energy dissipation rate, are responsible for the pellet size. A higher dissolved oxygen tension, corresponding to a higher energy dissipation rate, has no direct affect on the pellet size.

The hairy length of the pellets is compared in a similar way to the pellet size. Figure 9 shows the distributions of pellet hairy length at 38 h. Using the arithmetic mean approach, the mean pellet hairy lengths were calculated from the distributions. The mean hairy length of the pellets at the same specific energy dissipation rate is plotted against the oxygen fraction in inlet gas in Figure 10a. Figure 10a shows that the hairy length of the pellets was hardly affected by the oxygen fraction if the oxygen fraction was higher than 0.1. The oxygen
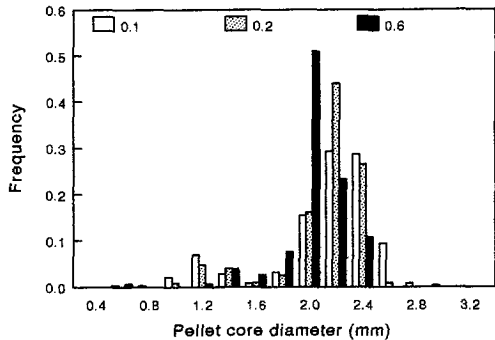

Figure 9. Distributions of pellet hairy lengths at different oxygen fractions (parameters with markers) in inlet gas at 38 h fermentation

fraction of 0.1 in inlet gas led to the average dissolved oxygen tension of about 20% of air saturation under the used conditions. When the oxygen fraction was 0.04 (the average dissolved oxygen concentration was about 5% of air saturation), the longer hairy length was measured. In this case, a very fluffy pellet was formed and it was difficult to determine the hairy length of these pellets accurately because the interface between the hair and the core was not clear any more. The data of the hairy length of pellets against the specific energy dissipation rate from our previous study are plotted in Figure 10b. Hairy length and specific energy dissipation rate can be correlated with

$$L_h = 0.000117 \epsilon^{-0.25} \tag{3}$$

Comparison of Figure 10a and Figure 10b leads to the conclusion that the hairy length of pellets was independent of the dissolved oxygen tension, but dependent on the mechanical forces. For the same mechanical force intensity, the hairy length of pellets decreased with fermentation time.

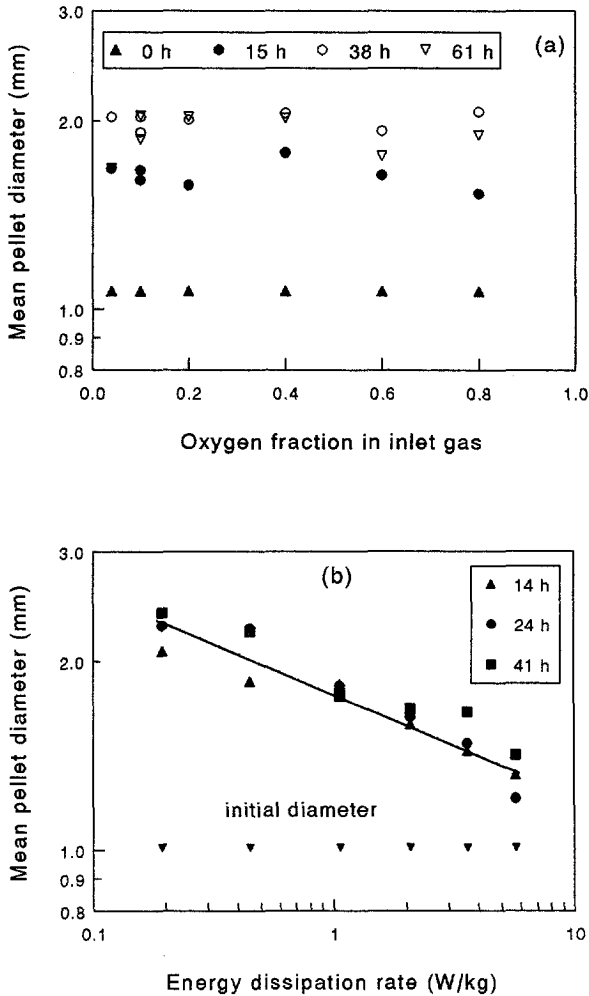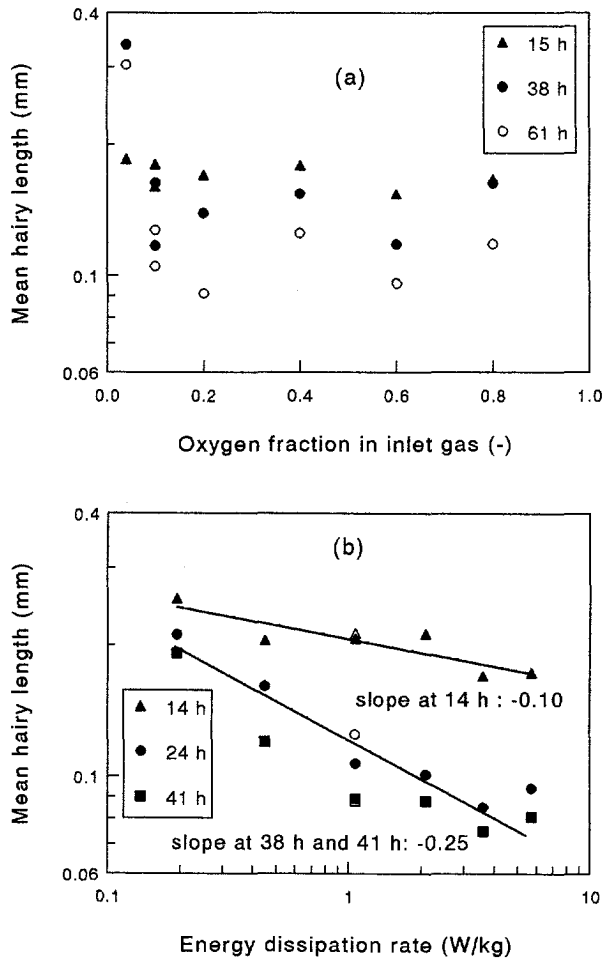**Figure 10.** Hairy length of pellets from the parallel batch fermentations. **a**: run at different oxygen fractions in inlet gas but at the same specific energy dissipation rate (see Table II). **b**: run at different specific energy dissipation rates in our previous parallel batch fermentations. The open marker is from a duplicate fermentation.

Because a limitation of oxygen mass transfer within the pellets is expected, the biomass per pellet surface area may be a function of the dissolved oxygen tension as discussed before. However, from Figure 2 and Figure 3 it is difficult to know how much the dissolved oxygen tension affects the biomass per pellet surface area because the dissolved oxygen tension and the mechanical forces were both varied in the previous set of parallel fermentations. Extra data are needed in order to discriminate between the two mechanisms. The biomass per pellet surface area, measured at different dissolved oxygen tensions but at the same specific energy

Figure 11. Biomass per pellet surface area from the parallel batch fermentations run at different dissolved oxygen tension but at the same specific energy dissipation rate (see Table II) and from our previous parallel batch fermentations run at different specific energy dissipation rates.

dissipation rate, is depicted in Figure 11. The figure shows that the biomass per pellet surface area increased with the average dissolved oxygen tension at a constant specific energy dissipation rate (1.0 W/kg). In the present parallel fermentations, the agitation intensity was the same in the different fermenters and the pellet size was comparable in the different fermenters. So, the increase of the biomass per pellet surface area as shown in Figure 11 can only be caused by the dissolved oxygen tension. The regression of the data of the present set of fermentations at 38 h and 61 h in Figure 11 gives Eq.(4).

$$m_{ps} = a_1 C_{O2}^{a_2} \qquad (a_1 = 0.07 \pm 0.01; \ a_2 = 0.33 \pm 0.03) \qquad \textbf{(4)}$$

where C_{O2} is the dissolved oxygen tension (kg/m^3), m_{ps} is the biomass per pellet surface area (kg/m^2) and a_i is the coefficient.

The data of our previous parallel fermentation are plotted in Figure 11 as well. The previous data match well with the present, despite the large difference in stirrer speed and the variation of pellet size in the earlier data. This confirms the former assumption that the biomass per pellet surface area is a function of the dissolved oxygen tension and it is independent of mechanical forces. From Figure 8b, we know that the pellet size of the previous fermentations at 41 h varied from 1.5 to 2.5 mm corresponding to a power input of 5.7 - 0.2 W/kg. Hence, the biomass per pellet surface area appears to be independent of pellet size. The regression of all the data in Figure 11 leads to a similar result as given in Eq.(4).

The increase of agitation intensity results in the increase of turbulent intensity and convective flow in a stirred vessel. Therefore, further interpretation of Figure 11 is that molecular diffusion is the dominant mechanism for oxygen transfer within pellets of the submerged fermentations. Turbulent diffusion and convective flow hardly occur within pellets. This supports the results from Cronenberg et al. (1994), Ngian and Lin (1975), and Huang and Bungay (1973) and differs from those of Wittler et al. (1986) and Miura et al. (1975). An exception may occur for pellets with a very high porosity. The pores in these pellets are so large and the pellets are so less rigid that deformation and convective flow in them may occur. This could influence the internal mass transfer.

The biomass per wet pellet volume is expected to be a function of the dissolved oxygen tension as well. From Eq.(4) and the relationship between the biomass per wet pellet volume and the biomass per pellet surface area, Eq.(5) can be derived.

$$\rho_{WPV} = 6\frac{m_{ps}}{d_p} = \frac{a_3}{d_P}C_{O2}^{a_2} \qquad (a_3 = 0.42\pm0.06) \qquad (5)$$

Where C_{O2} is the dissolved oxygen tension (kg/m^3), m_{PS} is the biomass per pellet surface area (kg/m^2), d_P is the diameter of the pellets (m) and ρ_{WPV} is the biomass per wet pellet volume (kg/m^3).

This equation states that smaller pellets under a higher dissolved oxygen tension have more biomass per wet pellet volume. The pellet size is a function of mechanical forces which is related to the agitation intensity. Therefore, the biomass per wet pellet volume is a function of both the dissolved oxygen tension and agitation intensity. The biomass per wet pellet volume is calculated from the total biomass and total wet pellet core volume in the 300 pellets. Based on Eq.(5), the data of the two sets of parallel fermentations (the previous one and the present one) are plotted in Figure 12. One fermentation was run at a constant agitation intensity and with varying dissolved oxygen tension. The other was carried out with varying agitation intensities and different corresponding dissolved oxygen tensions. Figure 12 shows that the biomass per wet pellet volume is correlated well by the variable of $C_{O2}^{0.33}/d_p$. Eq.(5) is plotted in Figure 12. Comparison of the data from the two sets of parallel fermentations with Eq.(5) shows good agreement. The two sets of data match each other as well, although the two were performed in different ways and different precultures were used.

A physical explanation for Eq.(5) is that the biomass per wet pellet volume is proportional to the amount of oxygen transferred into pellets per pellet volume. The amount of the oxygen transferred per pellet volume increases with the driving force of oxygen transfer in the pellets and the specific area of pellets. A higher bulk dissolved oxygen tension leads to a large
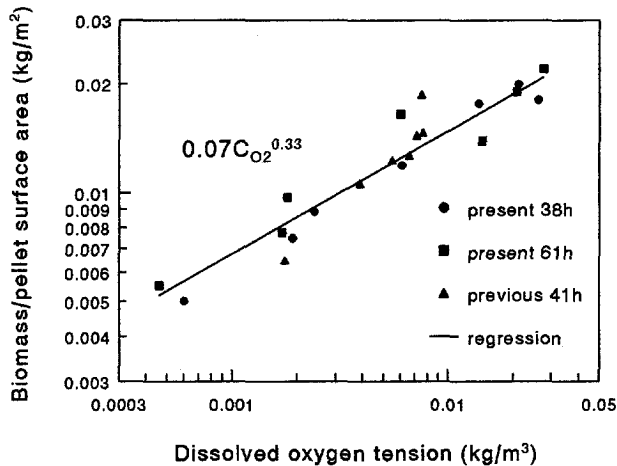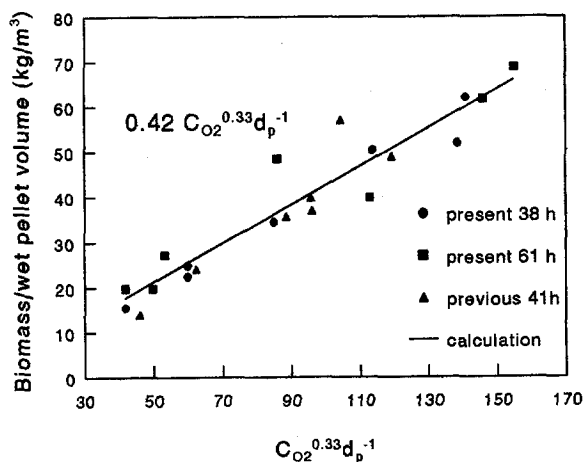
Figure 12. Biomass per wet pellet volume from the parallel batch fermentations run at different dissolved oxygen tension but at the same specific energy dissipation rate (see Table II) and from our previous parallel batch fermentations run at different specific energy dissipation rates.

driving force for internal oxygen transfer in the pellets. Smaller pellets have a relatively large specific surface area. Therefore, smaller pellets grew at a higher dissolved oxygen tension have more biomass per wet pellet volume. In our previous study the biomass per wet pellet volume was found to increase with specific energy dissipation rate. The reason of that is clear now. The higher agitation intensity led to a higher dissolved oxygen tension and a smaller pellet size.

In general, the dissolved oxygen tension is influenced by the oxygen consumption rate, the specific energy dissipation rate, the rheology of the broth, the oxygen concentration in the gas phase and the gas flow rate. This implies that for the same specific energy dissipation rate, the biomass per wet pellet volume could be different. So Eq.(5) is a more precise correlation than the one in our previous work.

The tensile strength of the pellets should increase with the biomass per wet pellet volume (Cui et al., 1997). Because the biomass per wet pellet volume is a function of the dissolved oxygen tension and pellet size, the strength of the pellets will be a function of the dissolved oxygen tension and pellet size as well. This means that higher dissolved oxygen tensions and larger mechanical forces lead to the formation of stronger pellets.

From the data of the dry biomass per wet pellet volume, it can be estimated how dense the pellet structure is. Using the same assumptions as in our previous work, namely that the wet hyphal density is 1100 kg/m^3 and the water content in the wet hyphae is 80%, the internal average porosity in the pellets can be calculated by

$$\epsilon_W = 1 - \frac{\rho_{WPV}}{0.2\,\rho_h} \qquad (6)$$

Combining of Eq.(5) and Eq.(6) gives

$$\epsilon_W = 1 - a_4 \frac{C_{O2}^{a_2}}{d_P} \qquad (a_4 = 0.0019 \pm 0.0003) \qquad (7)$$

Eq.(7) was compared with the pellet porosity calculated from dry biomass per pellet volume of the present and previous sets of parallel fermentations. The results showed that Eq.(7) matched the data well and $C_{O2}^{0.33}/d_P$ was a good group of variables for the description of the pellet porosity. Because Eq.(7) and the pellet porosity were derived from Eq.(5) and biomass per wet pellet volume, respectively, the conclusion for the biomass per wet pellet volume can be passed to the pellet porosity (actually, $1-\epsilon_w$). The pellet porosity is thus a function of the dissolved oxygen tension and pellet size. Because the energy dissipation rate influences both the dissolved oxygen tension and the size of the pellets, it affects the porosity of the pellets as well. Based on the same reasoning as for the biomass per wet pellet volume, the porosity of the pellets correlates better with the dissolved oxygen tension and pellet size than with the specific energy dissipation rate. Eq.(7) shows that again the amount of oxygen transferred into the pellets per pellet volume is the dominant mechanism. For the same size of pellets, the porosity decreases with increasing dissolved oxygen tension. For the same dissolved oxygen tension in fermentations, the smaller pellets have lower porosity.

Fig.13a shows the fraction of filamentous mycelia in the total biomass, obtained at a constant specific energy dissipation rate, against the dissolved oxygen tension. The fraction was about 30%. The level of the dissolved oxygen tension did not show an obvious effect on this fraction when it varied from 5 to 250% of air saturation. However, at the highest dissolved oxygen tension (about 330%) the fungi formed very dense pellets (the most dense pellets in Fig.12) and the fraction of free mycelium was close to zero, which differed from the rest of the observations. Dion et al. (1954) reported that aeration with pure oxygen in *P. chrysogenum* fermentation resulted in a quite different appearance of the mycelium compared to aeration with air. The hyphae became thickened, more branched, and shorter. Vecht-Lifshitz et al. (1989) stated that the hydrophobicity of cell walls increased with oxygen
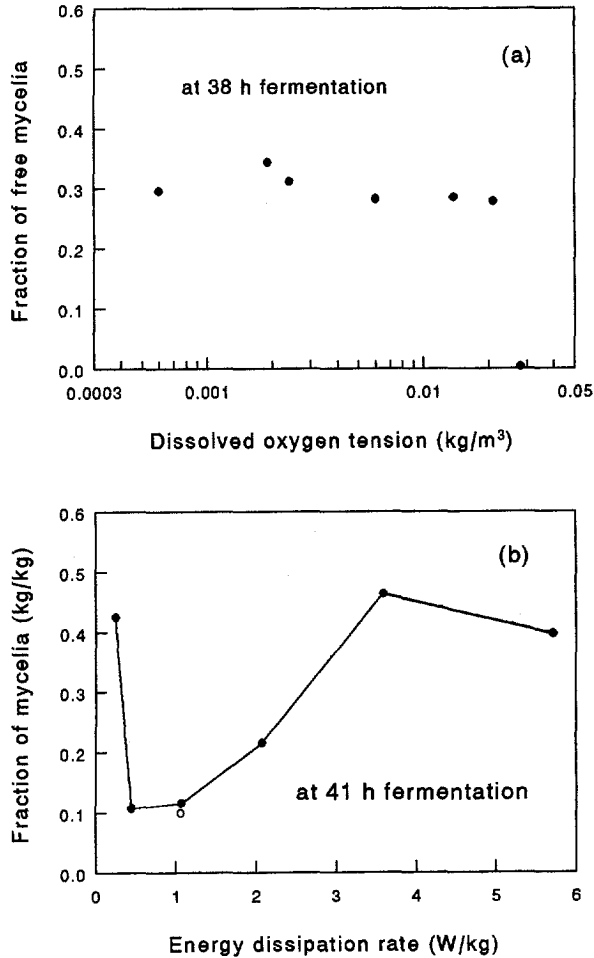
Figure 13. Fraction of free filamentous mycelial mass in the total biomass from the parallel batch fermentations. **a:** rub at different oxygen fractions in inlet gas but at the same specific energy dissipation rate (see Table II). **b:** run at different specific energy dissipation rates from our previous parallel batch fermentations. The open marker is from a duplicate fermentation.

tension, which enhanced the cellular aggregation. If one considers a pellet as an aggregation of filamentous mycelia, then a higher pellet fraction in the total biomass would be expected at a higher dissolved oxygen tension. Figure 13a shows that the dissolved oxygen tension in the range of 5-250% hardly influenced the fraction, but at a dissolved oxygen tension of about 330% the pellet fraction was about 1, which seemed to agree with Vecht-Lifshitz et al. (1989). The fraction of free filamentous mycelia from our previous experiments is plotted against the specific energy dissipation rate in Figure 13b. The data in Figure 13a and 13b

agree well for the specific energy dissipation rate of 1.0 W/kg. As reported in our previous study, the fraction increased with increasing specific energy dissipation rate. Figure 1 shows that the different specific energy dissipation rate in the previous parallel fermentations resulted in a different dissolved oxygen tension as well. From Figure 13a we know that the dissolved oxygen tension hardly influences the fraction of free filamentous mycelia when the dissolved oxygen tension is in the range of 5-250% of air saturation. Therefore the change in the fraction of free mycelium with the specific energy dissipation rate is most likely due to mechanical forces. The mechanical forces increase with increasing specific energy dissipation rate. The conclusion is that the fraction of free filamentous mycelia is a function of the agitation intensity and less or not dependent on the level of dissolved oxygen tension in the bulk.

From the above results and discussion, we come to the following hypothesis. The extension and branching of hyphae of pellets at the surface are restricted by mechanical forces, and the extension and branching in internal pellets are limited by the amount of available dissolved oxygen in a submerged fermentation. The increase of pellet sizes is controlled by the extension and branching of hypha at surface in the radial direction. Because the dissolved oxygen is available in the bulk under the studied conditions, the extension and branching are only affected by mechanical forces and are independent of the dissolved oxygen tension in the bulk. Therefore, pellet size is only related to the agitation intensity (mechanical forces) and not to the dissolved oxygen tension. The biomass per pellet surface area is a function of the extension and branching of hyphae within the pellets. Mechanical forces can be neglected and the amount of available oxygen is limited in the pellets. So, the extension and the branching within the pellets are influenced only by the dissolved oxygen tension, which explains that the biomass per pellet surface area is only a function of the dissolved oxygen tension. Based on this hypothesis, the biomass per wet pellet volume and the pellet porosity can be explained as a function of the dissolved oxygen tension and pellet size. The agitation of the impellers in a stirred bioreactor creates mechanical forces that shave hyphae off from the pellets. Because the filamentous mycelium in the bulk grow without dissolved oxygen limitation and the hyphae shaved from pellets contribute to the free filamentous mycelium mass, the fraction of filamentous mycelia in the total biomass rises with increasing agitation intensity. The dissolved oxygen tension has no obvious influence on this fraction. An exception is that the fraction drops to zero when the oxygen level is about 330% of air saturation. Observation of the fermentation shows that the broth suspension consists of dense pellets and clear medium. The explanation may be a physiological one.

CONCLUSION
The parallel fermentations of *A. awamori* were performed at different dissolved oxygen tension but at the same agitation intensity (1.0 W/kg). In the previous study, the parallel

fermentations were run at different agitation intensities (0.2-5.7 W/kg). The comparison of these two led to a better understanding of the relation between fungal morphology and operation conditions. Increasing agitation intensity enhances the mechanical forces that act on the fungal cells as well as G-L mass transfer. Pellet size and hairy length in a submerged fermentation were controlled by mechanical forces. The dissolved oxygen tension hardly had an effect on these. The filamentous mycelial fraction in the total biomass increased with increasing agitation intensity. Mechanical forces resulted in the chipping off of hyphae from the pellets. The chipped hyphae reseeded the free filamentous mycelia. The dissolved oxygen tension did not show obvious effects on this fraction, with the exception that this fraction was zero at the dissolved oxygen tension of 330% of air saturation.

The biomass per pellet surface area was found to be determined only by the dissolved oxygen tension. Mechanical forces hardly affected this parameter. Therefore, molecular diffusion was the dominant mechanism for oxygen transfer in the pellets and the turbulent diffusion and convective flow could be neglected. The biomass per wet pellet volume or pellet density was a function of both the dissolved oxygen tension and the pellet size. Higher dissolved oxygen tensions led to the formation of denser pellets. With the same dissolved oxygen tension, smaller pellets had a denser structure. The porosity of pellets was rather large and varied in the range of 90 - 70% within the experimental conditions used. The porosity decreased with increasing dissolved oxygen tension and decreasing pellet size.

NOMENCLATURE

a_i	: coefficient (i = 1 - 4)	-
B_f	: width of baffles	m
C_d	: distance between two impellers	m
C_{O2}	: dissolved oxygen tension in the bulk	kg m^{-3}
D	: diameter of impellers	m
D_{eff}	: effective diffusion coefficient of oxygen in pellets	m^2 s^{-1}
D_m	: molecular diffusion coefficient of oxygen in pellets	m^2 s^{-1}
d_p	: diameter of pellets	m
d_{crit}	: critical diameter of pellets	m
H	: level of liquid in stirred bioreactor	m
L_h	: hairy length of pellets	m
m_{PS}	: dry biomass per pellet surface area	kg m^{-2}
R_{O2}	: volume oxygen consumption rate in pellets	kg m^{-3} s^{-1}
T	: diameter of the stirred vessel	m

Greeks

ϵ	: specific energy dissipation rate	W/kg
ϵ_W	: porosity in pellets	%

ρ	: density of fluid	kg m^{-3}
ρ_{wp}	: dry biomass per wet pellet volume	kg m^{-3}
ρ_h	: density of hyphae	kg m^{-3}

References

Ayazi Shamlou, P., Makagiansar, H.Y., Lilly, M.D., Thomas, C.R., 1994, Turbulent breakage of filamentous microorganisms in submerged culture in mechanically stirred bioreactor, *Chem. Eng. Sci.,* **49**, 2621-2631.

Carlsen, M., Spohr, A.B., Nielsen, J., Villadsen, J., 1996, Morphology and physiology of an α-amylase producing strain of *Aspergillus oryzae* during batch cultivations, *Biotechno. Bioeng.,* **49**, 266-276.

Clark, D.S., 1962, Submerged citric acid fermentation of ferrocyanide-treated beet molasses: morphology of pellets of Aspergillus niger, *Can. J. Microbiol.,* **8**, 133-136.

Cronenberg, C.C.H., Ottengraf, S.P.P., Van den Heuvel, J.C., Pottel, F., Sziele, D., Schügerl, K, Bellgardt, K.H., 1994, Influence of age and structure of Penicillium chrysogenum pellets on the internal concentration profiles, *Bioproc. Eng.,* **10**, 209-216.

Cox, P.W., Thomas, C.R., 1992, Classification and measurement of fungal pellets by automated image analysis, *Biotechnol. Bioeng.,* **39**, 945-952.

Cui, Y.Q., Van der Lans, R.G.J.M., Luyben, K.Ch.A.M., 1997, Effects of agitation intensities on fungal morphology of submerged fermentation, *Biotechnol. Bioeng.,* **55**, 715-726.

Cui, Y.Q., Van der Lans, R.G.J.M., Luyben, K.Ch.A.M., 1996, Local power uptake in Gas-liquid systems with single and multiple Rushton turbines, proceeding of 14 international symposium on chemical reaction engineering, *Chem. Eng. Sci.,* **51**, 2631-2636.

Dion, W.M., Carilli, A., Sermonti, G., Chainl, E.B., 1954, The effect of mechanical agitation on the morphology of *Penicillium chrysogenum* thom in stirred fermenters, *Istituto Superiore di Sanita (Eng.ED),* **17**, 187-205.

Emerson, S., 1950, The growth phase in *Neurospora* corresponding to the logarithmic phase in unicellular organisms, *J. Bacteriol.,* **60**, 221-223.

Giuseppin, M.L.F., 1984, Effects of dissolved oxygen concentration on lipase production by *Rhizopus delemar*, *Appl Microbiol Biotechnol*, **20**, 161-165.

Kobayashi, T., Van.Dedem, G., Moo-Young, M., 1973, Oxygen transfer into mycelial pellets, *Biotechnol. Bioeng.*, **15**, 27-45.

Marshall, K.C., Alexander, M., 1960, Growth characteristics of fungi and actinomycetes, *J. Bacteriol.*, **80**, 412-416.

Metz, B, 1976, From pulp to pellets, Ph.D thesis of Technical University of Delft.

Miura, Y., Miyamato, K., Kanamari, T., Teramoto, M., Ōhira, N., 1975, Oxygen transfer within fungal pellet, *J. Chem. Eng. Jap.*, **8**, 300-304.

Ngian, K.F. and Lin, S.H., 1976, Diffusion coefficient of oxygen in microbial aggregates, *Biotechnol. Bioeng.*, **18**, 1623-1627.

Reichl, U., King, R., Gilles, E.D., 1992, Characterization of pellet morphology during submerged growth of *Streptomyces tendae* by image analysis, *Biotechnol. Bioeng.*, **39**, 164-170.

Sakurai, A., Imai, H., 1992, Effect of operational conditions on the rate of citric acid production by rotating disk contactor using *Aspergillus niger*, *J. Ferment. Bioeng.*, **73**, 251-254.

Schügerl, K., Wittler, R., Lorenz, T., 1983, The use of molds in pellet form, *Trends in Biotechnology*, **1**, 120-123.

Tramper, J., Van't Riet, K., 1991, Basic Bioreactor Design, Marcel Dekker, New York.

Trinci, A.P.J., 1970, Kinetics of the growth of mycelial pellets of *Aspergillus nidulans*, *Arch. Mikrobiol.*, **73**, 353-367.

Van Suijdam, J.C., Metz, B., 1981a, Influence of engineering variable upon the morphology of filamentous molds, *Biotechnol. Bioeng.*, **23**, 111-148.

Van Suijdam, J.C., Metz, B., 1981b, Fungal pellet breakup as a function of shear in a fermenter, *J. Ferment. Technol.*, **59**, 329-333.

Vecht-Lifshitz, S.E., Magdassi, S., Braun, S., 1989, Pellet formation and cellular aggregation in *Streptomyces tendea*, *Biotechnol. Bioeng.*, **35**, 890-896.

Vecht-Lifshitz, S.E., Ison, P. A., 1992, Biotechnological applications of image analysis: present and future prospects, *J. Biotechno.*, **23**, 1-18.

Wecker, A., Onken, U, 1991, Influence of dissolved oxygen concentration and shear rate on the production of pullulan by *Aureobasidium pullulans*, *Biotechnology letters*, **13**, 155-160.

Wittler, R., Baumgart, H., Lübberts, D.W., Schügerl, K., 1986, Investigations of oxygen transfer into *Penicillium chrysogenum* pellets by microprobe measurements, *Biotechnol. Bioeng.*, **28**, 1024-1036.

Zetelaki, K., and Vas, K., 1968, The role of aeration and agitation in the production of glucose oxidase in submerged culture, *Biotechnol. Bioeng.*, **10**, 45-59.

CHAPTER 6

Influence of Fermentation Conditions and Scales on the Submerged Fermentation of *Aspergillus awamori*

Y.Q.Cui, R.G.J.M. van der Lans, K.Ch.A.M. Luyben

Abstract

Aspergillus awamori is an interesting fungus for the industrial production of enzymes. To generate essential information, fermentations with this organism (CBS 115.52) were performed under various conditions. Experiments on autolysis showed that fungal cells autolysed seriously under depletion of substrate or oxygen. Its rate depended on both temperature and agitation. The ratio of the biomass production to the sum of biomass production and carbon dioxide production in time is used for deriving the yield and maintenance coefficient. This ratio can be used to estimate the biomass concentration from the CO_2 production on line as well. Pellets were the dominant morphology for most of the fermentations performed. The hairy length of the pellets first increased with time and then decreased. At a comparable specific energy dissipation rate, in the larger scale fermenters pellets had a larger hairy length than in the smaller. The fraction of pellet biomass in the total biomass decreased with time at the beginning of the fermentations (0-20 h) and then reached a more or less stable value. Both counting the number of pellets during the fermentations and observing pellets under agitated but non-growth conditions indicated that formation and breakage of pellets hardly occurred under the studied conditions.

Keywords: *Aspergillus awamori*; kinetics; morphology; scale; agitation intensity; stirred vessels.

INTRODUCTION

Aspergillus awamori has been used industrially for the production of enzymes such as glucoamylase, α-amylase, and protease.[1] In literature, much effort has been made on the possible use of this species for the production of other enzymes, such as xylanase,[2, 3] protopectinase,[4] chymosin[1,5]. The production level of one particular protein can be several tens of grams per litre of culture medium. For example, *Aspergillus awamori* can secrete more than 20 g/L of glucoamylase.[1] Another important advantage is that the organism has a long history of safe use for the manufacture of food products destined for human consumption and is regarded as nontoxigenic and nonpathogenic. Most works on *Aspergillus awamori*[6,4,3,1] are focused on strain improvements for a specific product since strain improvement has proved to be a powerful tool to increase the productivity of a given product. Once a strain is improved, production has to be carried out by fermentation. Fungal fermentation is widely recognized as a complex process in which numerous problems occur. Scale up and optimization of this process still rely on empiricism and tradition. Viscous and non-Newtonian media, bad mixing, poor mass transfer and difficulty in the control of morphology are common problems encountered in large scale fungal fermentations. This is irrespective of the kind of products. So knowledge on fungal fermentation, such as morphology, kinetics and operation parameter effects on fungi, is needed to understand and perform this fermentation properly on both small and large scales. However, this kind of information is scarce in literature.

The objective of this research was to generate essential information for *Aspergillus awamori* fermentations. Fermentation time profiles, kinetics (growth, maintenance, autolysis, yield, respiration), morphology development (pellet size, hairy length, fraction of free mycelial mass in the total biomass), the effects of operation parameters on growth and morphology and the mechanisms of the interaction between mechanical forces and pellets were studied. It is expected that the obtained information is relevant to other fermentations with filamentous microorganisms. *Aspergillus awamori* (CBS 115.52) was chosen as model strain. Batch fermentations using different substrates (glucose, sucrose) were performed under various conditions.

EXPERIMENTAL

Cultures of *Aspergillus awamori* (CBS 115.52) were maintained and spores produced on standard potato dextrose agar. The composition of the synthetic media used is given in Table I. Either a seed culture or a spore suspension were used for the inoculation of the

fermentations. The medium composition of the seed culture was the same as that of the fermentation medium. For the sterilizations steam was used which went through the medium in the fermenter. Part of this steam condensed in the medium during sterilization. Therefore the actual initial concentration of the medium might be not exactly the same as that given in table I due to different amounts of condensed water at each sterilization.

Table I. Synthetic fermentation medium

Ingredient	concentration	
Sucrose or Glucose	10	g/L
NH_4Cl	9.0	g/L
KH_2PO_4	1.5	g/L
$NaNO_3$	1.0	g/L
$MgSO_4.7H_2O$	1.0	g/L
$Cacl.2H_2O$	0.3	g/L
Yeast Extract	1.0	g/L

The fermentations were carried out in three different fermenters. The working volumes were 2, 15 and 100 L. The fermenter geometries are given in Table II. The fermenters with 2 and 100 L working volume were equipped with Rushton turbines. The fermenter with 15 L working volume had one stirrer with six tall blades instead of Rushton turbines. A torque meter was mounted into the shaft of this fermenter so that the power input could be measured.

Table II: Geometries of fermenters in used.

Terms	fermenter1	fermenter2	fermenter3
working volume of fermenter (V) in L	100	2	15
diameter of fermenter (T) in mm	395	130	215
number of impeller	3	2	1[†]
top impeller (D) in mm	130	45	
middle impeller (D) in mm	130		
bottom impeller (D) in mm	174	45	

†: a special stirrer with six tall blades (height: 305 mm, diameter: 140 mm)

The seed cultures were carried out in 2 L shaking flasks. The procedure of making the seed cultures in shaking flasks was as follows. The shaking flasks were filled with 500 ml or 400 ml of the medium. The flasks with the medium were first sterilized and then a certain amount of a spore suspension with a known concentration was added. The flasks were rotated in a rotary shaker at 200 rpm for 24 hours. The temperature was kept at 25 °C. The obtained precultures were inoculated into the fermenter. The set point of temperature was 25 °C. The pH was maintained at 4.5, using ammonia and phosphate. Antifoam was added if needed. Different stirrer speeds were used for different fermentations. The specific energy dissipation rates in the used gassed multi-impeller systems were estimated by calculation.[7]

Samples were taken during the fermentations. A part of the sample was used to determine the morphology. Another part was spun down to separate the solid biomass from the supernatant. With synthetic medium the initial fungal morphology obtained in the preculture was pellets. The pellet core size and hairy length of pellets were measured by means of image analysis.[8] At least 250 objects were analyzed for each sample. The biomass concentration (BM) and the fraction of free filamentous mycelia or pellets in the total biomass were determined in terms of dry biomass.[8] The number of pellets in a given amount of sample (20 ml) was counted by eye. From this the pellet number per volume in the fermentation broth was calculated. The concentrations of sucrose, glucose and fructose in the supernatant were determined by means of HPLC. A Bio. Red HPX 87N column was used at 85°C. The eluent was 15mM of Na_2SO_4 aqueous solution at a speed of 0.6 ml/min. The amount of injection was 10 μl. The total organic carbon contents (TOC) in the supernatant was measured by means of a DC-190 system, a product from DOHRMANN DIVISION, which featured a vertical quartz combustion tube packed with supported platinum catalyst. The furnace was maintained at 680 °C. Respiration data, DO_2, the addition of NH_4OH and H_3PO_4 were measured and registered during the fermentations.

An overview of media, size and type of the inoculations, fermenters and operation conditions used in the fermentations of this study are described in Table III. In total 15 fermentations with synthetic medium were run. Fermenter size, agitation intensity, substrate type, inoculation and oxygen concentration in the in-let gas were varied.

Table III: Fermentation description. Precultures were normally cultivated in shake flasks.

Fermentation code	medium	fermenter L	spore Sp/mL	ϵ W/kg	stirrer speed rpm	aeration L/min	morphology	remark
F1	glucose	100	$2.7\ 10^3$	1.3	300	18	P + M	
F2	glucose	100	$1.2\ 10^4$	1.3	300	18	P + M	
F3†	glucose	100	$2.1\ 10^4$	3.1	400	9	M	spore suspension
F4	glucose	100	$2.5\ 10^4$	3.1	400	9	M	
F5	sucrose	100	$1.2\ 10^3$	0.4	200	9	P + M	
F6	sucrose	100	$1.7\ 10^3$	0.8	250	9	P + M	
F7	sucrose	100	$1.5\ 10^3$	0.8	250	9	P + M	
F8	sucrose	100	$1.0\ 10^3$	3.1	400	9	M + P	
F9	sucrose	2	$6.3\ 10^3$	0.45	450	0.3	P + M	parallel
F10	sucrose	2	$6.3\ 10^3$	1	600	0.3	P + M	parallel
F11	sucrose	2	$6.3\ 10^3$	3.6	900	0.3	M + P	parallel
F12	sucrose	15	$2.8\ 10^3$	1	200	1.5	P + M	special fermenter
F13	sucrose	15	$9.5\ 10^3$	1	200	1.5	P + M	special fermenter
F14	sucrose	15	$1.8\ 10^4$	1.2	233	1.5	P + M	special fermenter
F15	sucrose	15	$1.5\ 10^3$	0.3	150	1.5	P + M	special fermenter

* : the fermentations in parallel were run parallel with different agitation intensitiesis.
P: stands for pellets; M: stands for free filamentous mycelia.
P + M : broth contains both pellets and free filamentous mycelia but pellets are dominant (>50%).
M + P : broth contains free filamentous mycelia and pellets but free filamentous mycelia are dominant (>50%)
† : Spore suspension was used as an inoculum in F3.

Two so-called cold mode experiments or dispersion experiments were carried out as well. Pellets were obtained and sieved from the broths (after 25 h of fermentation) of F5 and F15, respectively. The used fraction of pellets was between 2 and 2.6 mm sieves. The obtained pellets were put into the 15 L fermenter filled with the corresponding supernatant. The suspension was agitated at a specific energy dissipation rate of 2.1 W/kg. The temperature was kept at 25 °C. At regular intervals samples were taken. The pellet diameter was measured.

For convenience, the concept of the carbon mole was used and expressed as Cmol. It is the amount of substance which contains one mole of the element carbon.[9] The molar mass of *Aspergillus awamori* was assumed to be 25 g/Cmol which is the same as for yeast.

RESULTS AND DISCUSSION

General observations
Biomass decay during storage
It was found that the dry biomass concentration decreased when substrate or oxygen was depleted during a fermentation. To verify if this also happened during sample storage, experiments on biomass decay at three different conditions were carried out. The measured data are plotted against time in Fig.1. Decay was observed during the storage of samples at all tested conditions. The first was storage in a refrigerator at 4°C. The second was storage in a stirred fermenter where substrate was still available. Temperature and pH in this fermenter were maintained at fermentation conditions but inlet air was replaced by nitrogen gas. The third was storage in a bottle at a temperature of 22-25°C. The dry biomass concentration decreased quickly with storage time in all cases. This means that the composition of the supernatant of the samples changed also during its storage. Therefore, spinning down of the samples and subsequent dry biomass measurements were done immediately after a sample was taken.
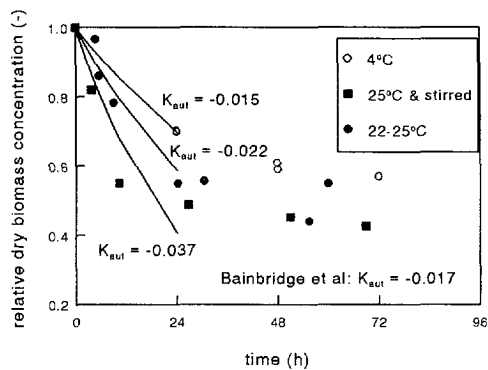

Figure 1. Decay of biomass during storage

In literature, autolysis kinetics of fungal cells of *Aspergillus nidulans* and *P. chrysogenum* has been reported as exponential.[10,11] This does not hold for our data with *Aspergillus awamori*. The autolysis constants obtained from regression depended on the chosen time period. A long time period gave a lower absolute autolysis constant than a shorter time period. The data in Fig.1 suggest two subsequent regimes, one of fast decay and the other of slow decay. This may be caused by the slow decay of the cell wall mass since the cell wall is strong and hard to be degraded. The decay in the first 24 hours was dominated by the fast leaking of cell contents out of the cells. This period is considered to be relevant for cell lysis and was used to determine the autolysis constants. The obtained autolysis constants were -0.015 h^{-1}, -0.022 h^{-1} and -0.037 h^{-1} for the respective conditions (Fig.1). Decay of biomass at 22-25°C was faster than at 4°C. Physical and chemical processes are faster at a higher temperature and this will lead to a faster decay of dry biomass at a higher temperature. Agitation can injure or damage the cells. Under starvation conditions, the cells are expected to become weaker and more vulnerable to mechanical forces. Mechanical damage will enhance leaking of cytoplasm from the cells. Another effect may be the ageing of cells. It was reported[12] that the size of vacuoles increased in hyphal cells with fermentation time. Therefore younger cells are expected to be stronger than older cells. The conclusion is that the autolysis constant is not a real constant, but will depend on chemical, physical and physiological conditions. The autolysis constants for unstirred conditions may be representative for fungal lysis within a pellet and the autolysis constants for stirred conditions for the filamentous mycelial autolysis during a fermentation.

Bainbridge et al.[11] measured the biomass decay of *Aspergillus nidulans* at 30 $^{\circ}$C in a stirred vessel where glucose was depleted but other cell nutrients were present in excess. Regression of their data resulted in an autolysis constant of -0.017 h^{-1} which is in line with the present observation.

Fermentation profile

Fig.2a shows a typical time course of biomass concentration (BM), sugar concentration, cumulative base and acid addition and respiration rate. The concentrations of biomass, sucrose, glucose, fructose and total sugar are depicted in Fig.2b. The results lead to the following remarks: I. CO_2 production rate was almost equal to oxygen consumption rate. In other words their ratio, the respiratory quotient (RQ), was about 1. II. During the fermentations with sucrose, sucrose was split into glucose and fructose. *Aspergillus awamori* first used glucose, then fructose. III. When the reducing sugar was used up, growth stopped. IV. Growth of biomass was accompanied by base consumption. Thereafter acid was consumed.
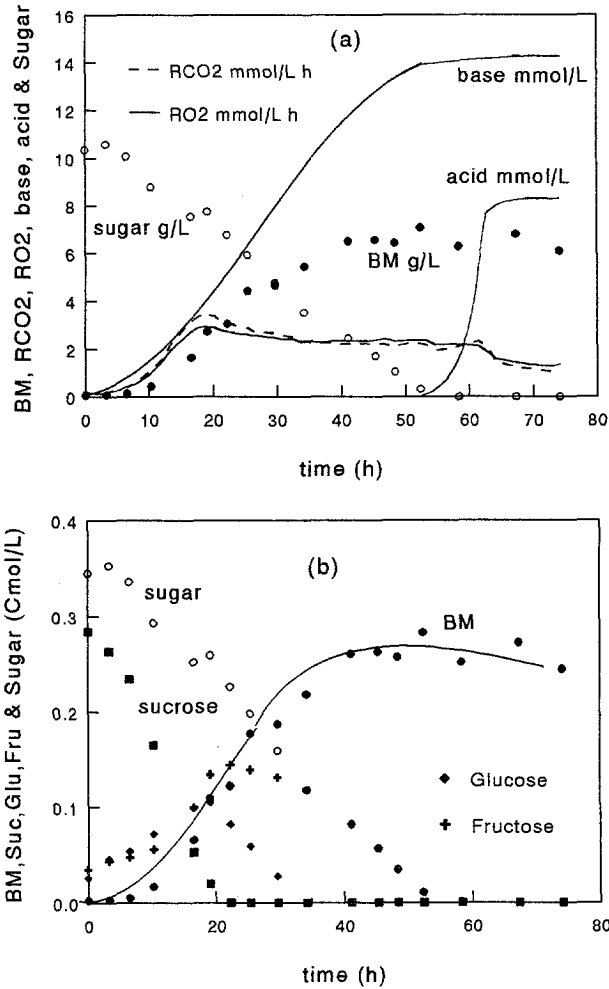
Figure 2. General course of fermentations. **a**: biomass grow, sugar consumption, base and acid addition and respiration; **b**: biomass, sucrose, fructose and Red. sugar (fermentation F5).

Reproducibility of fermentation and image analysis

Fig.3a shows a comparison of the two fermentations F6 and F7 which were performed under the same operation conditions. The time profiles of the biomass concentrations were very similar to each other. The biomass concentration of F6 was a little bit lower than that of F7. The decrease in sugar concentration was rather similar in the two fermentations except for a slightly higher initial sugar concentration in F7, which corresponds with the higher biomass
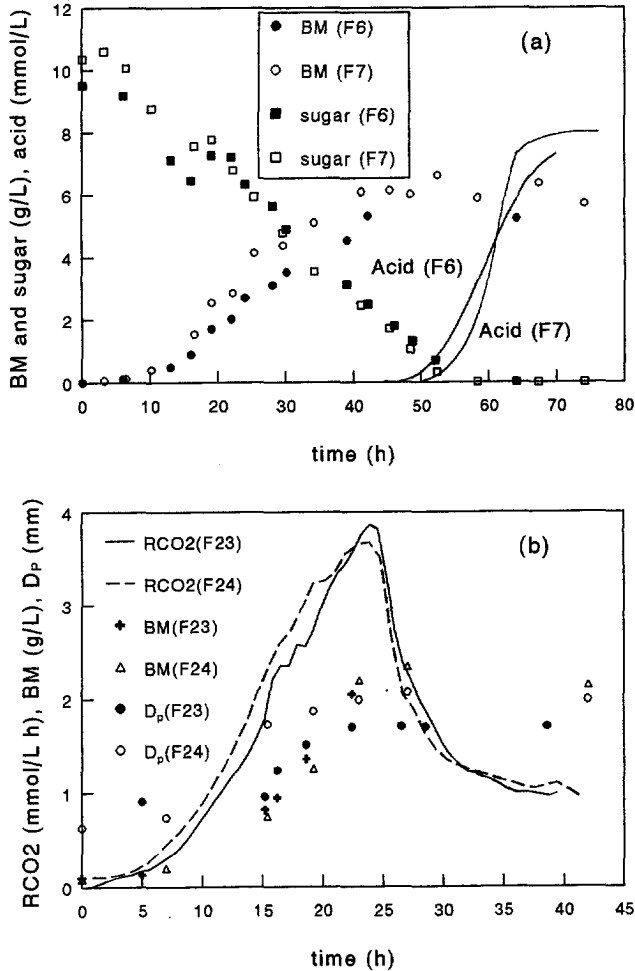
Figure 3. a: Reproducibility of biomass growth, sugar consumption and acid addition in duplo's fermentations, which were run at 250 rpm and in 100 L fermenter (F6 and F7). **b**: reproducibility of CO_2 production rate, biomass concentration and pellet size at 200 rpm in 15 L fermenter (F12 and F13).

concentration of this fermentation. This difference in initial concentration was due to water condensation during medium sterilization. Fig.3a shows that the addition of acid in F6 occurred a little bit earlier than in F7. These data show that the reproducibility of biomass concentration, sugar consumption and use of acid was good. Another set of data from duple fermentations, in the 15 L fermenter, are shown in Fig.3b. Biomass growth and CO_2 production rate were very comparable in these two fermentations, but pellet size differed

about 20-40% although the same agitation intensities were used. The reproducibility in fungal morphology appeared to be less good.

The less good reproducibility in fungal morphology may be caused either by a poor reproducibility in the morphology measurement or a poor reproducibility of the fermentations with respect to morphology. In literature, an increasing number of publications on the application of image analysis techniques [13,14,15,12] in fungal fermentations can be found. However, there is hardly any information on the reproducibility of such an analysis. To check the effect of the individual researcher on the quantification of the morphology, image analysis of samples from fermentation F7 was carried out by two researchers. In this case pellet size measured by different researchers was comparable. The measured hairy length of pellets differed about 20%. Measurements repeated by the same researcher were almost identical. Hence the limited reproducibility in morphology was not caused by the measurement method.

So the reproducibility of the morphology in the fermentations was limited. One of the reasons was that it was very difficult to control exactly the same start conditions for different fermentations. Analysing the results further, it appeared that the preculture had a strong effect on the pellet morphology which developed in the fermentations. Many variables influence spore germination, spore coagulation and pellet formation. The same number of spores will not always result in the same number of pellets. Cultivation of precultures that are seemingly treated in the same way may develop a totally different morphology. However, the reproducibility of biomass growth, sugar consumption and base and acid addition was good. A method to overcome the poor reproducibility in morphology is using identical precultures by running parallel fermentations.[8]

Carbon balance
The carbon balance was verified for the fermentations of F3 and F7. For the balance, carbon in biomass (equal to biomass concentration in Cmol/L), total organic carbon (TOC) in the medium or sugar carbon in the medium and carbon dioxide (Accum.CO_2) in the off-gas were taken into account. The results are depicted in Fig.4. In F7 (Fig.4a), the dominant morphology during the fermentation was pellets and sucrose was used as carbon source. In F3 (Fig.4b), free filamentous mycelia were dominant and glucose was used as carbon source. The figures show that the sum of carbon in biomass, CO_2 and carbon source (TOC in F7 and glucose in F3) was almost constant during the fermentations. This means that 1) the amount of possible by-products formed was negligible; 2) the data of TOC, BM, CO_2 and sugar had a good accuracy. In Fig.4a the reducing sugar concentration is presented as well. The comparison of organic carbon concentration and reducing sugar concentration (Red. sugar) shows that the total organic carbon was almost equal to the carbon in the sugars.
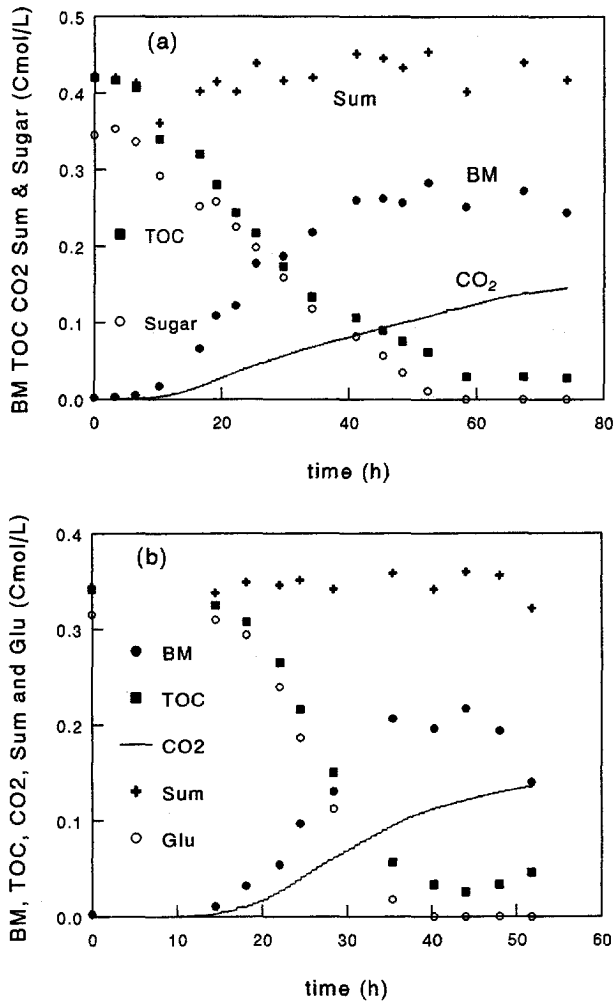
Figure 4. Carbon balance in two fermentations run at different conditions. **a**: F7 (250 rpm, sucrose as substrate and pellets dominant morphology; **b**: F3 (400 rpm, glucose as substrate and free filamentous mycelia dominant morphology).

Growth kinetics

Agitation effects on growth

Fig.5a depicts the dry biomass concentration of several fermentations against time. The plot shows that the fungi grew faster at higher stirrer speeds (F7: 250 rpm and F8: 400 rpm) than at a lower one (F5: 200 rpm). Fungal growth rate at 400 rpm was, however, not much different from that at 250 rpm. Power input is related to gas-liquid mass transfer rate so it
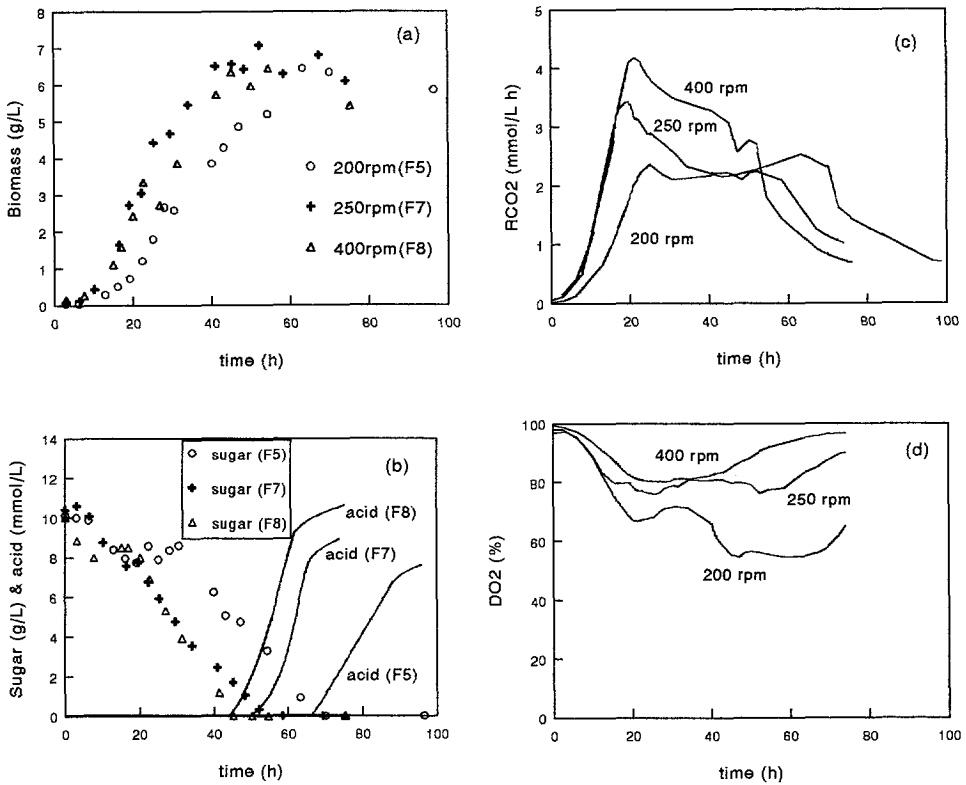
Figure 5. Time profile of several variables in three fermentations run at different conditions.
a: biomass growth; b: sugar consumption and acid addition; c: carbon dioxide production rate;
d: dissolved oxygen tension.

affects the dissolved oxygen tension in the bulk. Mechanical forces due to stirrer power input
will influence fungal morphology, may influence its metabolism and can damage fungi. The
levels of dissolved oxygen tension corresponding with the different power inputs are plotted
in Fig.5d. This graph shows that the dissolved oxygen tension in the bulk was always higher
than 50% during all three fermentations although a lower stirrer speed led to a lower level
of the dissolved oxygen tension. This means that there was no oxygen limitation for free
filamentous mycelia and the outer layer of pellets. Internal limitation, however, may still
occur within the pellets. A higher level of dissolved oxygen tension in the bulk will diminish
the extent of this internal oxygen limitation. This may explain that a lower power input led
to slower growth. Mechanical damage of fungi would have resulted in a slower growth at a
higher stirrer speed. Agitation also affects the fraction of pellet mass in the total biomass. In

general, filamentous mycelia is reported to be the dominant morphology at a higher stirrer speed and compact pellets at a lower speed.[8,16] The form of fungal morphology influences growth as well. Filamentous mycelia do not have an internal limitation of substrate or oxygen so that their growth is faster. But they are more easily damaged, which will lead to a slow net specific growth rate. The close growth profiles of fermentation F8 and F7 may very well be the result of the balancing between difference in morphologies, difference in mechanical damage and difference in mass transfer limitation.

The time profiles of substrate consumption of these fermentations are presented in Fig.5b. The sugar consumption at 200 rpm was the slowest and the sugar consumption profiles of F7 and F8 were similar, which corresponds to the observations on biomass growth.

Fig.5b shows the profiles of acid addition as well. Acid consumption started earlier at a higher stirrer speed. This corresponds to the depletion of substrate and the end of the growth phase.

The CO_2 production rates at different agitation intensities in Fig.5c show that stronger agitation leads to a higher CO_2 production rate but during a shorter period of time. Estimating the area below each curve shows that the areas are approximately equal. This means that about the same amount of CO_2 was produced in those fermentations although different agitation intensities were used.

Growth rate
The total length of hyphae and the number of branches were reported to increase exponentially in the early growth of filamentous fungi.[17,18,19] Eq.(1) is often used for describing fungal growth.

$$R_X = \mu \, C_x \tag{1}$$

where R_X is the growth rate per volume [Cmol/L h], μ the biomass specific growth rate [h^{-1}] and C_X the biomass concentration [Cmol/L].

Microorganisms will grow at their maximum specific growth rate if optimal medium conditions are maintained. It was attempted to determine the maximum specific growth rate of *Aspergillus awamori*. However, as a result of oxygen limitation in pellets, cell autolysis, mechanical damage, cytoplasm leaking and the presence of inhibiting compounds in the broth it was difficult to do this accurately. Therefore, the apparent specific growth rate was determined in the present study instead of the theoretical maximum specific growth rate. Based on the time profile of the biomass concentrations measured in the fermentations of F3 -

F8, the apparent specific growth rate at about 20 h was found to be 0.19-0.25 h^{-1}. The type of substrate used (glucose or sucrose) did not show an obvious effect on this rate.

In literature, the maximum specific growth rate of *Aspergillus oryzae*[20] was reported to be 0.27-0.29 h^{-1}, 0.36 h^{-1} for *Aspergillu nidulans*[21] and 0.22 h^{-1} for *Aspergillus niger* calculated from the maximum respiration data[22,23] by assuming that the biomass yield per oxygen was 1 kg/kg. The measured apparent specific growth rate of *Aspergillus awamori* is comparable to these relevant species.

Yield and maintenance coefficients

In general, the carbon from a substrate may be converted into biomass, CO_2 and products. Analysis of organic products in the supernatant by means of HPLC showed that no products were formed. This was also concluded from the carbon balance analysis. Therefore the carbon in the consumed sugar must be equal to the sum of the carbon in the biomass and the carbon in CO_2. The ratio of biomass concentration to the sum of biomass concentration and specific off-gas carbon dioxide production will then be equivalent to the ratio of biomass concentration to the reduction of the sugar concentration. In the following the yield and maintenance coefficient will be obtained from the time course of this ratio. There are two reasons to do this instead of using the ratio of the biomass concentration to the reduction of the sugar concentration. First, measuring carbon dioxide is easy and on-line in most laboratory and industrial fermentations. Second, the substrate concentration is sometimes difficult to determine, for example when a complex substrate is used such as wheat bran.

Fig.6 shows the ratio as a function of time in the fermentations of F3, F4, F5, F7 and F8. In these fermentations, the specific energy dissipation rate was varied from 0.5 to 3.8 W/kg (see table III). Obviously, agitation intensity did not influence the ratio under the studied conditions. The use of different substrates (F3 and F4: glucose; F5, F7 and F8: sucrose) did not affect the ratio either. Also the morphology (free filamentous mycelia in F3 and F4 and pellets/mycelia in F5, F7 and F8) did not appear to have a noticeable effect (see table III). However, Fig.6 shows that the ratio decreased with time. This may have been caused by maintenance, cell autolysis or mechanical damage to the cells. The latter two are far less important since morphology (autolysis within pellets) and mechanical forces (damage to mycelia) did not affect the ratio (see both Fig.6 and Table III). So maintenance was probably the main reason to cause the decrease of the ratio in Fig.6. By assuming that only maintenance caused the ratio decline, the maintenance coefficient can be estimated from the data in Fig.6. A detailed derivation for this is given in the Appendix. Based on Fig.6 and the derivation, the yield of biomass on substrate, $Y_{SX} = 0.78\pm0.06$ Cmol/Cmol and the maintenance coefficient, $m_S = (0.0044\pm0.0008)/(0.78\pm0.06) = 0.0056\pm0.0015$ Cmol/Cmol h
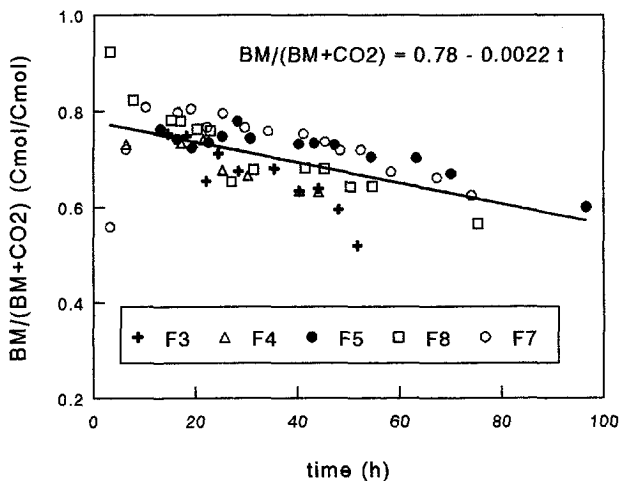
Figure 6. Ratio of biomass concentration to the sum of biomass concentration and accumulated carbon dioxide production as a function of time.

In literature, a yield value of 0.63 Cmol/Cmol for *Aspergillus awamori* on glucose at 25°C and 0.72 Cmol/Cmol for *Aspergillus nidulans* on glucose at 25°C were given by Roels[9]. Krzystek et al.[24] reported a yield value of 0.64 Cmol/Cmol for *Aspergillus niger* on sucrose at 32°C. The deduced yield of biomass on sugar with the present used strain was 0.78 ± 0.06 Cmol/Cmol which is higher than the ones from literature. This may indicate that the present strain was more efficient in biomass synthesis using sugar.

For *Aspergillus nidulans*, Roels[9] reported a maintenance on glucose of 0.016 Cmol/Cmol h. Righelato et al.[25] found a maintenance coefficient of 0.017 Cmol/Cmol h for *P. chrysogenum* on glucose at 25°C. Bainbridge et al.[11] used a maintenance coefficient of 0.0232 Cmol/Cmol h for *Aspergillus nidulans* on glucose at 30°C. Krzystek et al.[24] gave a maintenance coefficient of *Aspergillus niger* on sucrose of 0.026 Cmol/Cmol h at 32°C. The maintenance coefficient from this study was 0.0056 ± 0.0015 Cmol/Cmol h at 25°C. This is much lower. Therefore, the maintenance of this strain was rather low.

Respiratory quotient and yield and maintenance on oxygen

In fermentation F5 CO_2 production rate was almost the same as oxygen consumption rate (Fig.2a) so that the respiratory quotient, RQ value, was about 1. Similar values of RQ were found in the other fermentations as well. This indicates that the biomass reduction degree is probably the same as the used substrate (glucose or sucrose). It is about 4. Of course, this

is based on the condition that no product is formed or that the amount of possible by-products is negligible in comparison with the amount of biomass formation. Since the RQ-value equals about 1, the yield of biomass on oxygen $Y_{ox} = Y_{sx} / (1 - Y_{sx}) \approx 3.5$ Cmol/mol = 2.7 kg/kg. The maintenance coefficient on oxygen is about 0.0056 mol/Cmol h or 0.0072 kg/kg h.

Morphology

Morphology parameters studied in this work include pellet size, pellet density, hairy length of the pellets and the fraction of pellet mass in the total biomass. The emphasis will be on the development of these parameters in time. Pellet size is a common parameter studied in literature. The size is reported to decrease with agitation intensity.[26,27,8] Pellet density is an important parameter with respect to pellet internal mass transfer, tensile strength of pellets and the capacity of biomass production per volume in a given fermentation. The fraction of pellet mass in the total biomass is a morphology parameter and is related to the broth rheology. In a previous paper[8], the fraction was found to increase with agitation intensity. The hairy length of pellets is related to the surface structure of pellets. Higher agitation intensities will lead to a shorter hairy length of pellets.[8]

Pellet size
The core diameter of pellets in fermentations F5, F7 and F8 are depicted in Fig.7. The diameter increased rapidly during the first 20-30 h. Thereafter a more or less constant value is reached. Previous work with parallel fermentations[8] showed that the agitation intensity had a clear effect on pellet size. Fig.7 does not show a clear difference in pellet size at different agitation intensities. The fermentations in Fig.7 were carried out with different precultures. Therefore the sizes in Fig.7 are expected to be a result from both the difference in the agitation intensity and the difference in preculture.
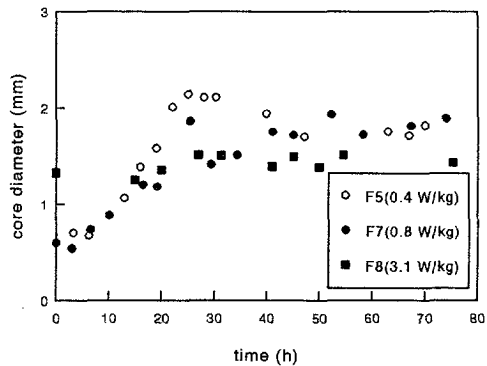

Figure 7. Time course of pellet core diameters in fermentations run at different agitation intensities in 100 L fermenter.

Hairy length of pellets

Time courses of the hairy length of pellets are given in Fig.8. First the hairy length increased and then it decreased slowly. This is rather similar to the time profiles of hyphal length of filamentous mycelia reported in literature [28,19]. Fungal pellet growth occurs by the extension and branching of hyphae in the outer zone of pellets. Extension of hyphae leads to an increase of the hairy length of pellets. However, the presence of mechanical forces restricts their length and the hyphae will be chipped off to some extent. Vacuole formation (Paul et al.[12]) will weaken the strength of hyphae and lead to a shorter hairy length in time even at the same agitation intensity. At a higher stirrer speed the hairy length of pellets was

Figure 8. Time course of hairy length of pellets in fermentations run at different agitation intensities in 100 L fermenter.

shorter. This is in agreement with previous work [8] with parallel fermentations in a 2 L fermenter. The difference in preculture conditions appeared not to influence the hairy length of pellets. The dissolved oxygen tension does not affect the hairy length of pellets significantly.[29]

Scale effects on hairy length

Fig.9 shows the hairy length as a function of the specific energy dissipation rate in 100 L and 2 L fermenters. Although in the both cases the hairy length decreased with agitation intensity, the hairy length in the 100 L fermenter was larger than in the 2 L fermenter at comparable conditions with respect to specific energy dissipation rate and fermentation time. This is a clear scale effect on the hairy length. Comparing the results of fermentations at two scales (10 L
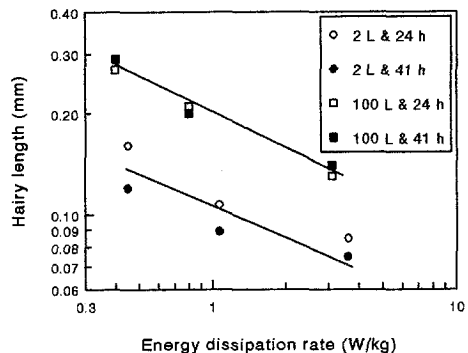
Figure 9. Effect of fermenter scale (2L and 100 L) on the hairy length of pellets in the fermentations F5, F7, F8, F9, F10 and F11.

and 100 L) with *Penicillium chrysogenum*, Smith et al.[30] reported that at similar energy dissipation rates less damage to filamentous mycelia and a higher rate of penicillin synthesis were observed in a 100 L fermenter than in a 10 L fermenter. This is well in line with our observation. Difference in circulation frequency and average velocity gradient at the two different scales may cause this effect. At a similar specific energy dissipation rate, the circulation frequency through the impeller zone, given by ND^3/V, and the average velocity gradient, given by $11N$, are lower in the 100 L fermenter than in the 2 L fermenter (N: stirrer speed, D: diameter of impeller, V: volume of reactor per impeller). The present data are insufficient to distinguish which of the two is the dominant factor. Smith et al.[30] stated that their data indicated that the circulation frequency was the dominant factor.

Fraction of pellet mass in total biomass

Fungal morphology in submerged fermentations is usually classified as one of two extremes, free filamentous mycelia or dense spherical pellets. In literature, mostly only one of the two is studied. In our fermentations a mixed morphology was generally present. Previous studies [8,29] showed that the fraction of pellet mass in the total biomass decreased with agitation intensity but that the dissolved oxygen tension had less effect on the fraction. Fig.10 shows that during the fermentation at a higher stirrer speed (400 rpm), mycelia were dominant. But at a stirrer speed equal to or lower than 250 rpm, the pellet form was dominant, which is in agreement with previous work [8]. The change of the fraction of pellet mass in the total biomass mainly occurred during the first part of the fermentation (t <40h). After that, the fraction stayed more or less constant.
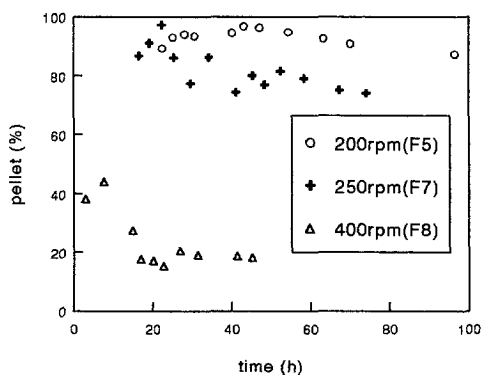

Figure 10. Time course of pellet mass fraction in the total biomass in the fermentations run at different agitation intensities in 100 L fermenter.

Physical picture behind the interaction between mechanical forces and pellets

Finally the change of the pellet number during a fermentation was examined in order to study the formation and destruction of pellets. Fig.11 shows the development of the number of pellets in fermentations of F13 and F14. The number of pellets under the studied conditions did not change noticeably. This implies that neither new pellets were formed nor pellets were

broken up during the studied fermentations. In literature, four types of pellet formation mechanisms are reported. 1). The spore coagulation type [31] where spore coagulation in the early stage of germination yields a dense hyphal aggregate which evolves into a pellet. 2). The noncoagulating type [31,32,18] where a single spore generates a pellet. 3). Development of pellets from hyphal elements [33,34]. Hyphal elements agglomerate first to loose clumps and then gradually develop into a pellet. 4). Pellet development from fragments of pellet breakage.[35]
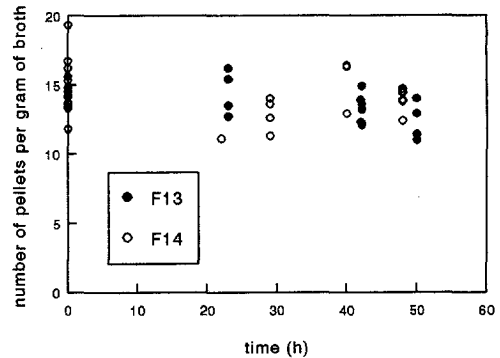
Figure 11. Number of pellets during the fermentations. **a**: fermentation F13; **b**: fermentation F14.

In the fermentations F13 and F14, the fermenters were inoculated with a preculture in which pellets were already formed and the inoculated spores had germinated. Therefore, the spore coagulation mechanism and the noncoagulation mechanism could not occur during these fermentations. Since no new pellet formation or destruction were observed during the fermentations, the third and fourth mechanisms did not occur either. The fermentation broth always contained filamentous mycelia (see Fig.10) but the formation of clumps and the development of the clumps into pellets were not observed. This is different from literature [33,34]. Besides measurement during the fermentation, pellet number and size were also measured in cold mode experiments. Pellets were obtained from F5 after 20 h of fermentation and F15 after 25 h and were kept in the refrigerator for two days. Pellets were sieved and stirred in the supernatant of a broth at a stirrer speed of 300 rpm which corresponded to a specific energy dissipation rate of 2.1 W/kg. Pictures of these samples are presented in Fig.12. No breakup of pellets was observed and the size of pellets hardly changed with agitation. These results illustrate that the tensile strength of the pellets was stronger than the mechanical forces in the present submerged fermentations. In literature [35,26], breakage of pellets and the formation of new pellets from fragments were reported. The present results from both the cold mode experiments and the fermentations contradict with these reported findings.

In literature [26,27,35], it is reported that pellets will be broken if they are larger than a critical size. The critical size is a function of agitation intensity. The observed similarity in the sizes
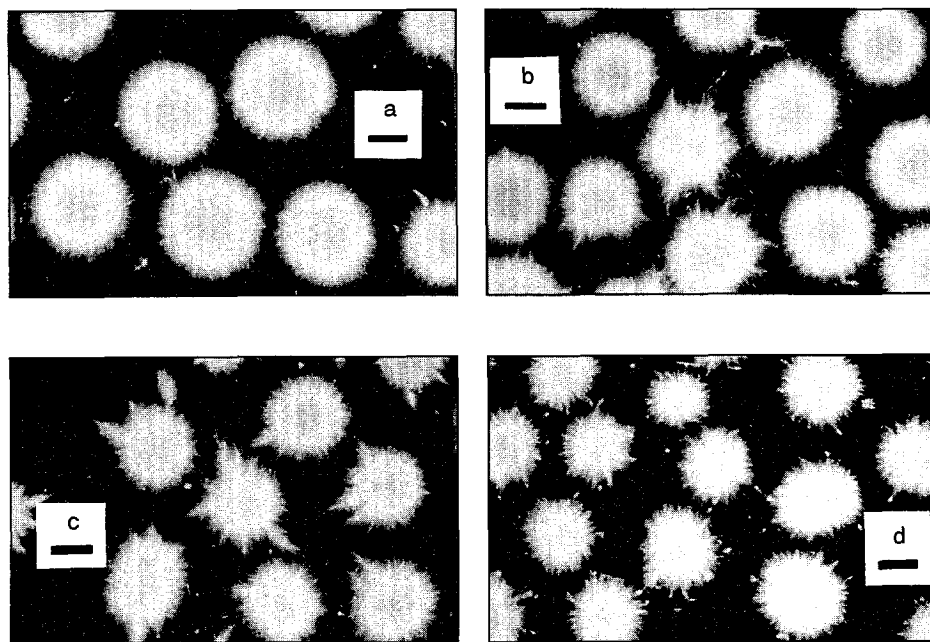
Figure 12. Picture of pellets before agitation and after agitation under ungrowth conditions (bar = 1 mm). **a**: pellets from F5 before agitation; **b**: pellets from F5 after 6.5 h of agitation; **c**: pellets from F15 before agitation; **d**: pellets from F15 after 26 h of agitation.

at different agitation intensities contradicts with such a statement. Our observation from several tens of fermentations with *Aspergillus awamori* suggests that the pellet size was influenced by the amount of available substrates per pellet, the density of pellets, agitation intensities and the time period of pellet growth. For the same density and the same agitation intensities, a higher sugar concentration in the bulk, a lower number of pellets and a longer period of growth led to the formation of a larger pellet than that in a lower sugar concentration, larger number of pellets and shorter growth period. The pellet size was controlled more by growth than by breakage.

CONCLUSIONS

Fermentations of *Aspergillus awamori* have been run in fermenters of 2 L, 15 L and 100 L working volume. Two kinds of substrates, sucrose and glucose, were used for the

fermentations. The cell mass was found to decay when substrate or oxygen was lacking. The decay rate depended on the physical conditions (temperature and agitation). The carbon balance showed that the measurements matched each other well. Morphology quantification, biomass growth and substrate consumption had a good reproducibility. The difference in the morphology of different fermentations under the same conditions, however, can be large.

The yield and maintenance of cells on substrate and on oxygen were determined. The yield of the used strain on either substrate or oxygen was higher at the studied conditions than that reported with relevant strains. The type of substrate had almost no influence on the ratio of biomass to the sum of biomass and carbon dioxide. This offered an approach to estimate biomass concentration from the CO_2 production, which is desirable both for obtaining on-line information of biomass growth and for the situation where biomass determination is difficult such as when a solid substrate is used.

Fungal morphology changed in time during a batch fermentation. The hairy length of pellets first increased and then decreased, which is similar to the observation of the hyphal length of filamentous mycelia during a fermentation. Pellets cultivated in the larger scale fermenter had a longer hairy length than in the smaller scale fermenters at a similar specific energy dissipation rate. The pellets grew in size during the first 20-30 h of the fermentations and thereafter the size stayed more or less constant. The fraction of filamentous mycelia increased during the first part of the fermentations (0-20h), after this, it reached a more or less stable value. This value was a function of agitation intensity.

The number of pellets during the fermentations was almost constant at the studied conditions. This suggests that formation of pellets and pellet breakage did not occur during the fermentations inoculated with pellet suspension as preculture. Cold mode experiments indicated that the pellets hardly broke up after several hours of agitation at an agitation intensity of 2.1 W/kg. It further proved that the pellets in the present study were stronger than the exerted mechanical forces. The pellet size was controlled more by growth than by agitation.

NOMENCLATURE

a_i	: constants	-
C_{CO2}	: accumulative CO_2 production per volume	mol L^{-1}
C_s	: substrate concentration	Cmol L^{-1}
C_{so}	: initial substrate concentration	Cmol L^{-1}
C_X	: biomass concentration	Cmol L^{-1}
D	: diameter of impeller	m
K_{aut}	: cell autolysis constant	h^{-1}

m_O	: maintenance coefficient of cells on oxygen	mol Cmol^{-1} h^{-1}
m_s	: maintenance coefficient of cells on substrate	Cmol Cmol^{-1} h^{-1}
N	: stirrer speed of impeller	s^{-1}
P_{num}	: number of pellets per volume	m^{-3}
R_s	: substrate consumption rate	Cmol L^{-1} h^{-1}
R_{O2}	: volume oxygen consumption rate in pellets	mol L^{-1} h^{-1}
R_x	: biomass growth rate	Cmol L^{-1} h^{-1}
R_p	: radius of pellets	m
R_{op}	: critical radius of pellets	m
r_p	: radial position in pellets	m
t	: time of fermentations	s
T	: diameter of the stirred vessel	m
V	: volume of fermenter per impeller	m^3
Y_{OX}	: yield of biomass on oxygen	Coml mol^{-1}
Y_{SX}	: yield of biomass on substrate	Cmol mol^{-1}

Greek

μ	: specific growth rate	s^{-1}
μ_{max}	: maximum specific growth rate	s^{-1}
ϵ	: specific energy dissipation rate	W/kg
ρ_p	: dry biomass per wet pellet volume	kg/m^3
ρ_h	: density of hyphae	kg/m^3

REFERENCES

1. Ward, M., Production of Calf Chymosin by *Aspergillus awamori*. in: *Genetics and molecular biology of industrial microorganisms* (C.L.Hershberger, S.W.Queener and G. Hegeman, eds.). American Society for Microbiology, Washington DC, 1996, pp 288-294

2. Smith, D.C. and Wood, T.M., Xylanase production by *Aspergillus awamori*. Development of a medium and optimization of the fermentation parameters for the production of extracellular xylanase and β-xylosidase while maintaining low protease production. *Biotech. & Bioeng.* 1991, **38**, 883-890,

3. Gouka, R.J., Hessing, J.G.M., Punt, P.J., Stam, H., Muster, W. and Van den Honde,l C.A.M.J.J. An expression system based on the promoter region of the *Aspergillus awamori* 1,4-β-endoxylanase a gene. *Appl. Microbiol. Biotechnol.* 1996, **46**, 28-35

4. Hours, R.A., Katsuragi, T. and Sakai, T. Growth and protopectinase production of *Aspergillus awamori* in solid-state culture at different acidities. *J. of Fermentation and Bioengineering*. 1994, **78**, 426-430

5. Berka, R.M., Bayliss, F.T., Bloebaum, P., Cullen, D., Dunn-Coleman, N.S., Kodama, K.H., Hayenga, K.J., Hitzeman, R.A., Lamsa, M.H., Przetak, M.M., Rey, M.W., Wilson, L.J. and Ward, M. *Aspergillus niger var. awamori* as a host for the expression of heterologous genes. in: *Applications of enzame biotechnology* (Kelly, J.W. and Baldwin, T.O., eds.). Plenum Press, New York, 1991,

6. Smith, D.C. and Wood, T.M. Isolation of mutants of *Aspergillus awamori* with enhanced production of extracellular xylanase and β-xylosidase. *World Journal of Microbiology and Biotechnology*. 1991b, **7**, 343-354

7. Cui, Y.Q., Van der Lans, R.G.J.M. and Luyben, K.Ch.A.M. Local power uptake in gas-liquid systems with single and multiple Rushton turbines. 14th International Symposium on Chemical Reaction Engineering, *Chem. Eng. Sci.* 1996, **51**, 2631-2636

8. Cui, Y.Q., Van der Lans, R.G.J.M. and Luyben, K.Ch.A.M., Effects of agitation intensities on fungal morphology of submerged fermentation. *Biotechnol. and Bioeng.*, 1997, **55**, 715-726

9. Roels, J.A., Energetics and Kinetics in Biotechnology, Elsevier Biomedical Press, Amsterdam, 1983, P.54 & 81

10. Trinci, A.P.J. and Righelato, R.C. Changes in constituents and ultrastructure of hyphal compartments during autolysis of glucose-starved *Penicillium chrysogenum*. *J. Gen. Microbiol*. 1970, **60**, 239-249

11. Bainbridge, B.W., Bull, A.T., Pirt, S.J., Rowley, B.I. and Trinci, A.P.J. Biochemical and structural changes in non-growth maintained and autolysing cultures of *Aspergillus nidulans*. *Trans. Br. Mycol. Soc*. 1971, **56**, 371-385

12. Paul, G. C., Kent, C.A. and Thomas, C.R. Hyphal vacuolation and fragmentation in Penicillium chrysogenum. *Biotechnol. & Bioeng*. 1994, **44**, 655-660.

13. Packer, H.L. and Thomas, C.R. Morphological measurements on filamentous microorganisms by fully automatic image analysis. *Biotechnol. & Bioeng*. 1990, **35**, 870-881

14. Cox, P.W. and Thomas, C.R. Classification and measurement of fungal pellets by automated image analysis. *Biotechnol. & Bioeng.* 1992, **39**, 954-952.

15. Riechl, U., King, R. and Gilles, E.D. Characterization of pellet morphology during submerged growth of *Streptomyces tendae* by image analysis. *Biotechnol. & Bioeng.* 1992, **39**, 164-170.

16. Metz, B. and Kossen, N.W.F. The growth of molds in the form of pellets-Literature review. *Biotechnol. & Bioeng.* 1977, **19**, 781-799

17. Trinci, A.P.J. Study of kinetics of hyphal extension and branch initiation of fungal mycelia. *J. Gen. Microbiol.* 1974, **81**, 225-236

18. Yang, H, Reichi, U., King, R. and Gilles, E.D. Mathematical model for apical growth septation, and branching of mycelial microorganisms. *Biotechnol. & Bioeng.* 1992, **39**, 49-58

19. Nielsen, J. and Krabben, P. Hyphal growth and fragmentation of *Penicillium chrysogenum* in submerged cultures. *Biotechnol. & Bioeng.* 1995, **46**, 588-598.

20. Carlsen, M., Spohr, A.B., Nielsen, J. and Villadsen, J. Morphology and physiology of an α-amylase producing strain of *Aspergillus oryzae* during batch cultivations. *Biotechnol. & Bioeng.* 1995, **49**, 266-276

21. Trinci, A.P.J. Kinetics of apical and lateral branching in *Aspergillus nidulans* and *Geotrichum lactis*. *Trans. Br. Mycological Society.* 1970, **55**, 17-28

22. Yano, T., Kodama, T. and Yamada, K. Fundamental studies on the aerobic fermentation part VIII. Oxygen transfer within a mold pellet. *Agri.Biol. Chem.* 1961, **25**, 580-584,

23. Kobayashi, T., Van Dedem, G., and Moo-Young. Oxygen transfer into mycelial pellets. *Biotechnol. & Bioeng.* 1973, **15**, 27-45

24. Krzystek, L., Gluszcz, P. and Ledakowicz, S. Determination of yield and maintenance coeffcients in citric acid production by *Aspergillus niger*. *Chem. Eng. J.* 1996, **62**, 215-222

25. Righelato, R.C., Trinci, A.P.J., Pirt, S.J. & Peat, A. The influence of maintenance energy and growth rate on the metabolic activity, morphology and conidiation of *Penicillium chrysogenum*. *J. Gen. Microbiol.* 1968, **50**, 399-412.

26. Van Suijdam, J.C. and Metz, B. Fungal pellet breakup as a function of shear in a fermenter. *J. Ferment. Technol.* 1981, **46**, 329-333

27. Taguchi, H., Yoshida, T., Tomita, Y. and Teramoto, S. The effects of agitation on disruption of the mycelial pellets in stirred fermenters. *J. Ferment. Technol.* 1968, **46**, 814-822

28. Ayazi Shamplou, P., Makagiansar, H.Y., Ison, A.P., Lilly, M.D. and Thomas, C.R. Turbulent breakage of filamentous microorganisms in submerged culture in mechanically stirred bioreactors. *Chem. Eng. Sci.* 1994, **49**, 2621-2631

29. Cui, Y.Q., Van der Lans, R.G.J.M. and Luyben, K.Ch.A.M. Effects of dissolved oxygen tensions and mechanical forces on Fungal morphology of submerged fermentation. *Biotechnol. & Bioeng.*, 1997, in press.

30. Smith, J.J. and Lilly, M.D. and Fox, R.I. The effect of agitation on the morphology and penicillin production of *Penicillium chrysogenum*. *Biotechnol. & Bioeng.* 1990, **35**, 1011-1023

31. Takahashi, J. and Yamada, K. Studies on the effect of some physical conditions on the submerged mold culture. Part II. On the two types of pellet formation in the shaking culture. *J. Agric. Chem. Soc.* 1959, **33**, 707-709

32. Burkholder, P.R., Sinnott, E.W. Morphogenesis of fungal colonies in submerged shaken cultures. *Am. J. Bot.* 1945, **32**, 424-431

33. Van Suijdam, J.C., Kossen, N.W.F. and Paul, P.G. An inoculum technique for the production of fungal pellets. *Eur. J. Appl. Microbiol.* 1980, **10**, 211-221;

34. Nielsen, J., Johansen, C.L., Jacobsen, M., Krabben, P. and Villadsen, J. Pellet formation and fragmentation in submerged cultures of *Penicillium chrysogenum* and its relation to penicillin production. *Biotechnol. Prog.* 1995, **11**, 93-98

35. Edelstein, L. and Hadar, Y. A model for pellet size distributions in submerged mycelial cultures. *J. Theor. Biol.* 1983, **105**, 427-452

Appendix

Linear regression of the ratio of biomass production to the sum of biomass production and CO_2 production with time in fig.6 gave

$$\frac{C_x}{C_x + C_{CO2}} = a_1 - a_2 t \tag{2}$$

Since $C_x + C_{CO2} = C_{S0} - C_S$

$$\frac{C_x}{C_{S0} - C_S} = a_1 - a_2 t \tag{3}$$

Where C_x is the concentration of biomass [Cmol/L], C_S the concentration of sugar [Cmol/L], C_{S0} the initial concentration of sugar [Cmol/L], C_{CO2} the cumulative CO_2 production per volume [Cmol/L], t the time of fermentation [h] and $a_1 = 0.78 \pm 0.06$ and $a_2 = 0.0022 \pm 0.0004$ h^{-1} the regression constants with the standard error.

After rewriting Eq.(3) to make C_x explicitly, differentiation gives:

$$\frac{dC_x}{dt} = -a_1 \frac{dC_s}{dt} + a_2 t \frac{dC_s}{dt} - a_2 (C_{s0} - C_s) \tag{4}$$

Fig.5b shows that the sugar was reduced almost linearly with the increase of time, which means that $\frac{dC_s}{dt}$ was constant. Then $t \frac{dC_s}{dt}$ equals $-(C_{s0} - C_s)$ approximately, hence Eq.(4) can be simplified into

$$\frac{dC_x}{dt} = -a_1 \frac{dC_s}{dt} - 2 a_2 (C_{s0} - C_s) \tag{5}$$

Fig.6 shows that the ratio did decline with time but not very much. This implies that the carbon used for cell maintenance is much less than for cell biomass synthesis i.e. $C_{S0} - C_S \approx C_x / Y_{SX}$. Using this relation and the definition of conversion rate ($R_s = -dC_s / dt$; $R_x = dC_x / dt$), Eq.(5) can be rewritten as

$$R_s = \frac{R_x}{a_1} - 2 a_2 \frac{C_x}{Y_{sx}} \tag{6}$$

According to the definition of yield and maintenance coefficients (Pirt, 1965), the substrate consumption rate can be expressed as:

$$R_s = \frac{R_x}{Y_{sx}} + m_s C_x \qquad (7)$$

where R_x is the biomass growth rate [Cmol/L h], R_s the substrate consumption rate [Cmol/L h], Y_{SX} the yield of biomass on substrate [Cmol/Cmol], C_X the biomass concentration [Cmol/L] and m_s the maintenance coefficient [Cmol/Cmol h].

The form of Eq.(7) is similar to that of Eq.(6). Comparison leads to $Y_{SX} = 0.78 \pm 0.06$ Cmol/Cmol and $m_s = (0.0044 \pm 0.0008)/(0.78 \pm 0.06) = 0.0056 \pm 0.0015$ Cmol/Cmol h.

CHAPTER 7

Aspects of the Use of Complex Media for Submerged Fermentation of *Aspergillus awamori*

Y.Q.Cui, J.Ouwehand, R.G.J.M. van der Lans, K.Ch.A.M. Luyben

Abstract

For the industrial production of enzymes using fungi often complex media containing a solid substrates are used. In this study fermentations with *Aspergillus awamori* were performed using wheat bran. The results are compared with previous work on synthetic medium. Major differences are that the wheat bran was not consumed completely as glucose or sucrose and that fungi growing on the wheat bran particles (adhesion growth) may occur depending on the inocula used. If the spore concentration was higher than 1.3×10^5 spores per mL, adhesion growth dominated. If the concentration was lower than 1.8×10^4 spores per mL, wheat bran free pellets and clean wheat bran particles dominated. In between these two values the broth suspension consisted of wheat bran free pellets, clean wheat bran particles and adhesion colonies. The solid substrate suppressed the growth in free filamentous mycelial form. A method was developed to separate the wheat bran particles from the pellets. The kinetics with complex medium appeared to be essentially the same as with synthetic medium. The ratio of biomass production to the sum of biomass production and CO_2 production was a function of time and independent of operation conditions, morphology and substrates (sucrose, glucose or wheat bran). Gas-liquid mass transfer coefficients during the fermentations were determined and compared with a correlation from the literature.

Keywords: *Aspergillus awamori*; solid substrate; morphology; biomass determination; adhesion growth; stirred vessels.

INTRODUCTION

For the industrial production of enzymes and antibiotics fungal fermentations using complex media with a solid substrate are often used. However, the information on such fermentations with respect to growth, kinetics and morphology is scarce in literature. The use of a complex medium may influence morphology and growth kinetics and will hamper biomass determination. For submerged fungal fermentations in synthetic media, two extreme types of morphology, pellets and free mycelia, are known. Most research on fungi is focused on these morphologies [1,2,3,4,5, 6,7]. But when a solid substrate is used fungal growth on the solid surface may occur, which creates a third type of fungal morphology. Biomass concentration is perhaps the most basic parameter which is routinely followed during the course of a fermentation. Many derived parameters, such as yield coefficient, specific growth rate and oxygen uptake rate, require knowledge of the biomass concentration. Determining dry mass is a long established and accurate method, however, it is tedious. When a solid substrate is present, the use of this method becomes difficult or impossible. Separation of the biomass from the solid substrate is needed to determine the biomass instead of the total solid mass. Spectrophotometric turbidity measurements are very popular for single cell cultures. However, this method is not directly applicable for fungi. In order to apply this method, the broth needs a pretreatment such as homogenization[8]. When solid substrate is present this method cannot be applied at all. Measuring chitin concentration in a sample has been reported as another approach[9]. Chitin exists in fungal cell walls and it is absent from most other organisms. It can be used as a measure of biomass concentration. However, the chitin content of hyphae may change with age and growth conditions. Moreover, vacuoles and empty regions within hyphae are reported to increase with age[10]. Therefore the chitin content per biomass will not be constant, which may lead to a poor accuracy of this method.

The composition of solid substrates is mostly complicated and not very well defined. This makes the description of the fungal metabolism and monitoring of a fungal fermentation very difficult. Another problem is that the carbon source in a solid substrate is commonly a large molecule. Direct uptake of such a molecule hardly occurs. Degradation into a suitable form is needed before the final uptake can take place. This means that the proper enzyme must be formed to enable such a degradation. The amount of the suitable substrate is not only dependent on the consumption rate but also on the speed of the degradation. The final substrate which is being used by the microorganism may change during the fermentation. All of these facts make the description of a fungal fermentation on complex medium difficult.

In the present study, fermentations of *Aspergillus awamori* with different substrates (wheat bran, wheat bran + glucose) were carried out under different conditions. The factors influencing fungal growth on the surface of wheat bran were studied. Methods to quantify the

biomass concentration in complex medium were tested. Information on adhesion growth, kinetics, growth, respiration, morphology is obtained during the fermentations. Inoculation size, agitation intensity and the fermenter scale were varied in the different fermentations. The results were compared with those[11] from the fermentations with synthetic medium.

EXPERIMENTAL

Cultures of *Aspergillus awamori* (CBS 115.52) were maintained and spores produced on standard potato dextrose agar. The fermentations were carried out in 15, 100 and 1800 L fermenters. Fermenter geometries are presented in Table 1. The composition of the complex

Table I: Geometries of fermenters in use

terms	fermenter1	fermenter2	fermenter3	fermenter4
working volume of fermenter (V) in L	1800	100	15	2
diameter of fermenter (T) in mm	1250	395	215	130
number of impeller (D) in mm	2	3	3	2
daimter of top impeller (D) in mm	440	130	74	45
diamter of middle impeller (D) in mm		130	74	
diamter of bottom impeller (D) in mm	440	174	74	45

Table II Complex fermentation medium

Ingredient	concentration	
wheat bran	40	g/L
$(NH_4)_2SO_4$	5	g/L
KH_2PO_4	1.5	g/L
$MgSO_4.7H_2O$	0.75	g/L
KCl	0.75	g/L

This medium + 5 g/L glucose is used for fermentation (F23)

Table III Composition of wheat bran

components	percentage
water contents	16%
protein	15%
starch	22%
fat	3%
rest (cellulose, mineral,...)	44%

medium used is given in Table II. Wheat bran is the carbon source and its composition is presented in table III. Both a seed culture and a spore suspension were used for the inoculation of the fermentations. The medium composition of the seed culture was the same as that of the corresponding fermentation medium. The seed cultures were prepared either in 2 L shaking flasks or in a 60 L fermenter. The procedure for preparing a seed culture for the shaking flasks was the same as that reported earlier[11]. The procedure for making the seed

culture in the 60 L fermenter was as follows. The fermenter was filled with 45 L medium and sterilized. Then 4 L spore suspension with 4.5×10^6 spores per ml was added. The fermenter was stirred at 200 rpm for 67 h. The temperature was maintained at 25 °C. The obtained seed culture was used for the inoculation of the 1800 L fermenter. The fungal morphology in the seed culture (both 2 L shaking flasks and 60 L fermenter) was a mixture of filamentous mycelia, small clumps and small pellets.

For sterilizations, steam was used. Some steam condensed in the medium during sterilization. Therefore the actual initial concentration of the medium might differ between fermentations. The obtained precultures were inoculated into the fermenter. The temperature set point was 25 °C. The pH was maintained at 4.5, using ammonia and phosphate. Antifoam was added if needed. Different stirrer speeds were used for different fermentations and the specific energy dissipation rates in the used gassed multi-impeller systems were calculated[12]. Samples were taken from the fermenter during the fermentations. Pellet core size and the hairy length of the pellets were measured by means of image analysis[7]. At least 250 objects were analyzed for each sample.

In some cases fungi did grow on the wheat bran particles. If this growth occurred, it was impossible or too difficult to determine the biomass concentration. In other cases, adhesion did not occur and the biomass concentration could be measured after separating the biomass from the wheat bran. Several methods to separate the biomass from the wheat bran were tested. It was found that an aqueous salt solution such as NaCl was a good medium to achieve this separation. Na^+ and Cl^- are the two most common ions that exist in the broth. This means that the addition of NaCl would not influence the sample very much. Na_2SO_4 could be used as well. Salt was used to create a solution with a density in between that of wheat bran and pellet particles. Therefore, pellets float and wheat bran settles in such a solution. The detailed procedure of the "NaCl solution" method was as follows. First the sample was put into a sieve with a pore size of 70 μm and the medium went through the sieve. Thereafter demineralized water (about 3-4 times (v/v) of the amount of the sample) was added to wash the solid part. The cleaned sample was removed from the sieve and put into a beaker. Then some water was added to it. The next step was to add a certain amount of concentrated NaCl solution to reach the desired density. After that the pellets started floating in the upper part of the medium and the wheat bran would stay at the bottom. The upper part was separated quickly from the lower part. This process could be repeated as many times as needed. The last step was to wash out the salt from the separated wheat bran and pellets with demineralized water. Because the wheat bran particles were brown and flat and the pellets mostly spherical and white, it was easy to check if the separation was successful. After the separation was finished, the pellet mass and the wheat bran mass were maesured. This approach could also be used to quantify the fraction of attached growth in the total growth

by separating pellets, attached and clean wheat bran particles.

The medium, the size and the type of the inocula, the fermenters and the operation conditions used for the various experiments are described in Table IV. In total, more than 9 fermentations with complex medium have been run. In addition, shake flask experiments were performed in order to study the adhesion growth. Spore suspension was used as inoculum. The spore concentrations were varied between 1.8×10^4 and 1.3×10^5 spores per ml. The medium and the temperature used for the shake flask experiments were the same as for the fermentations in the stirred vessel. The pH was not controlled. The shaking speed was 200 rpm. The cultivation in shake flask lasted about four days.

Table IV. Fermentation description

Code code	medium	fermenter L	spore Sp/ml	preculture	ϵ W/kg	agitation rpm	aeration L/min	morphology	remark
F1	glucose	100	2.7 10³	shake flask	1.3	300	18	P+M	Cui et al.,[11] (1997)
F2	glucose	100	1.2 10⁴	shake flask	1.3	300	18	P+M	:
F3	glucose	100	2.1 10⁴	spore	3.1	400	9	M	:
F4	glucose	100	2.5 10⁴	shake flask	3.1	400	9	M	:
F5	sucrose	100	1.2 10³	shake flask	0.4	200	9	P(85%)+M(15%)	:
F6	sucrose	100	1.5 10⁴	shake flask	0.8	250	9	P(70%)+M(30%)	:
F7	sucrose	100	1.0 10³	shake flask	3.1	400	9	M(80%)+P(20%)	:
F8)	sucrose	2	6.3 10³	shake flask	0.2	300	0.3	P+M	Cui et al.,[7] (1997)
F9	sucrose	2	6.3 10³	shake flask	0.45	450	0.3	P+M	:
F10	sucrose	2	6.3 10³	shake flask	1	600	0.3	P+M	:
F11	sucrose	2	6.3 10³	shake flask	1	600	0.3	P+M	:
F12	sucrose	2	6.3 10³	shake flask	2.1	750	0.3	P+M	:
F13	sucrose	2	6.3 10³	shake flask	3.6	900	0.3	M+P	:
F14	sucrose	2	6.3 10³	shake flask	5.7	1050	0.3	M+P	:
F15	wheat bran	2000	8.0 10³	stirred tank	1.3	150	300	free P	this paper
F16	wheat bran	100	1.3 10⁵	spores	1.3	300	18	P+WB	:
F17	wheat bran	100	3.4 10⁵	shake flask	6.4	500	18	P+WB	:
F18	wheat bran	100	2.3 10⁵	shake flask	1.3	300	18	P+WB	:
F19	wheat bran	100	8.0 10⁵	shake flask	1.3	300	18	P+WB	:
F20	wheat bran	100	1.3 10⁴	shake flask	1.3	300	18	free P	:
F21	wheat bran	100	1.8 10⁴	shake flask	3.1	400	17	free P	:
F22	wheat bran	15	1.8 10⁴	shake flask	0.36	300	5	free P	:
F23	WB + G	100	8.8 10⁴	shake flask	1.3	300	18	P+WB	:

* : Most of the results from the fermentations using synthetic medium (F1-F14) have been reported in the perious works[7, 11]. Here the part of these results are used for the comparison with those from the present fermentations using complex medium (F15-F23)

For convenience, the concept of the carbon mole was used and expressed as Cmol. It is the amount of substance containing one mole of the element carbon.[13] The molar mass of *Aspergillus awamori* was assumed to be 25 g/Cmol which is the same as for yeast.

RESULTS AND DISCUSSION

Fermentation profile

Biomass, mass of the residual wheat bran, total solid mass, respiration data, and consumption of base and acid from fermentation F21 are plotted in Fig.1. The figure shows the following. 1) The CO2 production rate was almost equal to the oxygen consumption rate. The respiratory quotient, defined as the ratio of the CO_2 production rate to O_2 production rate[13], was around unity. 2) Growth of biomass was accompanied by base consumption. After the biomass concentration reached the highest point, acid was needed to maintain the pH at set point. This indicates that base was used for the biomass formation from substrate. When the substrate was depleted, the demand for base was stopped. The use of acid probably corresponds to cell autolysis. 3) The highest respiration rate occurred just a little bit earlier than when the highest point of the biomass concentration was reached.
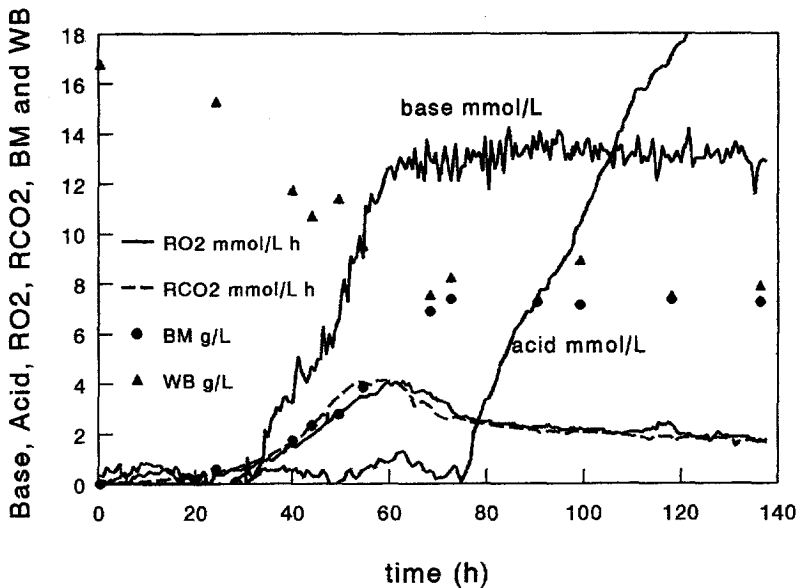
Figure 1. Time profiles of biomass concentration (BM), substrate concentration of wheat bran (WB), CO_2 production rate (RCO$_2$), oxygen consumption rate (RO$_2$), base and acid addition in F21.

During fermentations with wheat bran also solid mass was measured. Fig.2 depicts the results from F21. The increase of biomass corresponded with the decrease of wheat bran. After a growth phase of about 70 h, the mass of wheat bran remained almost constant at about 9 g/L. Probably the remains consist of fibres which are difficult to break down. The biomass

concentration was the highest at about 50-70 h. This seems to be the time when the easy degradable part of the substrate in the wheat bran was used up. Both the total solid mass and the sum of pellet mass and wheat bran mass did not change very much any more after that and were approximately equal to each other. Here, total mass is the mass of solid particles which are equal to or larger than 0.07 mm.
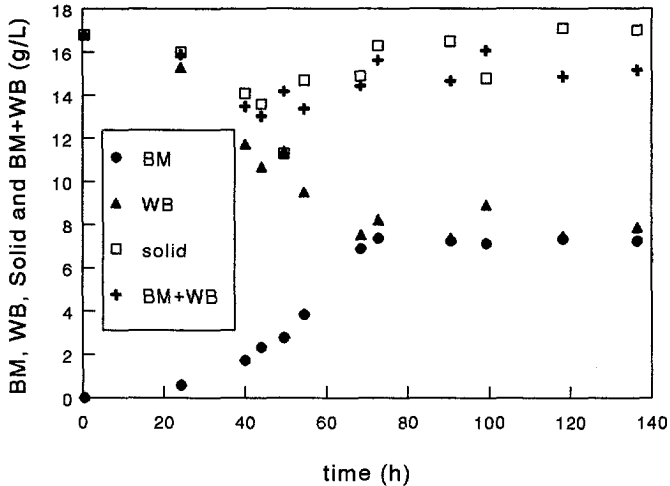

Figure 2. Time profiles of solid mass in the fermentation (F21) with complex medium.

In general, carbon from the substrate will be converted into biomass, products and CO_2 during fermentation. To verify if organic products were formed, the supernatant was analyzed. No products were found. In the case of the fermentations with synthetic medium[11], no organic products were found either and the carbon balance was closed. Although the carbon balance could not be checked because of the use of the complex substrate, it is assumed that organic products were not formed or that their amount was negligible under the studied conditions.

Adhesion
Fig.3a is a picture of some particles in the broth taken from F21 (100 L) at 45 h. It shows a mixture of wheat bran free pellets and clean wheat bran particles. Adhesion growth of fungi on wheat bran was not visible. For comparison Fig.3b shows a picture of particles in the broth taken at 46 h from F16 where fungi grew on the wheat bran particles. When adhesion growth will occur and how to control it have not been reported yet in literature according to our knowledge, although it may be an important for industrial processes. For most fungal fermentations, a desired morphology exists with respect to productivity. To be able to achieve
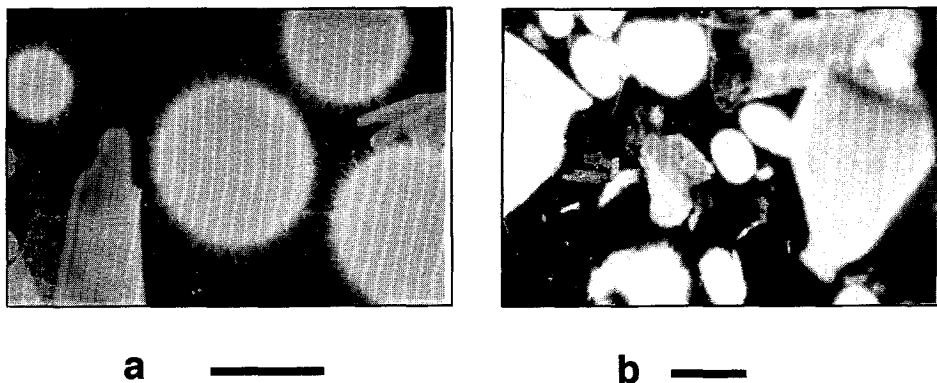
Figure 3. Picture of broths (bar = 1 mm) **a**: wheat bran free pellets and clean wheat bran particles in F21 at 45 h; **b**: growth of fungi on wheat bran in F16 at 46 h.

and control the desired morphology, the relation between operation conditions and fungal morphology must be known. In our fermentations, it was noticed that the adhesion between fungi and wheat bran occurred only in some fermentations. When adhesion occurred, the fungi grew on the surface of the wheat bran and the shape of the colony was flat and irregular due to the irregular shape of the particles. In the extreme case, hardly any spherical wheat bran free pellet could be observed in the broth. In some cases, a mixture of adhesion growth, clean wheat bran particles and wheat bran free pellets appeared in the broth. In other cases, wheat bran free pellets and clean wheat bran particles dominated fully in the broth and adhesion hardly occurred. Substrate limitation was first regarded to be a possible cause for adhesion growth. The addition of soluble substrates, such as glucose or sucrose, in the fermentation medium should then prevent the adhesion. To verify this, a fermentation with both wheat bran and glucose (F23) was carried out. Fungi, however, still grew on the surface of the wheat bran particles. Comparison of several fermentations (table IV) showed that the size of inocula i.e. the spore concentrations played an important role. If the spore concentration was higher than 1.3×10^5 spores per ml, adhesion growth dominated. If the concentration was lower than 1.8×10^4 spores per ml, wheat bean free pellets were the dominant morphology. The spore concentration varied between 1.8×10^4 and 1.3×10^5 spores per ml in the shaking flask experiments. The obtained broth suspensions were observed to be a mixture of adhesion growth, wheat bran free pellets and clean wheat bran particles in varying amounts. The percentage of adhesion growth in the total growth increased with increasing spore concentration. This was independent of agitation intensity and fermenter scale.

Growth, yield, maintenance and respiration

In previous work using synthetic medium[11], it was reported that the ratio of biomass concentration to the sum of biomass concentration and specific CO_2 production was a function of time only. The ratio was independent of operation conditions, morphology and type of substrates (sucrose or glucose). Yield and maintenance coefficients could then be deduced from the time course of this ratio. For the present fermentations with complex medium, the results of HPLC analysis of the supernatant of the broth showed that no products were formed or that their amount was negligible compared to the amount of biomass. Therefore the amount of the carbon from the wheat bran consumed was equal to the sum of the carbon in the biomass and the carbon in the off gas in the form of CO_2 production in a similar way as with the fermentations on synthetic medium.
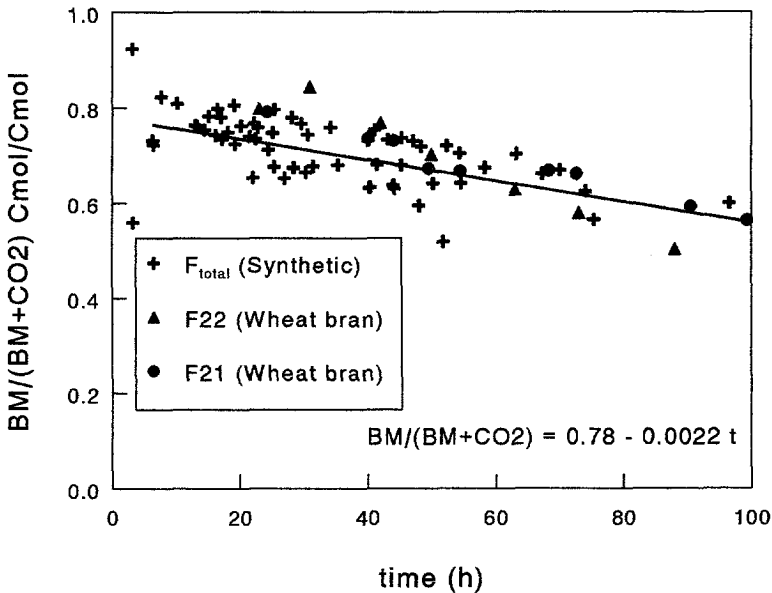
Figure 4. Ratio of biomass production to the sum of biomass production and produced CO_2 from the fermentation with wheat bran compared to those with synthetic medium[11].

From the nine fermentations with complex medium, four were dominated by a mixture of wheat bran free pellets and clean wheat bran particles. By using the developed separation approach, the dry biomass in three of these four fermentations was measured. Off-gas analysis was performed for two of these three fermentations. The ratio of biomass concentration to the sum of biomass concentration and specific CO_2 production was calculated for these two fermentations and depicted in figure 4 together with previous data from

synthetic medium[11]. Fig.4 shows that the ratio was not significantly different from the results obtained with synthetic medium. The use of wheat bran did not affect the ratio. Starch was the major part in wheat bran which was used for growth. The degree of reduction of starch is equal to that of sucrose and glucose. The length of the basic carbon chain in starch and sucrose is the same as for glucose (6 carbons). So it is reasonable to assume that the relation between the ratio and the fermentation time is independent of the substrate used, the morphology (filamentous mycelia or pellets), the scale of the bioreactor and the operation conditions. Therefore the correlation for the ratio as a function of time, as reported in our previous paper[11], can be also used in the case of fermentations with wheat bran. This correlation reads as follows:

$$\frac{C_x}{C_x + C_{CO2}} = \frac{C_x}{C_{S0} - C_S} = 0.78 - 0.0022\, t \qquad (1)$$

Where C_x is the concentration of biomass (Cmol/L), C_S the concentration of substrate at time t (Cmol/L), C_{S0} the concentration of sugar at time of zero or initial concentration (Cmol/L), C_{CO2} the accumulative CO_2 production per volume(Cmol/L) and t the fermentation time (h).

It was reasoned that the decrease of the ratio with time was caused by maintenance and hence that yield of biomass and maintenance coefficient on substrates can be deduced from Eq. (1).[11] This results in $Y_{SX}=0.78\pm0.06$ Cmol/Cmol and $m_S=0.0056\pm0.0015$ Cmol/Cmol h. Since the respiration quotient is about one in fermentations with complex medium, the yield of biomass on oxygen, $Y_{OX} = Y_{SX} / (1 - Y_{SX}) = 3.5$ Cmol/mol and the maintenance coefficient of biomass on oxygen, $m_O = m_S = 0.0056$ mol/Cmol h.

The observed maximum specific growth rate is influenced by the type of nutrients, temperature, pH, various necessary trace elements, the presence of inhibiting chemicals and the formation of vacuoles.[11] To circumvent these effects, the apparent maximum specific growth rate was estimated using the first part of the time course of the biomass concentration. The used period was between 20 and 30 h. It was the period when the amount of biomass was high enough to allow an accurate measurement and when the effects of vacuoles and inhibiting compounds on fungal growth are still relatively small. The estimated rate can be considered as an apparent maximum specific growth rate. In total two time profiles of biomass growth were measured in complex medium fermentations. The estimated growth rate was 0.15-0.17 h^{-1} which is lower than 0.2-0.25 h^{-1} obtained[11] from the synthetic medium fermentations. Since starch is the major component in wheat bran used for growth, degradation of starch was needed before direct utilization. Therefore the rate of enzyme hydrolysis of starch probably retarded the fungal growth.

Estimation of biomass concentration

In general, the biomass concentration in fermentations with complex medium is difficult to determine although the information is very important for controlling a fermentation. On-line information is even more preferable. Fig. 4 has shown that the ratio of biomass formation to the sum of biomass formation and carbon dioxide production was a function of time. This ratio hardly depends on the type of the substrates used and the operation conditions. The amount of byproducts is negligible in comparison with the biomass formation. Therefore, Eq.(1) may be used to estimate the biomass concentration from off-gas data.[11] Such an approach can be applied for a relevant industrial process as well, both on-line and off-line.

Fungal morphology in complex medium

In the fermentations with complex medium, pellet growth or adhesion growth was absolutely dominant. Free filamentous mycelia were hardly present in comparison. The used energy dissipation rate varied from 0.36-6.4 W/kg. In the fermentations with synthetic medium at similar specific energy dissipation rates, the free filamentous mycelial mass constituted 20-80% of the total biomass.[11] The presence of wheat bran particles in the fermentation medium seemed to promote the aggregated growth form.
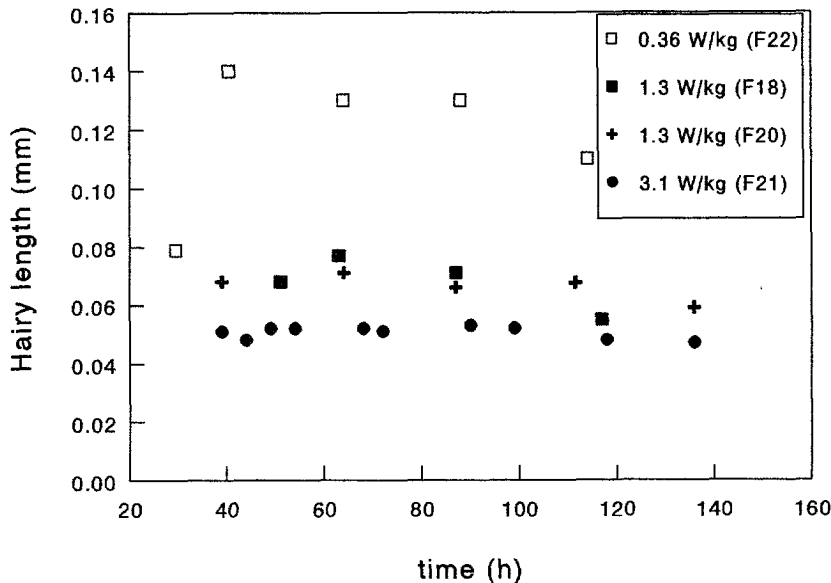

Figure 5. Hairy length of pellets and fungal colonies on wheat bran as a function of specific energy dissipation rate in the fermentations F22, F18, F20 and F21.
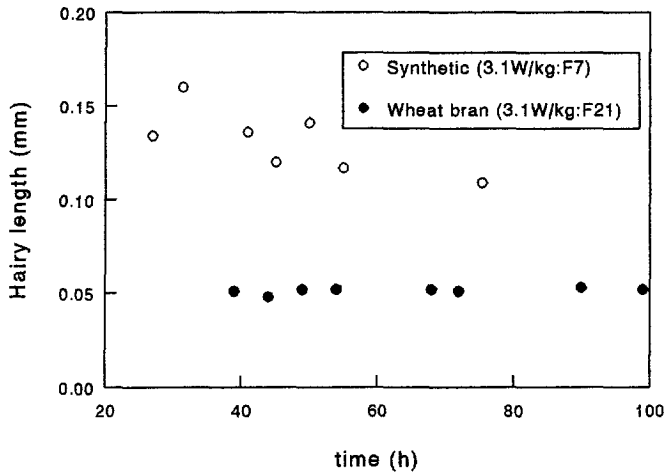
Figure 6. Comparison of the hairy lengths of pellets in the fermentation with sucrose (F7) and those in the fermentation with wheat bran (F21) at the same energy dissipation rate.

Both pellets and attached colonies on wheat bran had a hairy structure in their outer layer. The hairy length was used to describe their surface morphology. When no adhesion growth occurred, the size of pellets was measured. Fig.5 presents the time course of the hairy length in several fermentations. The hairy length appeared to be a function of agitation intensity. A strong agitation led to a shorter hairy length. This trend is the same as in the case of synthetic medium fermentations[7, 11]. Fig.6 depicts the hairy lengths of pellets cultivated both in synthetic medium (sucrose) and in complex medium (wheat bran) at the identical energy dissipation rate of 3.1 W/kg. The hairy length in sucrose medium was larger than in wheat bran medium. This corresponds with the faster growth in the synthetic medium (0.2-0.25 h^{-1}) than in wheat bran medium (0.15-0.17 h^{-1}). However, since the complex medium will also influence the hydrodynamic conditions in the stirred fermenter, no clear conclusion can be drawn from the observed difference in hairy length.

The pellet sizes in several fermentations are plotted as a function of time in Fig. 7. The pellet size did not change very much after the first 40 h. From the base and acid consumptions, respiration rate and biomass concentration profiles, the growth period in F21 is expected to end at about 65 h (see Fig. 1). The size did increase during this period, but thereafter remained constant. Without growth, a constant pellet size implies that the breakage of pellets probably did not occur in the complex medium fermentations. The time profile of the pellet size is similar in F20 and F22. Comparison of the pellet size in different fermentations
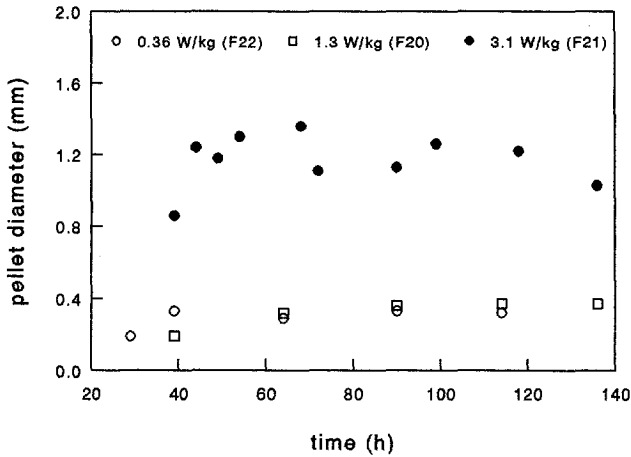
Figure 7. Pellet sizes in fermentation F21, F20 and F22 as a function of time at different power inputs.

indicates that the pellet size did not decrease with increasing power input (Fig.7). The pellets cultivated at the highest power input were even larger. The pellet sizes ranged from 0.3 to 1.2 mm. These are smaller than those[7,11,14] in synthetic medium fermentations, 1.0 - 2.5 mm. Since the precultures used were different, the difference in the size could be caused by the agitation intensity as well as the inocula used.

Mass transfer

During fermentations, the dissolved oxygen tension in the bulk and oxygen concentrations in the inlet air and off-gas were logged. From such data, the gas-liquid mass transfer coefficient can be calculated by

$$k_L a (C_{O2}^* - C_{O2}) \; V_t = Q_g (C_{O2_{inlet}} - C_{O2_{off-gas}})$$ (2)

Where $k_L a$ is the gas-liquid mass transfer coefficient (s^{-1}), C_{O2}^* the dissolved oxygen concentration saturated with gas phase (g/L), C_{O2} the dissolved oxygen concentration in bulk (g/L), $C_{O2inlet}$ the oxygen concentration in the inlet air (g/L), $C_{O2off-gas}$ the oxygen concentration in off-gas (g/L), V_t the working volume (m^3), Q_g the aeration flow rate $(m^3 \; h^{-1})$.

Fig.8 compares the gas-liquid mass transfer coefficient measured during fermentations with a correlation from the literature[15] at different power inputs and gas velocities. The substrates used were glucose, sucrose or wheat bran. Their initial concentrations were 10 g/L, 10 g/L and 40 g/L, respectively. The dominant morphology varied from filamentous mycelia
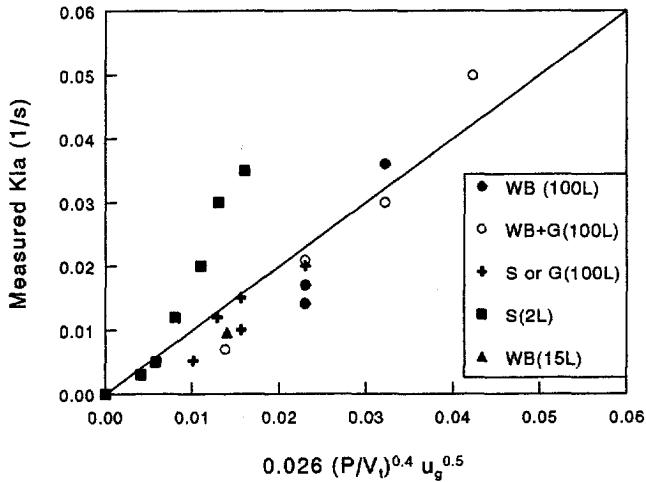
Figure 8. Gas-liquid mass transfer coefficients measured at different conditions during fermentations against those predicted by using the correlation from the literature[15].

to pellets. The comparison shows that the correlation matches the experimental data from the 100 L fermenter well. The correlation is claimed to be applicable for water or a low viscous medium. The broth in the synthetic-medium fermentations consisted of 5-7 g/L of biomass, 0-10 g/L of sugar and salt. For the complex medium fermentations it contained 0-8 g/L of biomass, 10-40 g/L of wheat bran and salt. From Fig. 8, it may be concluded that the broths were either not very viscous or the influence of the rheology in the present range on the gas-liquid mass transfer is negligible. The data measured in the 2 L fermenters are higher than predicted by the correlation. This may be caused by the relative large top surface or by the suction of air from the top place. If these data are excluded, the gas liquid mass transfer in the studied conditions can be described very well by this correlation.

CONCLUSIONS

Fermentations with *Aspergillus awamori* have been run in fermenters of 15 L, 100 L and 1800 L working volume using a complex medium (wheat bran). Due to the presence of wheat bran particles in the broth, adhesion growth may occur. The size of the inocula or the spore concentration was found to play an important role for this adhesion. When the spore concentration was lower than 1.8×10^4 spores per ml, no adhesion occurred. When it was higher than 1.3×10^5 spores per ml, adhesion dominated in fungal growth. If the concentration

was between these values, a mixture of wheat bran free pellets, clean wheat bran particles and attached colonies on wheat bran particles were observed. The addition of glucose to the medium did not influence the behaviour of fungal growth, so substrate limitation does not seem to be the trigger for growth onto the wheat bran particles.

The yields of biomass on carbon sources and on oxygen in the complex medium were the same as in the synthetic medium. This holds for the maintenance coefficient on carbon sources and on oxygen as well. The type of substrate had almost no influence on the ratio of biomass production to the sum of biomass production and carbon dioxide production. This offers an approach to estimate biomass production from the CO_2 production, which is desirable both for obtaining on-line information of biomass growth and for the situation where the biomass concentration is difficult to determine such as when a solid substrate is used.

The CO_2 production rate was almost equal to the oxygen consumption rate. In other words, the respiratory quotient was about 1, which was the same as with synthetic medium. Growth of biomass was accompanied by base consumption. After substrate depletion, acid was needed to maintain pH at the set point of 4.5.

Fungal morphology in the fermentations with complex medium changed with time and agitation intensity. The hairy length of pellets increased with time and then decreased, which was similar to the observation made with synthetic medium. Higher agitation intensities led to a shorter hairy length of pellets. A comparison of hairy lengths of pellets in different media shows that the pellets cultivated in sucrose medium have longer hairs than those in wheat bran medium. The solid substrate suppressed the growth in free filamentous mycelial form. The pellet sizes increased with time in the beginning (0-65 h) and then stayed more or less constant. Breakage of pellets is not a likely mechanism. Gas-liquid mass transfer during fermentations appeared to be well described by a correlation from the literature.

NOMENCLATURE

C_{CO2}	: accumulative CO_2 production per volume	mol L^{-1}
C_{O2}^{*}	: dissolved oxygen concentration saturated with gas phase	g/L
C_{O2}	: dissolved oxygen concentration in bulk	g/L
$C_{O2inlet}$	: oxygen concentration in the inlet air	g/L
$C_{O2off\text{-}gas}$	: oxygen concentration in off-gas	g/L
C_X	: biomass concentration	Cmol L^{-1}
C_s	: substrate concentration	mol L^{-1}
C_{s0}	: initial substrate concentration	Cmol L^{-1}
D	: diameter of impeller	m

m_s	: maintenance coefficient of cells	Cmol Cmol^{-1} h^{-1}
kla	: gas-liquid mass transfer coefficient	s^{-1}
P	: power input	W m^{-3}
Q_g	: aeration flow rate	m^3 h^{-1}
R_s	: substrate consumption rate	kg m^{-3} s^{-1}
R_x	: biomass growth rate	kg m^{-3} s^{-1}
R_p	: radius of pellets	m
t	: time of fermentations	s
T	: diameter of the stirred vessel	m
V_t	: total volume of reactor	m^3
u_g	: superficial velocity of gas	m s^{-1}
Y_{OX}	: yield of biomass on oxygen	Cmol/mol
Y_{SX}	: yield of biomass on substrate	Cmol/Cmol

Greek

μ	: specific growth rate	s^{-1}
μ_{max}	: maximum specific growth rate	s^{-1}
ϵ	: specific energy dissipation rate	W/kg
ρ_p	: dry biomass per wet pellet volume	kg/m^3
ρ_h	: density of hyphae	kg/m^3

REFERENCES

1. Dion, W.M., Carilli, A., Sermonti, G. and Chainl, E.B., 1954, "The effect of mechanical agitation on the morphology of *Penicillium chrysogenum* thom in stirred fermenters", *Istituto Superiore di Sanita (Eng.ED)*, **17**, 187-205

2. Clark D.S., 1962, "Submerged citric acid fermentation of ferrocyanide-treated beet molasses: morphology of pellets of *Aspergillus niger*", *Canadian Journal of Microbiology*, **8**, 133-136

3. Metz B, 1976, "From pulp to pellets", Ph.D thesis of Technology University of Delft.

4. Schügerl, K., Wittler, R. and Lorenz, T., 1983, "The use of molds in pellet form", *Trends in Biotechnology*, **1**, 120-123.

5. Yang, H, Reichi, U., King, R. and Gilles, E.D., 1992, "Mathematical model for apical growth septation and branching of mycelial microorganisms", *Biotechnol. and Bioeng.*, **39**,

49-58

6. Carlsen, M., Spohr, A.B., Nielsen, J. and Villadsen, J., 1995, "Morphology and physiology of an α-amylase producing strain of *Aspergillus oryzae* during batch cultivations", *Biotechnol. and Bioeng.*, **49**, 266-276

7. Cui, Y.Q., Van der Lans, R.G.J.M. and Luyben, K.Ch.A.M., 1997, " Effects of Agitation intensities on fungal morphology of submerged fermentation", *Biotechnol. and Bioeng.*, **55**, 715-726

8. Banerjee, U.C., Chisti, Y. and Moo-Young, M., 1993, "Spectrophotometric determination of mycelial biomass", *Biotechnol. Techniques*, **4**, 313-316

9. Matcham, S.E., Jordan, B.R. and Wood, D.A., 1985, "Estimation of fungal biomass in a solid substrate by three independent methods", *Appl. Microbiol. Biotechnol.*, **21**, 108-112.

10. Paul, G.C., Kent, C.A. and Thomas, C.R., 1994, "Hyphal vacuolation and fragmentation in Penicillium chrysogenum" , *Biotechnol. and Bioeng.*, **44**, 655-660.

11. Cui, Y.Q., Van der Lans, R.G.J.M. and Luyben, K.Ch.A.M., 1997, "Influence of fermentation conditions and scale on the submerged fermentation of *Aspergillus awamori*", submitted to *Enzyme Microbial Technology*.

12. Cui, Y.Q., Van der Lans, R.G.J.M. and Luyben, K.Ch.A.M., 1996, " Local power uptake in gas-liquid systems with single and multiple Rushton turbines", 14 international symposium on chemical reaction engineering, *Chem. Eng. Sci.*, **51**, 2631-2636

13. Roels, J.A., "Energetics and Kinetics in Biotechnology", Elsevier Biomedical Press, Amsterdam (1983), P.54

14. Cui, Y.Q., Van der Lans, R.G.J.M. and Luyben, K.Ch.A.M., 1997, "Effects of dissolved oxygen tensions and mechanical forces on fungal morphology of submerged fermentation", *Biotechnol. and Bioeng.* in press

15. Van't Riet, K. and Tramper, J., 1991, "Basic Bioreactor Design", Marcel Dekker, Inc. New York

CHAPTER 8

Physical Phenomena of Fungal Growth and Morphology in Submerged Fermentations

Y.Q.Cui, W.J. Okkerse, R.G.J.M. van der Lans, K.Ch.A.M. Luyben

Abstract

Generalizing results from fungal fermentations is difficult due to their high sensitivity towards slight variation in starting conditions, poor reproducibility and difference in strains. In this study an engineering model is presented in which oxygen transfer, agitation intensity, dissolved oxygen tension, pellet size, formation of filamentous mycelia, the fraction of filamentous mycelia in the total biomass, sugar consumption and biomass growth are taken into account. Two parameters were estimated from simulation, whereas all others are based on measurements or were taken from literature. Experimental data are obtained from the fermentations in both 2 L and 100 L fermenters at various conditions. Comparison of the simulation with experiments shows that the model can fairly well describe the time course of fungal growth (such as biomass and sugar concentrations) and fungal morphology (such as pellet size and the fraction of pellets in the total biomass). The model predicts that a stronger agitation intensity leads to a smaller pellet size and a lower fraction of pellets in the total biomass. At the same agitation intensity, pellet size is hardly affected by the dissolved oxygen tension, whereas the fraction of filamentous mycelia decreases slightly with an increase of the dissolved oxygen tension in the bulk. All of these are in line with observations at the corresponding conditions.

Keywords: Modelling; fungal fermentation; morphology; growth; operation conditions; stirred vessels.

INTRODUCTION

Fungal morphology in submerged cultures is usually classified as one of two extremes: individual filamentous mycelia, giving highly viscous and pseudoplastic fermentation broths, and dense, spherical colonies called pellets, leading to a low viscous suspension. In both cases mass transfer limitation may occur. With mycelia the viscous broth results in problems in bulk mixing and gas-liquid mass transfer, while internal diffusion limitation may occur within pellets. Whether fungi grow as individual filamentous mycelia or as pellets is influenced by a number of factors, such as the strain, medium, pH, temperature, mechanical forces, inoculum size and the dissolved oxygen tension. Control of the morphology is highly desired in industrial fungal fermentations. However, filamentous fungal fermentation is widely recognized as a complex process. In literature, much effort has been made to model fungal growth and morphology. Models for free filamentous mycelia include the description of spore germination, hyphal extension, hyphal segments and the number of branches as a function of time (Trinci and Saunders, 1977, Prosser and Trinci, 1979, Aynsley et al., 1990, Yang et al., 1992a, b., Nielsen and Krabben, 1995, Lejeune, 1996, Paul and Thomas, 1996). The simulation of pellet growth shows that the pellet size changes with time (Van Suijdam, 1980, Frederick et al., 1992, Edelstein and Hadar, 1983, Lejeune, 1996). Based on branching and extension of hyphae, Yang et al, (1992a and b) and Lejeune (1996) model theoretically the formation of pellets from free filamentous mycelia (or germinated spores). Assuming that pellets break up and the new pellets are formed from the obtained fragments, Edelstein and Hadar (1983), King et al.(1995), Tough et al.(1995) and Lejeune (1996) modelled the development of pellet populations. Edelstein and Hadar (1983) presented only a comparison of shapes of the measured and predicted distribution curve of pellet sizes, but gave no quantitative comparison. Tough et al. (1995) did not compare their model with experimental data. The highest class of a population of pellets predicted by a model (Lejeune, 1996 and King et al., 1995) is 5-10 times the observed one. So, quantitative predictions was not yet successful. In all these simulations, the change of pellet size and number is considered to be controlled by a growth and breakage mechanism. Previous work (Cui et al., 1997a & b) showed that in the model system used (submerged fermentation with *Aspergillus awamori* at different agitation intensities and different dissolved oxygen tensions) the breakage mechanism is of minor importance for pellet growth, while the chipping off of hyphae ('hairs') from the pellet surface is the dominant mechanism for governing the relationship between pellet size and mechanical forces. Moreover, the models reported in literature are either for filamentous hyphae or for pellets. In reality fungal morphology may change during the fermentation from pellets to filamentous mycelia and very often both of them exist simultaneously. It was shown that free filamentous mycelia were formed in pellet suspensions of fermentations inoculated with a pellet preculture and that the fraction of mycelia was influenced very much by agitation intensity (Cui et al, 1997a). Experimental observations from Cui et al., (1997a) and

Nielsen et al., (1995) show that the pellet fraction in the total biomass decreases with time during the fermentation. Such observations have not been modelled yet.

In this paper, we present a preliminary model to simulate a fungal fermentation in stirred vessels at different operation conditions. The inoculation was a pellet suspension. Fungal growth, pellet size, oxygen penetration in pellets and the fraction of free filamentous mycelia in the total biomass were modelled as a function of fermentation time, agitation intensity and oxygen concentration in the inlet gas. Gas-liquid mass transfer was taken into account so that the variation of dissolved oxygen tension in a stirred bioreactor was modelled in time. This is an important factor for growth and autolysis of pellets. Corresponding experiments were carried out to compare model simulations with experimental observations.

EXPERIMENTAL

Aspergillus awamori (CBS 115.52) was used as a model strain in the experiments. Cultures were maintained and spores produced on standard potato dextrose agar. The fermentations were carried out in a 100 L fermenter (140 L total volume) and 2 L fermenter (3 L total volume), respectively. The 100 L fermenter was installed with three Rushton turbines. The bottom impeller had a diameter of 17.4 cm, a blade height of 2.6 cm and a blade width of 3.2 cm. The top and middle one had a diameter of 13 cm, a blade height of 2.6 cm and a blade width of 3.2 cm. The 2 L fermenters were installed with two identical standard Rushton turbines (diameter : 4.5 cm). The composition of the media used is given in table I. A seed culture was used for the inoculation of the fermentation. The medium composition of the seed culture was the same as that of the fermentation medium.

Table I: Composition of the fermentation medium

Ingredient	concentration	
sucrose	10	g/L
NH_4Cl	9.0	g/L
KH_2PO_4	1.5	g/L
$NaNO_3$	1.0	g/L
$MgSO_4.7H_2O$	1.0	g/L
$CaCl.2H_2O$	0.3	g/L
Yeast Extract	1.0	g/L

The preparation of inocula for the 100 L fermenter was as follows. Four shaking flasks of 2 L were filled with 500 ml of the medium. The flasks with the medium were first sterilized and then 7 ml of a spore suspension with a concentration of 5.2×10^7 spores per ml was added. The flasks were rotated in a rotary shaker at 200 rpm for 24 hours. The temperature was kept at 25 ^{0}C. The obtained preculture was used to inoculate the fermenter. The initial fungal morphology of the preculture was small pellets. The mean core diameter of the pellets was about 0.7 mm.

The 100 L fermenter (140 L total volume) was filled with about 90 L medium which contained the nutrients for 100 L medium. For the sterilization of the medium in the fermenter, steam was used. A certain amount of steam condensed in the medium during sterilization. Therefore the actual initial concentration of the medium was measured after sterilization. Four flasks of preculture were transferred into the fermenter. The temperature set point was 25 $^{\circ}$C. The pH was maintained at 4.5, using ammonia and phosphate. Antifoam was added if needed. The stirrer speed was 250 rpm and the specific energy dissipation rate in the used gassed multi-impeller system was calculated (Cui et al, 1996). The power number of the bottom impeller with a non-standard geometry was corrected according to Carderbank and Moo-Young, (1961).

Fermentations in 2 L fermenter were run in parallel way. The set points of temperature and pH in 2 L fermenters were the same as in the 100 L fermenter. The detailed description has been given in literature (Cui et al. 1997a & b).

Samples were taken from the fermenters (100 L and 2 L) during the fermentations. The pellet core sizes were measured by means of image analysis (Cui et al.,1997a). At least 250 pellets were analyzed for each sample. The fractions of free filamentous mycelia and pellets in the total biomass were determined in terms of dry biomass fraction (Cui et al., 1997a). Part of the broth samples were spun down to separate solid biomass from the supernatant. The concentrations of sucrose, glucose, fructose and total organic carbon in the supernatant were determined by means of HPLC. A Bio. Red HPX 87N column was used at 85°C. Eluent was 15mM of $NaSO_4$ aqueous solution at a speed of 0.6 ml/min. The amount of injection was 10 μl.

MATHEMATIC MODEL

The model considers submerged fungal cultivation in which the broth consists of a mixture of pellets and filamentous mycelia in a stirred fermenter. A schematic description of the model is given in Fig.1. Pellets are divided into three distinct zones based on their structure. The first is the outer zone, or hairy part, which grows to the outside. Part of this outer zone is shaved off by hydrodynamic forces and the shaved off hyphae reseed the filamentous mycelia mass fraction. The severity of this shaving is a function of hydrodynamic forces. In the second zone, oxygen penetrates into it and fungal cells are active. The depth of this zone depends on the pellet density, growth rate and bulk dissolved oxygen tension. In the third zone of the pellets (so-called starvation zone in Fig.1), dissolved oxygen is depleted and autolysis occurs. The free filamentous mycelia in the bulk grow without oxygen or substrate limitation as long as dissolved oxygen and substrate are available in the bulk. The presence
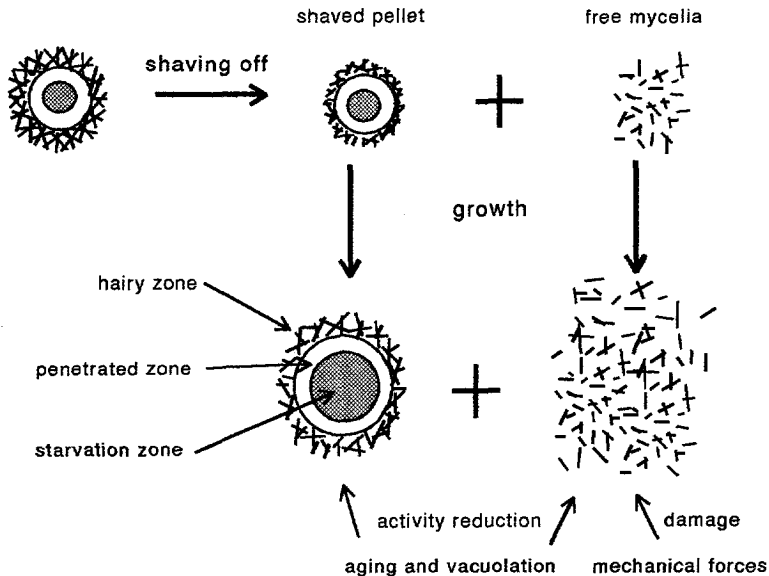
Figure 1. Schematic description of the presented model. Hairs of the pellet are shaved off by mechanical forces and are reseeded into mycelial growth. Both pellet and free mycelia grow. The mechanical forces damage and deactivate the free mycelia. aging and vacuolation result in the reduction of activity of both pellet and free mycelia.

of mechanical forces will deactivate filamentous mycelia. The magnitude of this deactivation depends on how large the mechanical forces are. In fungal hyphae, vacuoles are formed which increase in size with fermentation time. This will decrease the fungal hyphal activity per mass and lead to a reduction of specific growth rate. The bulk dissolved oxygen tension affects both pellet and filamentous growth. Gas-liquid mass transfer capacity and the oxygen consumption rate govern the bulk dissolved oxygen tension. The capacity of gas-liquid mass transfer is a function of power input, oxygen concentration in the inlet gas and the rheology of the fermentation broth. The combination of kinetics in the different pellet zones and the filamentous mycelia with the physical aspects of a stirred bioreactor will lead to a description of a submerged fermentation with a mixture of pellets and free filamentous mycelia.

Growth and deactivation kinetics

The growth of an individual hypha is confined to a region at its tip. New tips are created by branching and fragmentation. A relatively longer part of hyphae (several cells) behind the tip contributes to the tip extension. The extension rate of a hypha is proportional to its length if the total length is less than 15 mm (Trinci, 1974). Due to a linear extension rate of hyphae and the formation of new tips, the growth of free filamentous mycelia is effectively equivalent

to that of unicells. The exponential growth rate and Monod's expression for the specific growth rate are adopted in this work

$$R_x = C_x \mu \tag{1}$$

$$\mu = \mu_{m,t} \frac{C_s}{K_s + C_s} \frac{C_{O2}}{K_{O2} + C_{O2}} \tag{2}$$

where R_X is the biomass growth rate [kg m^{-3}s^{-1}], C_X the biomass concentration [kg m^{-3}], μ the specific growth rate [s^{-1}], $\mu_{m,t}$ the specific growth rate without substrate limitation at t hours of fermentation [s^{-1}], K_s the saturation constant of substrate [kg m^{-3}], C_s the local substrate concentration [kg m^{-3}], K_{O2} the saturation constant of dissolved oxygen tension [kg m^{-3}] and C_{O2} the local dissolved oxygen tension [kg m^{-3}].

Agitation is used to achieve a certain homogenization, gas dispersion and interphase mass and heat transfer for performing a submerged fermentation in a stirred vessel. Exposure of free filamentous mycelia to mechanical forces can result in damage and injury. It was reported that strong agitation led to a shorter hyphal length of filamentous mycelia (Dion and Kaushal, 1959, Metz et al. 1981, Ayazi Shamplou et al., 1994). The fungal mean hyphal length was found to be proportional to the specific energy dissipation rate to the power of -0.25 (Metz et al., 1976 and Cui et al., 1997a). This implies that mechanical forces can deactivate cells or decrease the specific growth rate of microorganisms. Such an inactivation mainly occurs for free filamentous mycelia since these are less protected. In order to describe this inactivation of free filamentous mycelia exposed to mechanical forces, its specific growth rate μ_f is expressed as.

$$\mu_f = \mu (1 - k_d \epsilon^{0.25}) \tag{3}$$

Where μ_f is the deactivated specific growth rate of free filamentous mycelia, μ the specific growth rate without mechanical damage, k_d the inactivation coefficient of hyphae due to mechanical damage and ϵ the specific energy dissipation rate [W/kg]. The higher the energy dissipation rate is, the more severely the hyphae will be deactivated. The inactivation is considered proportional to the specific energy dissipation rate with an exponent of 0.25, which is similar to the relation between the mean hyphal length and the specific energy dissipation rate.

The mechanical damage of hyphae and the inactivation of cells are complicated by other factors such as the formation of vacuoles in the cytoplasm, the increasing age and sizes of

the cells and the accumulation of toxic waste during fermentations. This can be illustrated by the variation of the hyphal length during fermentations. The common time profile of the fungal hyphal length in a stirred submerged fermentation as reported by Ayazi Shamplou et al. 1994, (main hyphal length) and Nielsen and Krabben, 1995, (total hyphal length) can be summarized as depicted in Fig.2. The hyphal length first increases as a result of growth. After some time, it starts
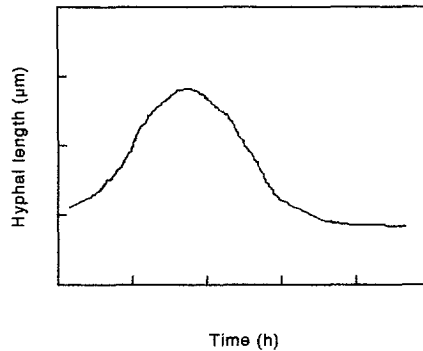

Time (h)

Figure 2. A general time profile of hyphal length at constant turbulent intensity summarized from the results of Ayazi Shamplou et al. (1994) and Nielsen and Krabben (1995)

to decrease despite a constant agitation intensity. After the decline phase, the hyphal length stays more or less constant. Previous measurements (Cui et al. 1997a) showed that also a rapid reduction of the hairy length of pellets occurred after a certain time of fermentation (14-24 h). This decrease can be explained by severe hyphal fragmentation as a result of the reduction of the hyphal tensile strength caused by the above mentioned factors.

Vacuolation occurs in hyphae as a natural process. The size of these vacuoles increases with fermentation time and eventually empty compartments will be formed in the hyphae. Paul et al. (1994) have measured the development of these vacuoles during a fermentation. The time profile of the volume percentage of the vacuoles in the cytoplasm corresponds to the time profile of the mean hyphal length. This strongly suggests that the reduction of the hyphal strength can be the result of the increase of vacuole size in hyphae. Below a certain volume fraction in the cytoplasm, the strength of the hyphae is not much influenced but above that value the strength of the hyphae decreases strongly. The reduction in strength of the pellet hairs reported in our previous study could be due to the effect of vacuolation as well. The reduction in strength will depend on strain, morphology and fermentation conditions. Data on these effects are lacking in literature. Considering that the reduction of the hairy length occurred at 14 - 24 h in our previous observation, we assume that a strong reduction in strength occurs after 20 hours of fermentation for *Aspergillus awamori* under the present studied conditions. In order to model this kind of kinetics mathematically, the following expression is chosen:

$$k_d = K_d (1 + \frac{t}{\tau})$$

(4)

Where K_d is the initial inactivation coefficient of hyphae caused by mechanical damage, t the time of fermentation [s], and τ the critical time of fermentation (20 h or 72000 s) when a strong reduction of hyphal strength occurs [s].

The formation of vacuoles in hyphae not only affect the strength but also the activity of fungal hyphae. A lower activity will result in a lower value of the maximum specific growth rate. The correction of the specific growth rate due to the formation of vacuoles in cytoplasm is expressed as

$$\mu_{m,t} = \mu_{max}(1 + \frac{t}{\tau})^{-0.5} \tag{5}$$

Substrate and oxygen consumption
In a fermentation, substrate and oxygen are consumed for growth, product formation and maintenance. In the case of no product formation, substrate and oxygen consumption rate are commonly described as (Roels, 1983):

$$R_S = \frac{R_x}{Y_{SX}} + m_S C_x \tag{6}$$

$$R_{O2} = \frac{R_x}{Y_{OX}} + m_{O2} C_x \tag{7}$$

Where R_S stands for the substrate consumption rate [kg m^{-3}s^{-1}], R_X for the biomass growth rate [kg m^{-3}s^{-1}], R_{O2} for the oxygen consumption rate [kg m^{-3}s^{-1}], C_X for the biomass concentration [kg m^{-3}], Y_{SX} for the yield of biomass on substrate [kg kg^{-1}], Y_{OX} for the yield of biomass on oxygen [kg kg^{-1}], m_S for the maintenance coefficient on substrate [kg kg^{-1} s^{-1}] and m_{O2} for the maintenance coefficient on oxygen [kg kg^{-1} s^{-1}].

Autolysis
Without substrate or oxygen, autolysis of cells will occur. The study of photomicrographs of cross sections of pellets showed that the centre of large pellets was autolysed (Clark, 1962). Oxygen limitation will occur in a pellet which is larger than a certain critical size. The critical size is a function of the pellet density, the bulk dissolved oxygen tension and the hyphal specific respiration rate. Trinci and Righelato (1970) and Bainbridge et al (1971) reported that for *Penicillium chrysogenum* and *Aspergillus nidulans* autolysis occurs when the mycelium is lacking substrate and that autolysis kinetics is an exponential one. In this study,

exponential autolysis kinetics is accepted. When the concentration of substrate or oxygen is lower than 1.0×10^{-6} g/L, autolysis occurs. Cell autolysis due to depletion is expressed as:

$$R_{aut} = K_{aut} C_X \qquad (8)$$

where R_{aut} is the autolysis rate of biomass [kg m^{-3} s^{-1}], C_X the biomass concentration [kg m^{-3}] and K_{aut} the autolysis constant [s^{-1}].

Shaving of hair from pellets

In a previous study (Cui et al., 1997a) it was shown that the outer hyphae (hairs) were shaved off from the outer zone of pellets due to mechanical forces in submerged fermentations. The breakage of pellets occurs less often when substrate and oxygen are available. This shaving process restricts the increase of pellet size during growth and the shaved-off hyphae reseed the free filamentous mycelial growth. It is assumed that shaving occurs only at the outer zone of pellets and that the shaving intensity is proportional to the specific energy dissipation rate.

$$R_{sha} = K_{sha} \epsilon R_{PG} \qquad (9)$$

where R_{sha} is the shaving rate of hyphae from pellet surface [kg m^{-3}s^{-1}], R_{PG} the growth rate of pellets [kg m^{-3}s^{-1}] and K_{sha} the shaving coefficient [kg/W].

Macrokinetics at the pellet level

The change in pellet size is much slower than the oxygen transfer process in pellets or in other words, the characteristic time of pellet growth is larger than the characteristic time of oxygen transfer in pellets. Therefore, the oxygen profile in pellets can be considered to be in a pseudo-steady state. In steady state, the mass balance of oxygen in a shell of a pellet leads to

$$\frac{D_{eff}}{r_p^2} \frac{d}{dr_p}(r_p^2)\frac{dC_{o2}}{dr_p} = R_{o2}\rho_p \qquad (10)$$

$$D_{eff} = D_m \epsilon_P = D_m (1 - \frac{\rho_p}{0.2\,\rho_h}) \qquad (11)$$

where D_{eff} is the effective oxygen diffusion coefficient [m^2 s^{-1}], r_p the radial position in pellets [m], C_{O2} the dissolved oxygen concentration [kg m^{-3}], R_{O2} the oxygen consumption rate [kg kg^{-1} s^{-1}], ρ_p the pellet density in dry weight [kg m^{-3}], ρ_h the wet hyphal density [kg m^{-3}] and

ϵ_P the porosity of pellet [-]. The water content in hyphae is assumed to be 80% so that the hyphal density in dry weight is 20% of ρ_h. Therefore $\epsilon_P = 1 - \dfrac{\rho_P}{0.2\,\rho_h}$

For Monod kinetics (Eq.2), Eq.(10) cannot be solved analytically. However, the saturation constants in Eq.(2) are rather low and in most cases the Monod growth kinetics can be approximated by zero-order reaction kinetics ($K_O = 0$ and $K_S = 0$) as has been used by many investigators (Michel et al. 1992, Van Suijdam, 1980). In the present study, the fermentation mode is batch, there are no substrate limitations for filamentous mycelia and pellet growth is mostly controlled by oxygen mass transfer before the sugar is depleted in the bulk. The error due to the use of the zero-order kinetics in pellets is negligible. For zero-order kinetics a critical radius of pellets exists. When pellets are larger than that, oxygen depletion occurs in part of the pellets. If the radius of this part is indicated by R_{0P}, then the boundary conditions for Eq.(11) become

$$
\begin{aligned}
\frac{dC_{O2}}{dr_P}\Big|_{r_P=0} &= 0 \\[2mm]
C_{O2}\big|_{r_P=R_P} &= C_{O2b} \\[2mm]
\frac{dC_{O2}}{dr_P}\Big|_{r_P=R_P} &= \frac{R_{O2}}{3\,D_{eff}}\Big(\frac{R_P^3 - R_{0P}^3}{r_P^2}\Big)
\end{aligned}
\tag{12}
$$

For zero-order kinetics the analytical solution of Eq.(10) under the boundary conditions of Eq.(12) gives the oxygen concentration as a function of the location in pellets, which is similar to a relation reported by Van' t Riet and Tramper (1991)

$$
\frac{C_{O2}}{C_{O2b}} = 1 + \frac{(\frac{\mu}{Y_{ox}} + m_{O2})R_P^2\,\rho_P}{6\,D_{eff}C_{O2b}}\Big(\frac{r_P^2}{R_P^2} - 1 + \frac{2R_{0P}^3}{r_P R_P^2} - \frac{2R_{0P}^3}{R_P^3}\Big)
\tag{13}
$$

In order to quantify whether the mass transfer controls a process, the Thiele modulus is used. The Thiele modulus is defined as the ratio of the kinetic rate and the diffusion rate. The Thiele modulus for zero-order kinetics is

$$
\phi^2 = \frac{(\frac{\mu}{Y_{ox}} + m_{O2})\,\rho_P R_P^2}{18\,D_{eff}\,C_{O2b}}
\tag{14}
$$

At $r_P = R_{0P}$, rearrangement of Eq.(13) and substitution of Eq.(14) give:

$$\phi^2 = (6\frac{R_{0P}^3}{R_P^3} - 9\frac{R_{0P}^2}{R_P^2} + 3)^{-1} \tag{15}$$

The radius of the oxygen depleted part in a pellet is a function of the Thiele modulus. When R_{op} is zero oxygen penetrates a pellet just fully and the Thiele modulus will be $3^{-1/2}$ (about 0.577). Based on the definition of R_{0P}, the solution of Eq.(15) is

$$\frac{R_{0P}}{R_P} = \cos(\frac{y+4\pi}{3}) + \frac{1}{2} \tag{16}$$

$$y = \cos^{-1}(\frac{2}{3\phi^2} - 1) \tag{17}$$

where cos and $\cos^{-1}$ are in radials. During a fermentation, pellet size, pellet density and dissolved oxygen tension change with time. This means that the Thiele modulus changes as well. Knowing the value of the Thiele modulus, the oxygen penetration in pellets and pellet growth kinetics can be calculated.

Bioreactor
Submerged fungal fermentations are generally carried out in stirred vessels. For a large scale fungal fermentation, mixing plays an important role for the fermentation performance. This role is diminished with the reduction of fermenter size and broth viscosity. In the present study, the size of the used fermenters varied from 2 to 100 L and the highest biomass concentration was about 6 g/L. For a 100 L fermenter filled with fungal fermentation broth, the measurement of pH pulse response curves showed that 95% homogenization time decreased from 60 to 20 seconds with the increase of stirrer speed from 200 rpm to 600 rpm. Considering that the 100 L fermenter was equipped with three impellers, the mixing time in each stage will be much lower than the measured overall mixing time. From the measured gas-liquid mass transfer coefficient, k_La, the characteristics time of oxygen transfer was calculated to be 83 seconds under fermentation conditions. Therefore, the system used can be considered as an ideal mixed bioreactor.

Due to the importance of the dissolved oxygen tension in all aerobic fermentations, a lot of effort have been devoted in literature to the prediction of the overall gas-liquid mass-transfer coefficient, k_La. In general, k_La is a function of the rheology of the broth (medium), the coalescing properties of the broth, the energy dissipation rate and the gas flow rate. For a

coalescing and nonviscous medium, a gross correlation (Van' t Riet and Tramper, 1991) can be expressed as

$$k_L a = 0.026 \left(\frac{P}{V_t}\right)^{0.4} u_g^{0.5} \tag{18}$$

The influence of viscosity on $k_L a$ in a stirred vessel is not very clear. Van' t Riet and Tramper, (1991) stated that when the viscosity of the medium is lower than 50 mPa.s, its influence can be neglected. If the viscosity is above 50 mPa.s, then $k_L a$ decreases with viscosity to a power of about 0.7.

Macrokinetics at the Bioreactor level

The size of pellets changes during the fermentation and is a function of growth rate, the oxygen penetration depth in the pellets, the shaving intensity, the autolysis rate and the rate of pellet density change. Its mathematic description may be given as follows:

$$4\pi R_p^2 \rho_p \frac{dR_P}{dt} = \frac{4\pi}{3}(\mu(1-K_{sha})(R_P^3-R_{0P}^3)\rho_p - K_{aut}R_{0P}^3 \rho_p - \frac{d\rho_p}{dt}R_p^3) \tag{19}$$

The change in pellet size is the result of growth minus shaving, autolysis and pellet density change. R_{0P}, the radius where the dissolved oxygen tension in the pellets is zero, is calculated from Eq.(16). The pellet density changed during our fermentations. But information on its time course is lacking. As a simplification pellet density is assumed to be a linear function of fermentation time. Knowing the pellet density ρ_p, the specific growth rate μ, the shaving coefficient K_{sha} and the autolysis coefficient K_{aut}, Eq.(19) can be integrated to calculate the pellet size at any moment. From the pellet size and pellet concentration (N_P : m^{-3}), pellet biomass concentration is calculated as

$$C_{xp} = N_P \rho_P \frac{4\pi}{3} R_p^3 \tag{20}$$

Three terms govern filamentous mycelial biomass. The first is growth. The second is the mass of hyphae shaved off from pellets. The third is autolysis which occurs only when substrate is used up. Hence, filamentous mycelial biomass is modelled as:

$$\frac{dC_{xm}}{dt} = \mu_f C_{xm} + K_{sha}\mu(R_p^3-R_{0p}^3)\frac{4\pi}{3}\rho_p N_P - K_{aut}C_{xm} \tag{21}$$

Under aerated conditions, oxygen in the gas phase is transferred into the liquid phase continuously. The dissolved oxygen is consumed by both filamentous mycelia and pellets. The dissolved oxygen concentration in the bulk is calculated as

$$\frac{dC_{O2}}{dt} = k_L a(C_{O2}^* - C_{O2}) - (\frac{\mu_f}{Y_{ox}} + m_{O2}) C_{xm} - (\frac{\mu}{Y_{ox}} + m_{O2}) \rho_P N_P \frac{4\pi}{3}(R_P^3 - R_{0p}^{\,3}) \qquad (22)$$

Considering the relationship between substrate consumption and biomass formation and the amount of substrate consumption for maintenance, the substrate concentration can be expressed as

$$C_s = C_{s0} - \frac{C_{xm} + C_{xp} - C_{x0}}{Y_{sx}} - \int_0^t (C_{xp} + C_{xm}) \, m_s dt \qquad (23)$$

Solving Eq.(19)-(23) and calculating the relevant parameters simultaneously will lead to the mathematic description of a fungal fermentation with a mixture of pellets and mycelia.

PARAMETER VALUES AND SIMULATION

The numerical calculation of the model was implemented in Psi-C.

For *Aspergillus oryzae*, a maximum specific growth rate of 0.27-0.29 h^{-1} was measured by Carlsen et al. (1996). Trinci (1970) reported that the highest specific growth rate of *Aspergillus nidulans* was 0.36 h^{-1}. Yano et al. (1961) and Kobayashi et al (1973) reported the maximum respiration rate of 6.1×10^{-5} kg kg^{-1} s^{-1} for *Aspergillus niger*. Assuming that the yield of biomass on oxygen is 1 g/g, this respiration rate corresponds to a maximum growth rate of 0.22 h^{-1}. In the present study, the observed highest apparent specific growth rate was about 0.2 h^{-1}. Because of the presence of pellets in the fermentation broth it is difficult to estimate the maximum specific growth rate from the observed specific growth rate. The maximum specific growth rate of *Aspergillus awamori* used in the model is assumed to be 0.27 h^{-1} (7.5 10^{-5} s^{-1}) for glucose and fructose.

The carbon source used during fermentation was sucrose. The time profile of the sugar concentration during the fermentations indicated that the used strain first consumed glucose and then took up the fructose (Cui et al, 1997c). The enzymatic hydrolysis of sucrose into glucose and fructose is much faster than the sugar uptake rate, which allows us to ignore the kinetics of sugar hydrolysis and to assume that the fermentation started with glucose and fructose.

The saturation constant for substrate in the Monod expression, K_s in Eq.(2), is an inverse measure of the affinity of the organism for the substrate. In literature, no saturation constants for *Aspergillus awamori* could be found. Pirt (1973) reported a glucose saturation constant of 0.005 kg/m^3 for *Aspergillus nidulans*. In this study, the saturation constants of glucose and fructose for *Aspergillus awamori* are assumed to be 0.01 kg/m^3. Since the fermentation mode is batch and the characteristic time for sugar transfer from the bulk to the pellet centre is much smaller than the one for dissolved oxygen transfer, limitation of sugar hardly occurs before it is depleted in the bulk. This means that the model simulation is not much influenced by this parameter.

The saturation constant for oxygen in the Monod expression, K_o in Eq.(2), is an inverse measure of the affinity of the organism for oxygen. In general, the saturation constants for oxygen are in the order of 10^{-4} kg/m^3 (Metz and Kossen, 1977). Kobayashi et al. (1973) reported an oxygen saturation constant of 1×10^{-4} kg/m^3 for *Aspergillus niger*. Michel et al. (1992) used 5×10^{-4} kg/m^3 as oxygen saturation constant for *P.chrysosporium* BKM-F-1767 and Lejeune (1996) used 3×10^{-4} kg/m^3 for *Trichoderma reesei* QM 9414. For *Aspergillus awamori*, the oxygen saturation constant is assumed to be 1×10^{-4} kg/m^3, which is in line with the above studies. In the bulk, the dissolved oxygen concentration is often much higher than the saturation constant. So in case of filamentous mycelia, dissolved oxygen limitation under the studied conditions hardly occurs and pellet growth is mainly controlled by oxygen transfer from the bulk into the pellets. Therefore the oxygen saturation constant will not have much effect on the model simulation under the present studied conditions.

Michel et al., (1992) used an autolysis constant of 0.009 h^{-1} for *P. chrysosporium* pellets. Fig.3 shows the reduction of dry biomass as a function of time under the condition of glucose or oxygen depletion from Bainbridge et al., (1971) and the present work. The data of Bainbridge et al. (1971) were obtained from glucose starved mycelium of *Aspergillus nidulans*. The present data I and II in Fig.3 are dry biomass concentrations measured in a broth stored in a refrigerator at 4°C. In the broth, sugar was still available but oxygen was depleted. The literature data and the present data are very comparable. Based on these data, the autolysis constant was
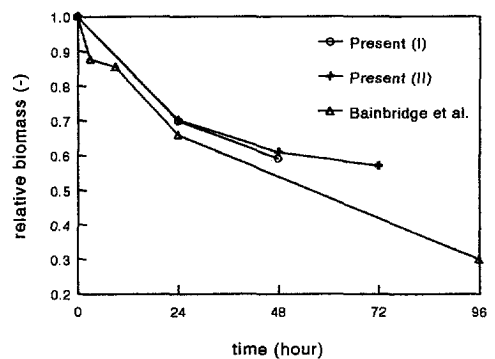

Figure 3. Cell autolysis due to substrate starvation. The present observations from two fermentations, referred as present I and present II, and literature data (Bainbridge et al., 1971).

estimated to be 0.01 h⁻¹. This is close to the autolysis constant used by Michel et al. (1992). In the present study, 0.01 h⁻¹ (2.8 10⁻⁶ s⁻¹) is used as the autolysis constant under the condition of oxygen starvation.

It is obvious to assume that part of the autolysed cells can be used as a substrate for the microorganisms. This means that autolysis due to the depletion of sugar will be diminished by digestion of parts of the autolysed cells. In our model we assume that 50% of the autolysed cells is digestible by cells.

A yield coefficient of 0.63 Cmol/Cmol was reported by Roels, (1983) for *Aspergillus awamori* grown on glucose. In a previous study (Cui et al. 1997c) the yield coefficients of the present strain on glucose and fructose were found to be 0.78 Cmol/Cmol or 0.65 kg/kg. It is higher than the values from literature. It seems that the present strain uses substrate very efficiently. The yield coefficients on glucose and fructose were assumed to be the same and constant during fermentation. The value of 0.65 kg/kg is used in this model. The yield coefficient of biomass on oxygen was found to be 3.55 Cmol/mol or 2.77 kg/kg. This means that the used strain is very efficient in the oxygen consumption as well.

Microorganisms use substrate and oxygen not only for growth but also for maintenance (see Eq.(6) and Eq.(7)). The maintenance coefficients of the present strain on substrate and oxygen were determined in a previous study (Cui et al. 1997c). It was found that the maintenance coefficient on substrate (m_s) was 1.9×10^{-6} kg kg⁻¹ s⁻¹ and the maintenance coefficient on oxygen (m_{O2}) was 2×10^{-6} kg kg⁻¹ s⁻¹.

The pellet density cultivated in a 2 L fermenter at a stirrer speed of 300 rpm was about 14 kg/m³. The preculture was cultivated in a shake flask at 200 rpm. A low dissolved oxygen tension was expected in the preculture. The low dissolved oxygen tension will lead to the formation of low density pellets (Cui et al. 1997b). The density of pellets in the preculture is assumed to be 10 kg/m³. For the model simulation, the change of pellet density with time, $\frac{d\rho}{dt}$, is needed (see Eq.(19)). As stated above it is assumed to increase linearly from time zero to 40 hours.
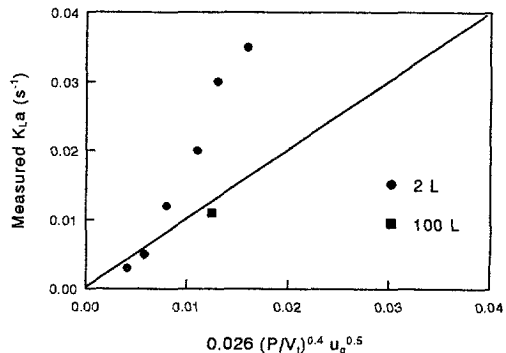

Figure 4. Comparison of the gas-liquid mass transfer coefficients from measurements and predictions by using Eq.(18) (Van 't Riet and Tramper, 1991).

In the case of lacking acrtual data on gas liquid mass transfer, k_La can be estimated by using Eq.(18). In the present study, the data of the dissolved oxygen tension, offgas analysis and gas flow rate allowed us to calculate the mass transfer coefficient for each fermentation. The values of k_La calculated from the fermentation data are given in Table II. Fig.4 shows the comparison of the values of k_La from fermentation with the values predicted from Eq.(18). In the low range of the mass transfer coefficients or for the 100 L fermenter, the prediction agrees with the experimental data. But the valus of k_La above 0.01 s^{-1} measured in the 2 L fermenter are larger than the prediction. Model simulation will be based on the values of k_La calculated from the fermentation data.

The value used for the model parameters and of other physical and chemical constants are given in Table III.

Table II. fermentation and simulation conditions

Fermenter	Stirrer speed rpm	Energy dissipation W.m^{-3}	oxygen in inlet gas %	K_La¥ measured s^{-1}	C_{x0} initial kg.m^{-3}	initial diameter mm	pellet† density kg.m^{-3}	remark
100 L	250	800	20.95	0.011	0.065	0.7	33	preculture I
3 L	300	194	20.95	0.003	0.13	1	14	preculture II
3 L	450	450	20.95	0.005	0.13	1	24	preculture II
3 L	600	1060	20.95	0.012	0.13	1	37	preculture II
3 L	750	2100	20.95	0.02	0.13	1	40	preculture II
3 L	900	3600	20.95	0.03	0.13	1	57	preculture II
3 L	1050	5700	20.95	0.035	0.13	1	50	preculture II
3 L	600	1060	4	0.012	0.13	1	17.5	preculture III
3 L	600	1060	10	0.012	0.13	1	24	preculture III
3 L	600	1060	20.95	0.012	0.13	1	41	preculture III
3 L	600	1060	40	0.012	0.13	1	55	preculture III
3 L	600	1060	60	0.012	0.13	1	62	preculture III
3 L	600	1060	80	0.012	0.13	1	60	preculture III

† observation at ca. 40 h of fermentation

¥ the gas-liquid mass transfer coefficient is calculated from the dissolved oxygen tension and the off-gas data

Table III. Parameter values used in model simulations

parameter	definition	value		remark
K_d	cell inactivation constant	0.11	-	fitted parameter
C_{O2}*	dissolved oxygen tension saturated with air	0.0084	kg m^{-3}	ref.Handbook (Perry)
D_m	oxygen diffusion coefficient	2.5×10^{-9}	m^2 s^{-1}	ref.Handbook (Perry)
K_{aut}	cell autolysis constant	0.0000027	s^{-1}	measured & Bainbridge; Michel
K_{O2}	oxygen saturation constant	0.0001	kg m^{-3}	ref.Kabayashi et al 1973
K_s	substrate saturation constant	0.01	kg m^{-3}	ref.Pirt.1973 (0.005)
K_{sha}	shaving coefficient	0.00006	-	fitting parameter
m_{O2}	maintenance coefficient on oxygen	0.000002	kg/kg s	observation
m_S	maintenance coefficient on substrate	0.0000019	kg/kg s	observation
Y_{OX}	biomass yield on oxygen	2.77	kg/kg	observation
Y_{SX}	biomass yield on substrate	0.65	kg/kg	observation
μ_{max}	maximum specific growth rate	0.27	h^{-1}	estimation

SENSITIVITY OF MODEL PARAMETERS

Shaving coefficient

The exposure of pellets to an agitation environment results in the shaving off of hair from pellets (Cui et al.,1997a). The shaving constant K_{sha} in Eq.(9) is chosen to describe the severity of this shaving effect. Comparison with all fermentation data led to a best fit value of 0.06 kg/W. This means that under specific energy dissipation rate of 1 W/kg, pellet growth will be reduced by 6% due to shaving hair out pellets. How sensitive the model is on this constant is studied by model calculations with different values of this parameter.

Fig.5a and Fig.5b show the relative change of the predicted pellet radius, biomass, the fraction of filamentous mycelia in the total biomass and sugar concentration in the bulk as a function of the change in the shaving coefficient. The Y-axis depicts the relative change in the output and the X-axis depicts the ratio of the shaving coefficient used in the sensitivity
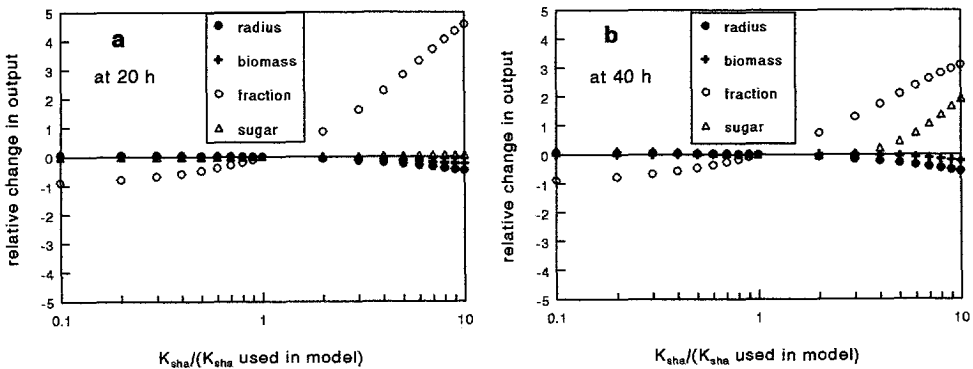

Figure 5. Sensitivity of model to the shaving coefficients with respect to pellet radius, biomass concentration, free filamentous mycelial fraction in total biomass and sugar consumption. **a**: at 20 h; **b**: at 40 h.

study to the one fitted from the model simulation. The relative change is defined as the change in output divided by initial output. Only the fraction of filamentous mycelial mass in the total biomass is sensitive to this parameter. A larger coefficient results in a higher fraction of filamentous mycelial mass in the total biomass, which is in line with the definition of the shaving coefficient. The comparison of the effects of this coefficient at different times shows that the fraction becomes less sensitive at later times.

Inactivation of hypha due to mechanical forces

Mechanical forces not only shave off the hair from the pellets but also damage the free

filamentous mycelia. The inactivation constant is used to describe such an effect on the filamentous growth. In the present model, the inactivation is expressed by Eq.(3) & Eq.(4). The value of inactivation constant used in Eq.(4) is 0.11 $(kg/W)^{1/4}$ obtained from a fit of the model simulation with the experimental data. It says that the mechanical forces will deactivate 11% of the hyphae at a specific energy dissipation rate of 1 W/kg. The results of a sensitivity analysis on this parameter are depicted in Fig.6a and Fig.6b. The two plots shows that the
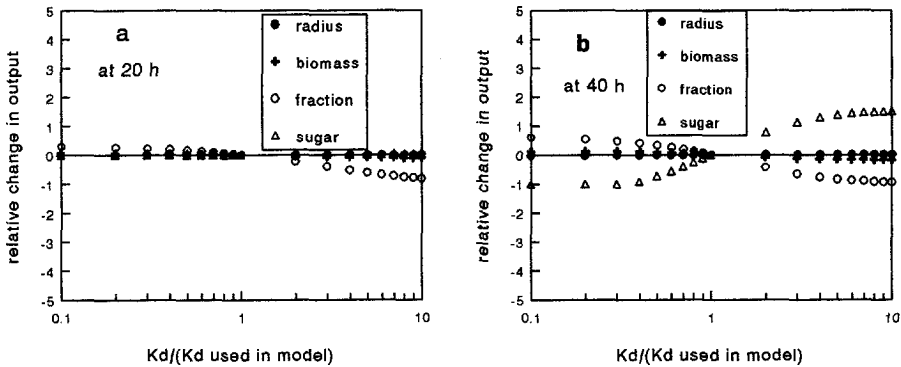

Figure 6. Sensitivity of model to the initial inactivation coefficient with respect to pellet radious, biomass concentration, free filamentous mycelial fraction in total biomass and sugar consumption. **a**: at 20 h; **b**: at 40 h.

filamentous mycelial fraction rises with decreasing the value of the parameter from 1.1 to 0.011 $(kg/W)^{1/4}$ or the ratio from 10 to 0.1. The relative change in the sugar concentration, the pellet radius and biomass concentration are much less sensitive than the fraction at 20 h. The relative change of sugar concentration is the most sensitive one in all variables at 40 h (Fig.6b). The explanation is that the sugar concentration simulated at 40 h is very low so that its relative change gets very sensitive. The sensitivity of pellet radius, biomass concentration, fraction and sugar concentration to the inactivation coefficient becomes larger with the increase of time.

RESULTS AND DISCUSSION

A batch fermentation of *Aspergillus awamori* was performed at 100 litre. The stirrer speed was 250 rpm, which corresponds to 0.8 W/kg specific energy dissipation rate. The preculture was a pellet suspension. The size of the pellets in the preculture was about 0.7 mm and the initial biomass concentration was 0.065 kg m^{-3}. During the fermentation, the biomass and the

pellet size increased, free filamentous mycelia appeared and the sugar was consumed. In previous studies (Cui et al., 1997a, 1997b), parallel fermentations have been performed at different agitation intensities and at different dissolved oxygen tensions at the same agitation intensity. The present model couples the fungal growth kinetics, the oxygen transfer in pellets, the quantitative description of the environment in the bioreactor at different operation conditions and the influence of the hydrodynamic conditions on the fungal morphology. By using different agitation intensities and different oxygen concentrations in the inlet gas, simulations of fungal fermentations at corresponding conditions were carried out. The fermentation conditions and the corresponding simulation parameters are given in Table II and Table III.
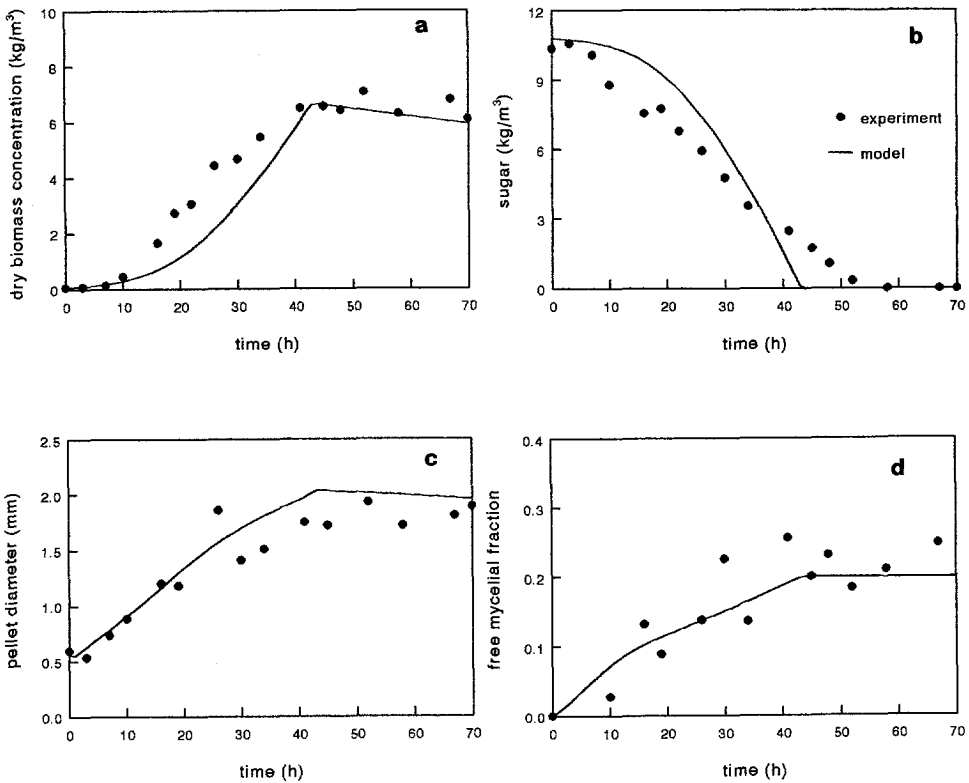

Figure 7. Observation (the markers) and model simulation (the lines) for the 100 L fermentation at a specific energy dissipation rate of 0.8 W kg^{-1}. **a**: time profile of biomass concentration, **b**: time profile of sugar consumption, **c**: time profile of pellet sizes; **d**: time profile of free filamentous mycelial fraction in the total biomass.

Fig.7a shows both the observed and the calculated biomass concentration in the 100 L fermentation. Without specification, biomass stands for the total biomass, which consists of both pellet mass and mycelial mass. The model predicts a slower biomass formation than found in the actual fermentation. Chemical elements analysis of the biomass showed that the biomass contained about 42% carbon [kg/kg]. A common biomass composition (Roels, 1983) is $CO_{0.5}H_{1.8}N_{0.2}$, which corresponds to 48% carbon in biomass [kg/kg]. Sugar has 40% carbon in mass. So if polysaccharide is formed and stored in the fungal cells, then the carbon content in the cells will be lower. But unfortunately the determination of polysaccharide formation was not done yet. Therefore no conclusive explanation for the low carbon content can be given in the present study. The measured sugar concentration in the period of 0 to 40 hours fermentation was lower than the one predicted by the model (Fig.7b), which corresponds to the time profile of biomass. However, full sugar depletion predicted by model is faster than measured. This implies that the actual substrate consumption rate at the later phase (30-50 h) was overestimated in simulation although inactivation term (see Eq.3) and aging term (see Eq.4) have been taken into account.

The predicted and observed time profiles of pellet sizes are depicted in Fig.7c. It shows that the pellet sizes increased rapidly during the first 40 h of the fermentation. After that the increase is much less. The predicted time profile of the pellet size matches the actual one well. The filamentous mycelia fraction in the total biomass during the fermentation was measured and simulated. The results are depicted in Fig.7d. In general, the fraction of filamentous mycelia in the total biomass increased with fermentation time. According to the model this is caused by two factors. On the one hand the pellet growth is limited by oxygen transfer while the filamentous mycelial growth is not. On the other hand the shaved off hyphae from pellets reseed the filamentous mycelial growth. Model and observation are in agreement. Knowing the mass transfer rate from the bulk to the pellets, the dissolved oxygen tension in the bulk and the oxygen consumption rate in the pellets, the oxygen penetration in the pellets can be calculated as a function of time. The calculated penetration depth of oxygen is presented in Fig.8. Molecular diffusion is assumed to be the dominant mechanism for oxygen transport in pellets. With the increase of pellet size, the oxygen depletion radius within a pellet increases as well. At 48h, all sugar is consumed and oxygen penetrates into the whole pellet since no oxygen is consumed any more. In literature (Clark,
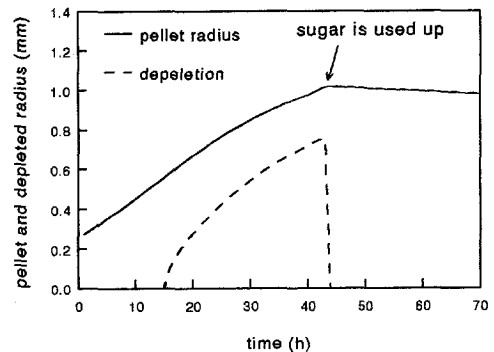
Figure 8. Calculated time profile of pellet sizes and oxygen penetration in pellets.

1962, Tough et al. 1995), it has been reported that hollow centres are formed in pellets if they are larger than a certain size. This is probably caused by lack of oxygen in the pellet centre.
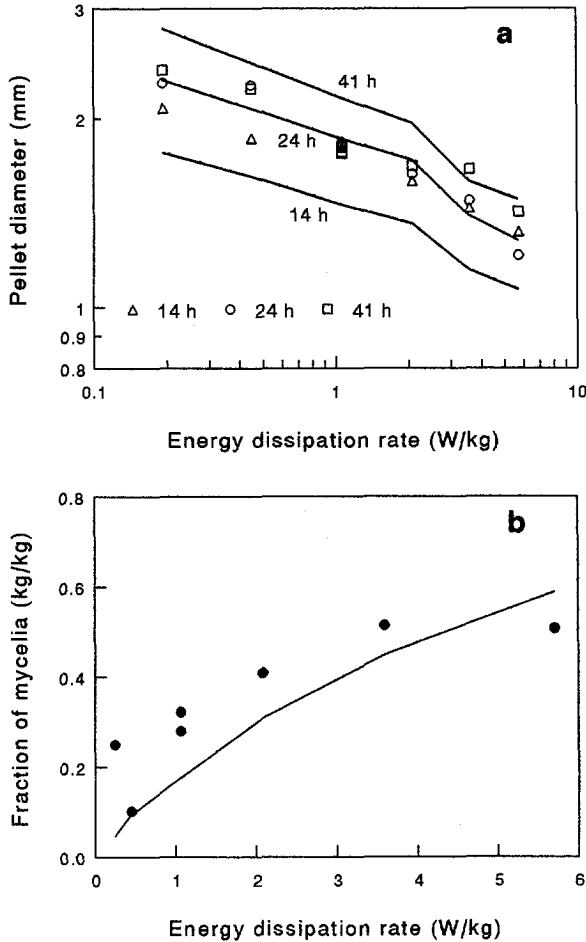
Figure 9. Observation (the markers) and model predictions (the lines) of the effects of the agitation intensity on pellet size (**a**) and free filamentous mycelial fraction in the total biomass (**b**) at 24 h.

It is well known that agitation intensity affects fungal morphology (Dion and Kaushal, 1959, Metz 1976, Ayazi shamplou et al., 1994, Cui et al., 1997a). Data from Cui et al. (1997a) from parallel fermentations under different agitation intensities are plotted in Fig.9a and Fig.9b. Using the corresponding conditions in the model, pellet sizes and filamentous mycelial fractions are calculated as well. The calculated values at different agitation intensities

are presented as curves. Model predictions are close to the experimental data. A higher
agitation intensity results in a smaller pellet size. Fig.9b shows the fraction of filamentous
mycelia in the total biomass. At the lowest specific energy dissipation rate, the measured
fraction is somewhat higher than the predicted one. The higher the agitation intensity, the
larger the filamentous mycelial fraction.

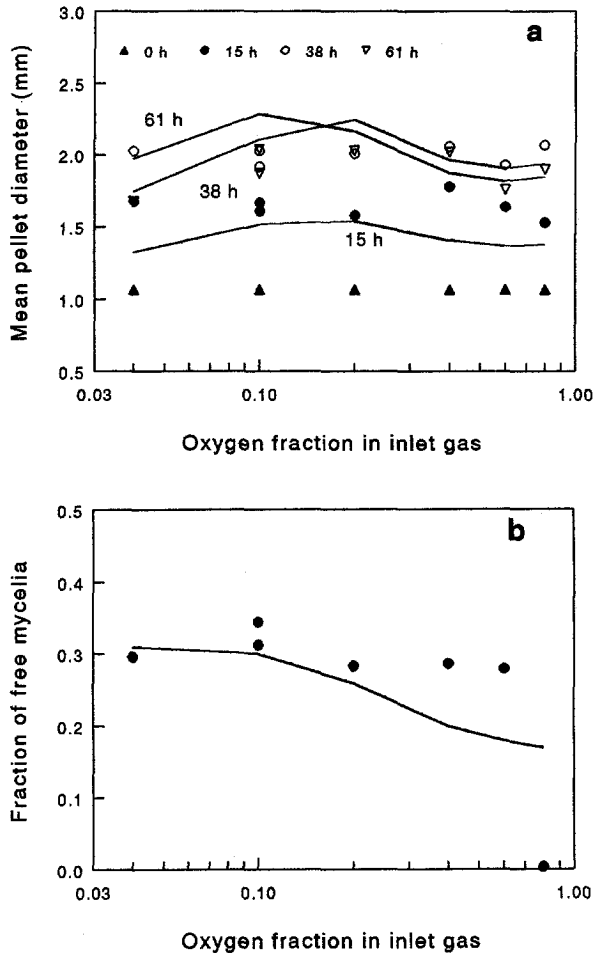**Figure 10**. Observation (the markers) and model predictions (the lines) of the effects of the
dissolved oxygen tension on pellet diameter (**a**) and free filamentous mycelial fraction in the total
biomass (**b**) at 38 h.

The effect of dissolved oxygen tension on fungal morphology has been studied previously
(Cui et al., 1997b). The fermentations were run in parallel under different dissolved oxygen

tensions but at the same agitation intensity. Fig.10a shows the pellet sizes measured in the parallel fermentations, together with the corresponding data calculated by the model. The model predicts that the pellet size formed at 10-20% oxygen fraction in inlet gas is somewhat larger than the others. The experimental data did not show this tendency. After 15 h of fermentation, the measured pellet size is larger than the one calculated by the model. The rest of the calculations match the observations reasonable well. Both the experimental data and the model predictions show that the dissolved oxygen tension has a limited influence on pellet size. The measured filamentous mycelial fractions are shown in Fig.10b again with the model simulations. The model predicts a tendency for the fraction to decrease with the increase of the dissolved oxygen tension, but the experimental data do not show this effect. In literature (Metz and Kossen, 1977, Vecht-Lifshitz et al. 1989) it is a common statement that a higher dissolved oxygen tension favours pellet growth. This could be interpreted as that a higher dissolved oxygen tension leads to a lower fraction of filamentous mycelial mass in the total biomass. Unfortunately no quantitative data have been reported, so a quantitative comparison with the model simulation and observations is impossible. The value calculated by the model is close to the measurements in our previous study. It was noticed that when the dissolved oxygen tension reaches 80% of the oxygen saturation concentration, filamentous mycelial fraction became zero, which was much different from the general tendency shown by the rest of data. This implies that some physiological factor plays a role as well while this factor was not taken into account in the present model.

The presented model demonstrates how a submerged cultivation with a mixture of pellet and mycelia in stirred vessels can be simulated with respect to fungal growth, fungal morphology and hydrodynamic conditions in fermenters. Since the macrokinetics at the bioreactor level is incorporated into the model, the effect of operation conditions, such as the agitation intensity, the gas flow rate and the oxygen concentration in the inlet gas on the fermentations can be predicted. Most of the parameters used for the simulation are based on measurements or reported values in literature. In total, two fitted parameters were used in the model, the shaving constant and the inactivation coefficient. The present model should be considered as an engineer model. Model predictions are in reasonable agreement with the observations at the different studied conditions. Some deviations between model simulation and observations exist. The predicted time course of fungal growth and morphology at different conditions allow one to obtain a reasonable idea on the behaviour of a fungal fermentation without actually conducting it.

Possible extensions and modifications of the model are, of course, of interest. The present model lacks the description on the morphology of free filamentous mycelia such as differentiation, branching, septation, product formation and vacuolation at different fermentation conditions. If these could be included more detailed information can be obtained

from a simulation. Furthermore, heterogeneity at the bioreactor level is ignored in the present simulation. Mixing is hardly a problem under the present conditions. However, in a large reactor or for a highly viscous fermentation broth insufficient mixing occurs. This will result in a heterogeneity in fermenters. In such a case, the local situation has to be used instead of the bulk situation. In principle, the combination of computational fluid dynamics or compartment models with the present model could give a description of fungal fermentation in a larger bioreactor.

CONCLUSIONS

A model is developed to simulate fungal growth and morphology in pellet and free filamentous mycelial culture in stirred fermenters. Fermentations of *Aspergillus awamori* in 100 L and 2 L fermenters have been run. The calculated time profiles of sugar consumption, biomass concentration, pellet size and the filamentous mycelia fraction match the observed ones. The penetration depth of dissolved oxygen into pellets during a fermentation is simulated. By using different energy dissipation rates in the model calculations, pellet sizes and the filamentous mycelial fractions in the total biomass are predicted. The model simulation agrees with literature data under corresponding conditions. The stronger the agitation, the smaller the pellet size and the lower the fraction of pellet mass in the total biomass becomes. The agreement between the observations and the calculations suggest that the hypothesis in the model that "hyphae are shaved off from pellet surface and reseed the growth of mycelia" is a good one. Also the effect of the dissolved oxygen tension on fungal fermentation is simulated. The comparison of the simulation with the data reported earlier shows a good agreement in terms of pellet size. However the model predicts that the fraction of the filamentous mycelial mass in the total biomass decreases with the increase of dissolved oxygen tension in the bulk while the data observed do not demonstrate such a tendency. Lack of data in literature prevented to verify if a higher dissolved oxygen tension favours pellet growth, which would mean that a higher dissolved oxygen tension leads to a lower fraction of filamentous mycelial mass in the total biomass.

NOMENCLATURE

C_{O2}	: dissolved oxygen concentration	kg m^{-3}
$C_{O2}{}^{*}$	: saturated dissolved oxygen concentration	kg m^{-3}
C_x	: biomass concentration	kg m^{-3}
C_{x0}	: initial biomass concentration	kg m^{-3}
C_s	: substrate concentration	kg m^{-3}

C_{s0}	: initial substrate concentration	kg m^{-3}
C_{O2b}	: dissolved oxygen tension in the bulk	kg m^{-3}
C_{xm}	: filamentous mycelial biomass concentration	kg m^{-3}
C_{xp}	: pellet mass concentration	kg m^{-3}
D_{eff}	: effective diffusion coefficient of oxygen in pellets	m^2 s^{-1}
D_m	: molecular diffusion coefficient of oxygen in pellets	m^2 s^{-1}
K_{aut}	: cell autolysis constant	s^{-1}
k_d	: inactivation coefficient	-
K_d	: initial cell inactivation coefficient	-
K_{O2}	: oxygen saturation constant	kg m^{-3}
K_s	: substrate saturation constant	kg m^{-3}
K_{sha}	: shaving coefficient	-
$k_L a$	: gas-liquid mass transfer coefficient	s^{-1}
m_{O2}	: maintenance coefficient on oxygen	kg kg^{-1} s^{-1}
m_S	: maintenance coefficient on substrate	kg kg^{-1} s^{-1}
P	: power input	W m^{-3}
N_P	: number of pellets per volume	m^{-3}
R_{aut}	: cell autolysis rate due to a substrate starvation	kg m^{-3} s^{-1}
R_{O2}	: oxygen consumption rate in pellets	kg m^{-3} s^{-1}
R_S	: substrate consumption rate	kg m^{-3} s^{-1}
R_x	: biomass growth rate	kg m^{-3} s^{-1}
R_{sha}	: rate of shaving hair from pellets	kg m^{-3} s^{-1}
R_p	: pellet radius	m
R_{op}	: critical radius of pellets	m
r_p	: radial position in pellets	m
t	: time	s
T	: diameter of the stirred vessel	m
V_t	: total volume of reactor	m^3
u_g	: superficial velocity of gas	m s^{-1}
Y_{OX}	: yield of biomass on oxygen	kg kg^{-1}
Y_{SX}	: yield of biomass on substrate	kg kg^{-1}
Y	: calculation parameter	-

Greek

μ	: specific growth rate	s^{-1}
μ_f	: specific growth rate of free filamentous mycelia	s^{-1}
μ_{max}	: maximum specific growth rate	s^{-1}
$\mu_{m,t}$	: specific growth rate without substrate limitation at t hours of fermentation	s^{-1}

ϵ	: specific energy dissipation rate	W kg^{-1}
ϵ_P	: pellet porosity	-
ρ_p	: dry biomass per wet pellet volume	kg m^{-3}
ρ_h	: density of hyphae	kg m^{-3}
ϕ	: Thiele modulus for zero-order kinetics	-
τ	: critical time of fermentation for severe hyphal strength reduction	s

REFERENCES

Ayazi Shamplou, P., Makagiansar, H.Y., Ison, A.P., Lilly, M.D., Thomas, C.R., 1994,"Turbulent breakage of filamentous microorganisms in submerged culture in mechanically stirred bioreactors", *Chem. Eng. Sci.* , **49**, 2621-2631

Aynsley, M., Ward, A.C., Wright, A.R., 1990, "A mathematical model for the growth of mycelial fungi in submerged culture", *Biotechnol. & Bioeng.*, **35**, 820-830

Bainbridge, B.W., Bull, A.T., Pirt, S.J., Rowley, B.I., Trinci, A.P.J., 1971, "Biochemical and structural changes in non-growing maintained and autolysing cultures of *Aspergillus nidulans*", *Trans. Br. mycol. Soc.*, **56**, 371-385

Carderbank, P.H., Moo-Young, M.B., 1961, "The power characteristics of agitators for the mixing of Newtonian and non-Newtonian fluids", *Trans. IChemE*, **39**, 337-347

Carlsen, M., Spohr, A.B., Nielsen, J., Villadsen, J., 1995, "Morphology and physiology of an α-amylase producing strain of *Aspergillus oryzae* during batch cultivations", *Biotechnol. & Bioeng.*, **49**, 266-276.

Clark, D.S., 1962, "Submerged citric acid fermentation of ferrocyanide-treated beet molasses: morphology of pellets of Aspergillus niger", *Can. J. Microbiol*, **8**, 133-136).

Cui, Y.Q., Van der Lans, R.G.J.M., Luyben, K.Ch.A.M., 1996, " Local power uptake in gas-liquid systems with single and multiple Rushton turbines", 14 international symposium on chemical reaction engineering, *Chem. Eng. Sci.*, **51**, 2631-2636

Cui, Y.Q., Van der Lans, R.G.J.M., Luyben, K.Ch.A.M., 1997a, "Effects of agitation intensities on fungal morphology of submerged fermentation", *Biotechnol. & Bioeng*, **55**, 715-726

Cui, Y.Q., Van der Lans, R.G.J.M., Luyben, K.Ch.A.M., 1997b, "Effects of dissolved oxygen tensions and mechanical forces on fungal morphology of submerged fermentation", *Biotechnology and Bioengineering* in press.

Cui, Y.Q., Van der Lans, R.G.J.M., Luyben, K.Ch.A.M., 1997c, "Influence of fermentation conditions and scale on the submerged fermentation of *Aspergillus awamori*", submitted to *Enzyme Microbial Technology*.

Edelstein, L., Hadar, Y., 1983, "A model for pellet size distributions in submerged mycelial culture", *J. Theor. Biol.*, **105**, 427-452

Kobayashi,T., Van Dedem, G., Moo-Young, M.B., 1973, "Oxygen transfer into mycelial pellets", *Biotechol. & Bioeng.*, **15**, 27-45

Dion, W.M., Kaushal, R., 1959, "The effect of mechanical agitation on the morphology of some common fungi growth in submerged culture", *Selected Scientific Papers from Instituto Superiore di Sanita*, **2**, 357-369

King, R., Büdenbender, CH., Oswald, G., 1994, "Mathematical models for growth and production of single pellets and pellet populations", *Conference on computer applications in Biotechnology Garmisch-Partenkirchen, Germany,* May 14-17, 1995.

Lejeune, R., 1996, "From spores to pellets: modeling the growth and morphology of filamentous fungi", *Ph.D thesis*, Vrije Universiteit Brussel, Belgium.

Metz B., 1976, "From pulp to pellet: an engineering study on the morphology of moulds", *Ph.D thesis, Delft University of Technology*

Metz, B., De Bruijn, E.W., Van Suijdam, J.C., 1981," Method for quantitative representation of the morphology of molds", *Biotechnol. & Bioeng.*, **23**, 149-162

Metz, B., Kossen, N.W.F., 1977, "Biotechnology Review, The growth of molds in the form of pellets, A Literature Review, *Biotechnol. & Bioeng.*, **19**, 781-799

Michel, F.C., Grulke, E.A., Reddy, C.A., 1992, "A kinetic model for fungal pellet lifecycle", *AIChE Journal*, **38**, 1449-1460

Nielsen, J., Krabben, P., 1995, "Hyphal growth and fragmentation of Penicillum chrysogenum in submerged cultures", *Biotechnol. & Bioeng.*, **46**, 588-598

Nielsen, J., Johansen, C.L., Jacobsen, M., Krabben, P., Villadsen, J., 1995, "Pellet formation and fragmentation in submerged cultures of *Penicillium chrysogenum* and its relation to penicillin production", *Biotechnol. Prog.*, **11**, 93-98

Paul, G. C., Kent, C.A., Thomas, C.R., 1994, "Hyphal vacuolation and fragmentation in Penicillium chrysogenum", *Biotechnol. & Bioeng.*, **44**, 655-660.

Paul, G. C., Thomas, C.R., 1996, "A structure model for hyphal differentiation and penicillin production using Penicillium chrysogenum", *Biotechnol. & Bioeng.*, **51**, 558-572.

Pirt, S.J., 1973, "Estimation of substrate affinities (K_S values) of filamentous fungi from colony growth rates", *J. Gen. Microbiol.*, **75**, 245-247

Prosser, J.I., Trinci, A.P.J., 1979, "A model for hyphal growth and branching", *J. Gen. Microbiol.*, **111**, 153-164

Roels, J.A., "Energetics and Kinetics in Biotechnology", Elsevier Biomedical Press, Amsterdam (1983), P.54

Tough, A.J., Pulham, J., Prosser, J.I., 1995, " A mathematical model for the growth of mycelial pellet populations", *Biotechnol. & Bioeng.*, **46**, 561-572

Trinci, A.P.J., 1974, "Study of the kinetics of hyphal extension and branch initiation of fungal mycelia", *J. Gen. Microbiol.*, **81**, 225-236

Trinci, A.P.J., Saunders, P.T., 1977, "Tip growth of fungal hyphae", *J. Gen. Microbiol.*, **103**, 243-248

Trinci, A.P.J., Righelato, R.C., 1970, "Changes in constituents and ultrastructure of hyphal compartments during autolysis of glucose-starved *Penicillum chrysogenum*", *J. Gen. Microbiol.*, **60**, 239-249

Van't Riet, K., Tramper, J., 1991, "Basic Bioreactor Design", Mercel Dekker, Inc. New York

Vecht-Lifshitz, S.E., Magdassi, S., Braun, S., 1989, "Pellet formation and cellular aggregation in *Streptomyces tendea*", *Biotechnol. & Bioeng.*, **35**, 890-896

Yang, H., Reichi, U., King, R., Gilles, E.D., 1992, " Measurement and simulation of the

morphological development of filamentous microorganisms", *Biotechnol. & Bioeng.*, **39**, 44-48

Yang, H., Reichi, U., King, R., Gilles, E.D., 1992, " Mathematical model for apical growth, septation, and branching of mycelial microorganisms", *Biotechnol. & Bioeng.*, **39**, 49-58

Yano, T., Kodama, T., Yamada, K., 1961, "Fundamental studies on the aerobic fermentation part VIII. oxygen transfer within a mold pellet", *Agri. Biol. Chem.*, **25**, 580-584

CHAPTER 9

Regime Analysis of Fungal Fermentation

Abstract

In the frame work of studying the technological aspects of fungal fermentations a regime analysis of fermentations with *Aspergillus awamori* is performed. The analysis mainly focusses on oxygen (transport and uptake) and the behaviour of fungal particles (spores, hyphae, and pellets) in fermentation fluids in order to understand the relation between input parameters and the results of fungal fermentations. The regime analysis on oxygen shows the following results. The gas-liquid oxygen transfer process is almost always slower than the oxygen uptake process in both pellet and filamentous mycelial fermentations. Controlling dominant morphology towards small pellets (below a critical value of about 0.5 mm) will reduce the oxygen limitation during fermentation. The gradients in the dissolved oxygen tension in production fermenters smaller than 10 m^3 are expected to be negligible. Increase of the dissolved oxygen tension by using increased top pressure or enrichment of oxygen in the inlet gas diminishes both mixing and gas-liquid oxygen transfer limitations effectively. Inhomogeneity may occur in both small (<0.1 m^3) and large scales (>10 m^3) of bioreactors. The overall mixing becomes worse with increasing aspect ratio of a bioreactor. The mixing can be improved by using a bioreactor with a low aspect ratio or a combination of radial and axial pumping impellers and/or optimizing the feeding location. Aeration does not influence mixing very much so mixing behaviour (measured or predicted) for an unaerated situation can be used as a good estimation for the corresponding aerated situation.

Fungal spores follow all the motions of turbulent flow during a fermentation so they only see viscous forces. But hyphae and pellets see both turbulent flow and viscous flow environments depending on the rheology of the broth. Destructive forces on hyphea and pellets are expected from both flow regimes.

Keywords: Scale-up; oxygen transfer; oxygen uptake; mixing; particles in turbulent flow; bioreactor.

INTRODUCTION

In the engineering field as well as in other fields such as the social field, systems encountered are complex in nature. Attempts to describe the behaviour of such systems lead to large sets of mathematical equations (Roels, 1983). Generally a complete description is impossible or requires too much time to realize. Moreover, the equations contain a massive number of parameters, most of which are difficult or even impossible to determine experimentally. Solving such sets of equations leads to other problems. Therefore, a methodology to simplify a complex reality into a model which still describes the relevant mechanisms accurately and can be solved within an acceptable time span and for reasonable costs is clearly wanted (Luyben, 1993). Regime analysis is such a methodology. The regime concept was introduced by Johnstone and Thring (1957). A technical definition of a regime is a state of interactions between different factors, which is ruled by one or several of those factors. For instance flow in pipes can be classified into the viscous flow regime and the turbulent flow regime. Two-phase gas-liquid flow in stirred bioreactors is often classified into the complete gas recirculation regime, the incomplete gas recirculation regime and the flooding regime (Nienow et al., 1977). Regime analysis is thus the analysis of the state of a system based on analysing the relevant subprocesses. In this methodology, the subprocesses are characterised by 'characteristic times', or time constants. The time constant of a subprocess is defined as the time span needed to complete a certain percentage of that subprocess, e.g. determined by the response of the system to a change of input. Definition and detailed quantification of time constants are given by Luyben, (1993), Moser, (1991) and Oosterhuis (1984). Regime analysis must answer several questions such as which subprocess is the slowest or the rate limiting step, will there be a change in regimes, and whether the regime is ruled by one mechanism or more mechanisms.

Fungi, filamentous microorganisms, are industrially interesting microorganisms due to their ability to produce large amounts of a primary metabolism product such as organic acid, or second metabolism products such as antibiotics, enzymes and heterogeneous proteins. Fungal cells are complex and can be considered as a small factory themselves. So far it is impossible to give a rigorous description of the behaviour of fungal cells. The physical and chemical environments required for their growth and formation of products are created in a bioreactor. A complete description of the hydrodynamics in a bioreactor is impossible as well. So a rigorous description of fungal fermentation is a near impossible task. Obviously simplifications are required. Regime analysis has been used as a tool for analysing fermentation processes (Oosterhuis, 1984, Sweere et al., 1987, Frandsen et al, 1993, Moser 1991). An analysis of the regimes in fungal fermentations will be presented in this work.

For a proper regime analysis it is important to know what conditions are wanted for the

micro-environment of the fungi. Basically, these needs are met by the physical transport of mass (substrates, oxygen and products) and heat. The needs can often not be satisfied fully due to economic or other restrictions. Sometimes they are conflicting with each other, for example, the need to reduce the mechanical damage of the cells and the need to increase the dispersion of gas. For the analysis of the micro-environment, knowledge of the interaction between physical transport and other relevant subprocesses at different conditions is required. In a fungal fermentation the hydrodynamic conditions in the bioreactor, fungal morphology and growth, broth rheology, and the formation and secretion of products are related to each other. Figure 1 gives a schematic description of a fungal fermentation.
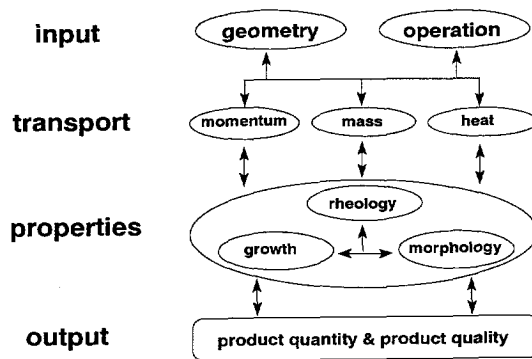

Figure 1. Scahematic description of a fungal fermentation

In this scheme four steps are visualised. The input, the first step, can be divided into operation variables ("operation"), geometrical variables ("bioreactor geometry") and others (medium, strains, cultivation conditions such as pH, temperature) which is mainly decided by microbiologists. "Geometry" and "operation" are determined by the design of a new bioreactor, or the modification of an existing one and by the optimization of operation conditions decided by a process engineer. Transport, the second step, is actual physical transport. It consists of momentum, mass, and heat transport. To transport all the nutrients to the microorganism and the products from the microorganisms, to remove the heat and to maintain a certain homogeneity these subprocesses are required in a fermentation. Under the certain conditions choosen, microorganisms will grow thereby obtain certain morphology, resulting in a certain rheology of fermentation broth. This is the third step. There is a strong interaction among the physiological factors, the morphological factors and the hydrodynamic factors. Finally the output (fourth step) of the fermentation will be a product, characterized by its quantity, quality and cost.

The present study focusses on the first three steps (input, transport and properties). The output (product quality and product quantity) is not taken into account here. The considered fermentation mode is batch. So substrate limitation can be ignored. Under those conditions, there are three processes in a fungal fermentation that are of primary importance. The first one is the extent of homogeneity in a fungal fermentation. The second is oxygen transport and consumption. The third one is the behaviour of fungal particles in the fermentation fluid. Possible limitations coming from other subprocesses are assumed not to interfere too strong with the whole process. For instance a heat transfer limitation can be reduced by increasing the heat transfer area or even pumping the broth through an external heat exchanger (Van 't Reit and Tramper, 1991). Since it is a batch fermentation the limitations of carbon, nitrogen, phosphate etc. are negligible.

CHARACTERISTIC TIMES

A characteristic time is a measure of the rate at which a subprocess is running and can be considered as the time needed by that subprocess to respond to a stepwise change in the input (Sweere et al., 1987). A small characteristic time means a fast mechanism and a large time means a slow mechanism. Homogenization, oxygen transfer and consumption, and fungal particle behaviour in turbulent flow of bioreactors will be studied in this work. The characteristic times of the relevant subprocesses are determined by the hydrodynamics and by the cell physiology and morphology. The hydrodynamics are controlled by the geometry of the bioreactor, the operation conditions and the rheology of the broth. The cell physiology and the cell morphology are determined by both the strain and cultivation conditions. The most relevant compound in the present case is dissolved oxygen. The morphology of fungi can vary from spherical compact colonies/pellets, to free filamentous mycelia. The morphology is influenced by the rheology of the broth and the internal mass transport in pellets. Thus, the characteristic times of the relevant subprocesses will be functions of operation conditions, geometries, rheology, morphology, or oxygen consumption rate, or a combination of these. The expressions used for the calculations of the characteristic times are given in Table I. The derivation of these expressions is presented in Appendix I-VII.

In the table only one characteristic time of overall oxygen consumption of pellets is given. The characteristic time for the intrinsic oxygen uptake is not explicitly expressed. But it is included in the derivation of the characteristic time (see Appendix VI). The expression of oxygen consumption by pellets given in table I should only be used for pellets larger than a critical value (see appendix VI). Under the present conditions, this critical diameter is estimated to be about 0.5 mm. When pellets are smaller than this critical value, the expressions for oxygen consumtion by free mycelia can be used. Mixing time and circulation time expressed in table I are for fully turbulent situations ($Re > 10,000$). When the flow is

Table I. Expressions of the characteristic times

Subprocess	expression for the characteristic time
Mixing	compartment model (Cui et al., 1996a)
Circulation of flow in one stage	$\dfrac{V/N_{stirrer}}{1.5\,ND^3}$
Gas-Liquid oxygen transfer	$1/(k_L a)$
Dissolved oxygen consumption by free mycelia	$\dfrac{0.63\,C^*}{C_x(\mu/Y_{OX}+m_{O2})}$
Dissolved oxygen consumption by pellets	$\dfrac{1\times10^{-4}}{3}\dfrac{R_p\rho_p}{C_{xp}D_{eff}}$
Particle response time	$10\dfrac{(\rho_p+\rho_L/2)\,d_p^2}{18\eta_f}$
Eddy life time	$l_E^{2/3}\epsilon^{-1/3}$

The expression for the characteristic time of dissolved oxygen consumption by pellets only holds for the situation when internal oxygen transfer is limiting. When the pellets are smaller than 0.5 mm, the characteristic time is the same for both free mycelia and pellets.

not fully turbulent mixing time increases considerably at decreasing Re number. A correction for Re number is made in the same way as Van 't Riet and Tramper (1991).

Evaluation of characteristic times
In the present study the submerged fungal fermentation of *Aspergillus awamori* (CBS 115.52) is used as the base case. Oxygen is mainly taken as a limiting compound. Both filamentous mycelia and pellets are considered as dominant morphology. Pellet size, biomass concentration, power input and bioreactor scale were varied. The geometry of the bioreactor

in all cases was taken as a stirred vessel of aspect ratio 2 with three Rushton turbines spaced 2 diameters apart. The gas flow rate per volume was kept constant at 0.5 vvm. The parameters of this strain are taken from Cui et al., (1997a) where the specific growth rate is 0.3 h^{-1}, the biomass yield on oxygen is 2, the maintenance coefficient is negligible and the density of pellets is 50 kg/m^3. The rheology of the broth was estimated from the literature correlations (Metz, 1976 and Van Suijdam, 1980). The subprocesses related to oxygen and the subprocesses related to fungal particle behaviour in fermentation fluids will be discussed below.

subprocesses related to oxygen
Characteristic times for the oxygen consumption of pellets on macroscale are presented as a function of pellet diameter in Figure 2 for different biomass concentrations. Small pellets (<0.5 mm) show no oxygen diffusion limitation and hence the characteristic times do not depend on the diameter any more. For larger pellets the characteristic time increases with size. With increasing size a larger part of the pellet faces depletion of oxygen. The characteristic time decreases with increasing biomass concentration. More biomass in the broth results in a quicker consumption of the dissolved oxygen.
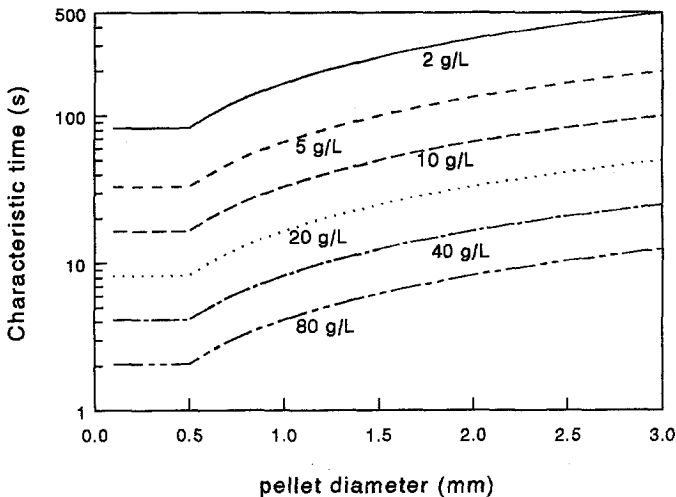

Figure 2. Characteristic times of pellets at different biomass concentrations are expressed as a function of pellet sizes

The biomass concentration influences not only the oxygen consumption rate but also the rheology of the fermentation broth. So the characteristic time of oxygen transfer from the gas

phase to the liquid phase will change as well. The characteristic times of mixing, oxygen transfer and oxygen consumption for both pellets and mycelia, are plotted in Figure 3 as a function of the biomass concentration.
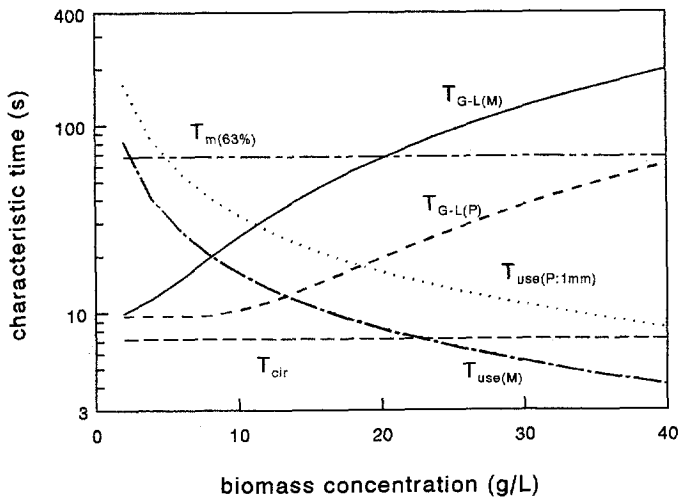

Figure 3. Characteristic times of mixing, G-L oxygen transfer, oxygen consumption of filamentous mycelia and oxygen consumption of pellets at different biomass concentrations

The homogenization time in Fig.3 does not depend on biomass concentration because the flow is assumed to be turbulent in all situations. However, this assumption does not hold if the biomass concentration is higher than a certain critical value. In general this critical value increases with the scale of the bioreactor and the power input. For our base case, it is about 20 g/L for a filamentous suspension and about 40 g/L for a pellet suspension. Therefore, the mixing time of a filamentous mycelia suspension in the right side of Figure 3 should be seen as an extrapolation. The oxygen transfer time increases and the oxygen consumption times decreases with increasing biomass concentration. Oxygen transfer in a pellet broth is faster than in a filamentous mycelial suspension. A change in regime occurs at biomass concentrations of about 10 g/L. Before the biomass concentration reaches about 10 g/L, the G-L oxygen transfer rate is faster than the oxygen consumption rate. The fluid circulation in the stage of the bioreactor is faster than the oxygen consumption as well. So no oxygen limitation and oxygen gradients are expected. When the biomass concentration is higher than about 10 g/L, the oxygen transfer process is slower than the oxygen consumption process. So limitation of oxygen occurs. When the biomass concentration is higher than about 20 g/L, the oxygen consumption process is faster than both the oxygen transfer and the liquid

circulation processes. Therefore, both gradients in the dissolved oxygen tension and oxygen limitation are expected in the fermenter. A large power input will be needed to decrease both the oxygen limitation and the mixing limitation.
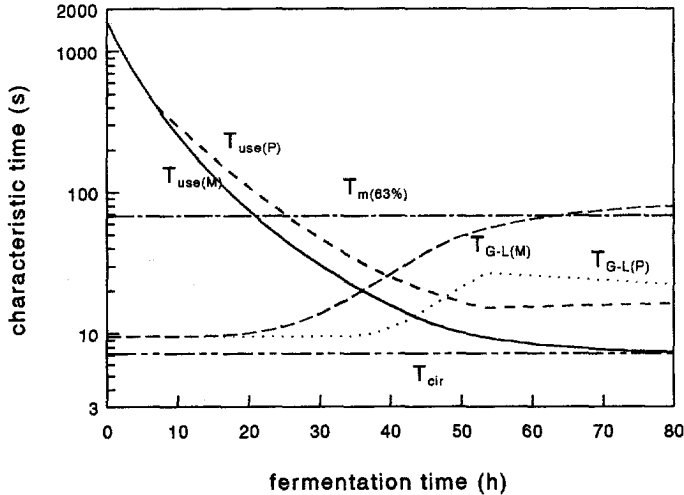

Figure 4. Time course of the characteristic times of different subprocesses in a fungal fermentation.

Fig.4 shows a simulated time course of the characteristic times in a fungal fermentation. The biomass growth in a batch fermentation is simulated both in pellet form and in filamentous mycelial form using the model and the same kinetic parameters as used by Cui et al., (1997b). The initial substrate concentration is assumed to be 40 g/L. Fig.4 shows that the oxygen consumption time decreases with the biomass growth but that the oxygen transport time increases. During the first part of a fermentation there are no limitations on a macroscale and biomass will grow exponentially. However after some 20 hours (under the used conditions) inhomogeneity in the bioreactor may occur. After about 35 hours oxygen limitation appears in case of a mycelial culture. In a pellet suspension this is some 10 hours because the broth is less viscous.

Increase of power input will enhance both mass transfer and mixing. Fig.5 shows the predicted characteristic times for mixing, oxygen transfer and oxygen consumption as a function of the total stirrer power input at a biomass concentration of 20 g/L.
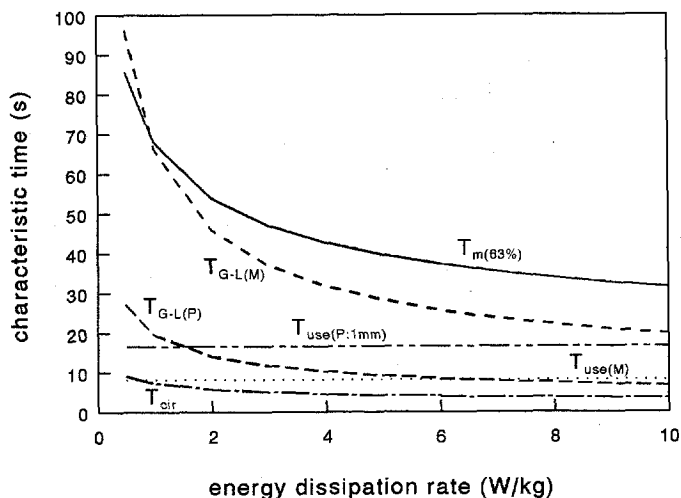
Figure 5. Characteristic times of subprocesses at different energy dissipation rates.

The characteristic times of oxygen consumption are constant and independent of the specific energy dissipation rate. The improvement of mixing and G-L oxygen transfer processes is more obvious at a relative low specific power input (smaller than 3 kW/kg) than at high values. Oxygen transfer is limiting for the filamentous mycelial fermentation in all cases at this biomass concentration. Controlling the morphology to be a pellet form will enable to diminish this limitation.

In practice bioreactors of different scales are used. For instance the bioreactor changes of course from a laborotory one to a production scale during the scale up of a bioprocess. Fig.6 depicts the characteristic times as a function of the bioreactor size. The characteristic times in Fig.6 are based on the same specific energy dissipation rate (1 W/kg) from stirrer and the same aeration flow rate per volume (0.5 vvm). When the bioreactor is smaller than 1 m^3, mixing time decreases with scale, since the smaller the bioreactor is the further the flow is from being fully turbulent (Re > 10,000). When the bioreactor is larger than 1 m^3 the flow is fully turbulent and mixing time increases with scale. The characteristic time of the G-L oxygen transfer decreases with scale, which is due to the fact that the superficial gas velocity increases with scale at a constant aeration flow rate per volume of 0.5 vvm. The oxygen transfer process is limiting for almost all scales. For both larger and smaller scales mixing is limiting. Gradients of dissolved oxygen tension and other chemicals such as acid or base and substrates are expected to occur in both large (> 10 m^3) and small (< 0.1 m^3) scales.
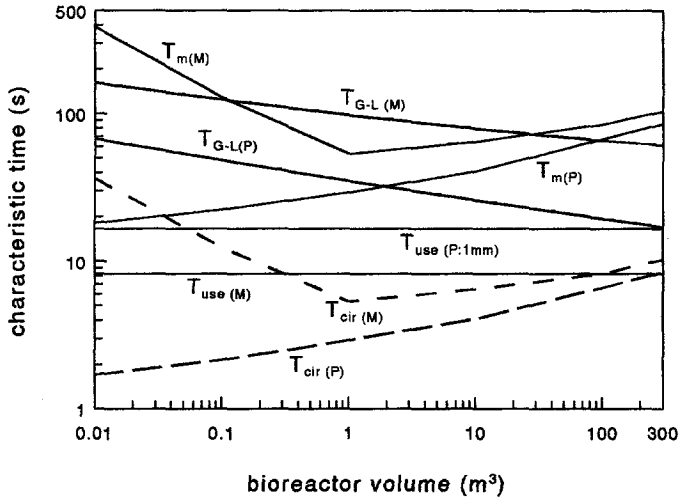
Figure 6. Characteristic times of subprocesses at different scales of bioreactors.

The oxygen consumption times of filamentous mycelia and pellets are influenced by the amount of the dissolved oxygen present. The characteristic times of mixing, oxygen transfer and oxygen consumption are plotted in Fig.7 for different relative oxygen concentrations. This relative concentration is definded as a ratio of actual oxygen concentration to the oxygen concentration in air at the standard condition (1 atm. and 25 °C).
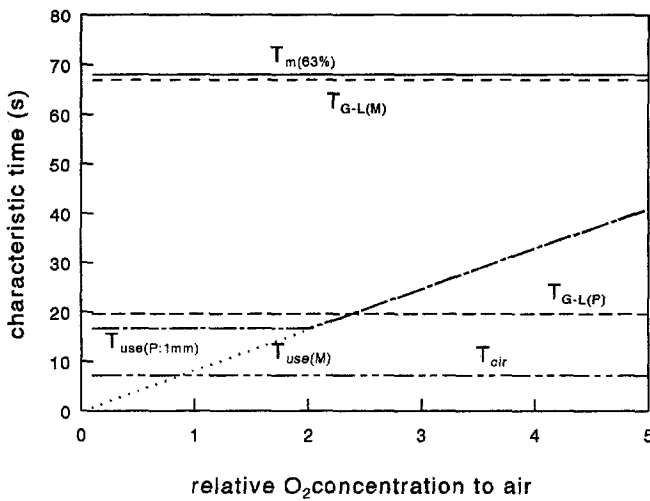

Figure 7. Characteristic times of subprocesses at different dissolved oxygen tensions.

The oxygen consumption time of mycelia increases with increasing dissolved oxygen tension (see table I). For pellets the curve can be divided into two regimes. If the oxygen saturation concentration is lower than a critical value the oxygen can only penetrate part of the pellets. In other words the internal oxygen transfer is the limiting process. This critical value is 2 times the air saturation concentration for a pellet with a diameter of 1 mm. When the oxygen saturation concentration is higher, the intrinsic oxygen consumption rate of the cells determines the process. So the characteristic time of pellets is constant for low values and increases with the oxygen saturation concentration for high values. The G-L oxygen transfer time is defined to be the time span to transport 63% of the saturated dissolved oxygen so that this characteristic time is independent of the oxygen saturation concentration (see table I and appendix V). In a similar way the mixing time is not influenced by the saturated dissolved oxygen tension as well. The mixing time is the largest one in all cases, which is more relevant to blending a chemical from the feeding pipe. For instance an inhomogeneity in a fed batch fermentation, in which the feeding pipe is located at top, can be a problem. The circulation time on the other hand is almost the smallest one. This means that the dissolved oxygen concentration is mixed in each stage very well. If there is no considerable difference in oxygen transfer rate between stages, the oxygen is mixed very well overall as well. The characteristic time of G-L oxygen transfer in a filamentous mycelial broth is almost as large as mixing time so G-L oxygen transfer is a limiting process. This can be improved considerably by controlling the morphology to pellets. If the pellets are smaller than a critical value, internal oxygen transfer limitation can be avoided.

subprocesses related to particle behaviour

In case of submerged fungal fermentations, one often deals with a three-phase (G-S-L) system, in which liquid is the continuous phase, gas bubbles are the discrete gas phase and filamentous mycelia and pellets are considered to be the discrete solid phase. For a dilute solid suspension such as in the beginning of a fermentation, the effect of the solid particles on the turbulent flow can be neglected. However, the presence of a solid phase above a certain value (30% v/v, Caulet et al., 1996), changes the turbulence structure by a modification of the energy cascade transfer process in a turbulent flow. On the other hand, the turbulent flow influences strongly the solid particles with respect to movement and damage. Damage to the cells can cause a decrease in growth rate, retardation of the metabolism, and release of intracellular substances (Bronnenmeier and Märkl, 1982). It influences morphology as well (Dion and Kaushal, 1959, Cui et al., 1997c, Metz, 1976). Stresses or forces induced by fluid flow are generally recognized as the cause for fungal cell damage in a stirred bioreactor (Metz, 1976, Ayazi Shamlou et al. 1994, Cui et al., 1997c). When a particle or a cell fully follows all the turbulent motions of the fluid, the dominant destructive forces are shear forces from the viscous regime. However, if a particle can not follow the turbulent fluid motions completely the turbulent destructive forces may become

dominant. In general a particle following all the motions faces a lower destructive force than one following not all or only part of the motions.

Turbulent flow is commonly described as a random movement of eddies in the liquid in different directions superimposed on the main flow of the liquid. The relative response of particles to a turbulent motion is derived in Appendix VII. This relative response is a function of eddy size, particle size, specific energy dissipation rate and the viscosity of the medium (Eq.31, Eq.32 and Eq.34). Fig.8 depicts the estimated response of particles relative to the motion of the smallest eddies at different viscosities.

Figure 8. Predicted relative response of particles to the motions of the smallest eddies at different medium viscosities. The specific energy dissipation rate used is 1 W/kg. The parameter with the different lines is the particle diameter.

For a batch fungal fermentation the apparent viscosity of broth varies from about 1 mPa.s at the start of the fermentation to 1 Pa.s at the end when the filamentous mycelial biomass concentration is about 20 g/L. The smallest eddy is about 30 μm at a specific energy dissipation rate of 1 W/kg and a viscosity of 1 mPa.s and about 5.6 mm at a specific energy dissipation rate of 1 W/kg and a viscosity of 1 Pa.s. Fig.8 shows that if a particle is smaller than about 10 μm, it will follow the smallest eddies in a stirred vessel fully. This is independent of the broth rheology encountered in a fungal fermentation. The size of a spore of *Aspergillus awamori* is about 10μm. So spores can be considered to follow turbulent motions in a stirred vessel fully. Mechanical forces acting on the spores are induced by viscous flow and the spores do not see a turbulent environment. Particles with a size of 1-10

mm hardly respond to the motion of the smallest eddies in a low viscous broth (such as 1-30 mPa.s) but do in a viscous broth (above 30 mPa.s). Those particles resemble fungal pellets. Therefore pellets are expected to face both turbulent forces and viscous forces depending the rheology of the broth. The size of filamentous mycelia in submerged fermentations is about several hundreds of micrometers. The size difference between filamentous mycelia and pellets is not very large. So filamentous mycelia face both turbulent and viscous forces as well. However, they 'see' viscous forces much later than pellets. These calculations are based on a specific energy dissipation rate of 1 W/kg.

The size of the smallest eddies decreases with increasing power input. Figure 9 depicts the relative response as a function of specific energy dissipation rate at a medium viscosity of 1 mPa.s.

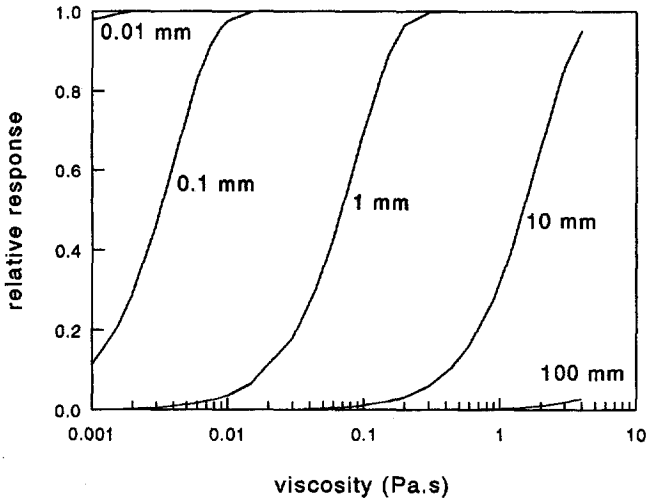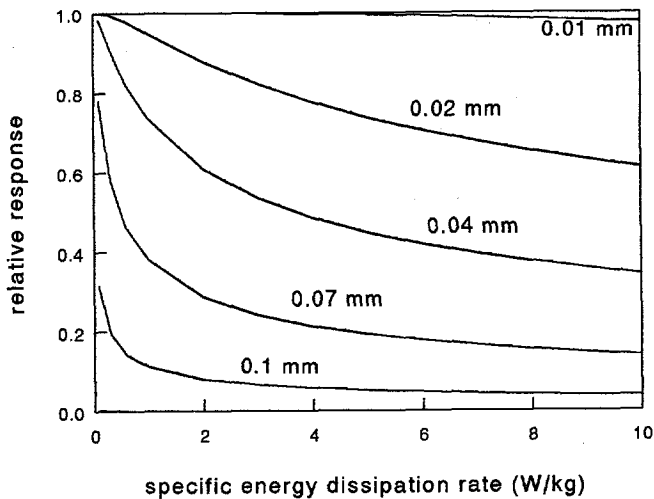**Figure 9**. Predicted relative response of particles to the motions of the smallest eddies at different energy dissipation rates. The viscosity of broth used is 1 mPa.s. The parameter with the different lines is the particle diameter.

Particles smaller than 0.01 mm follow the motion of all the smallest eddies in the stirred fermenter. This is independent of the power input used. Particles of about 0.1 mm follow only partly the motion of the smallest eddies in a medium (1 mPa.s) and the relative response decreases slightly with increasing power input. Particles larger than 0.1 mm do not follow the motion of the smallest eddies. So the difference in power input used at the start of fermentations (1 mPa.s) will not change the picture of the relative response of fungal particles

to the motions of the smallest eddies. Spores will only 'see' viscous flow, hyphae both viscous and turbulent flows and pellets only turbulent regime motions.

REDUCING THE LIMITATIONS OF DIFFERENT SUBPROCESSES

improvement of oxygen transport
Oxygen transfer is a function of power input, broth rheology, driving force and specific interfacial area between gas and liquid (related to gas dispersion). The power input into a bioreactor is restricted due to economical considerations and the factors like cell mechanical damage, undesired change of morphology or the removal of heat coming from higher agiation intensities. The rheology of the fungal fermentation broth affects the aeration coefficient $k_L a$. The broth rheology in a fungal fermentation can be improved by controlling the dominant morphology towards small pellets (smaller than 0.5 mm in diameter) without introducing internal oxygen transfer limitations. An increase of the driving force can be achieved by increasing the oxygen concentration in the gas phase, using an increased top pressure or choosing a bioreactor with a large aspect ratio. Normally gas is introduced into a bioreactor at the bottom. All of the gas goes through the region swept by the bottom impeller. This region is considered to be responsible for gas dispersion. Only part of the gas will go through the regions swept by the other impellers. So if gas is injected at each impeller gas dispersion might be improved at the same stirrer speed and broth rheology.

improvement of mixing in general
The model used to predict the mixing behaviour of a bioreactor was developed for a single-phase system (Cui et al, 1996a). However, the oxygen required in a fungal submerged fermentation comes from aeration. In the literature the effects of aeration on the mixing have been reported differently. Van 't Riet and Tramper (1991) concluded that aeration will double the mixing time compared to unaerated conditions at the same stirrer speed. Pedersen et al. (1994) concluded that mixing time decreased if a bioreactor is aerated. Groen (1994) claimed that the influence of aeration depended on the prevailing flow regime and is small in the generally encountered flow regime (less than 25% at constant stirrer speed). The mixing time in a 30 m^3 stirred reactor was measured at different operation conditions (stirrer speed and aeration rate) in the present study. The reactor geometry and the method and procedure used for these experiments are described by Cui et al., (1996a). Fig.10 shows the mixing number, a product of mixing time and stirrer speed, at different aeration flow rates.

The aeration flow rate varied from zero to the flooding flow rate which was estimated by using the correlation from Nienow et al. (1985). The mixing number remains more or less
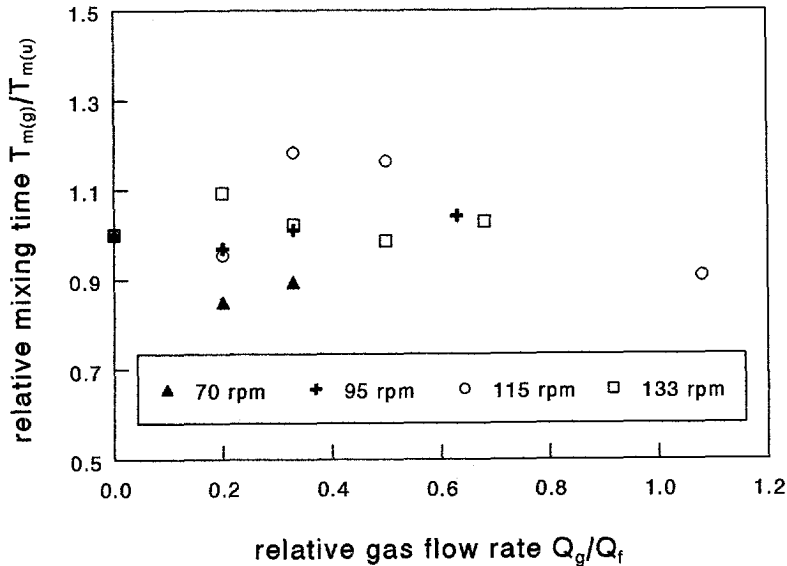
Figure 10. The ratio of aerated mixing time to unaerated mixing time in a 22.4 m³ bioreactor as a function of the ratio of the gas flow rate to the flooding gas flow rate. The flooding gas flow rate is calculated by using the correlation $Q_f = 30 N^3 D^{7.5} T^{3.5} g^{-1}$ from Nienow, et al., (1985).

constant although the relative gas flow, a ratio of actual gas flow rate to the flooding gas flow rate varied lot. The flooding flow rate is estimated by using a correlation, $Q_f = 30 N^3 D^{7.5} T^{3.5} g^{-1}$, from Nienow et al., (1985). The results show that aeration does not influence the overall mixing in a bioreactor very much in the normal operation range. Based on this results it is concluded that the predicted single phase mixing time can be used for the aerated system.

Mixing is dependent on the geometry and scale of the bioreactor and the type of impellers. However one should keep in mind that improving the mixing behaviour in an existing bioreactor is more often required than constructing a new bioreactor. Modifying the configuration and type of impellers and the location of feeding pipes in an existing bioreactor might be an economicallly viable option to achieve a better mixing. Although the construction of a new bioreactor might be better, it does, of course, cost more and is not as fast as the modification in an existing bioreactor. In the following, possible improvement of the mixing behaviour both by modofying and constructing a new bioreactor is discussed.

mixing: modification of existing bioreactors
Although Rushton turbines perform well with respect to gas dispersion and are often used in industry, they give a very limited axial mixing due to the fact that they are radial pumping

impellers. An improvement of the mixing behaviour while keeping a good gas dispersion performance can be expected by using a combination of a radial turbine at the bottom and axial pumping impellers at the other locations. For instance a Rushton turbine at the bottom and propellers in the middle and top positions may be used. The combination of different type of impellers in a multi-impeller system is the actual trend to attain good liquid mixing and good gas dispersion with less power input than that required by multiple Rushton turbines (Abrardi et al., 1990)

Gas is usually introduced into the bioreactor at the bottom for obvious reasons. However, the location and number of feeding points to introduce components such as acid, base, substrates, and product inducers can be changed relatively easily. The times needed to mix such components in a multi-impeller bioreactor entering at different feeding locations (outflow of bottom impeller, middle impeller and top impeller) has been estimated using the flow model. The results shows that the overall mixing time (63%) can be reduced by a factor of about 4 if the feeding point is changed from outer flow of top impeller to outer flow of middle impeller. Clearly the mixing of specific components can be improved considerablly just by feeding them at different locations. This could be an approach if the mixing of these components is the limiting factor.

mixing: construction of new bioreactors
Using the model (Cui et al., 1996a), the effect of scale and aspect ratio (i.e. the number of impellers) on the mixing behaviour were simulated. The flow was assumed to be fully turbulent in all the cases. The times needed to obtain 95% homogeneity were chosen to quantify the mixing time or the characteristic time of the blending subprocess. In order to make a proper comparison of the mixing behaviour of bioreactors at different scales, it was assumed that the bioreactors had a similarity in geometry, such as that the impellers (Rushton turbines) were equally distributed on the shafts, the number of impellers was proportional to the height of the liquid level, the ratio (T/D) of the impeller diameter to the vessel diameter was 1/3 and the distance between impellers is 3D. The specific power input was 1 W/kg. The characteristic mixing times predicted under these conditions are plotted in Fig.11 as a function of scale and aspect ratio of bioreactors i.e. the number of impellers.

The figure shows that mixing time increases strongly with the scale of the bioreactor in case of multi-impeller systems. This means that the extent of inhomogeneities in a bioreactor becomes larger with increasing scale. Mixing will become a problem in a large bioreactor. For the same scale of bioreactors at the same power input, the characteristic mixing time increases strongly with the number of impellers i.e. the aspect ratio of the bioreactor. For instance, the 95% mixing time of a 100 m^3 bioreactor with one impeller (i.e. its aspect ratio: 1) is about 20 seconds but in case of a 100 m^3 bioreactor with four impellers (i.e. its aspect

ratio: 4) it is 300 seconds. This is due to the fact that the fluid mixing between neighbouring stages is much less than the mixing within each stirrer stage. The exchange between stages is limited so that a kind of barrier exists between stages. Therefore, if insufficient mixing is a critical problem for a given process, the use of a bioreactor with a lower aspect ratio will be an option to improve the mixing behaviour.
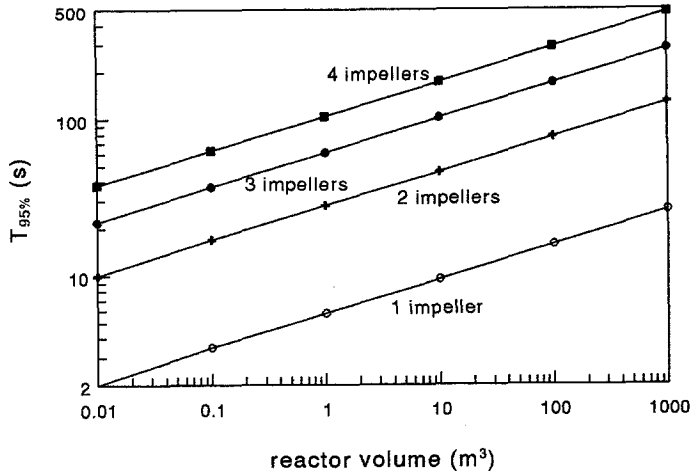
Figure 11. Mixing time predicted at the specific energy dissipation rate of 1 W/kg is plotted as a function of the scales of bioreactors and the number of impellers.

The above results are obtained using water as working medium. In the reality of a fungal fermentation, the broth shows viscous or even non-Newtonian behaviour. This will affect the fluid mixing in the bioreactor. The difference between the above prediction and the actual mixing will depend very much on whether the flow is turbulent. For a fully turbulent flow, macromixing is hardly dependent on the rheology of fluids. This means that in such a case the above results can be used for a fungal fermentation system. If the flow is not fully turbulent, the trend will be expected to be the same.

CONCLUSIONS

The gas-liquid oxygen transfer process is almost always slower than the oxygen consumption rate in both pellet and filamentous mycelia fermentations. The G-L oxygen transfer limitation gets worse with increasing biomass concentration. Controlling the dominant morphology in

a fermentation as a small pellet (below a threshold value of about 0.5 mm) will improve the oxygen transfer process without introducing internal oxygen transfer limitation. The gradients of dissolved oxygen tension in a bioreactor smaller than about 10 m^3 and larger than 0.1 m^3 are expected to be negligible. The increase of power input will improve the mixing and oxygen transfer. But this increase appears to be more effective in the range of up to 3 W/kg. Increasing the dissolved oxygen tension diminishes both mixing and G-L oxygen transfer limitations effectively. This could be achieved by increasing head pressure or oxygen concentration in the inlet gas.

The time span to homogenize the fluid in a bioreactor increases both with the scale of a bioreactor and the aspect ratio of a bioreactor. The use of a bioreactor with a low aspect ratio could be a option to improve the homogenization process without changing the scale of the bioreactor.

Fungal spores follow all the motions of the turbulent flow during a fermentation. So spores see only viscous flow. Hyphae and pellets see both turbulent flow and viscous flow depending the rheology of the broth. Therefore, destructive forces on hyphae and pellets are expected from both viscous forces and turbulent forces. A change of power input may lead to a change of fungal morphology.

NOMENCLATURE

A_p	projected area of particles	m^2
a_s	specific area of pellets	m^2
CF	circulation flow	m^3 s^{-1}
C_{O2}	dissoved oxygen concentration	kg m^{-3}
$C_{O2}{}^*$	saturated dissoved oxygen concentration	kg m^{-3}
C_{O2b}	dissoved oxygen concentration in bulk	kg m^{-3}
C_{XP}	biomass concentration of pellets	kg m^{-3}
C_X	biomass concentration	kg m^{-3}
C_{XM}	biomass concentration of filamentous mycelia	kg m^{-3}
C_{Re}	constant	-
D	diamter of impeller	m
d_p	diamter of particles	m
D_{eff}	effective diffusion coefficient	m^2 s^{-1}
d_h	hyphal diameter	μm
F	drag force	N
Fl	flow number of an impeller (Q_g/ND^3)	-
Fr	impeller Froude number (N^2D/g)	-

H	height of fermenter	m
K_C	constant in the Casson mode	$(Pa.s)^{1/2}$
k_La	aeration constant	s^{-1}
L_e	main hyphal length in	μm
$Lhgu$	hyphal growth unit (L_t / tip number)	μm
m_{O2}	maintenance coefficient on oxygen	kg kg^{-1}
N	stirrer speed	s^{-1}
$n_{stirrer}$	number of stirrers	-
P	power input	W
P_g	aerated stirrer power input	W
P_i	individual stirrer power input	W
Q_g	gas flow rate	m^3 s^{-1}
Re	Reynolds number	-
R_P	radius of pellet	m
R_{0P}	dissolved oxygen depletion radius of pellets	s
T_{use}	time constant of oxygen consumption	s
T	diamter of bioreactor	m
T_{G-L}	time constant of Gas-Liquid oxygen transfer	s
T_{use}	time constant of oxygen consumption	s
T_m	mixing time of bioreactors	s
T_{Cir}	circulation time	s
t	time	s
V	volume of bioreactor	m^3
v_g	gas superficial velocity	m s^{-1}
u_r	relative velocity between particle and fluid	m s^{-1}
u_f	fluid velocity	m s^{-1}
u_p	particle velocity	m s^{-1}
Y_P	relative response of particle to motion of eddies	-
Y_{OX}	yield coefficient of biomass on oxygen	kg kg^{-1}

Greek letters

τ	shear stress	N m^{-2}
ν	kinematic viscosity	m^2 s^{-1}
η_a	apparent viscosity	Pa.s
η_f	fluid viscosity	Pa.s
τ	shear stress	N m^{-2}
τ_E	eddy lifetime	s
τ_0	yield stress	N m^{-2}
τ_P	particle response time	s

| ẋ | shear rate | s⁻¹ |

$\dot{\gamma}$	shear rate	s^{-1}
ρ_p	density of particle	$kg\ m^{-3}$
ϵ	specific energy dissipation rate	$W\ kg^{-1}$
μ	specific growth rate	s^{-1}
ϕ	Thiele modulus	-

REFERENCES

Roels J.A., 1983, Energetics and Kinetics in Biotechnology, Elseviers Biomedical Press, Amsterdam.

Luyben, K. Ch. A. M., "Regime analysis for the scale-down of biotechnological processes", *Proceeding of Bioreactor Performance at Helsingør, Denmark*, 15-17 March, 1993. p:159-169

Johnstone R. E. and Thring, M.W., 1957, Pilot plant, Models and scale-up methods in Chemical Engineering, McGraw-Hill, New York

Nienow A.W., Wishdom D.J., and Middleton J.C., 1977, "The effect of scale and geometry on flooding, recirculation, and power in gassed stirred vessels, F1, *2th European Conf. on Mixing, Cambridge, England, 30th March-1st April*

Oosterhuis N.M.G., 1984, "Scale-up of Bioreactors: a scale-down approach", Ph.D thesis, Delft University of Technology

Moser A, 1991, "Strategies in bioreactor performance studies, *Bioprocess Engineering*, **6**, 205-211

Sweere A.P.J., K.Ch.A.M.Luyben, Kossen N.W.F.,1987, Regime analysis and scale-down: tools to investigate the performance of bioreactor, *Enzyme Microb. Technol.,* **9**, 386-398,

Frandsen,S., Nielsen, J., Villadsen, J., 1993, "Application of regime analysis of yeast fermentation for down-scaling", *Proceeding of International Symposium on Bioreactor Performance,* 15-17 March, 1993, Helsingør, Denmark, P:171-179 {on backers' yeast

Douglas E.Leng, 1991, "Succeed at scale up", *Chemical Engineering Progress.*, June 1991, 23-31

Van 't Riet K. and Tramper J., 1991, "Basic Bioreactor Design", Mercel Dekker, Inc. New York

Cui, Y. Q., Van der Lans R.G.J.M. and Luyben K.Ch.A.M., 1997a, "Influence of fermentation conditions and scale on the submerged Fermentation of *Aspergillus awamori*", to be submitted into *Enzyme and Microbial Technology*

Metz, B., 1976, "From Pulp To Pellet, an engineering study on the morphology of moulds", Ph.D thesis of Delft University of Technology.

Van Suijdam J.C., 1980, "Mycelial pellet suspensions, biotechnology aspects", Ph.D thesis of Delft University of Technology

Cui, Y. Q., Van der Lans R.G.J.M. and Luyben K.Ch.A.M., 1997b, "Physical phenomena of fungal growth and morphology in submerged fermentations", to be submitted into *Biotechnol. & Bioeng.*

Caulet P.J.C, Van der Lans R.G.J.M. and Luyben K.Ch.A.M., 1996, "Hydrodynamical interactions between particles and liquid flows in biochemical applications", *Chem. Eng. J.,*, **62**, 193-206

Bronnenmeier R. and Märkl H., 1982, "Hydrodynamics stress capacity of microorganisms", *Biotechnol. & Bioeng.*, **24**, 553-578

Dion W.M. and Kaushal R., 1959, "Effect of mechanical agitation on the morphology of some common fungi grown in submerged culture", *selected Scientific papers from Istituto Superiore di Sanita (Eng.Ed)*, **2**, 357-369

Cui, Y. Q., Van der Lans R.G.J.M. and Luyben K.Ch.A.M., 1997c, "Effect of agitation intensities on fungal morphology of submerged fermentation", *Bioeng. & Biotechnol.*, **55**, 715-726

Ayazi Shamlou P., Makagiansar H.Y., Lilly M. D. and Thomas C.R., 1994, " Turbulent breakage of filamentous microorganisms in submerged culture in mechanical stirred bioreactors", *Chem. Eng. Sci.,* **49**, 2621-2631

Cui, Y. Q., Van der Lans R.G.J.M., Noorman H.J. and Luyben K.Ch.A.M., 1996a, "Compartment mixing model for stirred reactors with multiple impellers", *Trans IChemE.*, **74**, 261-271

Pedersen A.G., Nielsen, J., Villadsen J., 1994, "Characterization of bioreactors using isotope tracer techniques", Proc 6th Europ Congress on Biotechnology, (Elsevier Science BV), p.931-

934.

Groen D.J., 1994, "Macromixing in Biorecactors", Ph.D thesis of Delft University of Technology

Nienow,A.W., Warmoeskerken M.M.C.G., Smith J.M., and Konno M., 1985,"On the flooding/loading transition and the complete dispersal condition in aerated vessels agitated by a Rushton turbine", *Fifth European Conference on Mixing,* paper 15, 143-155, BHRA, UK

Abrardi A., Rovero G., Baldi G., Sicardi S. and Conti R., 1990, "Hydrodynamics of a gas-liquid reactor stirred with a multi-impeller system", *Trans IChemE,* **68**, 516-522.

Cui, Y. Q., Van der Lans R.G.J.M. and Luyben K.Ch.A.M., 1996b, "Local power uptake in gas-liquid systems with single and multiple Rushton turbines", 14th International Symposium on Chemical Reaction Engineering, *Chem. Eng. Sci.,* **51**, 2631-2636

Metzner, A.B. and Otto,R.E., 1957, "Agitation of non-Newtonian fluids", *AIChE J.,* **3**, 3-10

Revill, B. K., 1982, Pumping capacity of disc turbine agitators- a literature review, *4th Europ Conf on Mixing,* (BHRA, Fluid Engineering, 24 April), B1: 11-24.

Hinze J.O., 1971, "Turbulent fluid and particle interaction", *Prog. heat mass transfer,* **6**, 433-452

Davies J.T., 1972, Turbulence Phenomena, p. 53-63, Academic Pres, New York, London.

Ezimora G.C. and Lübbert, 1997, "Catchment area of the cavities behind a Rushton turbine in gassed -stirred-tank reactor", *Chem. Eng. Sci.,* **52**, 1673-1677

Appendix I: Oxygen transport and consumption

The cultivation of fungi requires oxygen, which is commonly supplied by aeration. The whole process of oxygen transport and consumption consists of a chain of six subprocesses. 1) air (oxygen) transport into the reactor and dispersion of the gas; 2). oxygen transfer from gas to liquid. 3). oxygen transport in the bulk by mixing. 4). oxygen transfer from the liquid to the surface of the fungal particles. 5). oxygen transport within the fungal particles. 6). oxygen consumption by the fungi. The oxygen transport from the liquid to the surface of fungal particles is a much faster subprocess than the others and can be ignored normally (Van Suijdam, 19980).

For a fungal fermentation a bioreactor is normally filled with a suspension of pellets and free filamentous mycelia. If the fluid in the fermenter is assumed to be well mixed the mass balance on the dissolved oxygen can be described as one of the following two cases:

I: there is no limitation of oxygen in the pellets:

$$\frac{dC_{O2}}{dt} = k_L a(C_{O2}^* - C_{O2}) - (\frac{\mu}{Y_{Ox}} + m_{O2})(C_{xp} + C_{xm})$$ (1)

II: there is a limitation of oxygen in the pellets:

$$\frac{dC_{O2}}{dt} = k_L a(C_{O2}^* - C_{O2}) - (\frac{\mu}{Y_{Ox}} + m_{O2}) C_{xm} - a_s D_{eff} \frac{dC_{O2}}{dr}$$ (2)

Characteristic time of oxygen transfer

From Eq.1 it follows that the time constant for oxygen transfer is

$$t_{G-L} = \frac{1}{k_L a}$$ (3)

This time constant corresponds with the time span needed to reach 63% of the final value after a step change in the oxygen concentration. This is the so-called characteristic time of gas-liquid mass transfer. The aeration constant $k_L a$ is a function of stirrer power input, superficial gas velocity and rheology of the broth.

Dissolved oxygen is consumed during a fermentation. Without gas-liquid oxygen transfer, the dissolved oxygen concentration will drop. In case I the time span needed to consume 63% of the available amount of dissolved oxygen in the bulk saturated with gas phase will be

$$t_{use} = \frac{0.63\, C^*}{C_x(\mu/Y_{Ox} + m_{O2})}$$ (4)

This expression is derived from Eq.1 assuming no gas-liquid oxygen transfer. In case II the time span needed to consume 63% of the bulk dissolved oxygen by pellets is

$$t_{use,P} = \frac{1}{3} \times 10^{-4} \frac{R_p \rho_p}{C_{xp} D_{eff}} \qquad (5)$$

The detailed derivation of this equation is given in Appendix V.

Appendix II: G-L mass transfer

For a low viscous medium, the aeration constant can be estimated by the following correlation (Van 't Riet and Tramper, 1991).

$$k_L a = 0.026 \left(\frac{P_g}{V}\right)^{0.4} v_g^{0.5} \qquad (6)$$

The correlation was obtained from a large amount of literature data and can be used for low viscous media. However, in case of a fungal fermentation the broth is often very viscous and behaves as a Non-Newtonian fluid with a yield stress or shows a shear thinning behaviour. The influence of rheology on the gas-liquid mass transfer has been studied (Van 't Riet and Tramper, 1991). The published results did not lead to a widely accepted correlation yet. Van 't Riet and Tramper (1991) concluded from the literature that when the viscosity of the medium is lower than 50 mPa.s, it appears to have no influence on the gas-liquid mass transfer. But when the viscosity is higher than 50 mPa.s $k_L a$ will decrease with it to a power of 0.7. Therefore in the present study $k_L a$ for a Newtonian medium is mathematically described as

$$k_L a = 0.026 \left(\frac{P_g}{V}\right)^{0.4} v_g^{0.5} \left(\frac{\eta + 0.05}{0.05}\right)^{-0.7} \qquad (7)$$

Appendix III: Rheology

The rheological behaviour of a fluid can be classified into Newtonian and non-Newtonian fluids depending on whether it obeys Newton's law of viscosity ($\tau_{yx} = \eta \, du_x / dy$). A Newtonian fluid can easily be described since its rheological behaviour is characterized only by its viscosity, a constant. Strictly speaking one can only use the term of viscosity in case of Newtonian fluids. The behaviour of non-Newtonian fluids can be classified using three criteria, shear thinning or shear thickening, with yield stress or without yield stress, time-dependent or time-independent. A shear thinning fluid is called pseudoplastic, a shear thickening fluid dilatant. A fungal fermentation broth is reported mostly to be pseudoplastic

with a yield stress. To describe the rheology of a pseudoplastic fluid with a yield stress, the Casson model has often been used (Metz, 1976 and Van Suijdam, 1980).

$$\tau^{1/2} = \tau_0^{1/2} + K_c \dot{\gamma}^{1/2} \tag{8}$$

This model contains two parameters, the yield stress τ_0 and the consistency index K_c. A pseudoplastic fluid with a yield stress is difficult to deal with in most theoretical and empirical expressions for the momentum, mass and heat transfer. Apparent viscosity is introduced to overcome this problem. Based on Eq.8 the apparent viscosity can be expressed as:

$$\eta_a = \frac{\tau}{\dot{\gamma}} = K_c^2 + \frac{\tau_0}{\dot{\gamma}} + 2 K_c \left(\frac{\tau_0}{\dot{\gamma}} \right)^{1/2} \tag{9}$$

In the literature, a lot of work has been done to correlate the rheology of a fungal fermentation broth with the free filamentous mycelial biomass concentration, the morphology of hyphae and the volume fraction of pellets. Due to large deviations and the complexity in the system, it is not possible to give a general correlation. Based on a huge amount of experimental data, Metz (1976) presented a correlation for the rheology of a filamentous mycelial suspension cultivated in a batch mode. If average values of the morphology parameters are used, the following equations will be obtained from his work:

$$\tau_0 = 0.0021 \, C_{xm}^{2.5} \tag{10}$$

$$K_c = 0.017 \, C_{xm} \tag{11}$$

For a pellet suspension, Van Suijdam (1980) reported

$$\tau_0 = 3.4 \times 10^{-5} \, C_{xp}^3 \tag{12}$$

$$K_c = 0.013 \, C_{xp} - 0.1 \tag{13}$$

Appendix IV: superficial gas velocity and shear rate
In order to make a proper comparison it is assumed that all scales of the bioreactors

considered are equipped with three Rushton turbines and are operated at an aeration flow rate per volume, Q_g/V_t, of 0.5 vvm. The superficial gas velocity, v_g, is defined as:

$$v_g = \frac{Q_g}{\frac{\pi}{4} T^2} \tag{14}$$

The power input of an individual impeller is:

$$P_i = N_p \rho_f N^3 D^5 \tag{15}$$

Under ungassed conditions, the power number N_p is about 6 (Nienow et al.,1977). When gas is introduced into stirred bioreactors the power number decreases and is a function of the bioreactor geometery, stirrer speed and gas flow rate (Cui et al., 1996b). The specific energy dissipation rate is:

$$\epsilon = \frac{P}{V_t \rho_f} \tag{16}$$

The total power input P is a sum of the power input from aeration and the power input of impellers. A prediction of the power input of impellers at aeration conditions in the multi-impeller stirred tank has a poor accuracy (Cui et al., 1996b). But in general the ungassed power input of impellers can be used as a rough estimation of the total power input. The volume of the bioreactor is:

$$V_t = \frac{\pi}{4} T^2 H \quad [H=2T, \; T=3D] \tag{17}$$

The averaged shear rate in stirred bioreactors can be expressed as (Metzner and Otto, 1957):

$$\dot{\gamma} = k_s N \tag{18}$$

where k_s is about 10-13. A value of 12 is used for k_s in the present study. Rearrangement and combination of these equations give the shear rate as a function of the scale of the bioreactor and the specific energy dissipation rate for this specific case:

$$\dot{\gamma} = 37 \epsilon^{1/3} V_t^{-2/9} \tag{19}$$

Appendix V: *characteristic time of pellet oxygen consumption*
In this appendix the time span needed to consume 63% of the dissolved oxygen in the bulk by pellets is derived. Assuming that the pellet size is the same the specific area of the pellets can be expressed as:

$$a_s = \frac{C_{xp}}{\frac{4\pi}{3}R_p^3 \rho_p} 4\pi R_p^2 = \frac{3\,C_{xp}}{R_p \rho_P} \tag{20}$$

The Thiele modulus for zero-order kinetics is (Cui et al., 1997b)

$$\phi^2 = \frac{(\frac{\mu}{Y_{Ox}} + m_{O2})\rho_p R_p^2}{18\,D_{eff}C_{O2b}} \tag{21}$$

The relationship of the Thiele modulus with the pellet radius R_p and the radius R_{0P} where oxygen is fully depleted is (Van 't Riet and Tramper, 1991)

$$\phi^2 = (6\frac{R_{op}^3}{R_p^3} - 9\frac{R_{op}^2}{R_p^2} + 3)^{-1} \tag{22}$$

If $R_{op} = 0$, then $\phi^2 = 1/3$. The critical pellet radius can than be estimated as

$$R_p = (\frac{6\,D_{eff}C_{O2b}}{(\frac{\mu}{Y_{Ox}} + m_{O2})\rho_p})^{1/2} \tag{23}$$

Assuming that $D_{eff} = 2.5 \times 10^{-9}$ m^2/s, $C_{O2b} = 4.2 \times 10^{-3}$ kg/m^3 (50% saturation with air at 1 atm), $\mu = 0.3$ h^{-1}, $\rho_p = 50$ kg/m^3, $Y_{ox} = 2$, and m_{O2} is relatively small, then the estimated R_p is about 250 μm. In view of the denser outer layer in pellets, the dissolved oxygen penetration depth is assumed to be about 100 μm. Therefore, dC_{O2}/dr will be about $C_{O2b}/0.0001$. Substituting this into Eq.(2) and assuming no gas-liquid mass transfer and oxygen consumption of the free filamentous mycelia in the bulk, dissolved oxygen will be transported into the pellets with a time constant of

$$t_{use,P} = \frac{\Delta r}{a_s D_{eff}} = \frac{0.0001}{a_s D_{eff}} \tag{24}$$

Combination of Eq.20 with Eq.24 gives the charactertistic time of oxygen consumption in the pellets.

Appendix VI: mixing and circulation time

Mixing or blending is an important process in most (bio)chemical conversions. In the present study two time constants, overall mixing time and stage circulation time, are considered to be important in the multi-impeller stirred bioreactor. The overall mixing time is predicted using the compartment model from Cui et al., (1996a). In bioreactors equiped with multiple Rushton turbines the stage or compartment per impeller is formed due to poor exchange flow between stages. So a stage circulation time is introduced into the multi-impeller bioreactor to describe the circulation process in each stage. It is defined to be the time span needed for the circulation flow to finish a circle within the stage. The circulation flow induced by Rushton turbine can be expressed as (Revill, 1982)

$$CF = 1.5 \, ND^3 \qquad\qquad (25)$$

So the stage circulation time is

$$T_{Cir} = \frac{V/n_{stirrer}}{1.5 \, ND^3} \qquad\qquad (26)$$

Appendix VII: particles in turbulent flow

Strictly speaking, a discrete particle suspended in a moving fluid faces many different kinds of forces (Hinze, 1971), such as gravity, buoyancy, flow resistance or drag, pressure gradient, shear lift, rotational forces and maybe the impact forces due to collision with other particles or objects present in a moving fluid. The particles to be considered in a fungal fermentation are spores, free filamentous mycelia, pellets and solid substrates. The density of those particles are close to the fermentation medium, which means that gravity force and buoyancy force can be ignored. The momentum balance of particles including those forces is too complex to solve. As Hinze (1971) stated, the turbulent multi-phase system presents many insurmountable problems. We will discuss here only the resistance force or drag force and disregard other forces, mainly because other forces are not known for the general case (Caulet et al., 1996).

Whenever a relative motion exists between a particle and the surrounding fluid the fluid will exert a drag force upon the particle. The drag force on the particle is given by

$$F = C_{drag} A_p \, \rho_f u_r^2 / 2 \qquad\qquad (27)$$

where F is the drag force, C_{drag} the drag coefficient, A_P the projected area of the particle, ρ_f the density of fluid and u_r the relative velocity between the particle and encountered fluid. The drag coefficient C_{drag} is a function of the shape of the particle and the Reynolds number of the particle:

$$Re_p = \frac{d_p \rho_f u_r}{\eta_f} \qquad (28)$$

Where d_p is the diameter of the particle, η_f the viscosity of the fluid and Re_P the Reynolds number of the particle. For a spherical particle and $Re_p < 1000$ the drag coefficient is (Caulet et al., 1996)

$$C_{drag} = \frac{24}{Re_p}(1 + 0.14\,Re_p^{0.7}) \qquad (29)$$

In a common fungal fermentation, the size of the particles varies from a few micrometres to several millimetres (spores, hyphae and pellets). Power input varies around 1 W/kg. The Reynolds number of those particles varies approximately in the range of 0.01 to 1000. The term between brackets in Eq.29 varies from 1 to 18. As a simplification a constant value of 10 is used and called C_{Re}. The application of the momentum balance or Newton's law on a particle gives:

$$\rho_p \frac{\pi}{6} d_p^3 \frac{du_p}{dt} = -3\,C_{Re}\pi \eta_f d_p (u_p - u_f) \qquad (30)$$

Rearrangment of this equation gives:

$$\frac{-du_p}{(u_p - u_f)} = C_{Re}\frac{18\,\eta_f}{\rho_p d_p^2} dt \qquad (31)$$

Integration of Eq.31 from the time when the particle enters into an eddy to the time when it leaves from this eddy leads to

$$-\ln\frac{(u_p - u_f)}{(u_{P_0} - u_f)} = C_{Re}\frac{18\,\eta_f}{\rho_p d_p^2}\tau \qquad (32)$$

Where u_p is the velocity of particles in the coordinate system of an eddy, τ the time span for a particle to stay in an eddy and u_{P0} the initial velocity of the particles. The characteristic response time of a particle to a change in its environment, i.e. to a change of the above force,

is an important quantity for its behaviour in a flow fluid (Hinze, 1971). It is often defined as the time span to reach 63 % of the final value after a change in its environment. From Eq.(30), we obtain the 63 % response:

$$\tau_p = C_{Re} \frac{\rho_p d_p^2}{18 \eta_f} \tag{33}$$

If added mass (Caulet et al, 1996) is taken into account :

$$\tau_p = C_{Re} \frac{(\rho_p + \frac{1}{2}\rho_L) d_p^2}{18 \eta_f} \tag{34}$$

If we consider the case that a particle meets an eddy and stays in it, the interaction time will be an eddy lifetime. The characteristic time of an eddy or its lifetime is a function of the eddy size and the energy dissipation rate. Depending on the eddy lifetime the particle will respond to the eddy motion differently

$$Ln \frac{u_f - u_p}{u_f - u_{p0}} = -\frac{\tau_E}{\tau_p} \tag{35}$$

where τ_E is the eddy lifetime. Let the relative response of a particle to an encountered eddy in an eddy lifetime be $y_p = u_p / u_f$ and assume that the fluctuation velocity of the particle is zero in the coordinates of the eddy. Rearrangement and the introduction of the relative response result in

$$y_p = 1 - e^{-\frac{\tau_E}{\tau_p}} \tag{36}$$

In a turbulent flow, the energy in a large eddy will be transferred into the smallest ones in a cascade way. Finally the energy is dissipated in the smallest eddy in which viscous forces are dominant. According to the Kolmogoroff theory (Davies 1972), the size of the smallest eddies can be expressed as:

$$l_K = \nu^{3/4} \epsilon^{-1/4} \tag{37}$$

From the energy dissipation rate and the kinetic viscosity of the fluid, one could calculate the size of the smallest eddy. The eddy lifetime is defined as the time needed for one revolution of the eddy. The lifetime of an eddy at any size can be calculated as

$$\tau_E = \frac{l_E}{u_E} = l_E^{2/3} \epsilon^{-1/3} \tag{38}$$

In above the various time constants are derived. The table I shows their final expressions. Based on those expressions the regime analysis of the fungal fermentation is performed.

Summary/Samenvatting

Fungal Fermentation: Technological aspects

Summary

Fungal Fermentation: Technological aspects

A joint research programme on fungal fermentation, involving Unilever Research Vlaardingen, Hannover University and Delft University of Technology, was set up . In this programme Hannover focused on physiological aspects while the technological aspects was studied in Delft. The research described in this thesis mainly focuses on these technological aspects of a fungal fermentation.

Uncertainty in predicting the performance of a fungal fermentation at different scales and at different conditions, is problematic. In general the uncertainty is caused by incomplete understanding of the hydrodynamics in a bioreactor, the cell physiology and their interaction. The aim of the research presented in this thesis was to reduce this uncertainty. The research was conducted in three steps: 1) to develop the method to predict hydrodynamic behaviour of a stirred bioreactor, 2) to study the effects of environmental conditions on fungal morphology and growth, 3) to model the relevant mechanisms of fungal fermentations. Submerged fermentation of *Aspergillus awamori* was chosen as a model system. A stirred tank equipped with multiple Rushton turbines, as generally used in industry, was used to perform fermentations.

Hydrodynamics
The hydrodynamic study included two parts, the mixing behaviour of stirred bioreactors and the power uptake by individual impellers in multi-impeller fermenters at aerated conditions. For the first part a compartment model was developed to predict the mixing behaviour of stirred (bio)reactors with multiple impellers. Experimental data on mixing behaviour were obtained from a large scale bioreactor (30 m^3) at various conditions. Comparison of model calculations with the actual data showed that the model predicted the fluid mixing behaviour in a stirred bioreactor well. The model parameters are mainly based on theoretical considerations, which will increase the applicability of the model. In the second part, a large body of experimental data on the power uptake of Rushton turbines was collected from literature. It was found that the power uptake by impellers under a gassed conditions showed two regimes. Middle and top impellers reached the second regime at a much higher gas flow rate than single or bottom impellers under the same conditions. Using these data correlations on the local gassed power uptake of impellers were derived both for single-impeller and multi-impeller systems. Knowing the mixing behaviour and the impeller power input in multi-impeller bioreactors, is important for both scale up and optimization of a given fermentation. The correlations and the compartment model presented can be used for this.

Morphology and growth

The studied environmental conditions were mechanical forces (agitation intensity), dissolved oxygen tension, and the type of substrates (glucose, sucrose, wheat bran). Growth kinetics and the scale effect on morphology were looked at as well. Hyphal morphology was characterized by hyphal length and pellet morphology by its size, its surface structure or so-called hairy length, the dry mass per wet pellet volume, and the dry mass per pellet surface area. The effects of agitation intensity and dissolved oxygen tension on morphology were studied through two sets of **parallel** fermentations and a literature study. One set (seven parallel fermentations) was performed at different agitation intensities (0.2-5.7 W/kg) and the other set (eight parallel fermentations) at different dissolved oxygen tensions (5%-400% of air saturation) keeping the agitation intensity constant. It was found that the agitation intensity influenced strongly the hyphal length, the pellet size, the hairy length and the fraction of free filamentous mycelia in the total biomass, while the dissolved oxygen tension influenced mainly the internal structure of pellets.

Based on these experimental observations, the following mechanisms concerning the interaction of the hydrodynamic conditions in a bioreactor with fungal growth and morphology was proposed. The increase of the pellet size is controlled by the extension and branching of hyphae at the surface in radial direction. Since dissolved oxygen is sufficiently available in the bulk, extension and branching of hyphae in the outer zone of the pellets are affected by mechanical forces only and not dependent on the dissolved oxygen tension. Therefore, pellet size is related to the agitation intensity (mechanical forces) and not to the dissolved oxygen tension. On the other hand the biomass per pellet surface area depends on the extension and branching of hyphae within the pellets and it is a function of the dissolved oxygen tension. The agitation with impellers creates mechanical forces which 'shave off' hyphae from pellets. Since the filamentous mycelia in the bulk grow without dissolved oxygen limitation and the hyphae shaved off from the pellets contribute to the free filamentous mycelial mass, the fraction of filamentous mycelia in the total biomass rises with increasing agitation intensity.

Besides parallel fermentations, more than 20 other fermentations were carried out. The type of substrate (glucose, sucrose or wheat bran), the scale (2 L-2000 L), the specific energy dissipation rate (0.2-5.6 W/kg) and the inoculation size (1×10^3-1×10^7 spores per ml) were varied in the different fermentations. Growth rate, biomass yield coefficients on both substrate and oxygen, cell maintenance on both substrate and oxygen and cell autolysis coefficients were obtained from these fermentations. It was found that the time course of the ratio of the biomass production to the sum of biomass production and carbon dioxide production hardly changed over the range of fermentation conditions used. This offers an approach to estimate the biomass concentration from the CO_2 production, which is desirable for obtaining on-line

information of biomass growth, especially for the situation where biomass determination is difficult such as when a solid substrate like wheat bran is used. At a comparable specific energy dissipation rate, pellets in large scale fermenters appeared to have a larger hairy length than in the small scale fermenters. When wheat bran was used, sometimes adhesion growth (fungi growing on the wheat bran) occurred. A more detailed study of this phenomenon showed that inoculation size played an important role. Inoculation with a spore concentration higher than 1.3×10^5 spores per ml resulted in domination of adhesion growth in the broth suspension. If the concentration was lower than 1.8×10^4 spores per ml, wheat bran free pellets and clean wheat bran particles dominated the broth suspension. Between these two concentrations, the broth suspension consisted of wheat bran free pellets, clean wheat bran particles and adhesion growth particles.

The information obtained on the effects of the bioreactor micro-environment on the morphology is needed in order to be able to control the fungal morphology in a submerged fermentation. The results of the kinetic study allows both the prediction of growth and the estimation of biomass concentration on line. The latter is especially important when a solid substrate is used in a fermentation.

Modelling

An engineering model was developed in which oxygen transfer, agitation intensity, dissolved oxygen tension, pellet size, formation of filamentous mycelia, sugar consumption, and biomass growth are taken into account. Comparison of the simulation with experimental results shows that the model can fairly well describe the time course of a fungal fermentation. The model predicts that a stronger agitation intensity leads to a smaller pellet size and a lower fraction of pellet mass in the total biomass. At the same agitation intensity, pellet size is hardly affected by the dissolved oxygen tension, whereas the fraction of filamentous mycelial mass in the total biomass decreases slightly with an increase of the dissolved oxygen tension in the bulk. All of these are in line with observations at the corresponding conditions.

A regime analysis was performed with respect to the relevant mechanisms in a fungal fermentation. Comparison of the characteristic times of relevant subprocesses indicated that mixing and gas-liquid oxygen transfer were almost always slower than oxygen consumption. Controlling the morphology as pellets with a size below 0.5 mm improves the oxygen transfer and avoids the occurrence of an internal oxygen limitation within the pellets. Increasing operation pressure and enriching oxygen concentration in the inlet gas can reduce or prevent gas-liquid oxygen transfer limitation or the inhomogeneity of the dissolved oxygen distribution in a bioreactor. The mixing behaviour can be improved by using a lower aspect ratio of the bioreactor, equipping the bioreactor with both Rushton turbines (good at gas dispersion) and axial pumping impellers (improving axial mixing), and choosing a proper location for feeding

(base, acid, substrate and inducer), for instance feeding at the middle of bioreactors in stead of at the top.

The main outcome of the work described in this thesis can be summarized as follows.

❑ Mixing behaviour and power dissipation in a bioreactor equipped with multiple Rushton turbines can be predicted using the developed compartment model and the obtained correlations.

❑ Fungal morphology in submerged fermentations can be controlled by controlling the agitation intensity, the dissolved oxygen tension, and the inoculation size.

❑ Inhomogeneities and gas-liquid oxygen transfer limitations in large scale fungal fermentations are inevitable. Modifying the bioreactor geometry (lowering the aspect ratio, adding axial pumping impellers, optimizing feeding points), and increasing the driving force for gas-liquid oxygen transfer (using a higher operation pressure and/or higher oxygen concentration in the inlet gas) can improve the situation.

Samenvatting
Schimmelfermentatie: Technologische aspecten

Het onderzoek beschreven in dit proefschrift maakte deel uit van een onderzoeksprogramma op het gebied van schimmelfermentaties, dat gezamenlijk werd uitgevoerd door Unilever Research Laboratories in Vlaardingen, Universität Hannover en de Technische Universiteit Delft. In Hannover lag de nadruk op fysiologische aspecten; in Delft werden vooral de technologische aspecten bestudeerd.

In de industriële praktijk blijkt het moeilijk het verloop van een schimmelfermentatie bij verschillende omstandigheden correct te voorspellen. Daarvoor worden de hydrodynamica in een bioreactor, de fysiologie van de schimmel en de wisselwerking daartussen nog onvoldoende begrepen. Het onderzoek waarvan in dit proefschrift verslag wordt gedaan had tot doel kennis en begrip van deze processen te verhogen teneinde met meer succes het verloop van een fermentatie te kunnen voorspellen. In het onderzoek lag de nadruk op achtereenvolgens 1) het voorspellen van het hydrodynamisch gedrag van een geroerde bioreactor, 2) het bestuderen van de invloed van effecten in de micro-omgeving van de cel op de morfologie en de groei van de schimmel en 3) het modelleren van de schimmelfermentatie door mathematische beschrijving van de relevante mechanismen. Ladingsgewijze fermentatie met de schimmel *Aspergillus awamori* in een geroerd vat voorzien van meerdere Rushton turbineroerders, zoals niet ongebruikelijk in de industrie, werd gebruikt als modelsysteem.

Hydrodynamica
Het onderzoek naar de hydrodynamica richtte zich enerzijds op het menggedrag van geroerde bioreactoren met meerdere roerders in het algemeen en anderzijds op de vermogensinbreng van de individuele roerders terwijl belucht wordt, in het bijzonder. Een compartimentenmodel werd ontwikkeld waarmee het menggedrag van een geroerde (bio)reactor voorspeld kan worden. Validatie van het model gebeurde door metingen van het menggedrag in een grote bioreactor (30 m^3). Het bleek dat het model het menggedrag van een waterige vloeistof in een geroerde bioreactor goed voorspelt. Doordat de parameters in het model een mechanistische achtergrond hebben wordt een brede bruikbaarheid van het model verwacht. Voor het beschrijven van de vermogensinbreng van beluchte Rushton turbineroerders werd een grote hoeveelheid literatuurdata verzameld. Met deze data kon worden vastgesteld dat er twee stromingsregimes zijn te onderscheiden. In het geval van een enkele roerder of voor de onderste roerder vindt de overgang naar het tweede regime bij een veel lagere gastoevoer plaats dan bij hoger geplaatste roerders bij overigens dezelfde omstandigheden. Correlatie van de data leverde vergelijkingen op om de lokale vermogensinbreng van begaste roerders te voorspellen in systemen met een of meer roerders. Kennis van het menggedrag in een

bioreactor en van de vermogensinbreng van de roerders is nodig voor opschalen en optimaliseren van een gegeven fermentatieproces. Model en correlaties kunnen daarbij gebruikt worden.

Morfologie en groei

De invloed van schuifkrachten als gevolg van het roeren, van de zuurstofconcentratie en van het substraat (glucose, sucrose of tarwezemelen) op morfologie en groei werden onderzocht. Ook werd gekeken naar groeikinetiek en de invloed van de schaalgrootte op de morfologie. De morfologie van schimmel wordt beschreven met parameters, zoals de lengte van de hyfen in het geval van mycelium. In dit proefschrift wordt de morfologie van een pellet beschreven door de afmetingen, met een maat voor de oppervlaktestructuur (de haarlengte) en met twee maten voor de dichtheid, de droge massa per nat pelletvolume en de droge massa per pelletoppervlak. De invloed van de roersnelheid en van de zuurstofconcentratie op de morfologie werden bestudeerd door twee verschillende experimenten uit te voeren, waarbij een aantal fermentaties parallel verliepen. Bij het ene experiment (zeven fermentaties) was de roerintensiteit in iedere fermentor verschillend (vermogensinbreng 0,2-5,7 W/kg). Bij het andere experiment van acht fermentaties werd de zuurstofconcentratie in het beslag constant gehouden op waardes die verschilden per fermentor (5%-400% van de verzadigingswaarde van lucht), terwijl de vermogensinbreng door de roerder steeds hetzelfde was. De roerintensiteit bleek vooral invloed te hebben op de uiterlijke kenmerken van de morfologie: hyfenlengte, pelletgrootte, haarlengte en hoeveel van de biomassa in myceliumvorm groeide. De zuurstofconcentratie in het beslag had vooral invloed op de interne structuur van de pellets.

Aan de hand van de waarnemingen werd de hiernavolgende hypothese opgesteld met betrekking tot de mechanismen die een rol spelen bij de wisselwerking tussen de hydrodynamica en de groei en morfologie van schimmels. De pelletgrootte neemt toe door groei van hyfen aan het oppervlak in radiale richting. Indien er in het beslag voldoende zuurstof beschikbaar is, wordt deze groei en dus de pelletgrootte alleen beïnvloed door afschuifkrachten (roerintensiteit) en niet door de zuurstofconcentratie. De dichtheid van een pellet neemt echter toe door de groei van hyfen naar binnen toe en is wel afhankelijk van de zuurstofconcentratie in het beslag omdat deze de mate van indringing van zuurstof bepaalt. Het roeren veroorzaakt afschuifkrachten waardoor de hyfen aan het oppervlak van de pellets afbreken; de hyfen worden 'afgeschoren'. Dit afgeschoren materiaal draagt bij aan de toename in het beslag van vrij mycelium, dat geen last heeft van zuurstofbeperking. De relatieve hoeveelheid hiervan neemt daardoor toe bij harder roeren.

Naast de parallel uitgevoerde fermentaties werden nog 20 fermentaties uitgevoerd, waarbij het substraat (glucose, sucrose of tarwezemelen), de schaal (2 - 2000 liter), het mechanisch

ingebracht vermogen (0,2 - 5,6 W/kg) en de entconcentratie (1×10^3-1×10^7 sporen per milliliter) werden gevarieerd. Groeisnelheid, de biomassa-opbrengstverhoudingen ten opzichte van substraat en zuurstof, de onderhoudsbehoefte van de schimmel aan substraat en zuurstof en autolysecoëfficiënten konden worden bepaald. Het verloop in de tijd van de verhouding tussen biomassaproductie en de som van biomassaproductie en koolzuurproductie bleek vrijwel constant onder alle gebruikte omstandigheden. Dit gegeven kan gebruikt worden om tijdens een fermentatie de biomassaconcentratie te schatten aan de hand van de gemeten koolzuurgasproductie. Dit is vooral aantrekkelijk indien andere methodes om de biomassaconcentratie te bepalen problemen geven, bij voorbeeld bij het gebruik van een vast substraat zoals tarwezemelen. Verder bleken pellets in grote fermentoren bij een vergelijkbare mechanische vermogenstoevoer een grotere haarlengte te hebben. Bij het gebruik van tarwezemelen werd soms adhesiegroei (groei op de tarwezemelen) waargenomen. Nader onderzoek wees uit dat de entconcentratie daarbij een belangrijke rol speelde. Indien werd geënt met een spoorconcentratie boven 1.3×10^5 ml^{-1}, dan overheerste adhesiegroei in de schimmelsuspensie. Maar bij een concentratie onder 1.8×10^4 ml^{-1} werden vooral pellets zonder tarwezemelen en onbegroeide tarwezemelen waargenomen in het beslag. Werd een concentratie gebruikt tussen deze twee waardes in, dan waren alle vormen aanwezig.

De verkregen informatie over de effecten van de micro-omgeving van de cel op de morfologie is nodig om de gewenste morfologie te kunnen realiseren tijdens een fermentatie. Met de resultaten van het onderzoek naar de kinetiek kan de groei voorspeld worden. Ook kan daarmee de biomassaconcentratie tijdens de fermentatie geschat worden, wat vooral van belang is bij het gebruik van een vast substraat.

Model

Een praktisch model voor de simulatie van het verloop van een schimmelfermentatie werd ontwikkeld waarin zuurstofoverdracht, zuurstofconcentratie, roerintensiteit, pelletgrootte, myceliumproductie, substraatconsumptie en biomassagroei werden meegenomen. Het model blijkt vrij goed in staat te zijn de experimentele resultaten te beschrijven. Het model voorspelt dat verhogen van de roersnelheid leidt tot de ontwikkeling van een kleinere hoeveelheid kleinere pellets. Bij dezelfde roerintensiteit blijkt de zuurstofconcentratie weinig invloed te hebben op de ontwikkelde pelletgrootte. De relatieve hoeveelheid mycelium neemt iets af met hogere zuurstofconcentraties. Deze resultaten komen overeen met de waarnemingen.

Met de verkregen resultaten was het mogelijk een regime-analyse uit te voeren met betrekking tot de relevante mechanismen in een schimmelfermentatie. Uit het vergelijken van de karakteristieke tijden van deze subprocessen blijkt dat menging en gas-vloeistof-zuurstofoverdracht bijna altijd langzamer zullen zijn dan zuurstofconsumptie. Indien er voor wordt gezorgd dat de morfologie van de schimmel voornamelijk bestaat uit pellets kleiner dan 0,5 mm dan zal het zuurstoftransport het minst geremd worden doordat interne

zuurstoflimitatie in de pellets wordt vermeden en de negatieve effecten op de zuurstofoverdracht door een verhoogde viscositeit zo klein mogelijk zijn. Verder verhogen van de zuurstofoverdracht is mogelijk door te werken onder verhoogde druk of met met zuurstof verrijkte lucht. Het menggedrag kan verbeterd worden door een andere keuze van roerdertypen (de onderste roerder bijvoorbeeld een Rushton turbineroerder die het gas goed dispergeert en overigens axiaal pompende roerders die de axiale menging verbeteren), door optimaliseren van posities van de toevoeren van base, zuur, substraat en inductor (bijvoorbeeld in het midden in plaats van aan de top) of door toepassen van een lagere hoogte-diameterverhouding van de reactor.

De belangrijkste resultaten van het in dit proefschrift beschreven werk kunnen als volgt samengevat worden:

❑ Menggedrag en vermogensinbreng door de roerders in een bioreactor voorzien van meerdere Rushton turbineroerders kunnen voorspeld worden door gebruik te maken van de in dit proefschrift beschreven compartimentenmodel en correlaties.

❑ Schimmelmorfologie in een fermentor kan geregeld worden met behulp van de roersnelheid, de zuurstofconcentratie en de entconcentratie.

❑ Concentratiegradiënten en zuurstoflimitatie door onvoldoende zuurstofoverdracht kunnen niet vermeden worden bij een schimmelfermentatie op grote schaal. Wel kan een bestaande situatie verbeterd worden door het wijzigen van de geometrie (lagere hoogte-diameterverhouding, toepassen van axiaal pompende roerders, optimaliseren van toevoerposities) en het verhogen van de drijvende kracht voor zuurstofoverdracht (hogere werkdruk, verhoogde zuurstofconcentratie in het toegevoerde gas).

List of Publications in This Thesis

Cui, Y.Q., Van der Lans, R.G.J.M., Noorman, H.J., Luyben, K.Ch.A.M., 1996, "Compartment mixing model for stirred reactors with multiple impellers", *Trans IChemE.*, **74, Part A**, 261-271

Cui, Y.Q., Van der Lans, R.G.J.M., Luyben, K.Ch.A.M., 1996, "Local power uptake in gas-liquid systems with single and multiple Rushton turbines", 14th International Symposium on Chemical Reaction Engineering, *Chem. Eng. Sci.*, **51**, 2631-2636

Cui, Y.Q., Van der Lans, R.G.J.M., Luyben, K.Ch.A.M., 1997, "Effects of agitation intensities on fungal morphology of submerged fermentation", *Biotechnol. & Bioeng.*, **55**, 715-726

Cui, Y.Q., Van der Lans, R.G.J.M., Luyben, K.Ch.A.M., 1997, "Effects of dissolved oxygen tension and mechanical forces on fungal morphology of submerged fermentation", *Biotechnol. & Bioeng.*, in press

Cui, Y.Q., Van der Lans, R.G.J.M., Luyben, K.Ch.A.M., 1997, "Influences of fermentation conditions and scale on the submerged fermentation of *Aspergillus awamori*", Submitted.

Cui, Y.Q., Ouwehand, J.N.W., Van der Lans, R.G.J.M., Luyben, K.Ch.A.M., 1997, "Aspects of the use of complex medium for the submerged fermentation of *Aspergillus awamori*", Submitted.

Cui, Y.Q., Okkerse, W.J., Van der Lans, R.G.J.M., Luyben, K.Ch.A.M., 1997, "Physical phenomena of fungal growth and morphology in submerged fermentations", Submitted.

Cui, Y.Q., Van der Lans, R.G.J.M., Luyben, K.Ch.A.M., "Regime analysis of fungal fermentation", to be submitted.

Acknowledgement

The work presented in this thesis was funded by Unilever Research Laboratory Vlaardingen and was carried out at the Kluyver Laboratory, Delft University of Technology, the Netherlands. Many people have been involved, have cooperated and helped in the completion of this thesis. I would like to take this opportunity to thank all of these people.

My first acknowledgement goes to my promoter, Prof. Karel Luyben, who has given me the opportunity, stimulating guidance, encouragement, and kind help to perform this research. I want to express my acknowledgement specially to Dr.Rob van der Lans, my supervisor, for his valuable discussions and suggestions, detailed explanation, critical comments on my thesis, and correction of my mistakes.

I acknowledge the fruitful regular meetings with M. Bosse, B.J. van Schie, H. Stam, M.Giuseppin, J. Hunic, W.Musters, from Unilever Research Laboratory Vlaardingen and Prof. K.Schügerl, D.Siedenberg, and S.Müller from Hannover University.

I am grateful to J.P.Lispet, J.Houwers, and P.V.Kroon for their technical support, to D.C.Reuvers, C. Ras , G. v.d.Steen, and S.H.van Hateren for the analysis of my samples, and to M.Santos da Silva from Unilever Research Vlaardingen for his help in spore multiplication. I am grateful also to Dr.ir.B.H.A. van Kleeff for allowing and helping me to use the education laboratory to run two parallel fermentations.

Many students have been involved in this work. In this aspect I am indebted to Ir.P.G.M. Lelieveld, ir. J. Ouwehand, ir.L. Boon, ir.M. de Jong, ing. R.Hennep, ir.W.J. Okkerse, and drs. M.van Rijswijk for their contribution.

Lots of other people have helped in one way or another in my four years of study. I would like to thank my dear roommates, Aukje, Philippe, Peter, John, Mos, Henk, and Hans, for a good room atomsphere, Marc for translating my stellingen from English to Dutch, Leslie for checking my English in the stellingen. In the four year study I have got so many helps in different manners that it is difficult to count and address them all. Here, please excuse me for being not able to mention all of your names. Finally, my thanks are extended to all the members in the Kluyver Laboratory, whose enthusiasm, friendship have made my stay a pleasant one.

I owe my parents a lot. No matter what happens to them, they always give me their love and support by all means. I regret that my mother, who died Jan. 28, 1996, is not able to see my thesis. The support from Lou Yuan, my wife, is indispensable for me to finish my Ph.D study.

Curriculum Vitae

The author was born on April 7, 1958 in Shenyang, China. In 1975, he graduated from 16th Secondary School, Jinzhou, Liaoning province, China. After that he was a farmer for three years at Laobian Farm in Liaoning province. In 1978 he entered the Chemical Engineering Department of Dalian Institute of Technology and in 1982 he received the degree of BSc in Chemistry of Fine Chemicals. After this, he was employed as a process engineer on dye synthesis in Second Chinese Film Corp., P.R.China. In 1983 he started his post graduated study at Chemical Engineering Department, Dalian Institute of Technology and in 1986 he received his degree of MSc in Chemical Engineering. From 1986 to 1989 he worked as a junior researcher at Biochemical Engineering Department, Institute of Chemical Metallurgy, Academica Sinica, P.R.China. In 1989 he came to The Netherlands as a research fellow at Organic Chemistry Department, Delft University of Technology. In 1990 he started a post graduated study at Biochemical Engineering Department, Delft University of Technology and in 1992 he received his Masters in Biotechnology from the Institute for Biotechnology studies Delft Leiden. In 1992-1996 he was employed as AIO (Ph.D study) under the guidance of Prof. K.Ch.A.M.Luyben at the Kluyver Laboratory of Biotechnology, Delft University of Technology. The results of this four-year study is presented in this thesis. The author is working as a postdoc at the Kluyver Laborotory of Biotechnology since the first of January of 1997.